Methods to Develop Composite Action in Non-Composite Bridge Floor Systems: Part I

by

Brad Schaap, B. S.C.E.

Thesis

Presented to the Faculty of the Graduate School of

The University of Texas at Austin

in Partial Fulfillment

of the Requirements

for the Degree of

Master of Science in Engineering

The University of Texas at Austin

May 2004

Methods to Develop Composite Action in Non-Composite Bridge Floor Systems: Part I

Approved by
Supervising Committee:

Michael D. Engelhardt

Richard E. Klingner

Dedication

To my loving mother and father,

whose encouragement prepared me for anything,

and

to Amy,

whose love made me strive to complete it.

Acknowledgements

I would like to thank the Texas Department of Transportation for their support which made this study possible.

Further thanks go to Dr. Michael D. Engelhardt and Dr. Richard E. Klingner for their guidance and supervision throughout the project in addition to their support in the classroom. I must also extend my gratitude to Dr. Young-Kyu Ju, a visiting scholar from South Korea, for his immense assistance in all aspects of this project.

Special thanks goes to Christopher Heinz of Drillco for his support. Also, I must thank Wayne Wallace of Applied Bolting Technology Products for his support. It is obvious from my interactions with each of these men that his respective company is lucky to have him.

Most of all, I would like to thank my research partner and friend, Brent Hungerford, for his cooperation from start to finish.

May 2004

Abstract

Methods to Develop Composite Action in Non-Composite Bridge Floor Systems: Part I

Brad Schaap, M. S. E.

The University of Texas at Austin, 2004

Supervisor: Michael D. Engelhardt

Over six percent of the bridges in Texas are considered structurally deficient, with about 3500 bridges posted for load, meaning that they do not meet today's design load ratings. More than one out of every eight bridges is proposed to be replaced, at a cost of $15 billion, because of insufficient capacity or roadway geometry. Economic methods of rehabilitating the structurally inadequate bridges are highly desirable. Creating composite action in currently non-composite bridge floor systems may be such a method, given that two out of every five bridges are composed of steel girders topped with concrete slabs.

This thesis, combined with that of Hungerford (2004), investigates the viability of post-installing shear connectors. Of the fifteen connectors investigated, the static load-slip characteristics of twelve post-installed shear

connectors was assessed, resulting in the recommendation of seven connectors for further testing. A static single-connector direct-shear test was performed on each tested connector, in lieu of the more traditional push-out test. Data on the coefficient of friction between the steel beam and concrete slab was also collected, as some of the connectors rely on friction at the steel-concrete interface as the primary shear force transfer mechanism.

Table of Contents

List of Tables

List of Figures

CHAPTER 1
INTRODUCTION

1.1 GENERAL

Of the nearly 49,200 bridges in Texas, almost 3,000 are considered structurally deficient by the National Bridge Inventory (United States 2002). Over 3,500 bridges are posted for load (Figure 1.1), meaning that they do not meet today's design load ratings (United States 2002). More than one of every eight bridges or other structures is proposed to be replaced because of substandard load-carrying capacity or substandard geometry (United States 2002). With a replacement cost estimated at over $15 billion, alternative economically feasible methods of rehabilitating these structurally inadequate bridges are highly desirable. Creating composite action in currently non-composite bridge floor systems may be such a method.

Figure 1.1: Load posting sign

In Texas, approximately two out of every five bridges are made of steel girders topped with concrete slabs (United States 2002). A significant number of

older bridges with steel girders were not designed for composite action, and hence have no shear connectors. Simply connecting the steel girders and the concrete slab using shear connectors can increase their flexural capacity by 50 % or more. Figure 1.2 shows a typical bridge that is a candidate for such strengthening by creating composite action. The steel-concrete interface is shown in the upper-right corner of the figure.

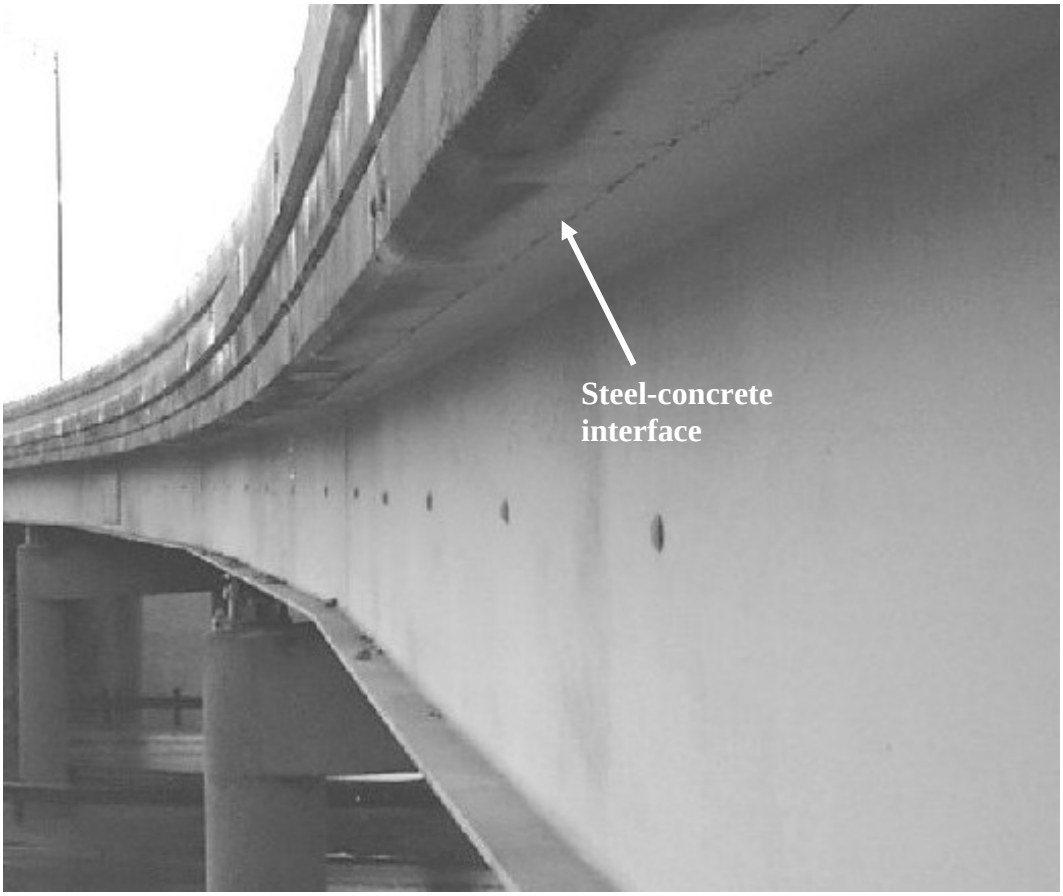

Figure 1.2: Typical candidate bridge for strengthening

Today, nearly all floor systems of bridges and buildings are designed to take advantage of composite action. Figure 1.3 shows the changes in distribution of stresses that result from connecting a steel girder with a concrete slab. In the

left-hand diagrams in Figure 1.3, the steel girder is not connected to the concrete slab. Slip occurs at the steel-concrete interface, and the steel girder and concrete slab act as independent flexural members. The flexural capacity of the concrete slab alone is usually quite small. Consequently, only the steel girder, acting alone, provides flexural resistance. In this case, equilibrium requires the neutral axis to be at mid-height of the steel girder, if the section is doubly symmetric. The right-hand diagrams in Figure 1.3 display a composite girder, in which the steel and concrete work together. Composite action is achieved by connecting the steel girder with the concrete slab to transfer horizontal shear at the steel-concrete interface. In a composite cross-section under positive moment, the neutral axis moves upward, and the stiffness and strength of the cross-section are increased substantially.

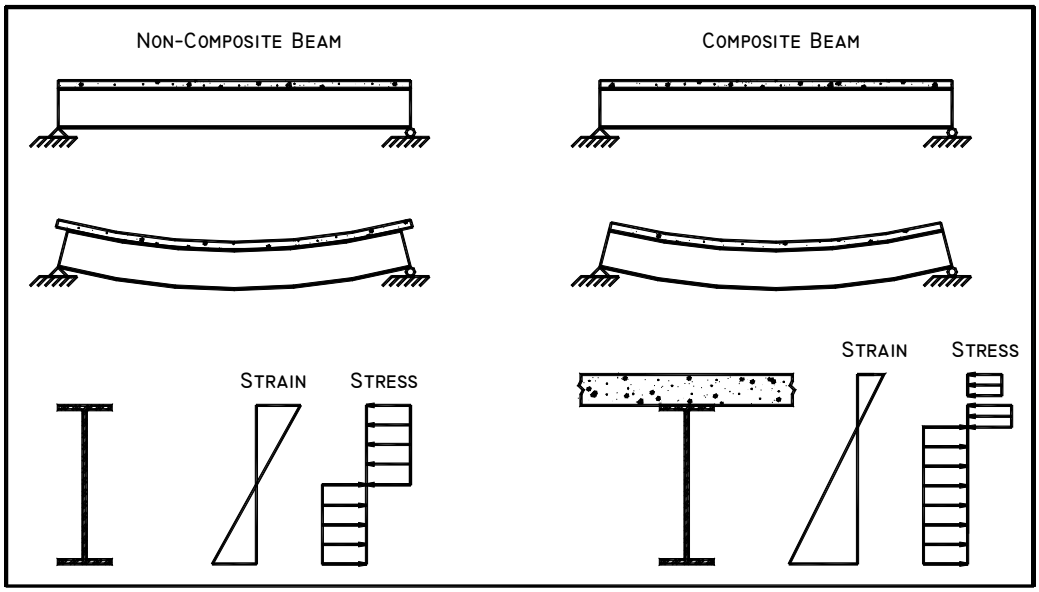

Figure 1.3: Advantage of composite girder

Creating composite action is a potentially appealing retrofit option for an existing non-composite bridge, because it requires only installation of connectors that can transfer shear between the steel girder and concrete slab. These

connectors then, in turn, allow the existing steel girder and concrete slab to work together in a more efficient manner, and therefore to carry larger loads. For new bridges, composite action is achieved by welding shear studs to the top of the steel girders before the concrete slab is cast. This welding is normally accomplished using a stud gun, which makes the process very rapid, economical, and effective. After the studs are welded to the top flange of the steel girders, the concrete slab is then cast around them. The shear studs are then fully embedded in the concrete slab, thereby allowing the transfer of large shears between the steel girders and the concrete slab.

In the case of an existing bridge, this approach is not possible, since the slab is already in place. Consequently, to take advantage of composite action in existing bridges, economical and practical methods for post-installing shear connectors are needed. This research addresses ways of developing composite action in currently non-composite bridge floor systems as an economical way of strengthening bridges to meet increased load requirements.

1.2 SCOPE OF THIS PROJECT

This thesis is one component of an ongoing larger investigation funded by the Texas Department of Transportation (TxDOT) to investigate the feasibility of creating composite action in existing non-composite bridges as a method of increasing the bridge's load rating. The overall project investigated 15 potential methods for achieving composite action (Figure 1.4). The objective of this project is to investigate economical, practical, and structurally effective methods of developing composite action.

In this thesis, the term "connection method" refers to any way of connecting the concrete slab and steel girder to transfer shear. This includes mechanical fasteners, and adhesives applied at the steel-concrete interface. The

term “connector” refers to any type of metal fastener, and excludes adhesive-only connections.

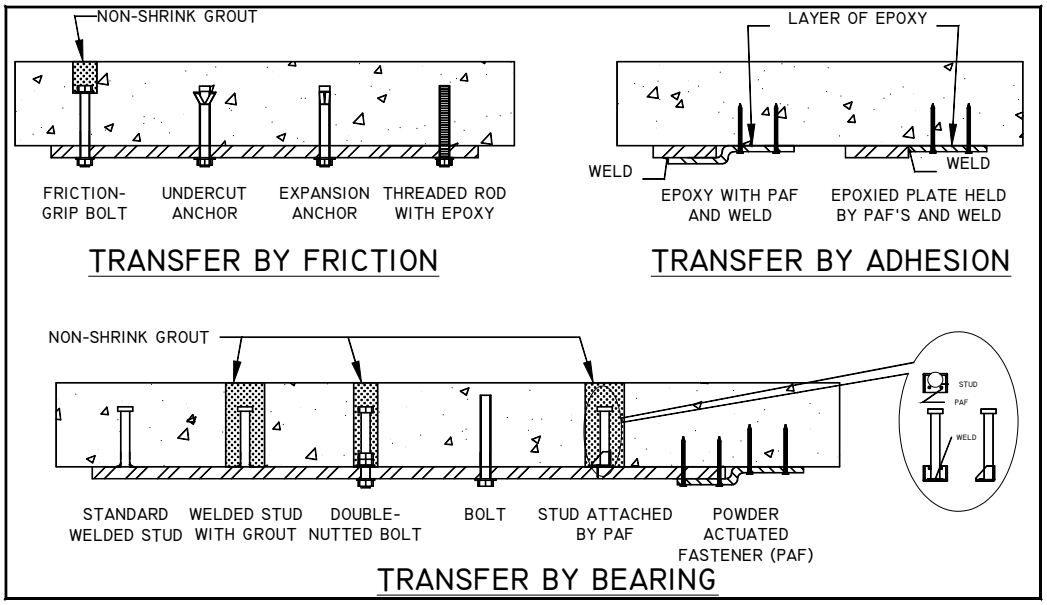

Figure 1.4: Shear-transfer methods investigated in this thesis

To determine the viability of the retrofit shear-connection methods, structural performance, constructability, and cost must be assessed. Structural effectiveness is evaluated using the ultimate strength and deformation characteristics of the connection method through static testing, as well as its fatigue characteristics under cyclic testing. An ultimate goal of this research project is to use the data gathered from testing to develop recommendations for design procedures. Figure 1.5 shows a flowchart of the testing program.

In addition to evaluating the structural effectiveness of the retrofit shear connection method, the constructability of the various retrofit techniques must also be considered. Comparisons are made based on the ease of constructability and the required tools for each connection method. Finally, the relative cost of the materials and installation equipment required to strengthen a sample

representative bridge for each connection method are estimated, as an additional factor affecting the feasibility of retrofitting.

Since both static and cyclic load cases are considered in bridge design, the project is divided into several facets for investigating the structural behavior of different shear-connector methods. Currently, the experimental testing is scheduled as follows:

1) single-connector, direct-shear static tests;
2) single-connector, direct-shear fatigue tests;
3) group-connector, direct-shear static tests;
4) group-connector, direct-shear fatigue tests; and
5) full-scale girder tests.

Static tests were first performed on single connectors to determine the strength and general behavior of the connection method considered. Connection methods exhibiting relatively low capacity or stiffness were eliminated from further investigation. Those exhibiting significant capacity with low slip were investigated further.

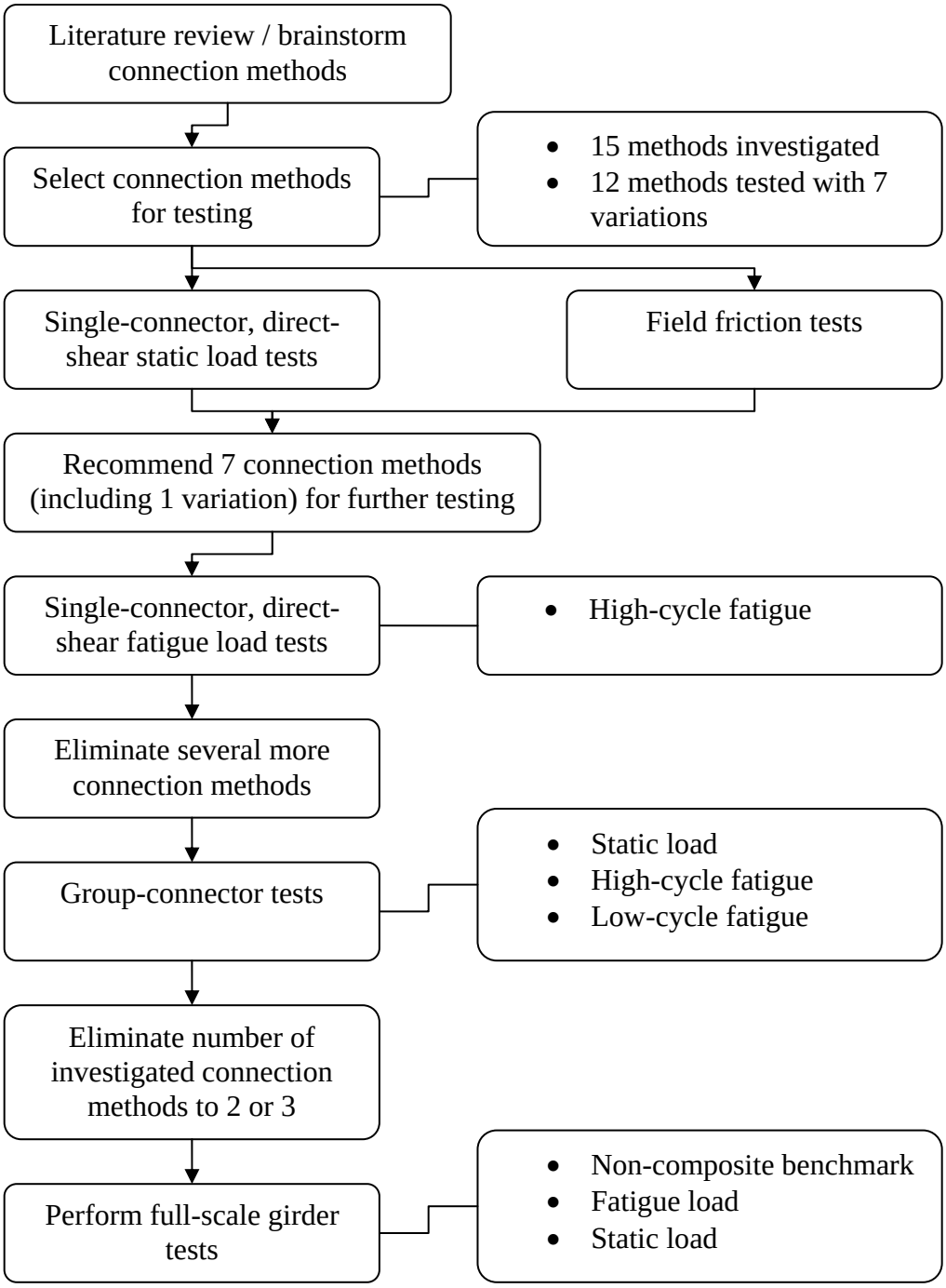

Figure 1.5: Preliminary flowchart of TXDOT Study 4124

Since bridges are subjected to relatively high cyclic stresses compared to most buildings, understanding the behavior of the connection method in fatigue is essential. Therefore, tests are currently planned on single connectors subjected to cyclic loading. Traditionally, high-cycle fatigue tests have been performed on shear connectors used in bridges. Many research papers written in the last decade, however, suggest that low-cycle fatigue should be investigated as well, due to the high cyclic loads expected in bridges.

Following cyclic tests on single shear connectors, the next phase of the project calls for static tests on groups of connectors (Task 3). Such tests are intended to provide data on load sharing and load redistribution among connectors. Furthermore, the majority of data on shear connector performance reported in the literature is based on tests conducted on groups of shear connectors. Consequently, the group-connector tests planned for this research program are intended to provide data directly comparable to that from past test programs on conventional welded shear studs. As with the static tests, the group effects of the investigated connection methods under cyclic loading must be understood. Therefore, a group fatigue test is anticipated. In the final stage of this project, large-scale tests on composite girders constructed with retrofit shear connectors are intended to provide a more comprehensive evaluation of the proposed shear-connector methods.

1.3 SCOPE OF THIS THESIS

The research reported in this thesis addresses the structural performance and constructability of various shear-connection methods. A test program for single connectors subjected to direct shear is described in this thesis, and in that of Hungerford (2004). This thesis also covers background literature of the fatigue behavior and design of shear connectors, including the related AASHTO (2002)

and AISC LRFD (2001) requirements. Recommendations are laid out for test setups for single connectors in high-cycle fatigue. Key variables affecting fatigue are discussed in detail.

This thesis primarily covers the anticipated static load-slip behavior, constructability, and cost-effectiveness. The first is evaluated using single-connector, direct-shear static test results of the following connection methods:

1) post-installed welded stud;
2) stud welded to plate;
3) double-nut bolt;
4) high-tension, friction-grip bolt;
5) expansion anchor; and
6) undercut anchor.

The behavior of the other shear-connection methods is described in Hungerford (2004). Details of various connection methods are described in Chapter 3.

1.4 HISTORICAL DEVELOPMENT OF COMPOSITE GIRDERS

The historical development of composite girders is briefly discussed in this section. Background information is also provided on the composite design provisions in design specifications for highway bridges published by the American Association of State Highway and Transportation Officials (AASHO 1961, AASHTO 2002).

One of the first questions that arises when designing for composite action is whether the concrete slab and steel girder work together naturally simply by friction and bond between the members. A natural bond, formed by microscopic mechanical interlock between the steel and concrete paste (Chapter 2), has been demonstrated (Cook 1977). Consequently, some degree of composite action can be developed without mechanical shear connectors. A number of investigators

have reported, however, that composite action developed between steel and concrete by bond or friction, separately or in combination, without mechanical shear connectors, may not be reliable. Tests performed at Iowa State on a greased girder, along with earlier tests, led Caughly to conclude that the amount of natural bond could not be determined; he recommended a mechanical anchor (Cook 1977). In addition, it is widely believed that the natural bond in a bridge is quickly broken after only a few cycles of truck loading. In 1929, Caughly and Scott discussed the design of a composite steel girder and concrete slab with a need for a mechanical shear connector (Cook 1977). Recent field load tests conducted on an older non-composite bridge by Bowen *et al*. (2003) also examined the degree of composite action developed by bond and friction, and showed that some composite action was developed at low load levels. At higher load levels, however, measurements showed that slip occurred at the steel-concrete interface and that the composite action was essentially lost. Those investigators concluded that composite action due to bond and friction was not sufficiently reliable to be counted on for capacity determinations.

Although some composite action can be achieved through bond and friction, research has clearly demonstrated that shear connection between steel and concrete are needed for reliable composite action. When composite construction was first gaining recognition, engineers and fabricators used a variety of connectors, such as plates, angles, channels, Z-sections, Ts, small sections of I-beams, square bars, and concrete reinforcing rods (Cook 1977).

Research into composite action for cast-in-place connectors started in the 1950's. In 1956, the then Committee on Bridges and Structures of the American Association of State and Highway Officials (AASHO) adopted detailed design requirements for composite construction requiring the slab and girder to respond to loading as a unit (Viest *et al*. 1997). Three types of connectors were included:

spiral, channel, and stud connectors. While spiral and channel connectors had been investigated and implemented in construction, stud connectors were new. The new provisions became a part of the 1957 edition (AASHO 1957) of the specification. Soon, bridges were constructed using composite design throughout the country. The economy and ease of construction of the stud connector made spiral and channel connectors virtually obsolete within only a few years. (Viest *et al*. 1997) Since the late 1950's, most research on composite systems has been performed using cast-in-place welded headed studs.

The 1961 American Association of State Highway Officials (AASHO 1961) Specifications allowed shear connectors designed by considering only static strength. The design equations used in the 1961 AASHO (AASHO 1961) Specifications limited the slip at the interface of the girder and slab to a value that would preclude yielding of the connector. The useful capacity of the connectors was derived from static tests of composite girders with shear connectors and from push-out specimens (Viest, Fountain and Siess 1958). Design equations divided the useful capacity by a factor of safety in an effort to ensure that the ultimate strength of the member could be developed prior to yielding of the connectors. Tests showed that fatigue was not a controlling mode of failure when composite design was performed using the 1961 AASHO Specifications (Toprac 1965). Spacing of the shear connectors was based an elastic analysis. Thus, design of composite girders using the 1961 provisions was very conservative (Slutter and Fisher 1966).

The behavior of cast-in-place connectors in high-cycle fatigue was investigated in the 1960's. Results of computer models using finite-element analysis were compared to experimental results in the 1980's and 1990's. In the past decade, low-cycle fatigue tests have also been performed.

In current practice for both buildings and bridges (AISC LFD 2001, AASHTO 2002), the static strength of composite girders is computed using a plastic cross-sectional analysis. The number of shear studs is also based on plastic analysis. For bridges, the required number of shear studs is also evaluated based on elastic fatigue considerations.

Although prestressed concrete has become the preferred structural system for bridges in many parts of the world, composite construction still has many advantages (Haensel 1998). For example, a major advantage of steel over prestressed concrete for bridge girders is the relative ease of maintaining or strengthening structural elements. In Germany, many new bridges reunifying the east and west halves of the country use composite construction (Haensel 1998).

CHAPTER 2
BACKGROUND: COMPOSITE ACTION AND BEHAVIOR AND DESIGN OF SHEAR CONNECTORS FOR STATIC AND FATIGUE LOADING

2.1 COMPOSITE ACTION

The concept of strengthening bridges by creating composite action in existing non-composite bridge floor systems is not new. The 50-year-old Spruce Street Bridge in Scranton, Pennsylvania is an early example, strengthened in 1945. Its weight limit was almost doubled, to 30,000 pounds, by removing the concrete deck, installing spiral shear connectors, and casting a new deck (Cook 1977). The goal of the project discussed in this thesis, however, is to avoid the costly removal and replacement of the concrete deck and simply connect the existing concrete and steel members.

In this thesis, the term "connection method" refers to any method for connecting the concrete slab and steel girder for the transfer of shears. This includes mechanical fasteners, as well as adhesives applied at the steel-concrete interface. The term "connector," on the other hand, refers to some type of metal fastener and does not include any adhesive-only connections.

2.1.1 General Design Considerations

Slutter and Fisher (1966) performed the research that forms the basis of today's design standards for composite girders. Their research changed the AASHO (1961) code from focusing on static loading using a very conservative

allowable load, to using a less conservative, more economical fatigue loading approach. Bridges are designed for fatigue loading to account for repeated application of live loads throughout the life of the bridge. Since fatigue occurs under service loads, most fatigue design is based on elastic analysis. In addition, complete composite interaction (defined in Section 2.1.2) is assumed, as this corresponds closely with experiments even when an inadequate number of shear connectors are provided. Only the cracked section of the concrete slab should be considered when computing the strength and stiffness of the composite section because cracks form from shrinkage (Slutter and Fisher 1966).

Elastic theory of composite action is based on the shear flow at a section given by Equation 2.1, which is reported in any mechanics of materials text. Computations of elastic response of a composite girder are normally based on the transformed section. With this approach, the concrete slab is transformed into an equivalent steel section by reducing the effective width of the slab by the ratio of the modulus of elasticity of steel to the modulus of elasticity of concrete.

$$S_r = \frac{V_r \times Q}{I} \qquad \textbf{(2.1)}$$

Where: S_r = range of shear flow at cross-section (kips/in.);

V_r = range of applied shear at cross-section (kips);

Q = first moment of area of portion of cross-section above the steel-concrete interface about center of gravity of transformed section ($in.^3$); and

I = moment of inertia of transformed section ($in.^4$).

The variables used are consistent with those given by the current AASHTO (2002) specifications. Further discussion of the AASHTO (2002) specifications is given in Section 2.9. Knowing the shear strength of the

connector or connectors at a cross-section, the required spacing at the cross-section can be calculated using Equation 2.2:

$$s_{req} = \frac{Z_r}{S_r} \qquad \textbf{(2.2)}$$

Where: s_{req} = required spacing of connectors (in.); and

Z_r = shear strength of connectors at cross-section (kips).

Increasing the shear strength of the individual connector (thereby increasing the shear strength at a cross-section), increases the required spacing, allowing fewer connectors.

As an alternative to the elastic approach described above, the required number of shear studs can also be computed based on plastic theory. Plastic theory simply requires enough connectors to develop the lesser of the strength of the steel girder or concrete slab (C or T) between points of zero moment and maximum moment, where:

$$C = 0.85 \times f_c^{'} \times b \times a \qquad \textbf{(2.3)}$$

Where: C = maximum possible compression force in concrete slab (kips);

f_c' = compressive strength of concrete (kips);

b = effective width of concrete slab (in.); and

t = depth of concrete slab (in.).

$$T = A_b \times f_y \qquad \textbf{(2.4)}$$

Where: T = maximum possible tension force in steel girder (kips);

A_b = area of girder ($in.^2$); and

F_y = minimum specified yield strength of steel girder (ksi).

Research has shown that the connectors can be evenly spaced (Toprac 1965), and the required number of connectors obtained by dividing the lesser of C

or T by the connector shear strength. Increasing the shear strength of the individual connector decreases the required number of connectors.

Creating composite action in the candidate bridges (discussed in Chapter 4) will be most effective in the positive bending moment region, where the compressive strength of the concrete can be used to form a wide compressive flange (Gilbert and Bradford 1995). This raises the neutral axis, allowing the steel to carry more tension (Figure 1.3). Longitudinal reinforcement can be used in negative bending regions.

2.1.2 Composite Action and Composite Interaction

The four combinations of composite action and composite interaction, shown in Figure 2.1, are described below. Composite action primarily deals with the stresses on a cross-section, while composite interaction deals with the strains on a cross-section.

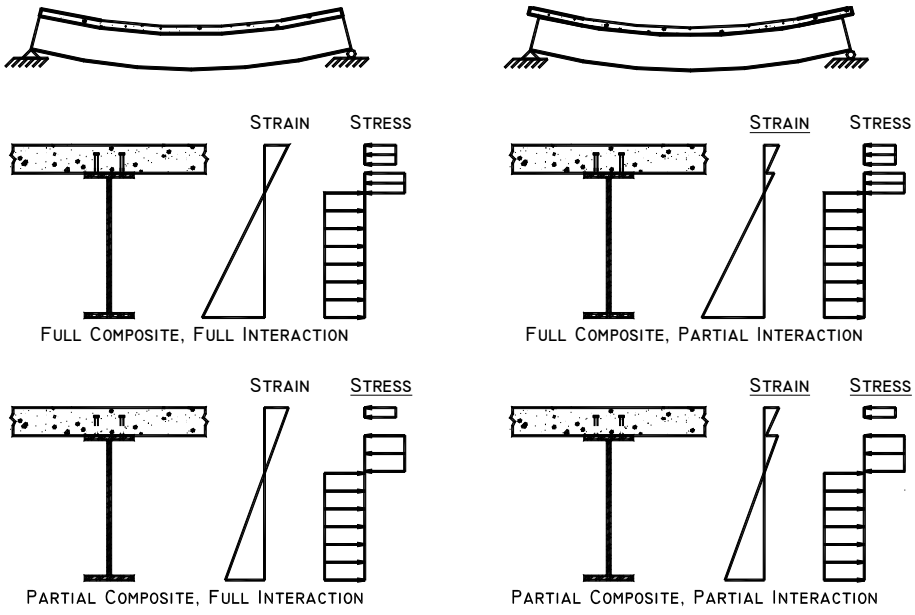

Figure 2.1: Composite action and interaction

2.1.2.1 Fully Composite Action

A girder is defined to be "fully composite" when sufficient shear studs are provided to develop the full flexural strength of the given cross-section (that is, the flexural strength of the member is governed by the strength of the steel girder and concrete slab; girder strength is not governed by the strength of the studs). Generally, a designer can assume essentially no slip between steel and concrete for elastic analysis at service loads. The sufficient number of shear studs, N_f, is the number of connectors which allows the composite girder to achieve its full ultimate strength and is obtained by calculating the force required to be transferred at the steel-concrete interface at the ultimate load state (Faella, Martinelli and Nigro 2003). When the number of shear studs supplied is greater than N_f, the girder is said to be "fully composite," and the ultimate strength is not affected by the number of shear connectors. The upper-left and upper-right stress of Figure 2.1 show fully composite cross-sections.

2.1.2.2 Partially Composite Action

A girder is defined to be "partially composite" when its flexural strength of the girder is governed by the strength of the shear studs. A designer must account for slip between the steel girder and concrete slab for elastic analysis at service loads. The ultimate strength of a partially composite girder is less than that of a fully composite girder because the concrete cannot achieve its full plastic limit state, as the force in the slab is limited by the strength of the connectors. The decrease in flexural strength can be related to the degree of shear connection N/N_f, where N is the number of connectors actually used (Faella, Martinelli and Nigro 2003). The shear connectors must have the slip capacity required to achieve the desired load capacity (Johnson and Molenstra 1991). Further discussions on the maximum slip required by the bridge, as well as the slip

capacity of the welded headed shear stud, are given in Sections 2.1.7 and 2.5.5 respectively.

The minimum degree of shear connection, N/N_f , is limited by codes to between 25 and 50 % in buildings to allow for some degree of ductility after the section has reached its capacity (Viest *et al*. 1997). In addition, it is recognized by many researchers that sudden shear failure can occur in bridges with low percentages of interaction (Viest *et al*. 1997). Johnson and Molenstra (1991) warn that N/N_f must exceed a value dependent on the span, type of loading, and load-slip relation of the connector, to prevent sudden premature shear failure.

Johnson and Molenstra (1991) also warn against the use of partial composite design at the interior support of continuous girders because of large tensile forces which occur in excess of yield due to strain hardening before either adjacent span fails. They point out that partial shear connection is now specified for sagging (positive) bending only, in BS 5950 (1990) and in Eurocode 4 (1994). It is also not allowed in the current AASHTO (2002) provisions, although it once was, as discussed in Section 2.9.2. In addition, since welding is not typically allowed on the tension flanges of girders, a reason exists to investigate post-installed connection methods that require no welding, such as the double-nut bolt discussed in Chapter 3. The lower-left and lower-right stress diagrams of Figure 2.1 show partially composite cross-sections. While the steel member achieves a fully plastic stress distribution, the concrete does not achieve its full capacity, because the shear connectors can transfer only a limited force to the slab.

2.1.2.3 Partial Composite Interaction

Faella, Martinelli and Nigro (2003) recognize that slip occurs at the steel-concrete interface because shear connectors are not stiff enough to prevent it, even for fully composite design. Slip at the steel-concrete interface results in

partial shear interaction, which primarily affects the stiffness of the composite member. The slip at the steel-concrete interface is shown in the upper-right and lower-right strain diagrams of Figure 2.1, where a discontinuity exists at the steel-concrete interface.

Experiments by Alsamsam in 1991 on simply supported girders and Ansourian in 1981 on continuous girders show that even for full shear connection, the effect of partial shear interaction results in an increase of experimental deflection of about 30 to 40 % over the calculated deflection for full interaction (Faella, Martinelli and Nigro 2003). Those authors show that the deflection calculated accounting for partial shear interaction is always greater than the calculated deflection for fully composite design assuming full interaction. They report that the ratio of the calculated deflections is proportional to the degree of shear connection, N/N_f (Faella, Martinelli and Nigro 2003). Flexibility is greatly affected by partial shear connection versus full shear connection due to an even more pronounced partial shear interaction (Faella, Martinelli and Nigro 2003).

2.1.3 Achieving Composite Action

Composite action is achieved by connecting the steel girder with the concrete slab to permit transfer of horizontal shears at the steel-concrete interface. The standard welded headed stud's root transfers most of the horizontal shear acting at the steel-concrete, while the head prevents uplift of the slab (Matus and Jullien 1996). Due to local crushing of the concrete, the stud bends and transfers shear through flexure (Cook 1977).

The headed stud is welded to the girder using a special gun that arcs electricity between the girder flange and a fluxing agent in the stud, forming a pool of molten metal around the base of the stud. The pool is contained by a ceramic annulus and the gun pushes the stud into the molten metal, forming a

uniform weld. The studs are about 3/16-in. longer than listed in the AISC manual (AISC LRFD 2001), as the welding process reduces their length to that specified (Cook 1977).

Based on research performed on full-scale girders, studs fail progressively through the connectors as each gradually loses effectiveness during the life of the girder under fatigue loading (Toprac 1965). That is, a composite girder does not fail once the first connector fails, but rather gradually reduces in effectiveness as the horizontal shears redistribute to other connectors.

Tadros, Badie and Girgis (2001) report that a stud does not necessarily need a head because the reinforcement confines the concrete around the connector adequately even through fatigue. Those authors point out that the AASHTO LRFD Specifications (1998) requires the use of continuous top and bottom transverse reinforcement over the girder lines (Tadros, Badie and Girgis 2001). Upon completion of the fatigue resistance investigation performed by those three researchers, it was evident that providing continuous top and bottom reinforcement in the deck and slab can provide adequate confinement to the concrete (Tadros, Badie and Girgis 2001).

2.1.4 Basic Mechanisms of Shear Transfer

As described in Section 2.1.3, a connector capable of transferring the horizontal shear is required to achieve composite action. The three basic methods of transferring shear between a concrete slab and a steel girder are:

1) bearing;
2) friction; and
3) adhesion.

Table 2.1 lists the primary mechanisms of force transfer for the connectors discussed in this project (described in Chapter 3). If applicable, the secondary

shear-transfer mechanism, which engages after loss of friction, is also listed and marked.

Table 2.1: Mechanism of shear transfer for each connection method

Connection Method	Mechanism
Welded Headed Stud, Double-Nut Bolt, Saw Teeth, Expansion Anchor†, Undercut Anchor†, Welded Threaded Rod†, Adhesive Anchor†, Concrete Screw†, Powder-Actuated Fasteners†, Rivets†, High-Tension, Friction-Grip Bolt†	Bearing
High-Tension, Friction-Grip Bolt, Expansion Anchor, Undercut Anchor, Welded Threaded Rod, Adhesive Anchor, Concrete Screw, Powder-Actuated Fasteners, Rivets	Friction
Epoxy Coating	Adhesion

†Denotes secondary shear-transfer mechanism

2.1.4.1 Bearing

Bearing is the most common mechanism for transferring shear at the steel-concrete interface in composite girders. The welded headed stud, the most common shear connector used in practice, transfers the shear from the top flange of the steel girder through a weld, and then to the slab by the connector bearing on the concrete. Other stud-type bearing connectors are connected to the steel girder by bearing (for example, double-nut bolt) or friction (for example, high-tension, friction-grip). Chapters 1 and 3 show diagrams of these connectors.

2.1.4.2 Friction

Using friction to transfer the shear between the concrete slab and the steel girder provides a shear connection with high stiffness. This mechanism requires

tension in the connector to create a normal compressive force at the steel-concrete interface. Shear is transferred completely by friction as long as it is less than the product of the coefficient of friction and the normal force. Friction is an ideal mechanism for fatigue loading, since no slip occurs, and thus incremental slip and incremental collapse is not a problem (that is, low-cycle fatigue, discussed in Section 2.1.8). When transferring shear by friction, the coefficient of friction at the steel-concrete interface is a critical design parameter. This issue is discussed further in Chapters 7 and 8.

2.1.4.3 Adhesion

Adhesion at the steel-concrete interface is one of the simplest mechanisms for connecting concrete to steel. In a retrofit situation, this could be accomplished by attaching a plate to the underside of the slab using a structural adhesive, and then connecting the plate to the girder by a weld, adhesive, powder-actuated fasteners, or other means. Adhesive has been shown to provide good performance in fatigue and possess a high ultimate strength by researchers at the University of Arizona (Epoxy 1963).

2.1.5 Effect of Tension and Moment in the Connector

Before using a model for composite action based only on the shear strength of the connector, it is important to understand the effects of possible tension or moment on the connector's shear strength. Studs in a bridge undergo shear and tension simultaneously (Viest *et al*. 1997). Those authors observe that the tensile forces can be large yet localized, and decrease the shear capacity of the connector by only a small amount. For example, they calculate that a tensile force applied to the connector equal to half the yield strength decreases the shear by only about 10 to 12 % according to current shear-tension interaction formulas for connectors (Viest *et al*. 1997). As discussed above, the stud transfers the load

through flexure as well. Viest *et al*. (1997) assert that researchers are unclear what effect the combination of shear, tension, and bending has on the connector's shear strength, but warn that it likely decreases under the combination.

2.1.6 Effect of Friction on the Behavior of the Bridge

Oehlers, Seracino and Yeo (2000) investigated the effect of friction on the behavior of the bridge and the life of the shear connectors. They assert that friction between the concrete slab and steel girder is beneficial because it reduces the shear carried by the shear connectors. The compressive force created by the loading element on top of the bridge increases the normal force between the slab and girder, enabling friction to transfer the shear, and also subjecting the connector to compression, increasing the connectors' capacity (Oehlers and Bradford 1995). Oehlers, Seracino and Yeo (2000) assert that friction extends the life of shear connectors above what is typically designed for because of the compressive loading force.

Oehlers, Seracino and Yeo (2000) assert that the effect of friction must be assessed in design to simulate the actual behavior of the shear connection and to accurately estimate the actual forces applied to the shear connectors. These researchers used a simple mathematical model to predict the beneficial effect of friction on the fatigue life (Oehlers, Seracino and Yeo 2000).

Oehlers, Seracino and Yeo (2000) report that the distribution of the normal compressive force in a shear span is highly non-uniform, whether or not friction is included in their analysis. No significant effect on the normal force distribution is observed when friction is taken into account in the analysis (Oehlers, Seracino and Yeo 2000). A concentrated truck load was applied at the quarter-point of the span, resulting in regions of a tensile normal force distribution around the load point (Oehlers, Seracino and Yeo 2000).

The three researchers report that despite high compressive forces at the interface along most of the length of the bridge, the girder does completely resist slip due to friction, as might be expected. They observed that slip occurred throughout the entire girder, except at the transition point where the shear flow changes direction. The horizontal shear shifts to the stiffest cross-section, until friction is overcome all at once, in which case the entire slab slides over the girder (Oehlers, Seracino and Yeo 2000).

Oehlers, Seracino and Yeo (2000) applied a concentrated load at the quarter-point and report that the shear flow on the connectors in the shorter span reduced relatively uniformly even though the compressive force distribution is non-uniform (Oehlers, Seracino and Yeo 2000). Friction increases the shear flow on the connectors in the longer span, however, because the transition point shifts toward the shorter span due to the concentrated load. The shift of the transition point toward the shorter shear span (making it shorter) increases the shear flow on the connector in the longer shear span adjacent to the applied load (Oehlers, Seracino and Yeo 2000).

The required resistance of the stud is reduced due to friction near the supports of a simply supported girder subjected to a moving point load, but is increased over the remainder of the girder (Oehlers, Seracino and Yeo 2000). At design points away from the supports, the increased shear flow in the studs is larger because of the increase in force due to the shift in the transition point being greater than the decrease due to friction (Oehlers, Seracino and Yeo 2000). Oehlers, Seracino and Yeo (2000) show that friction reduces the shear flow in regions where the shear is highest, but increases shear flow in the remainder of the girder under a moving load. They assert that the increase in shear flow is offset by the reduction due to partial interaction (Oehlers, Seracino and Yeo 2000).

Those researchers show that even a small amount of friction at the steel-concrete interface can substantially increase the fatigue life of the shear connectors. They suggest a simple hand analysis to assess the remaining life of the connectors based on the number of load cycles. This technique can help the designer determine if a more complex computer simulation is necessary. This approach could be beneficial to designers using the retrofit technique described in this thesis as partial shear connection may be used making the strength of the bridge directly dependent on the connectors (Oehlers, Seracino and Yeo 2000).

2.1.6.1 Testing Coefficient of Friction between Concrete and Steel

Oehlers, Seracino and Yeo (2000) use a coefficient of friction, μ, of 0.8 in their computer model to represent friction based on tests performed by Singleton in 1985 that show that the dynamic coefficient of friction between steel and concrete ranges from 0.7 to 0.95 under cyclic loading. In contrast, Cook (1989) summarizes the results of 27 tests on dry and wet surfaces to show the coefficient of friction between steel and concrete, μ, ranges from about 0.35 to about 0.65, with a mean of 0.50. Cook (1989) also reports that previous research has shown that the coefficient of friction is higher for concrete or grout cast against a steel plate than for the case of a steel plate attached to already hardened concrete. Cook (1989) performed 44 of his own tests and reports that the coefficient of friction has a mean of 0.43, a minimum of 0.39, and a maximum of 0.46. He asserts that the surface condition of the concrete and the magnitude of the applied normal force do not change the results significantly. Cook (1989) recommends using a design value for the coefficient of friction of 0.40 with a resistance factor, Φ, of 0.65, resulting in a design strength that is a 2 % lower fractile of test data.

2.1.7 Maximum Slip in Composite Girders

Since experiments performed on shear connectors measure the applied load and corresponding slip relationship, it is important to understand what maximum slip could occur between the concrete slab and steel girders in a typical candidate bridge (Chapter 4). Analytical and laboratory experiments have been performed by various researchers to assess the maximum relative slip between the two components of the bridge. Although a vast amount of research has been performed on the subject, no consensus exists on a solution. Several loading conditions and limit states may be appropriate to define maximum slip:

1) ultimate capacity of structure;
2) serviceability deflection; or
3) fatigue loading.

Johnson and Molenstra (1991) estimate that the maximum slip, s_{max}, of a composite girder subjected to its design ultimate load may be a function of about 20 independent variables, not including the geometric and constitutive properties. They point out that investigating each of these variables is impossible due to technical and economic constraints.

Johnson and Molenstra (1991) report that the two most significant parameters governing maximum slip are the degree of shear connection and the span of the composite girder. They use several sources in their research of maximum slip, including nonlinear numerical analyses, test data, and parametric studies. Their results show that distributed loading always gave higher maximum slips than combinations of point and distributed loads. They also report that a simply supported girder has a higher maximum slip than a continuous girder of the same span.

Johnson and Molenstra (1991) present Equation 2.5 based on four ratios they found always increase the maximum slip when the other three are held constant and performing computer analysis using an interpolation method:

$$s_{\max,p} = s_o \times \left(\frac{L}{h}\right)^{\alpha} \times \left(\frac{w_p - w_{pa}}{w_{pa}}\right)^{\beta} \qquad \textbf{(2.5)}$$

Where: α = -0.13 and -0.24 for N/N_f of 0.5 and 0.75 respectively;

β = 1.03 and 1.70 for N/N_f of 0.5 and 0.75 respectively;

L = length of simply supported bridge;

h = depth of composite section; and

w_p = design load per unit length.

$$w_{pa} = 8 \times \frac{M_{pa}}{L^2} \qquad \textbf{(2.6)}$$

Where: M_{pa} = plastic moment resistance of steel girder;

$$s_o = \frac{M_{pa} \times L \times h_a}{6 \times E_a \times I_a} \qquad \textbf{(2.7)}$$

Where: s_o = elastic end slip with zero shear connection when steel girder carries load w_{pa} per unit length;

h_a = depth of steel girder;

E_a = modulus of elasticity of steel girder; and

I_a = moment of inertia of steal girder.

Consistent units must be used. The coefficient of variation of the errors is 4.9 and 8.0 % for an N/N_f of 0.5 and 0.75 respectively. Table 2.2 shows the maximum slip for the typical candidate bridge given in Chapter 4 calculated using the equations given in this section.

Some researchers have found a correlation between the yield strength and ultimate slip of the connector in tests. Johnson and Molenstra (1991) ran most of

their analysis on steel with a yield strength, F_y, of 51 ksi, and a few tests with an F_y of 40 ksi. The reductions in s_{max} at N/N_f of 0.5 range from 33 to 48 % for a reduction in F_y of 23 % (Johnson and Molenstra 1991).

Oehlers and Sved (1995), derived Equation 2.8 for the slip that a bridge would undergo:

$$S_{\max} = M_{\max} \times L \times \frac{K_1}{3} - P_{\max} \times L \times \frac{K_2}{4} \qquad \textbf{(2.8)}$$

$$K_1 = \frac{h_s + h_c}{(EI)_s + (EI)_c} \qquad \textbf{(2.9)}$$

$$K_2 = \frac{(h_s + h_c)^2}{(EI)_s + (EI)_c} + \frac{1}{(EA)_s} + \frac{1}{(EA)_c} \qquad \textbf{(2.10)}$$

Where: M_{max} = maximum moment in span; and

P_{max} = force exerted by connectors at maximum moment section.

Subscripts "s" and "c" denote the steel and concrete properties, respectively, already given. Oehlers and Sved (1995) conclude that concrete cracking, which has been shown to occur at low load levels does not affect s_{max} significantly. They also suggest, however, that connector yield may have an effect on s_{max}. This equation is valid only for low degrees of connection, that is, 0.5 and below (Oehlers and Sved 1995).

Toprac (1965) shows that the failure of an individual stud in a girder does not affect the end slip or deflection, even considering the girder and slab in his specimens were debonded using a thin layer of oil at the steel-concrete interface. Slip at the steel-concrete interface is negligible for service loads (Gilbert and Bradford 1995). It has been shown, however, that end slip increases with the number of cycles for all full-scale girder fatigue tests (Toprac 1965). This is discussed further in Section 2.1.9.

The end slip, s_y, occurring for simply supported girder without shear connection under a uniformly distributed load, may be evaluated when the steel profile yields as follows (Faella, Martinelli and Nigro 2003):

$$s_y = \frac{q_y \times L^3}{24 \times E \times I_{abs}} \times \frac{h_a + h_c}{2} \quad \textbf{(2.11)}$$

Where: q_y = uniformly distributed load applied to bridge.

This parameter approximates the maximum possible slip (Faella, Martinelli and Nigro 2003). Faella, Martinelli and Nigro (2003) conclude that the influence of the other parameters (EI_{full}/EI_{abs}, cylinder concrete strength, f_c, steel yielding stress, type of loading, α_c and β_c) is negligible.

Viest *et al*. (1997) suggest Equation 2.12 for calculating slip along a simply supported bridge with a linear-elastic connector subjected to a uniformly distributed load based on partial interaction:

$$s(x) = \frac{qh}{EI_{abs}\alpha^3}\left(\frac{1-\cosh(\alpha L)}{\sinh(\alpha L)}\cosh(\alpha x) + \sinh(\alpha x) + \frac{\alpha L}{2} - \alpha x\right) \quad \textbf{(2.12)}$$

$$\alpha^2 = \frac{k_s}{EA_{eq}} \times \frac{EI_{full}}{EI_{abs}} \quad \textbf{(2.13)}$$

$$EA_{eq} = \frac{(EA)_T \times (EA)_B}{(EA)_T + (EA)_B} \quad \textbf{(2.14)}$$

$$EI_{abs} = (EA)_T + (EI)_B \quad \textbf{(2.15)}$$

$$EI_{full} = EI_{abs} + EA_{eq} \times h^2 \quad \textbf{(2.16)}$$

Where: q = uniformly distributed load applied to bridge;

k_s = shear stiffness of connector per unit length;

h = distance between centroids of girder and slab; and

x = location along bridge (0 for end slip of simply supported bridge).

Subscripts "B" and "T" correspond to the girder and slab properties respectively.

Tadros, Badie and Girgis (2001) performed fatigue loading on a full-scale girder test with a 40-ft girder and an 8-in. slab using one headless 1¼-in. diameter stud every 6 in. Measurements show a maximum slip of 0.049 mm (0.002 in.) after 4,800,000 cycles of HS25-loading at the critical shear section and another 4,800,000 cycles at midspan (Tadros, Badie and Girgis 2001).

Table 2.2: Maximum slip for typical candidate bridge under ultimate loading

Equation 2.5 (N/Nf = 0.50)	Equation 2.5 (N/Nf = 0.75)	Equation 2.7 No connectors	Equation 2.8	Equation 2.11 No connectors	Equation 2.12
0.13-in.	0.07-in.	0.29-in.	0.10-in.	0.11-in.	0.20-in.

The values given in Table 2.2 vary somewhat, with an average of 0.15.

The second limit state listed at the beginning of the section deals with the serviceability deflection criteria. Hungerford (2004) showed using a finite-element model that the typical candidate bridge may undergo a slip of 0.13 in. when typical serviceability deflection limits are reached.

The third limit state discussed at the beginning of the section dealt with fatigue loading. Toprac (1965) shows that the ultimate end slip for four full-scale girder tests ranges from 0.07 in. to 0.31 in. with an average of 0.20 in.

The dimensions of the typical candidate bridges (Chapter 4) vary somewhat, and no consensus on what the ultimate slip a bridge undergoes exists, as shown in Table 2.2. Based on the results of the three limit state criteria listed

at the beginning of this section, in this document, the maximum slip that a composite girder may undergo is estimated as 0.2 in.

2.1.7.1 Design Slip at Which Shear Connector Strength Should be Taken

Now that the ultimate slip a connector may undergo in a bridge has been estimated in several ways, it is relevant to discuss the slip at which the design shear should be taken based on the load-slip relationship of the connector. Johnson and Molenstra (1991) indicate the lack of standard definitions of ultimate slip capacity, s_c, or slip under service loads, s_s, and a connector. The authors define the ultimate slip capacity as the slip at which the load falls to $0.95 \times Q_u$ on the descending branch of the load-slip curve. Other authors use $0.8 \times Q_u$ (Johnson and Molenstra 1991). Hegger *et al*. (2001) recommend designing for a low range of slip to obtain good performance of the composite girders under service loads. Those authors also discuss the advantages of the connector possessing a yield plateau for good and stable behavior, which allows for redistribution among the connectors (Hegger *et al*. 2001). They recommend limiting the slip at which the shear connector strength should be taken, s_c, to 6.0 mm (0.24 in.) (Hegger *et al*. 2001).

Many researchers argue that the provisions for shear connector design need a serviceability (stiffness) and a strength limit state. Topkaya (2002) performed push-out tests on ¾-in. diameter studs to obtain the behavior of the connector during the first hours and days after casting of the concrete. He proposes taking the design strength of the connector, Q_d, attained at 0.03 in. of slip, which corresponds to a slip equal to 1/25th of the stud diameter. He found that taking loads at slips 0.005-in. greater than and less than the design slip only alters the load by about 5 % on each side (Topkaya 2002).

As discussed in the section above, design slip is taken as 0.2 in. in this document. More discussion on the ultimate slip capacities obtained in laboratory experiments for static, high-cycle fatigue, and low-cycle fatigue is given in Sections 2.5.5, 2.6.4, and 2.7.4, respectively.

2.1.8 Low-Cycle Fatigue

Although the static and fatigue behavior of various shear connectors has been investigated since the 1950's, during the last decade, additional research has been performed to investigate low-cycle fatigue. Low-cycle fatigue is a concern in structures subjected to repeated loads and having a connection that deforms beyond the elastic range (Gattesco and Giuriani 1996). After the connector has undergone inelastic deformation [Figure 2.2(a)], if the girder is in the elastic range, as is typical, the structure returns to its original, undeformed position upon unloading [Figure 2.2(b)], with no residual slip at the steel-concrete interface. If the slip recovered by the girder returning to its original position is larger than the slip recovered by the connector to obtain zero force on the connector, the connector will be subjected to a shear in the opposite direction [Figure 2.2(c)] (Gattesco and Giuriani 1996). If the connector undergoes a large enough shear in the opposite direction to yield the connector again, the connector may fail after being subjected to only a few load cycles, as this "alternate plasticity" in the stud can occur at every cycle (Gattesco, Giuriani and Gubana 1997). Those authors point out that since very little research has been performed on this phenomenon, and it is difficult to obtain the behavior of individual studs in bridges due to redistribution, low-cycle fatigue is quite complex, and its seriousness is unknown.

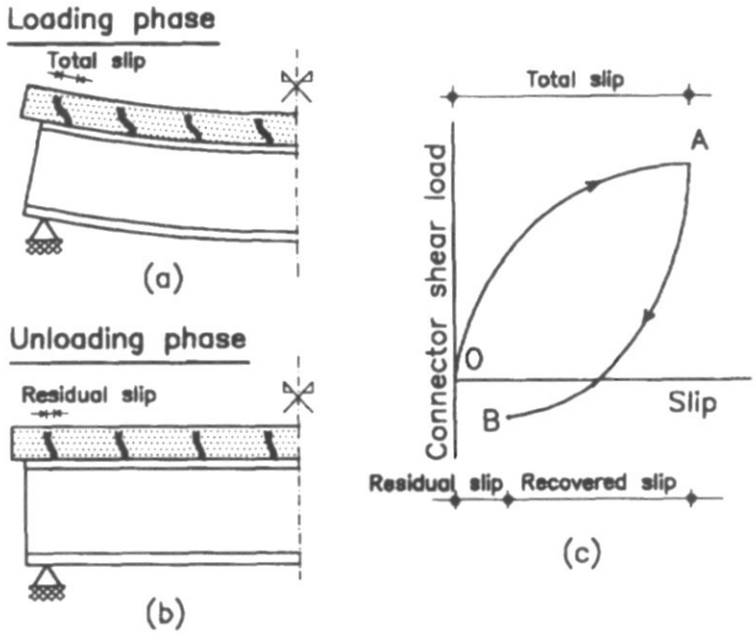

Figure 2.2: Low-cycle fatigue concerns (Gattesco and Giuriani 1996)

For a simply supported girder, shear studs near the supports are subjected to high shears and reversed loading, while the connectors close to midspan have low shears and are not subjected to reversed loading (Gattesco and Giuriani 1996). The reversed, inelastic loading is the cause of low-cycle fatigue failure. Gattesco and Giuriani (1996) demonstrated in three previous papers that the shear connectors carrying the most load can undergo reversed shearing during the unloading phase of the bridge. Moreover, the recovered slip can reach a value of about 50 % of the maximum slip. For very large ranges of load with reversed loading (over 10 % of the peak load), the incremental damage increases with every cycle (Gattesco and Giuriani 1996). This leads to incremental collapse, which is discussed in the next section.

The research performed by other researchers to investigate the behavior of welded studs under low-cycle fatigue loading conditions is described in Section

2.7. The effect of low-cycle fatigue on incremental collapse is discussed in the next section.

2.1.9 Incremental Collapse

Incremental collapse occurs when a collapse mechanism forms in the structure due to an aggregation of permanent deformation under the repeated application of live loads of high magnitude (Grundy and Taplin 2003). It can result in a structure becoming unserviceable through excessive deflections or in sudden collapse after the ductility of the shear connectors is exhausted (Grundy and Taplin 2003).

As discussed earlier, the stud connector transfers most of the shear between the concrete slab and steel girder at or near the root of the weld, creating a local crushed zone in the concrete. When the load on the connector reverses, as discussed in the section above, a gap can be created around the stud. As a result, the shear is transferred farther up the stud where the concrete is stiffer, resulting in more moment in the connector as the number of cycles increases. More slip occurs as the flexural forces on the stud increase. If the slip deflection continues to accumulate, the stud may fracture near the weld (Grundy and Taplin 2003).

Grundy and Taplin (2003) point out that classical theory of plasticity and laboratory tests (performed at Monash University in Melbourne, Australia over the past 30 years) demonstrate that a structure subjected to cyclic loads of high magnitude undergoes incremental collapse at a load level less than that required for static collapse under a single application of load.

Grundy and Taplin (2003) argue that incremental collapse is a serviceability limit state, since for ductile materials the static collapse is unaffected by a prior history of incremental collapse. They suggest that

incremental collapse is not a fatigue limit state because the shear connectors do not crack under service loads due to their ductility.

Incremental collapse of composite girders has been actively investigated since Grundy and Taplin (2003) performed tests on continuous girders composed of common structural materials (steel, reinforced and prestressed concrete, etc.). The authors report that for a continuous girder subjected to a moving patch load, theory predicts the results of tests quite accurately for all materials tested, except composite girders. For most materials, incremental collapse occurs at load levels of about 93 % of the ultimate static load, which can be predicted using plasticity theory. The effects of incremental collapse were seen by performing static tests after the cyclic tests. They report that fully composite girders, however, exhibit incremental collapse at loads as low as 53 % of the static strength. Due to asymmetry of the composite girder, Grundy and Taplin (2003) show that the static load capacity is significantly reduced (up to 23 % less than the load for static collapse for the girders tested in that experimental program) for low-cycle fatigue loading. They also show that an increase in slip at the steel-concrete interface under each load cycle, which is observed in experiments, could lower the capacity further. These points are discussed in more detail below.

The incremental collapse-to-static collapse capacity ratio varies from 0.53 to 0.69 in the tests performed on composite girders by Grundy and Taplin (2003) with an average of 0.61 based on seven tests. The general plastic theory predicts a ratio ranging from 0.94 to 0.98 with an average of 0.96 (Grundy and Taplin 2003). This shows that incremental collapse in composite girders occurs at lower loads than expected by general plastic theory.

Grundy and Taplin report that the deflection increases every cycle in approximately linear proportion to the amount by which the load exceeds the load at which no permanent deformation results. For the two-span girder tested, an

increase in the deflection of 0.1 mm every cycle would result in a permanent deflection of 20 mm, corresponding to span/200 for 200 cycles. In addition, if the incremental slip increases 0.002 mm per cycle, the permanent slip would reach 2.0 mm in just 1000 cycles. The authors warn that these are reasonable numbers for low-cycle fatigue loading and question the reliability of the girders under these limits, which are acceptable by today's standards (Grundy and Taplin 2003).

In the tests performed by Grundy and Taplin (2003), incremental collapse occurred with the formation of traditional plastic hinges and slip of the deck along the girder, preventing the cross-sections at the hinges from reaching the fully composite design strength due to slip. The two researchers report that the incremental collapse process is ductile until the connectors reach a large slip. Although only one of the seven of the test specimens failed by stud connector failure, it gives credence to the notion that incremental collapse is an ultimate limit state and also a serviceability limit state. The authors report that the ultimate limit state is preceded by evidence of distress (Grundy and Taplin 2003).

The three factors that reduce the static collapse beyond that calculated using general plastic theory, causing incremental collapse are (Grundy and Taplin 2003):

1) incremental collapse of a cross-section subjected to cyclic bending moment and axial force. This reduced the capacity to about 0.77 of static collapse in the laboratory experiments. (This was not considered in the general plasticity theoretical predictions.);
2) incremental collapse of continuous girders with slip of shear connection. This reduced the capacity to about 0.96 of static collapse. (This was considered in the theoretical predictions.); and

3) incremental slip of shear connectors. This reduced the capacity to about 0.85 of static collapse. (This was not considered in the theoretical predictions.).

First, classical plasticity theory predicts a reduction in the capacity of a cross-section subjected to repeated bending moment and axial force within the limits of static load capacity compared with monotonic loading to collapse (Grundy and Taplin 2003). This reduction phenomenon is particularly evident for monosymmetric cross-sections where the plastic neutral axis is offset from the elastic neutral axis, as in a composite girder (Grundy and Taplin 2003). This theory applies to materials with an infinitely ductile plastic plateau and an elastic unloading-reloading stress-strain relationship.

The second factor follows from the fact that slip at the steel-concrete interface of composite girders leads to a global collapse mechanism that reduces the load capacity of continuous girders (Grundy and Taplin 2003). As discussed in Section 2.1.2.3, slip occurs in composite girders regardless of the degree of shear connection. Even girders designed for full composite action can develop slip under repeated loading (Grundy and Taplin 2003). The effect of incremental collapse on the static collapse can be calculated, however, knowing the load-slip relationship of the connector (Grundy and Taplin 2003).

The third factor is a result of the growth in residual slip in the connector that occurs incrementally under each cycle. Taplin found that incremental slip occurs at virtually all levels of shear on the connectors (Grundy and Taplin 2003). Grundy and Taplin (2003) report that only a very small amount of increase in slip per cycle for low levels of applied shear permits the use of traditional fatigue assessment techniques without significant inaccuracy in the predictions. Gattesco and Giuriani (1996) report that incremental slip damage increases rapidly under each cycle for the blocks of cycles with a significant value of the reversed shear

(about 10 % of the peak load). The authors show that the increment of slip at the end of each cycle decreases to a constant value after the first few cycles. The increment of slip does not approach zero, however, suggesting that progressive damage occurs with each cycle. Gattesco and Giuriani (1996) report that damage occurs in the concrete in front of the connector and in the shank of the stud. The damage of the concrete mostly occurs in the first few cycles, while the stud shank deforms throughout the cyclic loading, explaining why the damage generally reduces to a constant value (Gattesco and Giuriani 1996). After the cyclic tests were complete, the specimens were tested to failure monotonically. The cyclic loading reduced the ultimate strength by almost 10 % and reduced the ultimate slip by about 30 % over the studs tested only monotonically (Gattesco and Giuriani 1996).

Grundy and Taplin assert that reversing the shear applied to the connector creates pinching in the load-slip relationship, resulting in an expanding loop that grows exponentially with the ratio of shear to static load capacity. This appears to occur at all load levels, with no lower bound (Grundy and Taplin 2003).

Grundy and Taplin have performed a significant amount of analysis to show that the large reduction in capacity due to incremental collapse is feasible, proving that it is not just an aberration of the tests. They are unclear, however, on how and to what extent the incremental growth in slip of the connector affects the general plasticity theory.

Grundy and Taplin show that the first two factors account for 83 % of the reduction in incremental collapse compared to static collapse for three test girders and 66 % for three other tests. They attribute the remainder of the reduction to incremental slip (Grundy and Taplin 2003).

Fortunately, Grundy and Taplin (2003) suggest that incremental collapse is not automatically a dominant or controlling limit state in practice. This is not to

say that incremental collapse should be ignored under high-magnitude, reversed cyclic loading, but only that it is not a concern for every bridge. Those authors note that the self-weight of the bridge is such a large component of the loading the bridge will experience that the cyclic applied shear is low, and normal fatigue-assessment techniques are satisfactory. The specimens test by Grundy and Taplin (2003) were relatively small, exacerbating the incremental collapse phenomenon. Incremental collapse must be considered significant, however, for short-span bridges (Grundy and Taplin 2003).

Grundy and Taplin indicate that little evidence exists in the bridge inventory that incremental collapse has caused any failures or even that static capacity has been exceeded causing any failure. They note that a large factor of safety (from 2 to 2.5) exists against collapse and incremental collapse is a concern when the loads approach the actual static capacity of the bridge. They warn, however, that load effects 40 % in excess of the design load occur and that a significant number of these overloads (between 50 and 5000) could lead to incremental collapse (Grundy and Taplin 2003).

2.1.10 Summary of Composite Action

Composite action was discussed in detail in Section 2.1, starting with general definitions commonly used by researchers on this subject. This section addresses general design considerations of composite action, and how to achieve it using a shear-transfer mechanism. The effect of tension, bending, and friction on the behavior of a welded headed stud was discussed because of its relevance to achieving composite action using shear connectors. Research on the probable maximum slip of the bridge at the steel-concrete interface was discussed along with several recommendations by researchers of the slip at which the shear connector design strength should be taken. Finally, the effects of a newly

researched area of the subject, low-cycle fatigue, is discussed. The findings of a field survey of bridges performed by the researchers to learn information on the condition of the bridges are discussed in the next section.

2.2 FAILURE MODES OF CONNECTION IN SHEAR

Three basic failure modes of the connection in shear exist (Klingner 2002):

1) connector steel failure in shear;
2) concrete cone breakout in shear; and
3) connector pryout.

2.2.1 Connector Steel Failure in Shear

Figure 2.3, taken from Klingner (2002), shows connector steel failure in shear, which involves bending of the connector leading to yielding and failure of the shank. This failure may exhibit shell-shaped spalling of the concrete ahead of the connector in the direction of the load. The spalling can occur prior to the maximum load being reached, increasing the deformation (slip) of the connector. Shear capacity is a function of the strength and cross-sectional area of the connector.

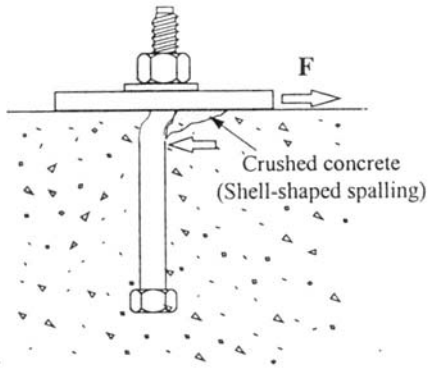

Figure 2.3: Connector steel failure in shear

2.2.2 Concrete Cone Breakout in Shear

Figure 2.4, taken from Klingner (2002), shows concrete cone breakout in shear, which often occurs near a free edge of the concrete member, and is most accurately predicted by the concrete capacity (CC) method as a function of concrete strength, edge distance, diameter, and effective embedment depth.

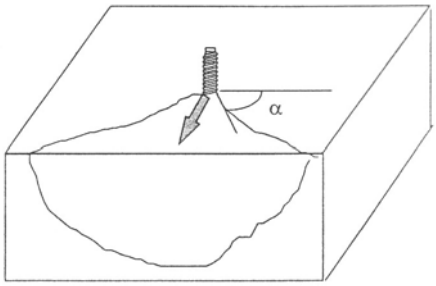

Figure 2.4: Concrete cone breakout in shear

2.2.3 Connector Pryout

Figure 2.5, taken from Klingner (2002), shows connector pryout, which consists of crushing of the concrete in front of the connector, as well as breakout of the concrete behind the connector opposite to the direction of loading. These concrete failures lead to connector pullout. Essentially, the connector rotates about the upper edge of the concrete closest to the applied load. This type of failure typically occurs with connectors with small embedment depths, at loads that can be estimated in terms of the tensile breakout capacity (Klingner 2002).

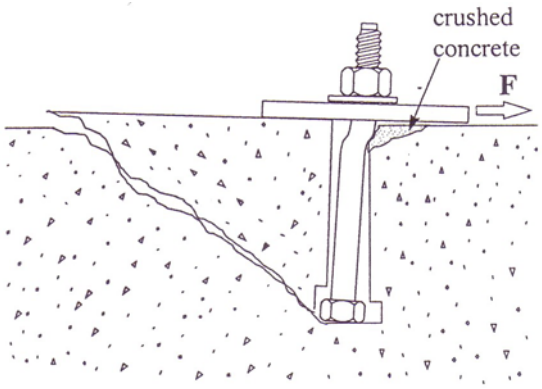

Figure 2.5: Connector pryout

2.3 RESEARCH ON WELDED HEADED STUD

The welded headed stud is the most-used, most-researched shear connector. The main findings of the research performed to date are discussed in this section. The typical test setup (the push-out test) and the more recent single-connector test, are discussed in Section 2.4.

The following bulleted definitions for static and fatigue loading conditions are commonly used in the field of composite girder design and shear connector research:

- "Pulsating load condition" is the condition in which the applied load is uni-directional; the load does not reverse, although it may reduce to zero and then be applied again (Nakajima *et al*. 2003).
- "Alternating load condition" is the condition of reversed cyclic shear (Nakajima *et al*. 2003).

Yamamoto *et al*. (2001) indicate that the main design factors for a new type of connector are:

1) embedment depth of connector;
2) diameter of connector shaft;
3) yield strength of connector; and

4) concrete compressive strength.

The selection of these parameters for the specimens used for testing in this project is discussed in Chapter 4 and Chapter 5.

It is well recognized that the shear-slip relationship of shear connections is generally nonlinear (Johnson and Molenstra 1991, Faella, Martinelli and Nigro 2003).

Increasing the size of the weld collar could improve the behavior of the stud (Hegger *et al*. 2001). Tests on connectors with larger than standard weld collars showed 10-percent higher strength and higher stiffness (Hegger *et al*. 2001). Hegger *et al*. (2001) note that actually increasing the size of the weld collar is difficult.

A potential disadvantage of the headed stud is that it requires welding to the top girder flange. The use of welded shear studs is questionable in some applications where the type and weldability of steel in the girders is unknown (Klaiber *et al*. 1983).

The following sections detail the major factors affecting the behavior of the welded headed stud.

2.3.1 Embedment to Diameter (H/d) Ratio

The ratio of the embedment depth (commonly called "height" because it often refers to welded headed studs, where the height of the stud equals its embedment depth) to diameter ratio is addressed in various codes. Tests have been performed by various researchers to investigate the minimum required H/d ratio. Most recently, Yamamoto *et al*. (2001) tested studs for a seismic retrofit application. They found large scatter in the shear stress data versus embedment depth, indicating that shear stress does not depend on embedment length (Yamamoto *et al*. 2001). When comparing the connector capacity versus

embedment depth, however, the data show that capacity can be increased when the embedment depth is over three times the diameter of the connector (Yamamoto *et al*. 2001). This shows that a minimum H/d ratio exceeding 3 is beneficial for post-installed connectors.

All specimens considered in creating the connector capacity design equation in the AISC LRFD (2001) and AASHTO (2002) provisions (discussed in Section 2.9) had an H/d ratio greater than 4, as recommended by previous tests (Driscoll and Slutter in 1961), since this is required if the full capacity of the connector is to be developed (Ollgaard, Slutter and Fisher 1971). For the experiments performed on this research project, an H/d ratio of 4 is targeted.

2.3.2 Diameter of Connector Tested

Almost all connectors are round, although a few exceptions are square in cross-section (Tadros, Badie and Girgis 2001). Most of the research performed on welded studs has used three different diameters: ½ in., ¾ in., and ⅞ in. It appears that most recently the ¾-in. stud is most prevalent. Topkaya (2002) chose the ¾-in. diameter, 5-in. tall stud because it is believed to be the most widely used in practice. Many other researchers have also used approximately ¾- x 5-in. stud connectors (Gattesco and Giuriani 1996, Hicks and McConnel 1996).

2.4 SETUPS FOR SHEAR TESTS

Several different types of test setups have been used to obtain the behavior of shear connectors. Girder tests, which most closely represent the bridge, were used in early research on composite design. In the late 1960's, the push-out test, which used only a few connectors, was common. Most recently, a single-connector, direct-shear test has been used to learn individual connector behavior.

In this section, two test setups are discussed;

1) multi-connector, push-out test; and

2) single-connector, direct-shear test.

Toprac (1965) shows that push-out tests could represent relatively accurately the behavior of welded headed studs upon comparing results to full-scale composite girders. An objective of the tests by Toprac (1965) is to determine if small-scale test results can be extrapolated to full-size girders in real bridges. Slutter and Fisher (1966) performed pilot tests using push-off tests, which are similar to the push-out test, except they use only one slab and one girder in the test setup. That is, the test setup nearly represents a bridge, with a concrete slab on top of a steel girder, connected with shear connectors. An axial load is applied to the concrete slab, however, that pushes off the concrete slab along the longitudinal axis of the structure, instead of applying gravity loads, like in a girder test. They compare the results of girder tests (gravity loads) and push-out (more precisely, push-off) tests and found them to closely correspond. They report that the push-out tests' mean results are approximately a lower bound of the girder tests. Thus, they decided to use push-out tests to observe more accurately the behavior of the shear connectors (Slutter and Fisher 1966).

Roberts and Dogan (1998) argue that push-out tests provide a conservative (lower-bound) estimation of stud strength due to the relatively high tensile forces induced in the studs, which lowers the shear capacity of the connectors, as discussed in Section 2.1.5. Although composite girder tests most accurately represent the behavior of a real bridge, several reasons are given by researchers to use a smaller, simpler push-out test:

1) Slutter and Fisher (1966) assert that the individual stud behavior cannot be determined when performing full-scale girder tests. Toprac (1965), however, shows that stud forces can be qualitatively evaluated using strain gauges placed on the steel girder under the connector.

2) Push-out tests are more economical because they use less materials, and require less testing equipment to test, than full-scale girder tests.

Taking the points listed above a step further, attempting to gather the "true" behavior of an individual connector in an economical manner, the single-connector test seems valuable.

A test that accurately simulates the behavior of a shear connector under cyclic loading is very important because small inaccuracies in modeling the behavior of the specimen can accumulate at each cycle leading to a different result after many cycles (Gattesco and Giuriani 1996). Those authors argue that the push-out test has shown some limitations and modeling inaccuracies which should be removed for subjecting a connector to a large number of cycles. Thus, a single-connector, direct-shear test has been used by researchers more frequently in the last decade (Gattesco and Giuriani 1996).

2.4.1 Multi-Connector, Push-Out Test

Johnson and Molenstra (1991) report that the load-slip curve obtained from a push-out test depends on the type of connectors, their spacing, the dimensions and reinforcement of the slab, the rib shape of any profiled sheeting used, the position of a connector within a rib, and the properties of the materials. Topkaya (2002) points out no standard procedure exists for push-out tests due to differences in test specimens, methods of casting, and test procedures. Eurocode 4 (1994) has several standard configurations for a push-out test. The most recommended configuration is shown in Figure 2.6, which is taken from a draft of Eurocode 4 (1994). As discussed in Section 2.5.1.1.1, significant scatter exists in the results from push-out tests. For instance, the concrete slabs and steel girder often separate in the direction normal to the interface before the ultimate capacity of the system is reached (Topkaya 2002). In addition, frictional forces at the base

affect the results (Topkaya 2002). Hungerford (2004) describes the shortcomings of the push-out test in detail.

2.4.1.1 Setup for Multi-Connector, Push-Out Test

Push-out tests are typically performed using a 2-slab, 1-girder setup with a W8x40 steel section using 4 welded shear studs per slab (8 studs total) (Thurlimann 1959). Some researchers have used 2 welded shear studs per slab (4 total) with 2 connectors in the transverse direction.

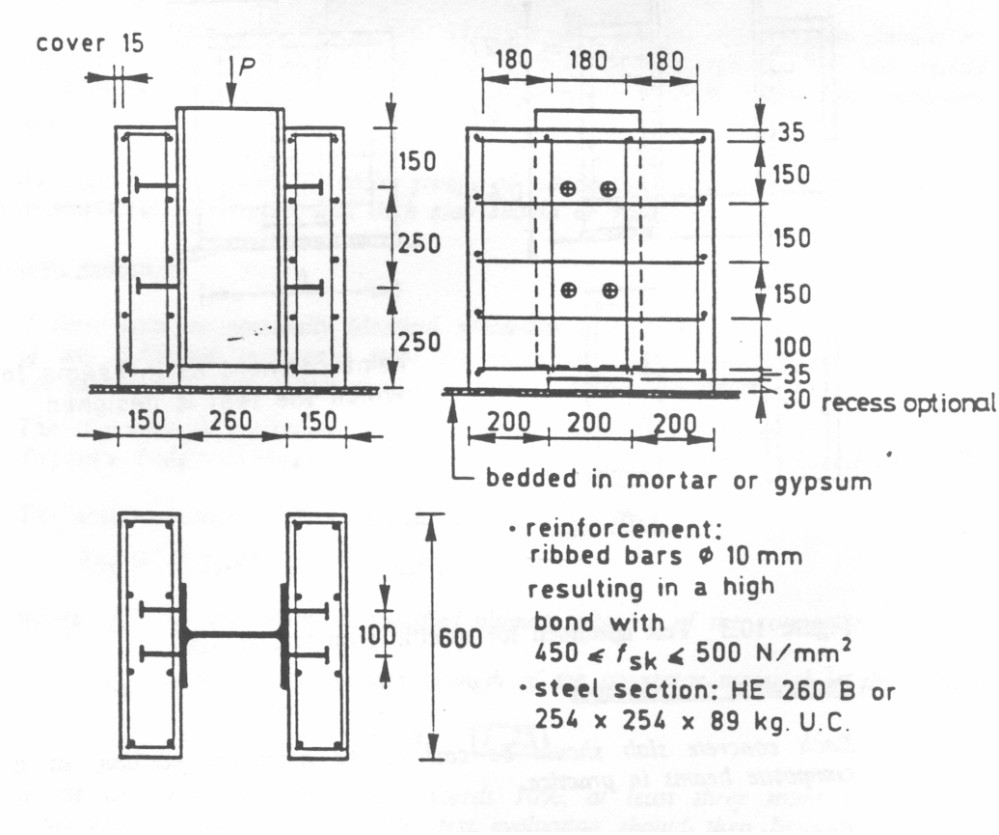

Figure 2.6: Push-out test configuration in Eurocode 4 (1994)

For cyclic load tests based on high-cycle fatigue, the fatigue endurance of the connectors is dependent on the applied stress range more than the magnitude of the peak load (Slutter and Fisher 1966). Gattesco and Giuriani (1996) point out

that tests are normally made using uni-directional cyclic loading so that the push-out test can be used.

Gattesco and Giuriani (1996) discuss several limitations of the push-out test. If the concrete blocks are fixed to the ground [Figure 2.7(a)], the observed shear capacities of the connectors are unrealistically increased due to the frictional force caused by the normal force, F_h, induced by the moment arm between the vertical reaction on the concrete block at the fixed connection and the shear on the connector. If rollers are used to allow sliding between the concrete blocks and the ground [Figure 2.7(b)], the moment caused by the vertical reaction and the shear on the connector is resisted in the concrete block, and therefore tension is still placed on the connector. Neither case accurately represents in the real structure (Gattesco and Giuriani 1996). Gattesco and Giuriani (1996) contend that only average values are obtained from the push-out test and it is impossible to obtain both the local slip and the shear of each connector with this type of test. Those authors warn that any local behavior of one connector, which may be important for the modeling of the shear-slip relationship under cyclic loads, would not appear in the push-out test.

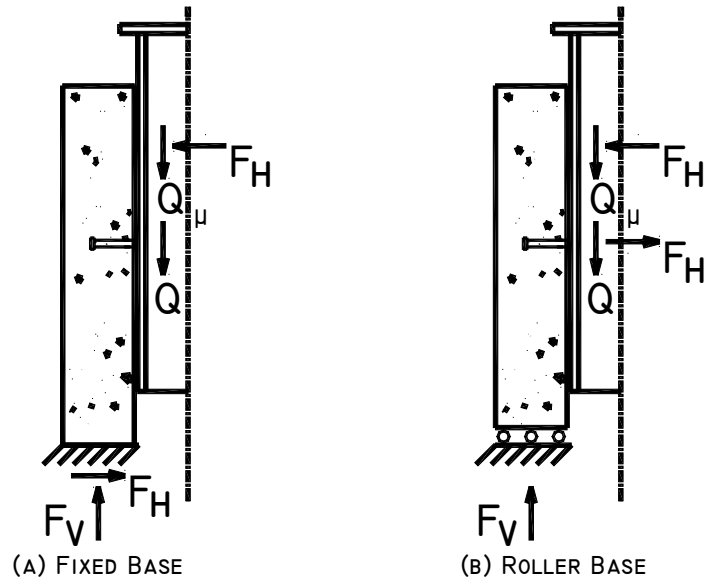

Figure 2.7: Concerns with push-out test [recreated from Gattesco and Giuriani 1996]

2.4.1.2 Typical Ranges of Measured Material Properties Used in Push-Out Tests

In general, the properties of the concrete and steel used by different researchers in push-out tests vary somewhat. Concrete strengths vary considerably, while the strength of the steel in the girder and connectors is fairly consistent, as described in the following sections.

2.4.1.2.1 Properties of Steel Stud Used in Push-Out Tests

The measured average ultimate tensile strength of a headed shear stud used in push-out tests is typically around 70 ksi, with a yield strength around 55 ksi based on a 0.2 % offset. Often, researchers only report either the measured ultimate tensile strength or the yield strength of the headed shear stud. The average ultimate tensile strength of the studs used by Ollgaard, Slutter and Fisher

(1971) is 70.9 ksi. The studs used in the experiments by Toprac (1965) have measured yield strengths of 54 and 57 ksi for the two studs tested and measured ultimate tensile strengths of 64 and 68 ksi respectively. The design specifications in the United States (AISC LRFD 2001, AASHTO 2002) are based on a specified minimum ultimate tensile strength of 60 ksi.

Yamamoto *et al*. (2001) show that the shear stress of the connector in a shear connector is proportional to the diameter of the connector, making it necessary to strengthen the shear strength of the connector when the steel diameter increases.

2.4.1.2.2 Properties of Concrete Used in Push-Out Tests

As mentioned above, the compressive strength of the concrete has varied for different experimental programs, and even sometimes within individual experimental program. Sometimes the variation is intentional, as with the research performed by Ollgaard, Slutter and Fisher (1971); other times, strengths vary from one specimen to another even using the same mixture design. The average cylinder strengths for each of seven girder specimens used by Toprac (1965) varied from 4150 psi to 5730 psi. Matus and Jullien (1996) use a fairly constant concrete strength of about 4300 psi. Most researchers have used concrete with a compressive strength of 4000 psi or higher. Very little research has been performed using concrete with a compressive strength as low as 3000 psi, as specified for a typical candidate bridge (Chapter 4), and is therefore used in the experimental program discussed in this thesis. The concrete used in a typical candidate bridge also has a specified 7-day tensile strength of 750 psi. To meet the specified tensile strength requirement, the concrete often can reach a compressive strength, fc, of 4500 psi after curing 28 days.

2.4.1.2.3 Properties of Steel Girder Used in Push-Out Tests

For the most part, research has been performed using wide-flange girders or two T-sections using A36 steel. Some researchers who have performed coupon tests on various locations of the steel section have reported typical variations between the flanges and the web.

2.4.1.3 Concrete Casting Direction

Slabs used in a push-out test can be cast in two directions: horizontally (as in a real bridge) or vertically (as in the typical vertical test setup shown in Figure 2.6). Slutter and Fisher (1966) cast the concrete for each specimen in the experiment horizontally onto a W8X40 A36 steel girder to mimic real procedures. Klaiber *et al*. (1983) cast the test specimens vertically so both slabs could be cast from the same batch of concrete, which reduces the variation in the strength of each of the concrete slabs. This advantage is typically cited by researchers who cast the specimens vertically usually in three lifts with thorough vibration after each lift (Klaiber *et al*. 1983). A disadvantage of casting specimens vertically, however, is that when using a cast-in-place shear connector such as a welded headed stud, it tends to introduce voids around the connectors that produce lower than expected strengths (Klaiber *et al*. 1983).

2.4.1.4 Reinforcement Used

Disagreement exists over the effect of the reinforcement on the results obtained in push-out tests. Since the concrete specimens are much smaller than the bridge floor slab that it represents, some feel that reinforcement is of minor or no importance. Johnson and Molenstra (1991) conclude, however, that higher strengths are obtained with wider slabs and more realistic reinforcement than in the standard test given by Eurocode 4 (1994).

Gattesco and Giuriani (1996) argue that the size of the concrete blocks is important in push-out tests because it influences the bearing capacity of the connection, noting that low ultimate capacities can be obtained for narrow slabs because cracking of the concrete involves the entire block.

Most researchers use several #3 and #4 reinforcing bars in the concrete slab specimens. Klaiber *et al*. (1983) used several #4 bars. In addition to the nominal amount of reinforcement, those researchers placed three #3 bars around the steel girder to hold it in place (one below the steel girder to hold it up, and two on the sides to hold it straight). The #3 bars were removed prior to testing. Thurlimann (1959) placed reinforcement similar to the reinforcement of a deck slab in an actual composite girder bridge.

Girder tests are usually performed using reinforcement representing that of a typical bridge. Toprac (1965) used #4 deformed bars spaced at 6-in. in the transverse direction, with #3 bars spaced at 12-in. in the longitudinal direction. He used two layers in each of the specimens with 1-in. cover on top and bottom, symmetrical about the web of the steel girder without any reinforcement directly above the web (Toprac 1965).

Based on the discussion above, it appears appropriate to design the reinforcing bar cage for test specimens to represent locations of reinforcement in existing (non-composite) bridges.

2.4.1.5 Number of Connectors Used Per Test

Johnson and Molenstra (1991) recommend that specimens have connectors at two or more different locations along the steel member to yield higher results in push-out tests. Most researchers who use the push-out test use eight connectors total (4 connectors per concrete slab specimen). Others, however, have used four connectors total (two in each slab) (Klaiber *et al*. 1983).

Nakajima *et al*. (2003) references the Japanese standard push-out test, which is similar to the setup used by Klaiber *et al*., in that it uses only four connectors instead of eight. The connectors are typically spaced at between 4 in. (Toprac 1965) and 6 in. (Klaiber *et al*. 1983) in the transverse direction.

Viest showed in 1956 that increasing the number of connectors per row influences the shear strength of each stud when the slab width and reinforcement are not changed (Ollgaard, Slutter and Fisher 1971). He concluded that the measured average connector strength increases as the number of studs in the transverse direction increases. Based on the results of one test using two connectors per slab rather than four, however, it does not appear that it makes a significant difference (Ollgaard, Slutter and Fisher 1971). Those authors point out that more reinforcement is available for each connector since the same reinforcement was used in every specimen. They note, however, that ultimate shear strength per connector does not increase for this type of specimen (Ollgaard, Slutter and Fisher 1971). They report that push-out specimens with either one or two rows of studs per slab exhibit the same average strength per stud (Ollgaard, Slutter and Fisher 1971).

2.4.1.6 Embedment

As mentioned in Section 2.3.1, typical embedment depth is four or more times the diameter of the connector, maximizing the capacity of the connector. Ollgaard, Slutter and Fisher 1971 used an embedment depth of 3 in. on a 6 in. thick concrete slab with ¾-in. headed studs, corresponding to four times the diameter of the connector.

2.4.1.7 Debonding

Topkaya (2002) shows that bond at the interface of the steel girder and concrete slab has a large influence on the initial stiffness of the studs. That author

recommends minimizing the natural bond (for example, using plastic sheets between the concrete and steel) to obtain conservative initial stiffness values. Other researchers have used a thin layer of wax at the steel-concrete interface to avoid bond and reduce friction (Gattesco and Giuriani 1996). Natural bond should be broken or eliminated because it is likely broken in a real bridge after only a few trucks have passed, as discussed in Chapter 1.

2.4.1.8 Foundation support (Boundary Conditions)

The support conditions of the two concrete slabs used in a push-out test have been a controversial issue of the test setup. Hicks and McConnel (1996) conclude that boundary conditions significantly influence the capacity of the shear studs. Moreover, Gattesco and Giuriani (1996) indicate the setup of the push-out test does not accurately simulate the actual behavior of the connector, since the boundary conditions of the concrete parts are quite different, as discussed in Section 2.4.1.1.

Figure 2.6 shows that the concrete slabs are typically set in mortar or on neoprene, resulting in a "fixed" boundary condition. Klaiber *et al*. (1983) used ¼-in. thick neoprene pads for uniform load distribution. Hicks and McConnel (1996) report that the push-out test using fixed boundary conditions exhibit capacities close to the resistances predicted by BS 5950 (1990). Generally, specimens with a British-style base condition [standard base, no recess (see Figure 2.6 for optional recess)], slightly underestimate the strengths predicted by BS 5950 (1990) by 10 %, while the German-style test configuration (with a recess) agrees with predicted strengths from BS 5950 (1990) more closely (Hicks and McConnel 1996). This suggests that code equations are consistent with the results of fixed-base tests.

Hicks and McConnel (1996) used "two-directional sliding bearings" on a standard push-out test, which allowed the concrete slabs to move in any direction in the horizontal plane. This resulted in the connectors failing at shears lower than predicted by both the BS 5950 (1990) and Eurocode 4 (1994) equations, even though the predicted failure mode was achieved in most cases. To ascertain the effect of the boundary conditions, Hicks and McConnel (1996) investigated various boundary conditions using an altered test setup.

Those authors conclude that the two-directional, roller-base condition does not accurately simulate the behavior of the shear studs obtained from a full-scale girder test because it causes increased separation between the concrete slabs and steel girder, resulting in high tension forces on the connector. They recommend this test setup for researchers who want to simulate the effects of high uplift forces on a bridge (Hicks and McConnel 1996).

Hicks and McConnel (1996) also tested "one-directional" bearings that only allowed movement lateral to the face of the slab of the specimen. This test setup appears not to induce any artificial friction forces in the transverse direction, and the results compare well with full-scale girder tests (Hicks and McConnel 1996).

2.4.1.8.1 Friction at the Base

Hicks and McConnel (1996) conclude that friction from the base in the transverse direction carries the majority of the load, based on strain-gage measurements. They conclude that frictional forces develop at the base of the slabs in the transverse direction increase the strength of the specimens by confining the connector and acting as additional transverse reinforcement in the British- and German-style push-out test setups (Hicks and McConnel 1996).

2.4.1.9 Applied Preload

Typically, a preload of about 10 % of the anticipated maximum capacity is applied to seat the specimens and ensure a uniform load distribution (Klaiber *et al*. 1983).

2.4.1.10 Testing Procedures

Most researchers test three replicates of each configuration to assess variability (Ollgaard, Slutter and Fisher 1971). Most tests are performed monotonically, although some researchers alternate the load. Alternating static tests consist of fully reversing loading cycles up to the peak load, and increasing the peak load at each cycle up to failure of the specimen (Nakajima *et al*. 2003). The load increment often ranges between one-tenth and one-fifth the anticipated ultimate load (Nakajima *et al*. 2003).

2.4.1.11 Measuring Slip

In the standard push-out test, slip is typically measured using four dial gauges or electronic displacement transducers. Thurlimann (1959) reports that the difference in the readings between individual dial gages is typically about 20 %, but could be as large as 100 % for static testing. He warns that a considerable variation in the readings must be expected for individual slip readings (as high as 100 %). Typically, the four readings are averaged to obtain the load-slip curve (Klaiber *et al*. 1983).

2.4.1.12 Measuring Separation

Cook (1977) indicates that almost every design specification recognizes that the concrete deck tends to separate from the steel girder under some types of loading. He reports that a concentrated load at midspan often causes a visible loss

of bond at the girder ends at relatively low load levels in bonded-aggregate composite girder tests.

In contrast, Viest *et al*. (1997) document that the effect of uplift is small for point loads. Some uplift exists at the supports for a point load acting on the slab. Also, large uplift exists below the loading point (Viest *et al*. 1997). In addition, immediately adjacent to these uplift regions, smaller regions of negative uplift exist (Viest *et al*. 1997). This is similar to the effect of friction reported by Oehlers, Seracino and Yeo (2000) discussed in Section 2.1.6, which gives credence to both observed phenomena.

Some researchers have measured the separation of the concrete slabs and steel girder. Klaiber *et al*. (1983) recommend that separation between the slab and girder be less than half the interface slip at the corresponding load level. Each of the specimens tested by those researchers met this criterion. Matus and Jullien (1996) show that after 25 load cycles, the slip is only 0.25 mm, and a separation of 0.06 mm exists between the slabs and the steel flanges. An and Cederwall (1996) measured a separation ranging from 0.4 to 1.3 mm (0.016 to 0.051 in.) in both normal- and high-strength concrete tests.

2.4.1.13 Type of Failure of Connectors or Concrete Specimen

In general, failure in push-out tests is observed by shearing of the connector (either above the weld or in the girder flange), preceded by tensile cracking of the slab (Klaiber *et al*. 1983). Some specimens fail by cracking or splitting of the concrete.

2.4.1.14 Advantages of Multi-Connector, Push-Out Tests

Matus and Jullien (1996) point out that the push-out test is often used because it is simple, costs less than a full-scale girder test, and is easier for measuring the load on a connector. It is the most widely used test for shear

connectors around the world. Gattesco and Giuriani (1996) point out that the push-out test captures the group effect of the eight connectors and reduces the scatter of the results. While this may be good for connectors used in bridges designed for full composite action, retrofit projects like the one described in this thesis, in which relatively few connectors may be used (if an exception for partial composite design is allowed by AASHTO), the variation in the behavior of individual connectors is important.

2.4.1.15 Disadvantages

As discussed before, the standard push-out test has several limitations:

1) Tension is induced in the connector. Many researchers have witnessed a gap between the concrete slabs and steel girder during testing (Nakajima *et al*. 2003). Nakajima *et al*. (2003) acknowledge that tension exists, but do not explain how much. Based on the numerical analysis performed by those researchers, it appears that the stud yields at the extreme fiber near the weld at very low levels of applied shear.
2) Unless multiple hydraulic loading jacks are used in a synchronized system, the push-out test can be performed only monotonically in most cases. Nakajima *et al*. (2003) point out that for this reason, little research has been done under reversed cyclic loading, which is important for low-cycle fatigue.
3) The sensitivity of the boundary conditions, and the effect of friction at the base of the concrete slabs has been shown to lead to inaccurate results (Gattesco and Giuriani 1996, Hicks and McConnel,1996).

By testing one connector at a time, the behavior of an individual connector and the surrounding concrete is more clearly defined, as discussed in Section 2.4.2. In addition, the research project reported in this thesis addresses more than

ten different post-installing shear-connection methods, so installing the eight connectors required in a push-out test would be very cumbersome.

2.4.2 Single-Connector, Direct-Shear Test

Gattesco and Giuriani (1996) used a single-connector, direct-shear test to obtain detailed information about connector behavior and to remove some limitations of the push-out test. They needed a test that could simulate as confidently as possible the actual behavior of studs under reversed cyclic loading. To that end, they proposed and described in detail a direct-shear test. Those researchers performed two pulsating static load tests and two alternating fatigue tests using the proposed single-connector, direct-shear test setup (Gattesco and Giuriani 1996).

Hegger *et al*. (2001) report results of tests designed to quickly investigate one stud at a time. Six connectors tested in a single-connector test setup exhibited 10- to 20-percent higher capacity than results from a push-out test (Hegger *et al*. 2001).

Nakajima *et al*. (2003) used a double-connector, direct-shear test. The tests were performed vertically, the plate had a stiffener, and the concrete block was sandwiched between two plates in the direction of the applied shear. The paper written by Nakajima *et al*. (2003) is an extension of work performed by previous researchers, attempting to capture the behavior of the welded stud under all four possible load conditions (pulsating and alternating, static and fatigue loading). Although several researchers (Yamanobe *et al*. 2001, Gattesco and Giuriani 1996) have performed alternating loading tests on connectors under static and low-cycle fatigue conditions respectively, Yamanobe's test setup requires two pairs of hydraulic jacks, while Gattesco and Giuriani did not perform pulsating

fatigue tests (Nakajima *et al*. 2003). The test setup used by Nakajima *et al*. (2003) is nearly identical to the setup proposed in this thesis in Chapter 4.

Yamamoto *et al*. (2001) used a single-connector, pulsating direct-shear test on their proposed shear connectors. Zhang, Klingner and Graves (2001) performed research on mechanical anchors using a single-connector, direct-shear test. They contend that connectors exhibiting good performance when tested individually in a single-connector test will also exhibit relatively good performance in a multiple-connector test. They also contend that connectors that show relatively poor performance when tested individually will also show relatively poor performance in multiple-connector tests (Zhang, Klingner and Graves 2001).

2.4.2.1 Typical Ranges of Measured Material Properties Used in Single-Connector, Direct-Shear Tests

For the most part, the material properties used in the single-connector tests have been similar to those used in push-out tests, although the ranges in the properties are narrower because fewer tests have been performed using single-connector, direct-shear setups. The single-connector tests do not use steel girders, but instead use a plate that represents the girder flange.

2.4.2.1.1 Properties of Steel Stud Used in Single-Connector, Direct-Shear Tests

Nakajima *et al*. (2003) used a steel stud with a yield strength of about 53 ksi. Gattesco and Giuriani (1996) used steel with a yield strength of about 50 ksi and an average ultimate tensile strength of about 70 ksi.

2.4.2.1.2 Properties of Concrete Used in Single-Connector, Direct-Shear Tests

Although many fewer tests have been performed using a single-connector test setup, the compressive strength of concrete has ranged from about 5000 psi to 6000 psi. Nakajima *et al*. (2003) tested two different concrete strengths: 6300 psi and 5800 psi. Gattesco and Giuriani (1996) used concrete with a cube compressive strength of about 4700 psi. To the author's knowledge, no single-connector tests have been performed using concrete with a compressive strength of 3000 psi, as would be found in the typical candidate bridges (Chapter 4). Recall that few researchers have used concrete with a compressive strength of 3000 psi in push-out tests, either.

2.4.2.1.3 Properties of Steel Plate Used in Single-Connector, Direct-Shear Tests

None of the researchers using a single-connector, direct-shear test cited in this thesis (Gattesco, Giuriani and Gubana 1997, Gattesco and Giuriani 1996, Nakajima *et al*. 2003) report a measured average ultimate tensile strength or yield strength of the steel used for the plate that represents the girder flange. It does not appear that the strength of the steel used in the plate is significant in the behavior of the shear connector.

2.4.2.2 Measuring Slip

As with the push-out tests, the relative displacement between the steel and concrete is measured in the direct-shear test. This is normally accomplished with electronic LVDTs or other electronic displacement transducers (for example, Nakajima *et al*. 2003).

2.4.2.3 Using Strain Gages to Evaluate Behavior of Stud

Several researchers have also used strain gages at the midheight of the shank of the stud to observe the strain behavior of the studs quantitatively

(Nakajima *et al*. 2003). This is not the same as measuring the strain on the girder flange under the connector, as used by Toprac (1965) to obtain the qualitative behavior of individual connectors.

2.4.2.4 Stiffening Plates

The steel plate representing the girder flange is stiffened by another longitudinal steel plate welded on the other side typically (to create a T-section, so that the loaded plate does not buckle or bend during the application of the load (Nakajima *et al*. 2003). A slender plate cannot handle the compressive forces applied for reversed cyclic loading, which tests using this setup have typically investigated.

2.4.2.5 Effect of Prestressing Block

Since the size of the concrete specimen is relatively small for a single-connector test, some researchers have prestressed the block to prevent premature cracking. For example, Gattesco and Giuriani (1996) prestressed the concrete block with a force approximately equal to the maximum force applied for the shear test, to prevent any transverse cracks. The prestressing bars create a strut and tie system to prevent cracking (Gattesco and Giuriani 1996).

Gattesco and Giuriani (1996) report that the horizontal and vertical prestressing ties influence the stud resistance less than 0.5 %. The maximum tensile force in the vertical ties is estimated to be less than 10 % of stud capacity, so that its effect to local concrete deformation around the stud can be neglected (Gattesco and Giuriani 1996).

The results of the experiments performed by Gattesco and Giuriani (1996) show that the single connector produces limited stresses in the concrete block. No macroscopic cracks developed until failure of the specimen. Therefore, the width of the concrete block used in single-connector, direct-shear tests is of minor

importance (Gattesco and Giuriani 1996). In the opinion of this author, however, cracking of the concrete is possible and may influence the slip. This is a reason not to prestress the specimen and to allow the passive reinforcement to behave as it would in the field. This is also a reason to make the size and spacing of reinforcing bars the same in an experimental specimen, as would be found in the field.

2.4.2.6 Reinforcement Used

Nakajima *et al*. (2003) used four 10-mm deformed bars in the longitudinal direction and two 6-mm stirrups spaced 200 mm (7.875 in.) apart to protect the premature cracks in the concrete block.

Hegger *et al*. (2001) show that providing more transverse reinforcement than the nominal amount in push-out specimens allows the load to increase after first yield, whereas using little or no reinforcement produces a flat plateau in the load-slip relationship after first yield. Thus, it is possible that a large amount of transverse reinforcement can cause load-slip behavior to deviate from that of the standard push-out test, which typically shows a plateau after yield.

2.4.2.7 Results

Gattesco and Giuriani (1996) compare their test results from two monotonic tests with results obtained using a standard push-out test, and found good agreement. As pointed out above, the compressive strength of the concrete is around 4700 psi. This is very close to that used by previous researchers, such as Ollgaard, Slutter and Fisher (1971), who used concrete with an average compressive strength of 4200 psi, although a large range of strength exists for the 48 specimens tested. Note that these strengths are above the specified compressive strength of the concrete (3000 psi) in a typical candidate bridge (Chapter 4).

Gattesco and Giuriani (1996) also report that the load-slip curves for monotonically loaded specimens exhibit very similar behavior to those obtained by other researchers. This suggests that although Gattesco and Giuriani proposed the single-connector, direct-shear test for fatigue loading, it could also be used for static tests.

2.4.3 Summary of Setups for Shear Tests

In this section, the setup and testing procedures commonly used by researchers to obtain the load-slip behavior of shear connectors (the multi-connector, push-out test and the single-connector, direct-shear test) were described. The effects of reinforcement, bond, embedment depth, material properties, and boundary conditions were discussed. Advantages and disadvantages of the multi-connector, push-out test were highlighted. An introduction to the single-connector, direct-shear test was given. Hungerford (2004) discusses the two test setups in detail. The results of experiments performed using each setup are discussed in the next four sections. The three strength limit states of the bridge (static, high-cycle fatigue, and low-cycle fatigue) are discussed. The findings of research performed on mechanical connectors are also discussed, as they are relevant to this project

2.5 STUD BEHAVIOR UNDER STATIC LOADING

Hungerford (2004) addresses the behavior and design of shear connectors under static loading. It is appropriate, however, to discuss some general characteristics here as well.

Although many researchers have investigated the static strength of the headed stud since the 1950's, perhaps the most extensive research on the static behavior of the headed stud was performed by Ollgaard, Slutter and Fisher (1971). They looked at the effect of the compressive and tensile strength, density,

and modulus of elasticity of the concrete, the diameter of the stud, the aggregate type and the number of connectors per slab in a standard push-out test (described in Section 2.4). Although their work is extensive, it does not investigate the strength or modulus of elasticity of the stud, the slab reinforcement, or geometry. Johnson and Molenstra (1991) investigated the effect of the strength and modulus of elasticity of the stud on the static capacity of the connector and found it to be influential. An and Cederwall (1996) investigated the effect of the slab reinforcement and found it to be important. They report that two layers of reinforcement give slightly higher (6 %) connector capacities in normal-strength concrete. They report that the reinforcement does not carry much load, but confines the concrete surrounding the studs (An and Cederwall 1996).

2.5.1 Results of Static Tests

The results of the static tests can be divided into two categories:

1) strength (ultimate, yield, design); and
2) stiffness (initial, plateau).

2.5.1.1 Strength of a Shear Connection Using a Welded Stud

Many design equations have been developed to estimate the ultimate static strength of the welded headed stud. Different researchers have found different variables to be influential on the static strength, as discussed in Section 2.5. Ollgaard, Slutter and Fisher (1971) created an equation strictly based on the concrete properties and the cross-sectional area of the stud. They report that the concrete exhibits substantial inelastic deformation before failure. Ollgaard, Slutter and Fisher (1971) conclude that the concrete is the controlling medium, based on the observed behavior at ultimate load. They produced Equation 2.17:

$$Q_u = 1.106 \times A_s \times f'_c{}^{0.3} \times E_c{}^{0.44} \qquad \textbf{(2.17)}$$

Where: Q_u = ultimate strength of connector, kips;

A_s = cross-sectional area of headed stud, in.^{2};

f_c' = specified compressive strength of concrete, ksi; and

E_c = elastic modulus of concrete, ksi.

Table 2.4 gives the static capacity for a ¾-in. diameter connector embedded in concrete with a compressive strength of 3000 psi for the equations given in this section. The equation given above has a coefficient of correlation of 0.89. Ollgaard, Slutter and Fisher (1971) report that the other investigated concrete properties (density and tensile strength) improve the coefficient of correlation only to 0.90. The AISC LRFD (2001) and AASHTO (2002) design provisions have adopted a simplified equation, using the same variables:

$$Q_u = 0.5 \times A_s \times \sqrt{f'_c \times E_c} \qquad \textbf{(2.18)}$$

Consistent units must be used; in this document, US customary units are used. Rounding off the coefficients to obtain the code equation reduces the coefficient of correlation less than 1.7 % for the 48 two-slab push-out tests performed by those authors (Ollgaard, Slutter and Fisher 1971). When comparing the data to ten other literature sources, the coefficient of correlation decreases 18 % to 0.72, and the standard error of estimate increases 90 % to 8.46 ksi based on Q_u/A_s (Ollgaard, Slutter and Fisher 1971).

Those researchers obtained the modulus of elasticity of the concrete by calculating the slope of the stress-strain curve. Comparing the values used for the elastic concrete modulus, E_c, obtained from the stress-strain curve to the calculation given by $57 \times \sqrt{f_c}$, shown in Table 2.3, it can be seen that while a few specimens show close correlation, most are far below the calculation, and some as low as half of the predicted value. This is important, because the values commonly used in design are based on $57 \times \sqrt{f_c'}$. The predicted values are

higher (they are an average of 15 % higher than tested values for the normal-weight concrete; using $33 \times w^{1.5} \times \sqrt{f_c}$ reduces the margin down only to 14 %, implying the density approximation is sufficient), the calculated connector strength will also be too high. Calculating connector strength using the $57 \times \sqrt{f_c}$ expression, the values increase by an average of 6.1 % for the normal-weight concrete specimens. Using the equation used in AISC LRFD (2001) and AASHTO (2002), connector strength is underestimated by an average of 9.6 % compared with the results from the stress-strain curve.

Table 2.3: Comparison of modulus of elasticity calculations

Concrete Density (pcf)	f_c (psi)	Measured E_c (ksi)	E_c based on $57 \times \sqrt{f_c}$ (ksi)	E_c based on $33 \times w^{1.5} \times \sqrt{f_c}$ (ksi)
148.1	5080	3740	4060	4240
147.6	3640	3510	3440	3570
147.4	4010	3580	3610	3740
140.5	4780	3180	3940	3800
138.6	2670	2190	2950	2780
142.6	4030	3170	3620	3570
140.5	4780	3180	3940	3800
89.1	4690	1510	3900	1900
108.2	4280	2060	3730	2430
99.2	4720	2430	3920	2240
113.4	4920	2530	4000	2800
97.7	3600	1840	3420	1910
111.1	4300	2190	3740	2530
111.4	3220	1880	3230	2200
112.3	4000	2060	3610	2480
111.1	4400	2210	3780	2560

Ollgaard, Slutter and Fisher (1971) conclude from a plot of Q_u/A_s versus $\sqrt{f_c \times E_c}$ used to derive the equation that an upper bound to the connector strength is approached when $\sqrt{f_c \times E_c}$ is about 130, as the test data tend to plot along a horizontal line. Since this corresponds to a value of Q_u/A_s of about 65 ksi, they conclude that the cap is related to the ultimate tensile strength of the connector. This led to capping Equation 2.17 and Equation 2.18 with Equation 2.19:

$$Q_u \le A_s \times f_u \qquad \textbf{(2.19)}$$

Where: f_u = ultimate strength of the stud material.

The ultimate strength of the connector material used in the tests, f_u, is 70.7 ksi, suggesting Q_u equal to $0.92 \times A_s \times f_u$ would be a more reasonable cap [see Equation 2.21 and Equation 2.22. It appears the cap is closer to 62 ksi, resulting in Q_u equal to $0.88 \times A_s \times f_u$. Either way, it does not seem conservative to use Q_u equal to $1.0 \times A_s \times f_u$.

Ollgaard, Slutter and Fisher (1971) witnessed no sudden failure at ultimate load, and observed a descending branch on the load-slip curve before failure. Failure either occurred by shearing off the studs or failure of the concrete slab.

As mentioned above and in the previous chapter, research has been performed on welded headed studs since the 1950's. In 1956, Viest suggested Equation 2.20 (in a slightly different form) to predict connector capacity:

$$Q_u = 930 \times d^2 \times \sqrt{f'_c} \qquad \textbf{(2.20)}$$

The variables are the same as those listed above except the units are lb and in. for this equation. Ollgaard, Slutter and Fisher (1971) found their results to be far below the capacities predicted by Equation 2.20, implying that it is grossly unconservative. This equation was used in the AASHTO provisions as late as 1977 (Cook 1977). For a ¾-in. stud embedded in 3000-psi concrete, Equation 2.20 gives a value about 33 % higher than the controlling equation used in the code today (Equation 2.18). Ollgaard, Slutter and Fisher (1971) note that the early equation is based on a compilation of limited data taken from several sources who used different experimental techniques and allowed other uncontrolled variables that contributed to the higher values predicted by the equation for girder and push-off tests. They note that the equation is intended only for use with concrete strengths below 4000 psi (Ollgaard, Slutter and Fisher 1971).

Different equations for shear-connector strength are used in codes throughout the world. In the United Kingdom, for instance, BS 5950 (1990) and Eurocode 4 (1994) are used for the design of shear connectors in concrete slabs (Hicks and McConnel,1996). Eurocode 4 (1994) uses Equation 2.21, with a cap similar to that used in the AISC LRFD (2001) and AASHTO (2002) design standards:

$$Q_u = 0.29 \times d^2 \times \sqrt{f'_c \times E_c} \leq 0.8 \times A_s \times f_u \qquad \textbf{(2.21)}$$

Consistent units must be used. Hicks and McConnel (1996) indicate that the first expression in Equation 2.21 is based on the work of Ollgaard, Slutter and Fisher (1971). The second expression in Equation 2.21 is the limitation based on the stud material for stronger concretes (Hicks and McConnel 1996). Both expressions give values about 25 % lower than the respective US expressions (Equation 2.18 and Equation 2.19).

Hicks and McConnel (1996) report that the predicted connector strength based on the method given by Eurocode 4 (1994) is 10 % lower than that of BS 5950 (1990) because Eurocode 4 uses the lower 5 % fractile resistance rather than a value closer to the mean.

Eurocode 4 (1994) grossly underestimates load-bearing capacity for eighteen standard push-out tests on welded headed studs in high-strength concrete (Hegger *et al*. 2001, An and Cederwall 1996). Eurocode 4 (1994) may not apply to full and partial shear connection in high-strength concrete, because of those tests (Hegger *et al*. 2001). In addition, An and Cederwall (1996) show that a stud connector is not nearly as ductile in high-strength as in normal-strength concrete. They show a sharp drop in the load-slip curve after maximum load. The research discussed in this and Hungerford's (2004) theses uses concrete with a relatively low compressive strength of 3000 psi.

Yamamoto *et al*. (2001) used Equation 2.22 and Equation 2.23, presumably taken from the Japanese code:

$$Q_u = 0.4 \times A_s \times \sqrt{f'_c \times E_c} \le 0.7 \times A_s \times f_y \qquad \textbf{(2.22)}$$

The first term of this equation is 20 % lower than the corresponding term of Equation 2.18, which is used in the AISC LRFD (2001) and AASHTO (2002) provisions. The second expression is 30 % lower than the strength cap of Equation 2.19.

The equations given so far have been functions of only the concrete properties and the diameter of the stud (excepting the cap equations). Oehlers and Johnson (1987) propose a simple expression for mean connector strength that also accounts for the constitutive properties of the steel:

$$Q_u = 5.0 \times A_s \times f_u \left(\frac{E_c}{E_s}\right)^{0.4} \times \left(\frac{f_{cu}}{f_u}\right)^{0.35} \qquad \textbf{(2.23)}$$

Where: E_s = modulus of elasticity of steel stud; and

f_{cc}' = specified cube compressive strength of concrete.

Consistent units must be used.

Johnson and Molenstra (1991) suggest Equation 2.24, which is based on the concrete and steel strength and stiffness:

$$Q_u = \left(4.1 - N^{-0.5}\right) \times \left(\frac{\pi * d^2}{4}\right) \times \left(\frac{E_c}{E_a}\right)^{0.4} \times {f_{cu}}^{0.35} \times {f_u}^{0.65} \qquad \textbf{(2.24)}$$

Where: N = number of studs in shear span.

Units of Q_u come from A_s and f_u. The other units do not matter.

Topkaya (2002) suggests Equation 2.25:

$$Q_u = 2.5 \times A_s \times (f'_c \times E_c)^{0.3} \qquad \textbf{(2.25)}$$

Topkaya (2002) also recommends a design strength based on yielding of the connector, changing the leading coefficient from 2.5 to 1.75.

Table 2.4: Predicted static capacity of ¾-in. connector in 3000-psi concrete

Equation	Q_u (kips)	Source
Equation 2.17	23.4	Ollgaard, Slutter and Fisher (1971)
Equation 2.18	21.4	AISC (LRF 2001) / AASHTO (2002)
Equation 2.19	26.5	Cap on AISC (LRF 2001) / AASHTO (2002)
Equation 2.20	28.7	Viest in 1956 (1977 AASHTO and prior)
Equation 2.21	15.8	Eurocode 4 (1994)
Equation 2.22	17.1	Japanese Code
Equation 2.23	19.1	Oehlers and Johnson (1987)
Equation 2.24	15.6	Johnson and Molenstra (1991)
Equation 2.25	17.2	Topkaya (2002)
Equation 2.25	12.0	Design Load, Topkaya (2002)

Notice from Table 2.4 that the code and research equations used around the world vary greatly, with the US specifications (AISC LRFD 2001, AASHTO 2002) predicting the largest values.

Equations previously presented in this section are derived from monotonic tests. Based on the work of Nakajima *et al*. (2003), the load-slip behavior is different for alternating-load tests. The alternating loading has a lower ultimate capacity and increases the slip for a given load as more cycles are incurred because a gap opens around the root of the weld. Nakajima *et al*. 2003 assert that the pulsating static test resembles a standard push-out test or a single-connector static direct-shear test.

Nakajima *et al*. (2003) report that mean maximum shear strength under pulsating load condition is about 25 % larger than under alternating load. These

findings demonstrate that low-cycle fatigue is affected by alternating loading (Nakajima *et al*. 2003).

Equation 2.17, Equation 2.18, and Equation 2.19 give the maximum static shear capacity of the connector. Ollgaard, Slutter and Fisher (1971) also derived an empirical expression for the shear-slip relationship:

$$Q = Q_u \times \left(1 - e^{-18\times\Delta}\right)^{2/5} \qquad \textbf{(2.26)}$$

Where: Q = shear;

Q_u = ultimate strength of connector; and

Δ = slip of connector.

This equation has a vertical slope at zero load. This was observed by Ollgaard, Slutter and Fisher (1971) in the load-slip curves due to the bond between the concrete slab and the steel girder. For a slip equal to 0.2 in., the equation predicts loads of 99 % of the ultimate load. As mentioned in Chapter 1, however, bond may be lost in a bridge after only cycles of service load. Therefore, it is believed that Equation 2.26 overestimates the initial stiffness of the connector. Since many researchers use it, it is believed much of the literature may overestimate the initial stiffness of the connector.

Ollgaard, Slutter and Fisher (1971) conclude that the deformed shape of the studs is different in normal-weight and lightweight concrete specimens, citing that the normal-weight provides more restraint. In normal-weight and lightweight concrete, the studs rotate through a large angle at the weld, and the concrete in front of the studs crushes.

2.5.1.1.1 Variations from Predicted Connector Capacities

As the section above shows, a great deal of variation exists in the expressions used to estimate the capacity of a connector. Also a great deal of variation exists within the tests performed to derive the design expressions.

Typically, the ultimate strength is the only property for which sufficient data are available to calculate and compare results. Many researchers exclude many low results attributable mainly to premature splitting that arises from the type of push-out test used (Johnson and Molenstra 1991). By excluding low results, however, valuable information may be lost. Consistently, the results contain a great deal of variation; for example data fall both well above and well below the predicted values given by Equation 2.17.

Thurlimann (1959) indicates that the loading rate affects the capacity of the specimen and suggests that little significance should be attributed to the ultimate strength of the connector. At that time, the AASHO (1961) design code limited the capacity of the connectors below a point in which the connectors yield, as discussed in Chapter 1, making the ultimate strength of the connector inconsequential. Given that the loading rate required to significantly increase the observed strength of steel is about 100,000 micro-strain, and that modern design approaches address elastic behavior, Thurlimann's 1959 suggestion is less valid today.

Looking at the data points used in the regression analysis performed to obtain Equation 2.17, a majority of points for ¾-in. diameter studs fall below the predicted values (about 30 out of 50). Most of these low points are in specimens using lightweight concrete, but several tests results using normal-weight concrete fall well below the respective predicted value. Ollgaard, Slutter and Fisher (1971) report that the tests showed a high variation in the ultimate strength of the shear connectors.

Ollgaard, Slutter and Fisher (1971) argue that the ultimate loads obtained from the tests of push-out specimens provide a lower bound to the strength of connectors in girders, although this point is contested by other researchers and by empirical evidence, as discussed below.

Klaiber *et al*. (1983) report the results of three benchmark tests performed on cast-in-place welded studs with ratios of predicted to observed strengths of 1.10, 1.08, and 1.01. Although some variation exists, and the results are unconservative, the authors conclude the experimental data closely match the expected values (Klaiber *et al*. 1983).

Topkaya (2002) reports larger scatter in test results for specimens cured for longer times. For example, specimens tested four hours after casting have relatively small scatter in the results, while specimens tested at eight and thirteen hours of curing exhibit larger scatter in the results.

Yamamoto *et al*. (2001) tested anchor bolts and report that the ratio of tested to predicted design strength of 0.87, 0.83, and 0.91 on three pilot tests using 16-mm connectors embedded 88 mm, again an unconservative result even using the Equation 2.22, which gives results 20 to 30 % less than the US design specifications (AISC LRFD 2001, AASHTO 2002). For 19-mm (¾-in.) connectors, the range of tested to predicted strength is 0.75 to 0.97 based on six tests (Yamamoto *et al*. 2001).

Johnson and Molenstra (1991) report curves for characteristic strength per stud differing about 15 % from predicted values, which they assert is in good agreement for this subject.

Nakajima *et al*. (2003) report the average of the results of the pulsating static load tests, which are closest to being represented by the standard push-out test, are about 22.5 % lower than the predicted of Equation 2.18. The results have a difference of about 5.7 %.

The US specifications (AISC LRFD 2001, AASHTO 2002) do not always predict connector strength accurately or conservatively. A significant difference in the ultimate strengths exists among test results and among various codes. Significant variation in the ultimate strength of the connectors can be expected

from one test to another. In addition, since most of the research cited above was performed on push-out test specimens using the average of eight connectors, even more scatter can be expected from single-connector tests.

2.5.1.2 Results Regarding Stiffness of Shear Stud

Occasionally, researchers investigate the stiffness of the connector. Johnson and Molenstra (1991) report that measurements on studs in girder tests have shown similar stiffnesses as push-out tests, and that wide scatter exists in both sets of data. In other words, that the initial slope of the load-slip curve can vary (Johnson and Molenstra 1991).

2.5.2 Results Regarding Diameter of Shear Stud

Yamamoto *et al*. (2001) report smaller-diameter connectors are slightly more efficient than larger-diameter cones based on strength and embedment depth. Those authors originally thought that using shallow connectors with 12- to 16-mm diameter would be advantageous, but recommend higher strength and larger diameter of connectors based on the results of their experiments.

2.5.3 Results Regarding Compressive Strength of Concrete

Yamamoto *et al*. (2001) conclude that the shear capacity of the connector increases with the compressive strength of the concrete, based on graphs of Q_u versus f_c. As shown in Section 2.5.1, most equations used to predict the capacity of shear connectors are based on the area of the connector and the compressive strength of the concrete.

2.5.4 Results Regarding the Effect of Cracks

The concrete cracking in negative moment regions of continuous girders must be considered (Faella, Martinelli and Nigro 2003). Cracks have been seen at

various loads during push-out tests. Matus and Jullien (1996) observed a few very thin cracks parallel to the connector axis on the outside surfaces of the concrete slabs, at the level of the connectors, at 85 % of ultimate loading. The maximum load was obtained when the slabs separated from the girder due to the failure of the connector's support (Matus and Jullien 1996). On the other hand, Ollgaard, Slutter and Fisher (1971) report that slab cracks were often visible just after the ultimate load was reached. Johnson and Molenstra (1991) excluded about half of the specimens considered because they failed by splitting. As mentioned in Section 2.5.1.1.1, excluding these specimens does not seem prudent.

2.5.5 Ultimate Slip Capacity under Static Loading

Oehlers and Coughlan (1986) show that fracture of the connector occurs at a slip of about $0.95 \times Q_u$ on the descending branch (Oehlers and Sved 1995). In the same paper, Oehlers and Coughlan show that the ultimate slip, s_u, (S_f in their paper) could be given as (Oehlers and Sved 1995):

$$s_u = (0.45 - .0021 \times f'_c) \times d \qquad \textbf{(2.27)}$$

Where: s_u = ultimate slip capacity of connector.

SI units should be used for this equation. This equation has a standard deviation of 0.048-in. using the data from the tests (Oehlers and Sved 1995).

The slip at maximum load, $s_{@Qu}$, is given by (in SI units):

$$s_{@Qu} = (0.41 - 0.0030 \times f'_c) \times d \qquad \textbf{(2.28)}$$

Where: $s_{@Qu}$ = connector slip at maximum load.

Oehlers and Sved (1995) report that the slip capacity of a connector is about 30 % of the diameter of the connector.

Johnson and Molenstra (1991) observed an ultimate slip capacity before stud failure of 2.4 mm (0.09 in.) on a 29.5-ft girder designed for 40 % composite

action. The remaining studs failed shortly after the first stud failed. These tests used small studs (13 mm or ½-in.), concrete with a high compressive strength (7250 psi), and a low degree of shear connection, resulting in low connector slip capacity (Johnson and Molenstra 1991).

From their tests, Johnson and Molenstra (1991) conclude that a 50-ft girder with only 50-percent shear connection requires connectors with an established slip capacity of at least 8.5 mm (0.33 in.). They warn that a 100-percent shear connection should be designed for if the slip capacity of the connector is only 4-mm (0.16-in.) because in several girders with 90-percent connection, s_{max} at ultimate load reached only 4 mm.

Johnson and Molenstra (1991) propose Equation 2.29 and Equation 2.30 based on pre-1985 data:

$$s_{@Qu} = (0.389 - 0.0023 \times f_{cu}') \times d \qquad \textbf{(2.29)}$$

$$s_u = (0.453 - 0.0018 \times f_{cu}') \times d \qquad \textbf{(2.30)}$$

Subsequent work has shown that slip at $0.95 \times Q_u$ on the descending branch is about 7.25-mm (0.29-in.) (Johnson and Molenstra 1991). Ollgaard, Slutter and Fisher (1971) report that slip at maximum load varies from 0.23 to 0.42 in. An and Cederwall report that the slip at maximum load ranges from 3.5 to 6.0 mm (0.14 to 0.24 in.) for normal- and high-strength concrete. Topkaya (2002) reports that such large slips at maximum load cause significant serviceability problems. Therefore, when defining the ultimate strength of the shear connectors, strength and serviceability criteria should be satisfied. This issue is still under scrutiny by AISC committees (Topkaya 2002).

Ollgaard, Slutter and Fisher (1971) show a photograph of a failed push-out slab specimen in which all four studs sheared off. The studs did not shear off at the same slip levels since the gaps between the studs and the slab are not the same

size, indicating that different amounts of plastic deformation occurred (Ollgaard, Slutter and Fisher 1971).

Eighteen standard push-out tests performed by Hegger *et al*. (2001) on welded headed studs in high-strength concrete (f_c of 13-14 ksi) show that the ductility criterion given by to Eurocode 4 (1994), which requires that the deformation capacity of the connector to at least 6 mm, is not fulfilled by any of the connector diameters tested.

Table 2.5: Calculated slip capacities of ¾-in. connector in 3000-psi concrete

Ultimate Slip, s_u		Slip at Ultimate Load, $s_{@Qu}$	
Equation 2.27	0.30-in.	Equation 2.28	0.26-in.
Equation 2.30	0.31-in	Equation 2.29	0.25-in

Table 2.5 shows that the equations give approximately the same values.

2.5.6 Variations on the Basic Welded Headed Stud to Improve Behavior

Several variations have been devised to improve the behavior of the standard welded headed stud. Hegger *et al*. (2001) report that using a group of connectors in the direction of the shearing force helps the ductility of the connector, although the full strength of both connectors cannot be relied on; some applicable reduction based on tests needs to be made. The first connector creates an area behind its base where the compression strains are lower so that the deformation to the following connector is lower. Although connector slip is the same, the distortions of the second connector are distributed over a greater height. This leads to better upwards redistribution of the forces along the shaft and hence to further relative displacement (Hegger *et al*. 2001).

Matus and Jullien (1996) state the welded headed stud exhibits low ductility. Since the concrete crushes in front of the connector under the applied

loads, the stiffness of the concrete and the composite girder is significantly reduced. This phenomenon increases the distance at which the resultant concrete efforts acts from the root causing the stud to yield in flexure and crushing more concrete. Breakdown of the shear connection can occur by the stud shearing failure or by crushing of the concrete, separately or in combination. Matus and Jullien (1996) assert that the strength of the connector cannot be predicted accurately using simple calculation due to the complex behavior of the concrete in front of the connector's root, which is under a triaxial stress state.

Matus and Jullien (1996) propose using a headed stud welded to a bracket that is attached to the steel girder using two powder-actuated fasteners. A flat yield plateau was observed that reflects the yield process of the support bearers and the zone around the powder-actuated fasteners. Most of the test specimens failed by tearing of the cold-formed bracket, although a few powder-actuated fasteners fractured. The proposed connector can be used for full or partial composite design due to its large ductility (Matus and Jullien 1996).

2.5.7 Using Strain Gages to Measure Connector Stresses

Toprac (1965) appears to have had the most success in using strain gages (albeit indirectly) to measure connector stresses and gain useful information on individual connectors in full-scale girder tests. He placed strain gages on the top flange of the girder below individual connectors. By measuring the variations in strain along the girder, he estimated which connectors were being stressed and were effective, and those which had failed or were ineffective. Toprac (1965) asserts that using strain gages to indicate the effectiveness of individual studs is reliable. He indicates that the strains measured by the gages increased as the fatigue test progressed, then decreased gradually to zero as the studs cracked.

When the studs completely sheared off, the compression strains are measured. The readings can be used qualitatively to describe the behavior (Toprac 1965).

Many other researchers, however, have report that placing a strain gage on the connector itself is not very useful. Nakajima *et al*. (2003) recognize that the strain measurements at midheight are somewhat meaningless since failure occurs at the weld of the stud. They note, however, that it is difficult to place a strain gage at the weld (Nakajima *et al*. 2003).

2.5.8 Summary of Stud Behavior Under Static Loading

The behavior of the welded headed stud subjected to static loading was discussed in Section 2.5. Several empirical equations used around the world are given, with significant variation in the predicted results from each. The effect of connector diameter, concrete compressive strength, and concrete cracks on the static capacity are discussed. The ultimate slip capacities of studs subjected to static loading are given. Several slight variations of the welded headed stud, given by several researchers, are summarized. Finally, the use of strain gages to measure the stresses on the connectors in a bridge is discussed. The behavior of the welded stud subjected to high-cycle fatigue loading is discussed in Section 2.6.

2.6 STUD BEHAVIOR UNDER HIGH-CYCLE FATIGUE LOADING

The prior research performed by investigators is described in this section, along with the testing procedures and results. The difference between uni-directional and reversed loading is distinguished. Finally, the ultimate slip capacity of the headed stud observed in tests is given and discussed.

Slutter and Fisher (1966) performed some of the first research on the fatigue life of welded shear stud connectors. Those researchers performed push-

off type tests, which are similar to push-out tests described in Section 2.4, to evaluate the number of cycles of load based on minimum stress and stress range.

The stress range is the only important variable in the mathematical formula recommended by those researchers (Slutter and Fisher 1966). They show that, for a given stress range, the specimens that underwent reversed loading had a higher fatigue life than those that were loaded monotonically. They concluded that there is no need exists to reverse the load; simply increasing the load to a maximum stress and reducing by the specified stress range monotonically will produce the critical failure mode. Previous research the University of Texas at Austin (Toprac 1965) showed that no direct relationship exists between the static strength and the fatigue strength of connectors, so simply reducing the factor of safety on the 1961 AASHO design provisions (which was the current specification at the time the research was performed) would be unwise (Slutter and Fisher 1966).

At the time this thesis was written, the current (2002) procedures used in AASHTO for strength design were being reviewed. The procedure used in the AASHTO (2002) specifications is based on elastic analysis for fatigue loading and plastic analysis for static loading, as described in Section 2.1.1. Thus, the connectors must be able to develop the yield strength of the girder or the crushing strength of the concrete. Research by Toprac (1965) and Slutter and Fisher (1966) shows that the number of connectors required to develop the ultimate strength of a member is significantly less than required from the design using the 1961 AASHO (AASHO 1961). It was known at the time the report by Slutter and Fisher was written that for most loading conditions uniform spacing, produces essentially the same response as the distributed spacing based on the intensity of the static shear in terms of ultimate strength and deflections (Slutter and Fisher 1966).

Research at Lehigh University and the University of Texas (Toprac 1965) shows that no direct relationship exists between the static strength and the fatigue strength of connectors. Therefore, simply reducing the calculated static design capacity used in the 1961 AASHO (AASHO 1961) specifications by a numerical factor can be unconservative, creating the need to perform fatigue tests to verify the applicability of any reduction factor. The tests also show that if the connectors are designed using fatigue life requirements (preventing fatigue failure), the loss of interaction between the girder and the slab was not sufficient to cause appreciable increases in stresses or deflections in the member. The initial tests, however, did not provide complete information on the fatigue strength of connectors nor the effect of other variables (for example, stresses) on the fatigue strength (Slutter and Fisher 1966).

The fatigue strength of headed studs in tests with constant load ranges is mainly influenced by the following parameters: (Bode, Leffer and Mensinger 2000)

1) A, the cross-section of the stud;
2) R, the ratio of the minimum load, P_{min}, to the maximum load, P_{max};
3) f_{cc}', the cube compressive strength of the concrete;
4) P, the peak of the cyclic load;
5) shape of profiled sheeting (if used).

Eurocode 4 (1994) considers only the range of shear stress, $\Delta P/A$ and limits the maximum load to 60 % of the static bearing capacity (Bode, Leffer and Mensinger 2000). Stress range is defined as the magnitude of the maximum stress minus the minimum stress applied using a negative sign for the minimum stress value if loading is reversed.

Toprac (1965) reports that stud failure due to fatigue begins near the supports of the simply supported test girder, where shears are high, and proceeds

toward the two load points, which were symmetric about the middle of the girder. He indicates that the pair of studs immediately above the reaction point typically show no signs of fatigue damage, such as cracking through the stud shank (Toprac 1965).

Viest *et al*. (1997) assert that the stiffness of the connector depends on the stud, its root, and the concrete. They indicate that the stress-strain curve for the concrete is nonlinear and substantial crushing and tensile cracking can occur around the connector. These phenomena are important under cyclic loads, since the concrete next to the stud can be compacted, crushed, and cracked rapidly, leading to progressively increasing slips for the same shear (Viest *et al*. 1997).

Toprac (1965) reports that all full-scale girder tests exhibit fully composite behavior and capacity under an initial static loading, although the capacities are not significantly higher than predicted. He also indicates that over the life of the fatigue tests, the specimens display a loss of composite action, which is shown by comparing the load versus centerline deflection at various points in the tests. By the end of a typical test, the plot of load versus centerline deflection is usually about halfway between fully composite and non-composite predictions (Toprac 1965).

Toprac (1965) defines failure as the point at which a significant loss of composite action occurs, since the deflection and end slip does not significantly increase until a significant loss of composite action occurs. The end slip and deflection remains fairly constant throughout the test until just before the girder fails completely.

Toprac (1965) found the stress range versus number of cycles (S-N) curve to be rather flat. Between 10,000 and 10,000,000 cycles, the stress range varies from about 20 to 13 ksi (Toprac 1965). Toprac (1965) had four specimens in a group; the number of shear connectors in each specimen varied based on different

design criteria. The number of studs used in the Category A specimens was determined using the 1961 AASHO (AASHO 1961) specifications with a maximum stress of 20 ksi in the tensile steel flange and a factor of safety of 3.70. Category B specimens were designed according to the AISC (1961) specifications with a factor of safety of 2.5 and ultimate strength design. Category C specimens were designed using the theoretical minimum amount of studs required for development of the full flexural static strength of the girder, similar to what would be used for design today (Toprac 1965). Specimen D used an amount of studs halfway between Category B and Category A. Group 1 contained the specimens which met the inspection standards of a Texas Highway Department inspector, whereas Group 2 failed one or more of the inspection criteria. Toprac (1965) notes that the specimens in Group 2 essentially behaved as those in Group 1, with the exception of Specimen 2-C.

The S-N curve used by Toprac (1965) includes all data from a group of tests, even though only one specimen was designed according to the 1961 AASHO (AASHO 1961) design specifications. It should also be pointed out that none of the tests reaches more than 4,500,000 cycles, so that author extrapolated to over twice as many cycles (10 million) in the reported numbers above (Toprac 1965).

2.6.1 Testing Procedures for High-Cycle Fatigue Loading

Most fatigue tests are performed using a push-out test (described in Section 2.4), applying a maximum and minimum load to the connectors to create a stress range. Although some variation exists on the frequency of the applied loading, most researchers apply cycles of load at about 3 Hz (for example, Toprac 1965) for high-cycle (traditional) fatigue and 0.1 Hz for low-cycle fatigue (Section 2.1.8). Slutter and Fisher (1966) loaded the specimens at rates of 250 or

500 cycles per minute (4 or 8 Hz). Slutter and Fisher (1966) loaded their test specimens at a rate that depended on the response of the specimen. The average shear stress is computed based on the nominal cross-sectional area of the studs. A single stress range and loading frequency is typically used for each specimen. Nakajima *et al*. (2003) report that loading frequency does not significantly affect fatigue life. Although most fatigue tests are load-controlled, some fatigue tests are performed under deflection control (for example, Roberts and Dogan 1998)

2.6.2 Results of Experiments on Studs Subjected to High-Cycle Fatigue Loading

Most researchers load all specimens to failure. In the tests performed by Slutter and Fisher (1966), failure typically initiates at the reinforcement of the stud weld and penetrates into the girder flange, causing a depression in the girder flange. A few specimens failed at the welds, which were found to have incomplete penetration. The mode of failure is not a significant variable in the tests (Slutter and Fisher 1966).

Slutter and Fisher (1966) observe that of the four studs tested per experiment, the two studs nearest the applied load fail in fatigue, and the remaining two shear off when they pick up the load for the specimens with higher stress ranges and lower minimum stresses. On the other hand, the load appears to be more evenly distributed over the four studs for the specimens with lower stress ranges and higher minimum stress levels, with all four studs showing fatigue damage. The fatigue life for ¾-in. diameter studs ranges from 27,000 up to 10,275,000 cycles, depending on the applied stress range. The fatigue life for the 7/8-in. diameter studs ranges from 33,000 up to 4,885,100 cycles (Slutter and Fisher 1966).

The general mathematical model assumed in the research by Slutter and Fisher (1966) is of the form:

$$Log(N) = A + B \times S_r \qquad \textbf{(2.31)}$$

Where: S_r = stress range applied to connector;

N = number of cycles to failure; and

A, B = numerical constants.

Slutter and Fisher (1966) show that the minimum stress level only slightly affects the fatigue life for the studs subjected to load reversal. In the research performed by Slutter and Fisher (1966), all specimens were loaded with a minimum stress of low magnitude. Failure is based on the initial fatigue fracture of the connectors. The tests under reversed loading have a significantly higher fatigue life than tests under pulsating (uni-directional) loading for a given stress range. Thus, those researchers decided to exclude data for load reversal tests when fitting a curve to the data. Slutter and Fisher (1966) came up with Equation 2.32:

$$Log(N) = 8.072 - 0.1753 \times S_r \qquad \textbf{(2.32)}$$

Those researches report from the tests and analysis that no significant difference exists between the fatigue life of the ¾-in. and 7/8-in. stud connectors.

The design equation for allowable stress range is proposed as:

$$Z_r = \alpha \times d_s^{\,2} \qquad \textbf{(2.33)}$$

Where: Z_r = allowable stress range of shear per stud;

d_s = diameter of stud;

α = 13,800 for 100,000 cycles;

10,600 for 500,000 cycles; and

7,850 for 2,000,000 cycles.

Units of lb and in. must be used. This equation can be applied conservatively for stud connectors with diameters of ⅞ in. and smaller (Slutter and Fisher 1966). Slutter and Fisher (1966) show that ½-in. diameter connectors exhibit a higher fatigue life than ones with diameters of ¾-in. and ⅞-in.

Toprac (1965) reports that all two-span girders tested in his experiments failed by shearing of all studs, with one span usually failing first. As discussed in Section 2.5.7, in all girder tests, stud failure was observed by measuring the strain in the top flange near the stud, before measurements of deflections and end slip indicated any significant deterioration of composite action (Toprac 1965).

Since Toprac (1965) performed one of the most extensive tests on fatigue of shear connectors, his results are discussed. Table 2.6 shows the number of cycles until the first stud failed, the first pair of studs failed, and all the studs in one span failed.

Table 2.6: Results from Toprac's (1965) research on high-cycle fatigue

Specimen	Cycles to failure of first stud	Cycles to failure of first pair of studs	Cycles to failure of first span
1-A	70,000	85,000	105,200
1-B	1,620,000	4,330,000	4,490,000
1-C	205,000	230,000	260,500
1-D	1,400,000	2,380,000	2,870,000
2-A	1,500,000	1,800,000	2,282,000
2-B	600,000	900,000	1,333,000
2-C	90,000	103,000	120,000

Bode, Leffer and Mensinger (2000) report that most of the observed lifetimes are less than half the predicted value, and some are less than reaching 10 %, based on Minor’s rule. For three tests, a maximum load of 50, 70, and 100 kN result in the failure at 641,700 128,050, and 53,600 cycles respectively.

Roberts and Dogan (1998) obtained the following results from their experiments. The number of cycles to failure varies from 8,951 to 15,160,820 for stresses ranging from 44.4 ksi to 6.05 ksi respectively for the girder tests. The stresses vary for different stud groups in the girder, but the very lowest and very highest stresses are reported here. Results of separate push-out tests show the number of cycles ranging from 47,024 to 18,477,755 for a stress range from 25 ksi to 9.2 ksi respectively. The average concrete strength is about 3700 psi (Roberts and Dogan 1998).

The Eurocode 3 (1993) fatigue design equation is given as follows (Roberts and Dogan 1998):

$$Log(N) = 15.801 - 5 \times Log(\tau_r) \qquad \textbf{(2.34)}$$

Where: τ_r = nominal stress range on stud.

The equation uses SI units and has a cutoff limit at 10^8 cycles. The results of the tests performed by Roberts and Dogan (1998) are larger than the lifetimes predicted by Eurocode 3 (1993). Those authors assert that Eurocode 3 (1993) is generally conservative and provides a satisfactory basis for fatigue assessment. See Section 2.4.1.1. Roberts and Dogan (1998) also report that the connectors in girder tests are subjected to higher shear stress ranges than for the push-out tests, which is believed to be due to the relatively high tensile stresses induced in the studs in push-out test specimens.

2.6.3 Uni-Directional Tests Versus Reversed Cyclic Tests

Two load conditions are used for testing the fatigue strength of connectors, pulsating (uni-directional) or alternating (reversed) loading.

For example, Nakajima *et al*. (2003) performed pulsating tests with a constant minimum load of 2.5 kN. In addition, they performed alternating tests with equal magnitude of the maximum and minimum load. Measurements were

taken every 10 to 600 seconds depending on the expected fatigue life (Nakajima *et al*. 2003).

Results of the main experiments performed by Slutter and Fisher (1966) indicate that the range of stress is more critical than the minimum stress, indicating that reversed loading is unnecessary and maximum load does not significantly affect the fatigue life. In contrast, Bode, Leffer and Mensinger (2000) show a significant influence of the peak load on the fatigue life for uni-directional tests, and assert that the concrete slab is split more under each cycle in the uni-directional test because the connectors subject the concrete to high stresses. Thus, the magnitude of the peak load significantly affects the fatigue life of the connectors in a uni-directional push-out test. Higher levels of peak load with the same cyclic stress range, lead to a further substantial increase of the slip between the concrete slab and the steel flange, exacerbating the splitting problem (Bode, Leffer and Mensinger 2000).

As discussed in Section 2.1.8, researchers have reported that reversed loading is important when investigating low-cycle fatigue. Nakajima *et al*. (2003) report that when the stress range is normalized using the static strength of the connector under a pulsating load, the life of the connector under the alternating load condition becomes shorter than under the pulsating load condition at about 50 % of ultimate strength. That is, when the stress (force) range is about 50 % of the ultimate strength, reversed loading needs to be performed (Nakajima *et al*. 2003).

2.6.3.1 Uni-Directional Test

The uni-directional test consists of applying a load in one direction, then unloading to either zero load, or a low stress level. For example, Toprac (1965)

performed girder tests keeping the minimum stress relatively constant at around 2 ksi, and varying the stress range from 10.5 to 17.8 ksi.

Nakajima *et al*. (2003) measured the strain at the midheight of the connector and conclude that the bending strain in the connector is larger for a uni-directional (pulsating) load than for a reversed (alternating) load. On the other hand, they report the axial strain to be larger in the reversed loading condition. They note that neither of these two observations explains the tendency of the fatigue strength characteristics (Nakajima *et al*. 2003).

2.6.3.2 Reversed Loading Test

Nakajima *et al*. (2003) report that when a stud is subjected to a shear stress range corresponding to approximately one-half of the connector's yield strength under a monotonic static test, the fatigue life under the alternating load condition is shorter than the one under the pulsating load condition. The yield strength noted here corresponds to when the static load-slip curve starts bending over. This range is equal to the yield magnitude. Thus, reversed loading (low-cycle) fatigue tests should be performed based on a stress range corresponding to the yield strength of the connector. The opposite tendency is observed, however, when the stud is subjected to the shear of a magnitude less than the yield strength of the connector (Nakajima *et al*. 2003). Thus, monotonic (pulsating) tests can be performed on stress ranges below the magnitude of the yield of the static tests.

2.6.4 Ultimate Slip Capacity under High-Cycle Fatigue Loading

End slip increases with the number of cycles for all full-scale girder fatigue tests (Toprac 1965). Some specimens show larger slips at the rocker end, while others slip more at the hinged end. No definite pattern exists (Toprac 1965). The maximum end slips are 0.31 in., 0.202 in., 0.22 in., and 0.07-in. for

Specimens 1-A through 1-D respectively. All specimens in Group 2 have an ultimate end slip of about 0.07-in. (Toprac 1965).

For Specimen 2-A, a maximum slip of about 0.098 in. was observed at the hinged support at 2,282,000 cycles (failure). The first stud was deduced to have failed at 1,400,000 cycles, with the first pair of studs failing at 1,800,000 cycles. The studs in the shear span with the smaller end slip did not completely fracture. Most of these studs, however, were visibly cracked on the side nearest the center of the girder and were easily removed from the girder flange by striking them with a hammer. Some had cracks through about 90 % of their area, and complete stud fracture was imminent in this shear span (Toprac 1965).

Roberts and Dogan (1998) performed pilot push-out tests on 10-mm studs and found the connectors have an ultimate slip of 8 mm (0.31 in.).

2.7 STUD BEHAVIOR UNDER LOW-CYCLE FATIGUE

Gattesco, Giuriani and Gubana (1997) and Grundy and Taplin (2003) have performed the majority of the research on low-cycle fatigue. Their findings are discussed in the sections below.

2.7.1 Testing Procedures for Low-Cycle Fatigue Loading

Gattesco, Giuriani and Gubana (1997) argue that the low-cycle fatigue life of shear connectors must be tested under applied strain, rather than simply applying a load to determine the high-cycle fatigue life of the connector. When a connector is beyond the elastic range, it undergoes an increase in incremental slip under a constant load range in each applied cycle. An individual connector in a bridge, however, is subjected to the induced slip caused by the global behavior of the structure, which does not grow. Rather, the maximum slip tends to a constant value after a limited number of cycles. Therefore, to study the low-cycle fatigue

resistance of the critical connector, its slip history is required (Gattesco, Giuriani and Gubana 1997).

In the tests of Gattesco, Giuriani and Gubana (1997), cyclic frequency was kept constant and equal to 0.1 Hz the quasi-static test. The first cycle ranged between maximum and minimum slips that were $2/3 \times s_{max}$ and $2/3 \times s_{min}$ respectively. Maximum and minimum values were reached in an incremental fashion after 20 cycles (Gattesco, Giuriani and Gubana 1997).

Gattesco and Giuriani (1996) used displacement control with a slip rate of 0.001 mm/s, measured by two LVDTs. The test protocol consisted of blocks of imposed displacement cycles, of which was performed using a range of shear between two constant shear values. Loading rate was kept constant at 500 N/s, which corresponds to about only 0.005 Hz for a range of 50 kN. This rate is very slow, as those researchers were interested in low-cycle fatigue. They conclude that the slip increment increases with the load range.

2.7.2 Measuring Separation

Gattesco and Giuriani (1996) checked the relative separation and relative transverse displacement using six dial gauges.

2.7.3 Results of Experiments on Studs Subjected to Low-Cycle Fatigue Loading

Gattesco, Giuriani and Gubana (1997) performed a significant amount of research on low-cycle fatigue, using displacement-controlled loads. Results of the tests are given in Table 2.7, in which the maximum applied slip is given in mm, along with the number of cycles to failure.

Table 2.7: Results of low-cycle fatigue tests by Gattesco, Giuriani and Gubana (1997)

s_{max} (mm)	Number of cycles to failure
0.80	33,338
1.0	18,400
1.0	13,200
1.25	5,274
1.5	3,040
2.0	3,230
2.0	1,440
3.0	432

The number of cycles to failure shown in Table 2.7 is very low, with a minimum of 432 cycles. Comparing the results of Table 2.7 (low-cycle fatigue) to Table 2.6 (high-cycle fatigue), one can see that the number of cycles to failure is typically one to three orders of magnitude lower for the former.

Gattesco and Giuriani (1996) measured the damage accumulated in terms of the slip increment, Δ_s, at the end of a block of cycles. Each block of cycles concluded when the slip increment, Δ_s, reached either a null value or a constant value (Gattesco and Giuriani 1996). Their monotonically loaded specimen failed by shearing of the stud shank preceded by a limited softening branch.

Another parameter in the cyclic plots of load versus slip is the slope of the unloading branch. Gattesco and Giuriani (1996) report that it tends to reduce by 15 to 25 % over 300 cycles due to permanent concrete crushing and deformation. Thus, at the end of the cyclic loading, the recovered slip is greater than at the beginning of the cyclic loading.

2.7.4 Ultimate Slip Capacity under Low-Cycle Fatigue Loading

The life of a connector subjected to low-cycle fatigue loading depends on the ultimate slip to which it is subjected. Gattesco, Giuriani and Gubana (1997) performed eight tests on 19-mm (¾-in.) studs and report that for a maximum slip value of about 1 mm, the number of cycles to failure is about 10^4; for higher values of maximum slip, life decreases rapidly. Their tests were displacement-controlled with a maximum applied slip equal to twice the minimum slip. Thus, slip was measured in just one direction. The load was reversed, however, because of the residual slip in the studs [Figure 2.2(c)]. The increase in residual slip after each load cycle, in other words, causes the load to be reversed (Gattesco, Giuriani and Gubana 1997).

2.7.5 Summary of Stud Behavior Under Low-Cycle Fatigue

Low-cycle fatigue of shear connectors has been investigated only recently, with most research performed in the late 1990's. Experimental results show that the low-cycle fatigue life of welded stud shear connectors is at ten one-thousand times less than the high-cycle fatigue life.

2.8 RESEARCH ON MECHANICAL ANCHOR USED AS SHEAR CONNECTORS

Mechanical anchors, usually proprietary, have been used as retrofit shear connectors. Only limited previous research has been performed on mechanical anchors for use as retrofit shear connectors in bridges. In this thesis, almost every anchor other than a welded headed stud is considered a mechanical anchor.

2.8.1 Research by Klaiber *et al*. on Post-Installed Shear Connectors

Klaiber *et al*. (1983) performed research on post-installed shear connectors to increase the shear capacity of bridges, tested two types of connectors: the double-nut, high-strength bolt; and the epoxied high-strength, friction-grip bolt.

Behavior under static loading was compared to that of the cast-in-place welded headed shear stud (Klaiber *et al*. 1983)

Although that research is similar to the research discussed here, major differences exist. First, those researchers investigated methods for strengthening, by post-tensioning bridges that had originally been designed as composite, and viewed adding shear connectors as a solution to a shear strength problem. Because the bridges in their investigation already used shear connectors in the original design, additional shear connectors could not increase the moment capacity significantly, according to the code specifications used at the time.

Another major difference between that project and this one is that Klaiber *et al*. (1983) tested only girders in flexure that were post-tensioned and had extra shear connectors, or girders that were only post-tensioned. Thus, no tests were performed to directly establish the effect of the post-installed shear connectors.

Further discussion of the behavior of mechanical anchors is given in the references given by Klingner (2002).

2.9 REVIEW OF AASHTO DESIGN REQUIREMENTS FOR SHEAR CONNECTORS

Section 10.38.5.1 of the 2002 AASHTO specification requires that shear connectors be designed for fatigue and checked for ultimate strength. The fatigue design equation is given by Equation 2.33, and the static strength of a headed stud is given by Equation 2.18.

Three major concerns exist with the current AISC LRFD (2001), and AASHTO (2002) requirements for the design of shear connectors (Viest *et al*. 1997):

1) no strength reduction factor, Φ, exists for the ultimate strength of the connector;

2) the ultimate strength of the connector is based on an average value, not an empirical lower bound; and
3) no requirement exists for the ductility of a shear connector.

The first two points can have important implications for achieving the slab or girder failure mode typically designed for today. Since the yield strength of the steel is a lower bound, the steel may not yield before the ultimate strength of the studs is reached. Viest *et al*. (1997) warn that a composite girder designed according to AASHTO provisions may respond unexpectedly if tested in the laboratory. Those authors believe, however, that the design strength would be achieved due to redistribution of shear among the studs, although the system may not be as ductile as anticipated (Viest *et al*. 1997).

Viest *et al*. (1997) note that US provisions (AISC LRFD 2001, AASHTO 2002) lack requirements for the slip capacity of shear connectors, since most tests indicate that they can undergo slips as large as 0.2 in. without fracturing.

In 1977, the AASHTO specifications used the design equation given by Equation 2.20, which gives an ultimate strength of 28.7 kips for a ¾-in. connector in concrete with a compressive strength of 3000 psi (Cook 1977). That is 33 % higher than the value given by today's Specification (Equation 2.18) value of 21.0 kips.

The AASHTO Specifications have changed over time based on the most current research [AASHO (1961), AASHTO (2002)]. Toprac (1965) asserts that the 1961 code was perhaps too conservative and Slutter and Fisher (1966) performed experiments to better understand the behavior of the connectors so predictions that are more accurate could be made.

2.9.1 Current Requirements of Spacing of Studs

The AISC LRFD (2001) Specification allows uniform spacing of studs because tests have shown that the flexural strength of composite girders is independent of stud spacing (Toprac 1965). Shear studs are assumed to be sufficiently ductile to redistribute shear among all studs.

A girder subjected to a concentrated load may require closer spacing of studs because it must have enough studs between the points of zero moment and the location of the concentrated load to develop the maximum at the concentrated load.

Structural plans of bridges designed in 2002 in Texas use six studs spaced at 6 in. at the ends of the bridge. For a 50-ft span, as for a typical candidate bridge (Chapter 4), studs are spaced at 18 in. elsewhere.

2.9.2 Removal of Partial Composite Design from AASHTO Provisions

The partial composite equation of Section 10.50.1.1 of the AASHTO (2002) provisions, $C = \Sigma Q$, was removed in the 1995 Interim edition. Prior to 1994, the partial composite provision was in the specifications, including the 1993 Interim Specifications. There was, however, no partial composite equation similar to the LFD Specification in the ASD Section 10.38.5.1.2 in the 1992 ASSHTO 15th Edition.

Section C10.50.1.1.1 of the Commentary of the 1995 Interim edition of the AASHTO specifications proposes removing the partial composite design equation because, although it was originally allowed in Load Factor Design section, it was overruled by the requirements of the Allowable Stress Design section (Article 10.38.5.1.2 of AASHTO 2002), which the LFD section references.

As Slutter and Fisher (1966) and Toprac (1965) point out, if enough connectors are provided to prevent fatigue failure, the structure does not exhibit significant loss of ultimate strength or increase of deflection under fatigue loading if the number of connectors is reduced. Therefore, partial composite design may be feasible (Toprac 1965). Hungerford (2004) discusses partial composite design in more detail.

CHAPTER 3
DESCRIPTION OF CONNECTION METHODS INVESTIGATED IN THIS STUDY

3.1 INTRODUCTION TO CONNECTION METHODS

In the early stages of this research project, the research team considered many methods for creating post-installed shear transfer in existing non-composite bridge floor systems. These connection methods encompass all three shear-transfer mechanisms presented in Chapter 2; namely bearing, friction and adhesion. The following connection methods were investigated, as shown previously in Figure 1.4.

- Post-Installed Welded Stud
- Post-Installed, Welded Threaded Rod
- Stud Welded to Plate
- Double-Nut Bolt
- Concrete Screw
- High-Tension, Friction-Grip Bolt
- Expansion Anchor
- Undercut Anchor
- Threaded Rod Adhesive Anchor
- Wedge Rod Adhesive Anchor
- Epoxy Coating
- Saw Cut Grooves
- Powder-Actuated Fastener/Rivet

The advantages and disadvantages of these connection methods were then considered in terms of their potential structural effectiveness, constructability and cost. This initial list of potential connection methods was then reduced to a smaller list of connection methods to be further investigated under static load testing. Figure 3.1 shows the connectors and related materials for the connection methods that were chosen for further investigation and static load testing. The descriptions of these connection methods, as well as the results of static load tests on these connection methods, are divided between two documents. Some of the connection methods are described here, and the remainder are described by Hungerford (2004).

*Welded headed stud and welded threaded rod not shown

Figure 3.1: Connectors investigated for project through testing*

The connection methods described in this thesis all include some type of connector. In this thesis, the term "connection method" refers to any way of connecting the concrete slab and steel girder to transfer shears. This includes mechanical fasteners, and adhesives applied at the steel-concrete interface. The term "connector" refers to any type of metal fastener and excludes adhesive-only connections. The term "basic connection method" refers to the connection method installed in its simplest form, as shown in the schematic diagrams of this chapter.

All connectors described here are passively installed as opposed to power-driven. That is, to install the connector, a hole must be drilled into the concrete (and possibly the steel) to allow space for the connector. Then the connector is inserted into the hole and held in place by various means, such as a weld or mechanical action. No adhesive is used in any of the connection methods described in this thesis. Hungerford (2004) covers the connection methods that use adhesive, as well as some connection methods that are power-driven.

The remainder of this chapter provides detailed descriptions of the connection methods reported in this thesis. Included is a discussion of the steps involved in the installation of each connection method. This is preceded below by a brief discussion of some of the tools needed as part of the installation process.

3.1.1 Tools Used for Installation of Connection Methods

The various shear connection methods described here require making holes in the concrete slab and sometimes in the top flange of the steel girder, to accommodate installation of connectors. The tools and techniques needed for making holes in the concrete and steel are described in this section. These tools and techniques can have an important impact on the constructability, cost and overall feasibility of the connection methods.

Two basic devices are used to drill a hole through concrete: a coring machine and a rotary hammer drill. A magnetically mounted Slugger™ drill is commonly used to drill through steel. Some connectors are installed from the top of the slab while others are installed from underneath the bridge, sometimes requiring placement of drilling equipment in the space between the top and bottom girder flanges. Some connection methods require work to be performed from both the top and bottom sides of the bridge deck.

3.1.1.1 Concrete Coring Machine

A concrete coring machine (Figure 3.2) is widely used to drill holes into concrete that are larger than 2 in. in diameter. It can drill a hole through a 7-in. thick concrete slab in about 15 minutes, but requires an electrical or fuel power supply and a constant supply of water. The larger diameter bit makes the coring machine more likely to hit embedded reinforcement than the rotary hammer drill, which uses smaller drill bits. Several additional disadvantages are discussed below.

The machine must be completely secured to the concrete while in use. This can be achieved by using anchors, vacuum suction, or a large weight, such as the wheel of a vehicle. If anchors are used, it is likely that many will be required, leading to a number of additional holes in the slab. Using vacuum suction utilizing a built-on apparatus is another option. This has been used successfully in many cases. If the concrete surface has debris or is not flat, however, the suction may not be adequate. Finally, the third option is to hold the machine down with the wheel of a vehicle.

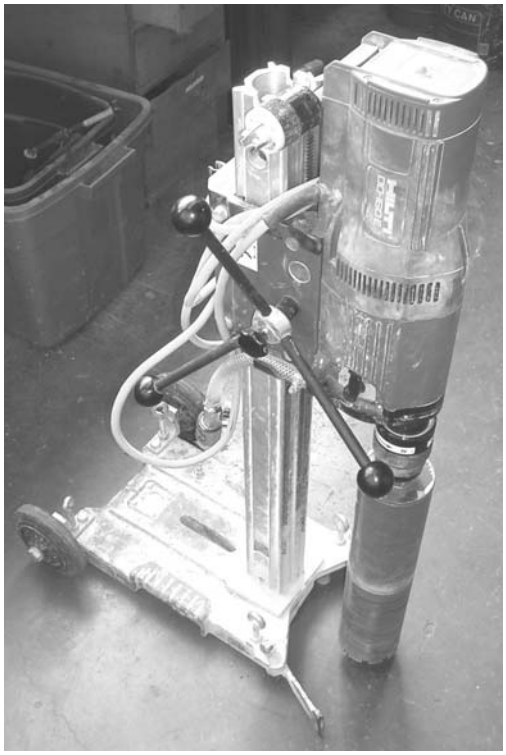

Figure 3.2: Concrete coring machine

The core bit requires a constant water supply to keep it cool. Typically, a standard garden hose is connected to the machine using an attached fitting. Providing this water supply may be problematic is some cases and may increase cost. In addition to the cost of supplying the water, the coring machine and coring bits are quite expensive.

For the reasons listed above, the use of a rotary hammer drill may be a more economical means of drilling holes in the concrete slab.

3.1.1.2 Concrete Rotary Hammer Drill

The second tool used for drilling through concrete is a rotary hammer drill, which can make holes up to 2 in. in diameter using a cruciform drill bit. For this research project, Hilti TE-52 or TE-55 drills (Figure 3.3) were used, with both

the rotary and hammer mechanisms functioning. Typical drill bits are shown in Figures 3.4 and 3.5. Although bits with diameters greater than 2 in. are available for the rotary hammer drill, they do not have the required length to penetrate the slab. Thus, drilling holes larger than 2 in. in diameter is very cumbersome with a rotary hammer drill. The rotary hammer drill can drill a 2-in. diameter hole through a 7-in. thick slab in about 10 minutes. It can drill a ¾-in. diameter hole using a carbide-tipped bit (Figure 3.5) in about 2 minutes. The drill is about 18-in. long, with the bit extending about another 8 in. The drill fits between the flanges of a 30-in. deep girder when drilling from underneath the bridge. The rotary hammer drill is hand-held and requires only an electrical power supply. It drills holes faster than the coring machine and does not require a constant water supply. The bit must simply be cooled from time to time in a bucket of water. The drill bits for the rotary hammer drill also can be quite expensive, but relative to the cost of the rehabilitation work, the cost is virtually negligible. The rotary hammer drill is less likely to hit reinforcement since it uses smaller bits than the concrete coring machine.

Figure 3.3: Rotary hammer drill

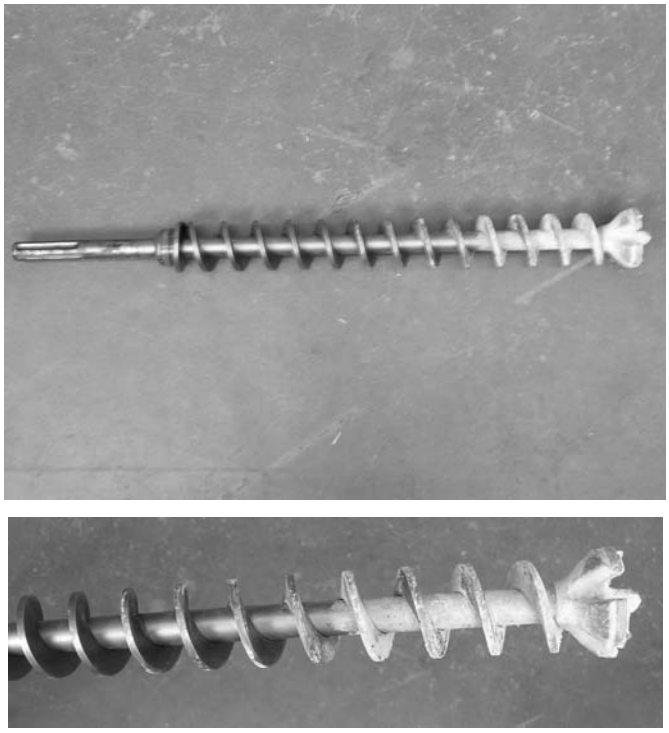

Figure 3.4: 2-in. rotary hammer drill cruciform bit

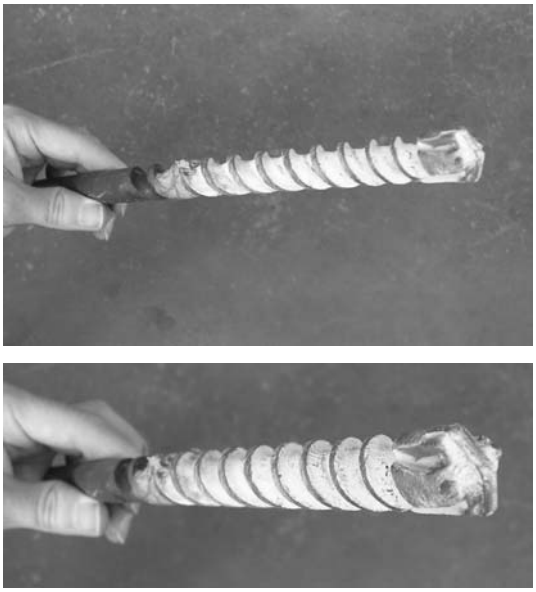

Figure 3.5: ¾-in. rotary hammer drill carbide- tipped bit

3.1.1.3 Special-Purpose, Hollow-Bit Drill for Steel

A special-purpose, hollow-bit drill (Figure 3.6), referred to as a "Slugger™" in this thesis, is a portable tool used for coring through steel using an annular bit. The drill is so named because it cores out the circumference of the hole, leaving a "slug" of solid steel in the middle, which is removed from the bit upon completing the hole. By drilling only the circumference of the hole, the tool requires less horsepower than a drill that uses a solid bit. The annular bit's thin wall and sharp teeth are delicate, however, and must be handled carefully. The drill can make a ¾-in. diameter hole through a 1-in. thick plate in about 3 minutes, and a 1-5/16-in. diameter hole in about 5 minutes. The drill is typically secured to the steel using a powerful magnet, enabling it to be used upside down with relative ease. This is important for connectors that require installation from the underside of the bridge. The base of the drill (not including the crank) is 20.5 in. high, 10.5 in. wide and 3.5 in. deep. Including the crank, the drill is 7 in. deep. The drill can easily fit between the flanges of a 30-in. deep girder when drilling from underneath the bridge. The Slugger™ drill requires an electrical power supply. While some Slugger™ drills have automatic coolant dispensers, a squirt-bottle of machine oil (Figure 3.7) is commonly used to keep the bit cool. In the field, this oil can be caught in a basin to protect the environment.

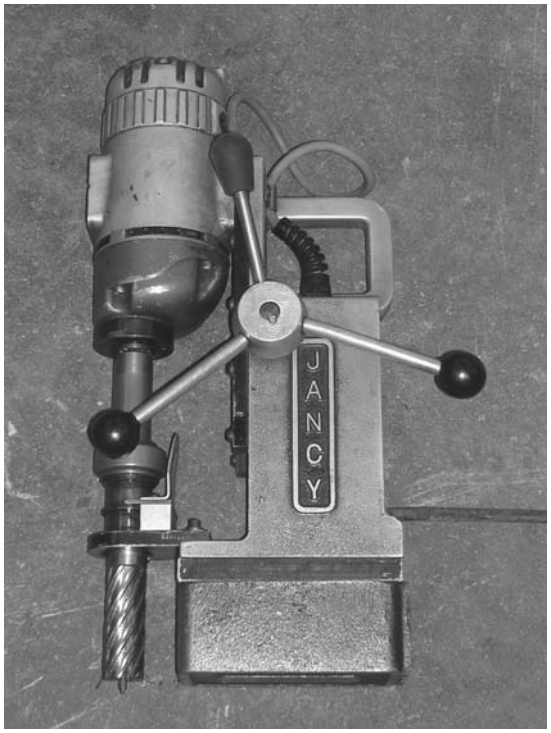

Figure 3.6: Slugger™ drill with 1¼-in. Slugger™ bit

Figure 3.7: Squeeze bottle with machine oil for cooling Slugger™ bit

3.2 SUMMARY OF CONNECTION METHODS COVERED IN MORE DETAIL IN THIS THESIS

In this thesis, results are presented for single-connector, direct-shear tests on the following six connection methods:

1) post-installed welded stud (POSST);
2) stud welded to plate (STWPL);
3) double-nut bolt (DBLNB);
4) high-tension, friction-grip bolt (HTFGB);
5) expansion anchor (KWIKB—KWIK Bolt II by Hilti Corp.); and
6) undercut anchor (MAXIB—Maxi-Bolt by Drillco).

Schematic diagrams of each of the connection methods, along with the conventional cast-in-place, welded headed shear stud, are presented below. The test designations presented in Chapter 5 are shown in parenthesis next to the name of the connection method so that the reader can refer back to this chapter and easily match the designation with the respective schematic diagram. Each diagram shows the concrete slab and the top of the steel girder to be connected. The schematics are drawn to a relative scale with a 7-in. thick concrete slab and a 12-in. wide, 1-in. thick girder flange. The connectors are ¾ in. in diameter and have an embedment depth of 5 in.

Each section contains information on the three characteristics of each connection method that were investigated in this project:

1) mechanism(s) of shear-transfer;
2) installation procedure and constructability; and
3) relative cost of connectors and installation tools.

Connection methods that use friction as the shear-transfer primary mechanism usually have a secondary shear-transfer mechanism of bearing, once the connector comes into contact with the edges of the hole in the steel and concrete.

The installation tools used for each connection method are given in the installation procedure. Based on the description of the installation procedures and required installation tools given in this section and in Section 3.1.1 respectively,

the reader can gain an initial understanding of construction difficulty associated with each connection method.

3.2.1 Cast-in-Place Welded Stud

The cast-in-place welded headed stud (Figure 3.8) is the most commonly used shear connection method for new construction. The studs are welded to the top of the steel flange before the concrete is cast. It uses bearing as the primary shear-transfer mechanism to the concrete, with the connector transmitting load from the steel flange through flexure and shear. Two studs are typically used per girder in the transverse direction of the bridge, so all diagrams show two connectors per section. From this point forward, the cast-in-place welded stud is often used as a benchmark, since it represents the standard of modern cast-in-place construction.

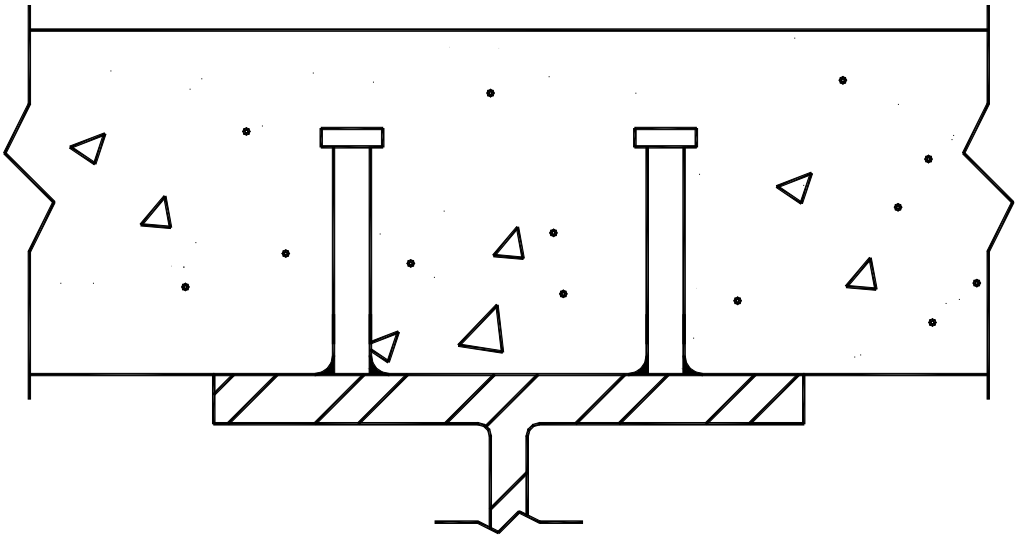

Figure 3.8: Cast-in-place welded stud (CIPST)

3.2.2 Post-Installed Welded Stud

The post-installed welded stud (Figure 3.9) is the retrofit connection method most similar to the cast-in-place welded stud. This connector is installed in four steps:

1) drill 3.5-in. diameter hole through concrete slab to top of girder flange using coring machine;
2) prepare surface of steel for welding by cleaning properly;
3) arc-weld stud to girder flange using stud welding gun; and
4) fill hole with grout.

The 3.5-in. diameter hole in the concrete is required so that the stud welding gun will fit to the bottom of the hole. The structural, non-shrink grout used to fill the hole is described in more detail in the following chapters. Bearing is the primary shear-transfer mechanism.

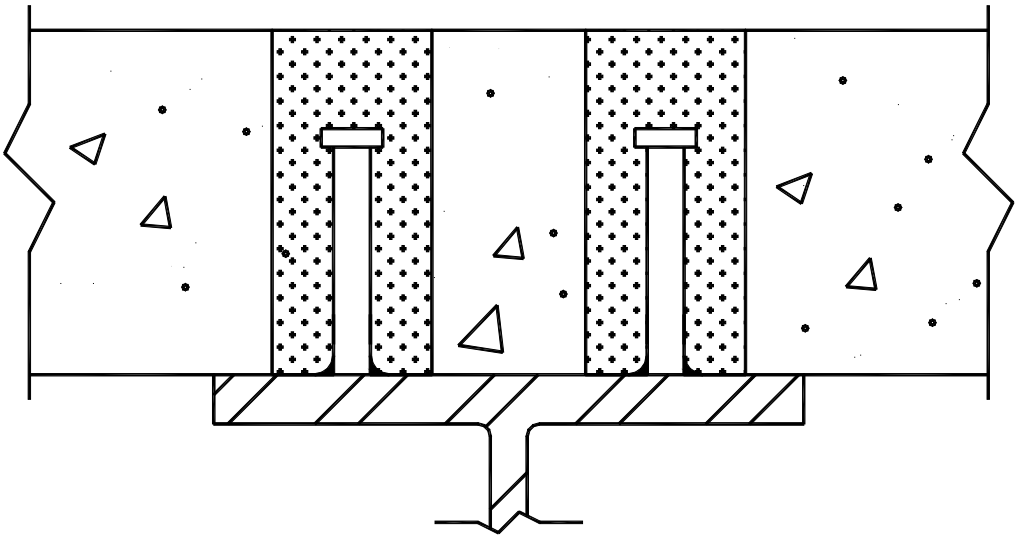

Figure 3.9: Post-installed welded stud (POSST)

3.2.3 Stud Welded to Plate

The stud welded to plate (Figure 3.10) is very similar to the post-installed welded stud. This connector is installed in five steps:

1) weld stud to 5- x 5- x ½-in. steel plate in shop;
2) drill 2-in. diameter hole through concrete slab using rotary hammer drill;
3) clean vertical surface of steel flange for welding;
4) fillet-weld ½-in. thick plate to girder flange; and
5) fill hole with grout.

The advantage of the stud welded to plate connection method over the post-installed welded stud is that a rotary hammer drill can be used instead of a coring machine. The tolerance on the location of the concrete hole must be greater, however, because the stud is pre-welded to the ½-in. plate in the shop and must fit into the hole while butting against the girder flange. The hole in the slab could be drilled from either the bottom or the top of the bridge deck. Drilling from the bottom may make it easier to locate the hole more accurately with respect to the edge of the girder flange. Bearing is the primary shear-transfer mechanism.

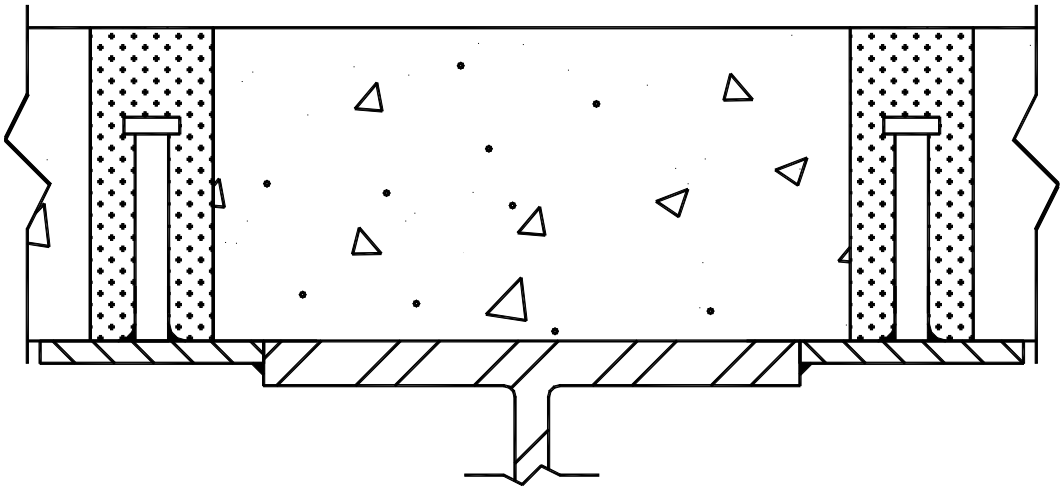

Figure 3.10: Stud welded to plate (STWPL)

3.2.4 Double-Nut Bolt

The double-nut bolt (Figure 3.11) connection method, reported by Klaiber *et al*. (1983), is installed in five steps:

1) drill 2-in. diameter hole through concrete from top of bridge using rotary hammer drill;
2) drill 13/16-in. diameter hole through steel flange from top of bridge using Slugger™ *drill;*
3) insert bolt from top of bridge, with two top nuts set to provide the desired embedment depth;
4) tighten bottom nut from bottom of bridge; and
5) fill hole with grout.

To make drilling through the steel easier, an alternative procedure may be implemented, in which case, the hole in the steel is drilled first from the bottom of the bridge. Next, a ¾-in. diameter pilot hole is drilled through the concrete from

the bottom. Then, a 2-in. diameter hole can be drilled through the concrete from the top using the pilot hole to ensure alignment of the holes in the steel and concrete.

A 2-in. diameter hole is used in the concrete to allow sufficient space for the nuts and washer. The two nuts on the top side of the girder flange are used to lock the bottom nut, allowing it to be tightened without holding the top nut. This allows the bolt to be tightened from only one side of the bridge. The bolt is longer than required for the bottom nut, so it can be held in place (for example, with pliers) while the bottom nut is being placed.

The double-nut bolt uses bearing as the primary shear-transfer mechanism Once the friction between the washers and the girder flange is overcome, the connector slides into bearing against the side of the hole in the girder. To reduce slip in the connection, the hole in the steel flange can be drilled to a tighter tolerance or the gap filled with grout.

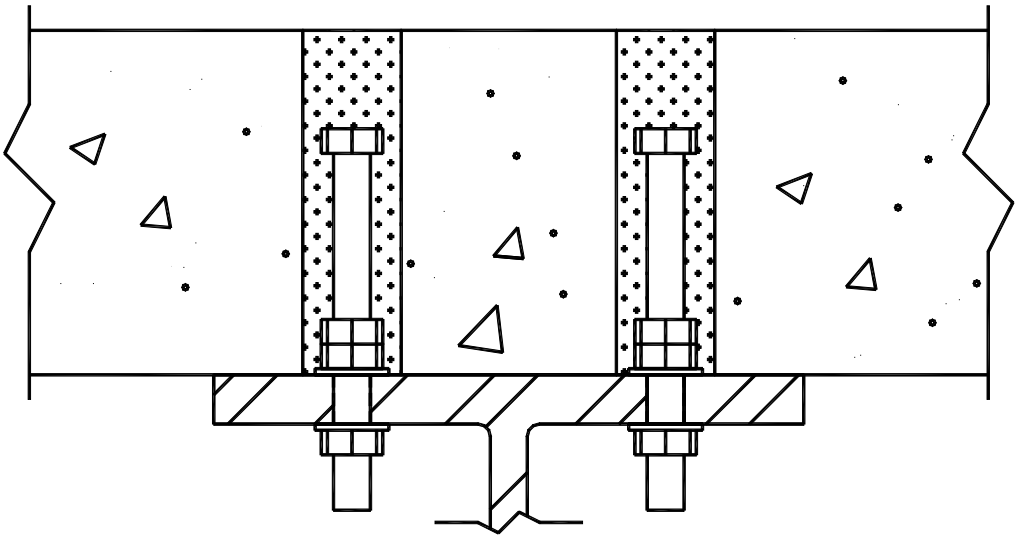

Figure 3.11: Double-nut bolt (DBLNB)

3.2.5 High-Tension, Friction-Grip Bolt

The high-tension, friction-grip bolt (Figure 3.12) connection method, reported by Klaiber *et al*. (1983), is installed in seven steps:

1) drill 13/16-in. diameter hole through steel girder flange from bottom of bridge using Slugger™ drill;
2) drill ¾-in. diameter hole through concrete from bottom of bridge using rotary hammer drill;
3) drill 2-in. diameter countersunk hole from top of bridge deep enough to allow bolt to meet required embedment depth using rotary hammer drill;
4) flatten bottom of countersunk hole to ensure flush surface for bolt head; alternatively, place epoxy or grout around bottom of hole to create flat surface;
5) insert bolt with washer under head into hole;

6) place bottom nut and washer and tighten to required full pre-tensioning from bottom of bridge; and
7) fill countersunk hole with grout.

The installation is started from the bottom to facilitate drilling through the steel. A load-indicating washer can be used to ensure proper pre-tension, as discussed in the next section.

Provided the connector is pre-tensioned to create a compressive force between the girder and slab, the high-strength, friction-grip bolt uses friction as its primary shear-transfer mechanism. Since the bolt is installed into the concrete with a narrow tolerance, when the friction is overcome, as the girder and slab undergo relative slip (in and out of page in Figure 3.12), the connector does not rotate in the hole in the concrete slab. Only the steel girder slides into contact with the connector, and bearing is the secondary shear-transfer mechanism of the connector. The hole in the girder flange can be drilled to a tighter tolerance or the gap filled with grout to reduce slip in the connection.

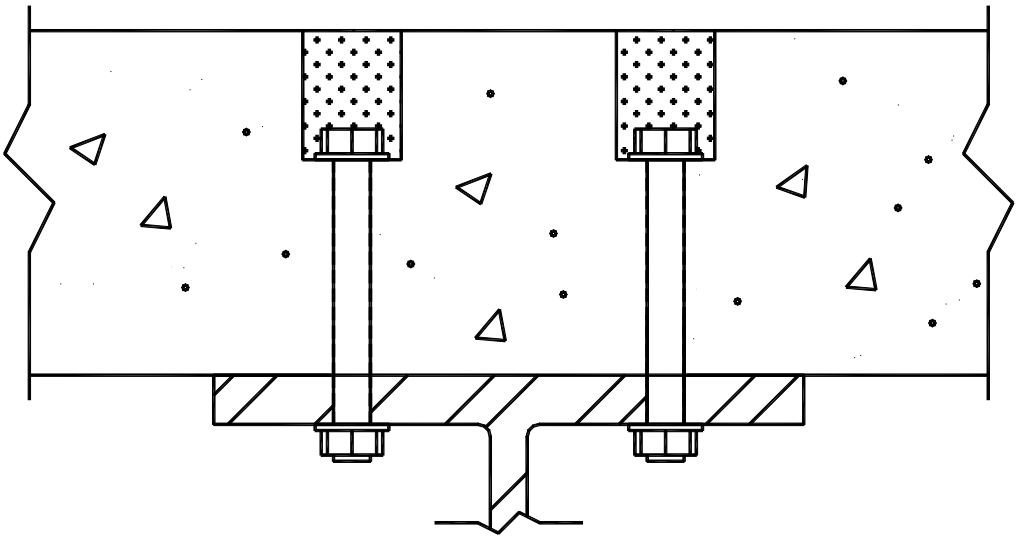

Figure 3.12: High-tension, friction-grip bolt (HTFGB)

3.2.5.1 Developing and Maintaining Pre-Tension with Various Washers

A structural concern in using high clamping forces is the effect, of under concentrated load, relaxation in the concrete, which reduces connector pre-tension. Since friction resistance depends on applied normal force, tension in the connector must be maintained. Several devices intended to ensure this are available, including load-indicating washers and Belleville washers. Each is discussed further here.

3.2.5.1.1 Load-Indicating Washers Used to Measure Pre-Tension

One device used to check pre-tension in a connector is a load-indicating washer. Various kinds of load-indicating washers are available (Grigorian, Yang and Popov 1992). These washers are placed between the bolt head and a standard washer. They have four or five small protrusions around the washer that are compressed as the bolt is tightened. The gaps between the protrusions are measured with a feeler gage supplied by the DTI manufacturer. The person tightening the bolt simply measures the gaps until the feeler gage can no longer be inserted, at which point the connector is pre-tensioned to the rated value for that washer. A specific load-indicating washer exists for each bolt diameter. "Squirter" Direct Tension Indicator (DTI) load-indicating washers have an orange silicone substance in the protrusions that is excreted as the bolt is tightened. The "Squirter" DTIs can be calibrated in a Skidmore, used to measure bolt tension, by gauging how much silicon is excreted when the desired connector pre-tension is obtained.

Load-indicating washers can be used to indicate the load only once, so a new washer needs to be used each time the tension is checked. This requires the nut to be removed each time, as well. Over time, this could become a problem because the risk of stripping the threads increases; since the connector is covered

with grout, it would be difficult to replace and would be made ineffective. Given that most of the creep would occur over the first year or two after installing the bolt, tension probably would need to be checked only a few times. The only way to remove and retighten the nut on the bolt is from underneath the bridge.

3.2.5.1.2 Belleville Washers Used to Maintain Pre-Tension

The Belleville washer is an alternative device that uses a spring-loaded washer to ensure little loss of pre-tension in the connector [Figure 3.13(A)]. These specially manufactured washers are cold-formed into a concave shape so that they act like springs. They can be used to maintain a high percentage of preload without removing the nut. To maintain the pre-tension in the connector, the washers must:

1) have enough deflection capacity to accommodate the creep of concrete; and
2) have enough load capacity to maintain the pre-tension.

Belleville washers can be thought of as structural springs. Used in parallel (all springs stacked the same way), they increase the allowable load, as shown in Figure 3.13(B). Used in series (all springs stacked opposing each other), they increase the allowable deflection, as shown in Figure 3.13(C).

Because Belleville washers are not designed for high loads, many have to be used in parallel to maintain the required pre-tension. In addition, the deflection capacity for Belleville washers, individually or stacked in series, is relatively small compared with the expected creep under tension load. Thus, although they have some advantages over the load-indicating washers, Bellville washers showed only limited usefulness in this test program.

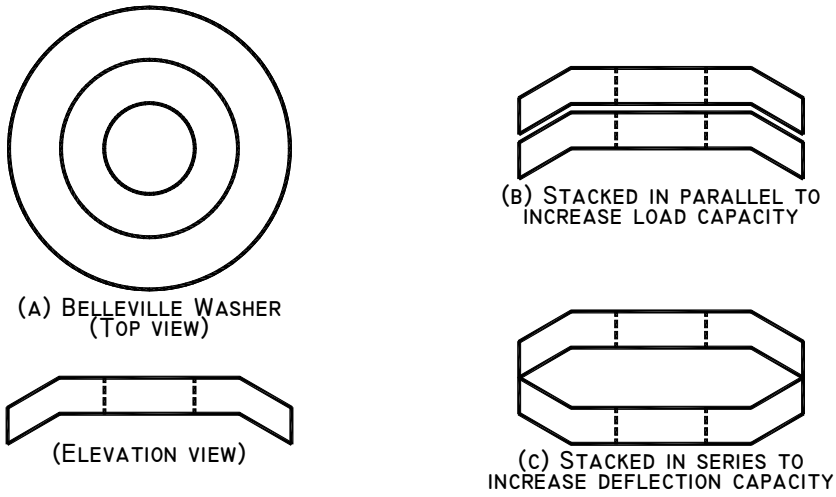

Figure 3.13: Belleville washer

3.2.6 Expansion Anchor

The expansion anchor (Figure 3.14) is a commercially available mechanical anchor. The expansion anchor used in these tests was the "KWIK Bolt II," manufactured by Hilti, Inc. It is installed in three steps:

1) drill 13/16-in. diameter hole through steel girder flange from bottom of bridge using Slugger™ drill;
2) drill ¾-in. diameter hole into concrete from bottom of bridge using rotary hammer drill, deep enough to allow connector to meet required embedment depth; and
3) tap connector into hole with hammer and tighten nut expanding sheaths into concrete for securing so pre-tension can be applied.

Of the connection methods discussed here, the expansion anchor is the easiest to install. Provided the connector is pre-tensioned, it uses friction as its primary shear-transfer mechanism to the concrete. The hole in the steel girder flange cannot be drilled to a tighter tolerance for this connector because the sheath

is larger than the connector shank. Since the connector requires an oversized hole in the concrete for installation, when the friction resistance is overcome, the connector rotates into contact with the concrete and steel girder flange (in and out of the page in Figure 3.14), and bearing is its secondary shear-transfer mechanism. The gap can be filled with grout to reduce slip.

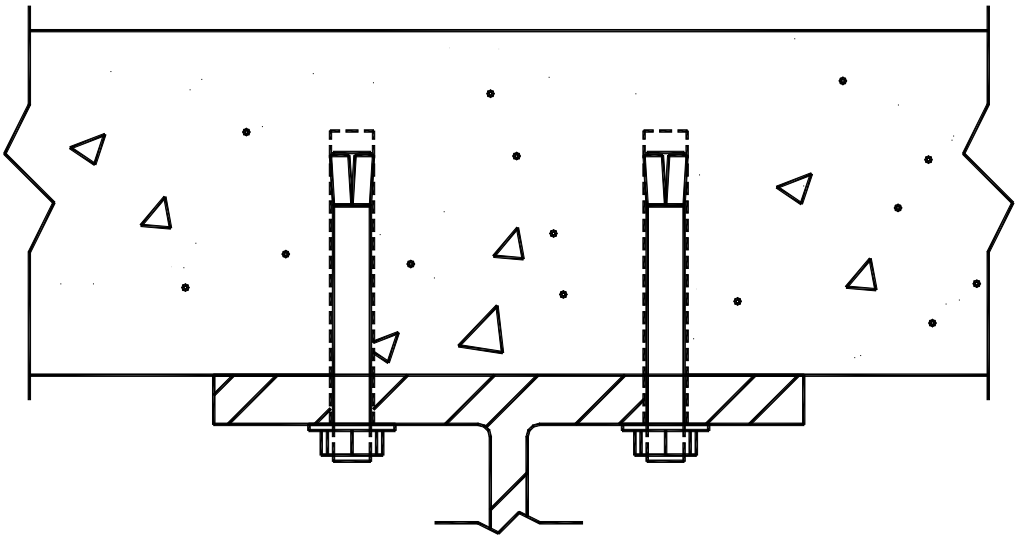

Figure 3.14: Expansion anchor (KWIKB)

3.2.7 Undercut Anchor

The undercut anchor (Figure 3.15) is a commercially available mechanical anchor. The undercut anchor used in these tests was the "Maxi-Bolt," manufactured by Drillco Devices, Ltd. It is installed in four steps:

1) drill 1-5/16-in. diameter hole through steel girder flange from bottom of bridge using Slugger™ drill;
2) drill 1¼-in. diameter hole into concrete from bottom of bridge deep enough to allow connector to meet required embedment depth using rotary hammer drill;

3) undercut hole using special high-speed undercutting drill with diamond cutting blades;
4) install connector and set using manufacturer-provided setting device; and
5) tighten nut to required pre-tension.

Although this connection method appears to be very easy to install, several practical installation problems exist. First, the undercutting drill is about 4 ft long, and would not fit between the girder flanges. Although a shorter (2-ft long) drill is available from the manufacturer, it may still be difficult to use between the girder flanges. Second, the diamond-tipped undercutting blades are very delicate and expensive to replace. Finally, the setting tool is somewhat awkward to use since it must be screwed onto the connector, set, and finally unscrewed. Practical difficulties of the undercut anchor are covered in Chapter 5.

Provided that the connector is pre-tensioned, the undercut anchor uses friction as its primary shear-transfer mechanism. Since the connector requires an oversized hole in the concrete for installation, when the friction resistance is overcome, the connector rotates into contact with the concrete and steel girder flange (in and out of the page in Figure 3.14), and bearing is its secondary shear-transfer mechanism. The hole in the steel flange cannot be drilled to a tighter tolerance for this connector because the sheath must be allowed to freely slide down the connector shank. The gap can be filled with grout to reduce slip.

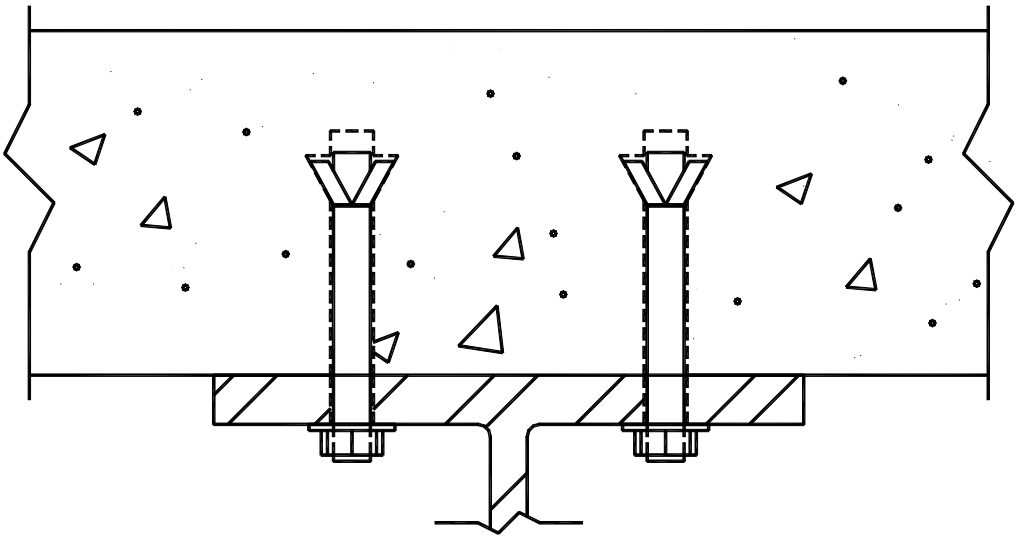

Figure 3.15: Undercut anchor (MAXIB)

3.3 SUMMARY OF CONNECTION METHODS DISCUSSED IN DETAIL IN THIS THESIS

The previous section has provided a brief overview of the connection methods considered in this thesis. The post-installed welded stud most closely replicates the standard cast-in-place welded stud used in modern design and construction for new bridges, and bearing is its primary shear-transfer mechanism. The stud welded to plate connection method is essentially the same as the post-installed welded stud connection method. The only difference is that the stud welded to plate connection method is pre-welded to a small plate in the shop and the plate is field welded to the vertical edge of the girder flange. The double-nut bolt is also quite similar to the welded stud. The only difference is that the nuts and washers transfer the shear from the concrete as opposed to the weld, as in the previous connection methods.

The next groups of connection methods use friction as the primary shear-transfer mechanism, until the friction resistance force is overcome, at which point the connector relies on bearing for a secondary shear-transfer mechanism. The high-tension, friction-grip bolt is a connection method that transfers the shear by applying a normal force at the steel-concrete interface and using friction. The expansion and undercut anchors are also intended to permit the development of a normal force at the steel-concrete interface when the anchors are pre-tensioned, and then to subsequently transfer shear by friction.

Several variations were implemented for some of the connection methods considered in this project to investigate how they influence the structural behavior of the connector. The following three variations were explored:

1) use of higher strength connector materials (for example, A36 and ASTM A-193 Grade B7 steel for undercut anchor);
2) filling gaps with grout (for example, fill space between undercut anchor and concrete and steel with grout); and
3) use of larger diameter connectors than used for basic connection method (3/4-in diameter, Chapter 4) (for example, use larger-diameter, high-tension, friction-grip bolt to maximize claming force to obtain the maximum possible force transfer by friction).

The installation requirements for the connection methods discussed in this thesis are summarized in Table 3.1. Cleaning the steel is grouped with flattening the bottom of the hole in the concrete (for example, for the high-tension, friction-grip bolt) because they both require flattening a surface, which may include chipping away small chunks of concrete with a chisel.

Table 3.1: Summary of installation requirements for connection methods discussed in detail in this thesis

Connection Method (number of installation steps)	Core hole into concrete	Drill hole into concrete using rotary hammer drill	Drill hole into steel	Clean steel for welding OR flatten concrete	Work from above or below deck
POSST (4)	X			X	Top
STWPL (5)		X		X	Both
DBLNB (5)		X	X		Both
HTFGB (7)		X, X*	X	X	Both
KWIKB (3)		X	X		Bottom
MAXIB (5)		X	X		Bottom

*Two holes of different diameters must be drilled into concrete.

The primary and secondary shear-transfer mechanisms between the steel girder and the concrete slab for each connection method discussed in this thesis are summarized in Table 3.2.

Table 3.2: Primary and secondary mechanisms of shear transfer

Connection Method	Mechanism of shear transfer to slab: Primary (Secondary)
Post-Installed Welded Stud (POSST)	Bearing
Stud Welded to Plate (STWPL)	Bearing
Double-Nut Bolt (DBLNB)	Bearing
High-Tension, Friction-Grip Bolt (HTFGB)	Friction (Bearing)
Expansion Anchor (KWIKB)	Friction (Bearing)
Undercut Anchor (MAXIB)	Friction (Bearing)

In an effort to consider the relative economy of the investigated connection methods, a cost analysis was performed including the price of the connectors and installation tools. Grout required for installation is also included in the analysis. The analysis was performed assuming 300 connectors, which is the number required for a 50-ft long span with six girders, with two connectors per section spaced at 2 ft. The figures have been normalized to the cost of the headed studs used in cast-in-place construction. The costs of the required materials and installation tools for the remaining connection methods are normalized as a multiple of the welded stud connection method. Results are presented in Table 3.3. These relative cost figures do not include the cost of labor, however, the relative ease of installation is given based on three categories: easy, medium, and hard. This information, combined with the relative material and installation equipment costs, should give the reader an idea of the more economical methods.

Table 3.3: Normalized cost of connectors and installation tools

Connection Method	Relative ease of installation	Cost of connectors and installation tools
Cast-in-Place Welded Stud (CIPST)	Easy	1.0
Post-Installed Welded Stud (POSST)	Easy	3.1
Stud Welded to Plate (STWPL)	Medium	5.6
Double-Nut Bolt (DBLNB)	Medium	11.9
High-Tension, Friction-Grip Bolt (HTFGB)	Hard	3.9
Expansion Anchor (KWIKB)	Easy	8.7
Undercut Anchor (MAXIB)	Easy	24.8

This chapter has given the reader a general background of the connection methods investigated to connect the concrete slab and steel girder to create composite action. These connection methods are discussed throughout the remainder of this thesis and the reader is encouraged to reference this chapter when reading the remaining chapters.

CHAPTER 4
DEVELOPMENT OF EXPERIMENTAL PROGRAM

4.1 INTRODUCTION TO EXPERIMENTAL PROGRAM

In this chapter, the development of the overall experimental approach for obtaining data on two issues related to the addition of shear connectors to existing non-composite bridge floor systems is described. These issues are: the coefficient of friction between steel and concrete in an existing bridge, and the static load-slip behavior of the connection methods described in Chapter 3. First, the development of the friction and static load tests used to address each of these issues is discussed. Next, the development of the test specimens and test setups used in each of the tests are described. This chapter also provides recommendations for a test setup for conducting fatigue tests on the connection methods. These recommendations are provided because fatigue tests are planned for the later stages of this overall research effort, as described in Chapter 1. Finally, the instrumentation required for the static load tests is given.

Because some of the investigated connection methods use friction as the primary shear-transfer mechanism, information was required on the probable range of the static coefficient of friction between an existing and weathered concrete slab and steel girder. As a result, a test was developed to obtain this information using girders from a bridge undergoing demolition, on which the top flange of existing steel girders was exposed.

The second type of test reported in this thesis is the single-connector, static load test. To accurately model the behavior of an investigated connection

method when subjected to shear, a direct-shear test was developed and performed on individual connectors.

4.2 DEVELOPMENT OF FIELD TESTS FOR COEFFICIENT OF STATIC FRICTION

Several connection methods investigated here rely on friction as the primary shear-transfer mechanism between the concrete slab and steel girder. Research by Cook (1989) shows that the coefficient of friction, μ, between a concrete slab and steel plate attached and loaded through an connector could conservatively be taken as 0.4. Cook also indicates that prior research shows that average values for μ are between 0.3 and 0.65. He recognizes the existence of a natural bond, microscopic mechanical interlock between the steel and concrete paste (Chapter 2), noting that previous research has shown that the coefficient of friction is higher for concrete or grout cast against a steel plate than for a steel plate attached to hardened concrete (Cook 1989). For the connection methods investigated in this project, natural bond is ignored, since it may have been broken over the life of a typical candidate bridge (discussed in Chapter 2).

With the points outlined above in mind, a test was developed to obtain data on the static coefficient of friction between an existing steel girder from a demolished bridge, and a concrete block that has been cast in the laboratory against a steel surface. Given that the concrete slab and steel girder in a typical candidate bridge have been weathered, it was believed necessary to obtain experimental values of the static coefficient of friction in the field to find out if they were affected by the weathered surface condition. The concrete block was cast on steel only to mimic the bottom surface of the bridge slab. No natural bond existed between the concrete block and the existing steel girders tested in the field.

In addition to the field friction tests, the researchers obtained the static coefficient of friction from the static load tests (Section 4.3) for the connection methods investigated that used friction as the primary shear-transfer mechanism. This was accomplished by dividing the applied shear at first slip by the corresponding clamping force obtained from a washer load cell. Results of these tests are presented in Chapter 6.

4.3 DEVELOPMENT OF SINGLE-CONNECTOR, DIRECT-SHEAR STATIC LOAD TESTS

Hungerford (2004) describes in detail the development and implementation of the single-connector, direct-shear static load test. A short overview is given here for completeness.

Most often, the behavior of a shear connector is obtained by performing a push-out test, as described in Chapter 2. As shown in Figure 4.1, the push-out test uses two concrete slabs attached to a steel girder by eight connectors. This type of test has several limitations. First, an additional friction force is created at the interface of the concrete slabs and the steel girder, as shown in the free-body diagrams in Figure 4.2, recreated from Gattesco and Giuriani (1996). This friction, labeled Q_μ in the figures, increases the observed shear capacity, Q, for connectors, since the total reaction, F_v, is the force measured during the test. Second, if a roller base is used, the connector is subjected to significant tension that is not present in the prototype situation. As pointed out by Gattesco and Giuriani (1996), small divergences in the test model, such as the two possible inaccuracies listed above, can lead to large inaccuracies in the behavior of a connection method, especially when performing fatigue tests due to the large number of cycles involved. Thus, it is important to model the shear test accurately.

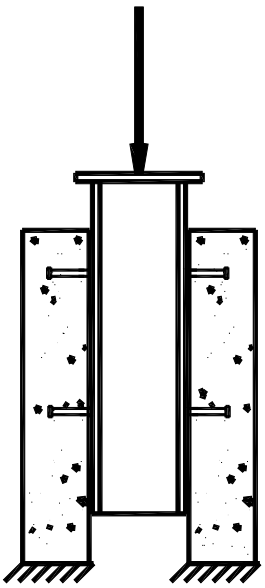

Figure 4.1: Standard push-out test

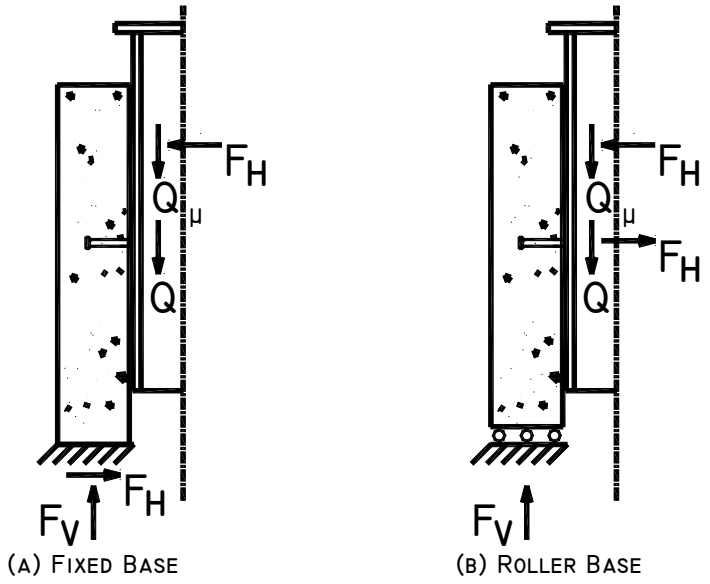

Figure 4.2: Free-body diagrams of standard push-out tests (Gattesco and Giuriani 1996)

In addition to these possible inaccuracies, the push-out test provides only average load and slip values, since it tests eight connectors in a single test. Since the behavior of an individual connector or small group of connectors can be critical for partial composite design, extrapolating this information from a push-out test can be questionable.

Given the limitations of the push-out test, a single-connector, direct-shear static load test was developed to determine the shear-slip relationship of the various connection methods under static loading. Since the model used for composite design addresses only the shear strength of the connection method, it was desired to design a test that measured the pure shear capacity of a connection method, minimizing the moment on the connection caused by eccentricity of applied shear. In addition, natural bond was broken to eliminate potentially unconservative results because bond may have been broken in the typical candidate bridge.

4.4 DEVELOPMENT OF SPECIMENS FOR SINGLE-CONNECTOR, DIRECT-SHEAR STATIC LOAD TESTS

In the following sections, the development of the test specimens, the embedment depth, and the materials used for the investigation are described.

4.4.1 Information on Typical Candidate Bridges

Since much of the research reviewed in this chapter includes equations that use specific parameters about the properties of a bridge and its shear connectors, several typical "candidate bridges" that could be strengthened by the retrofit shear connectors were surveyed as part of this project. The results of the field survey are given in detail by Hungerford (2004). The results are summarized here for completeness.

4.4.1.1 Bridges Surveyed in Field

A number of older non-composite bridges were surveyed to obtain information on typical characteristics of these bridges. The following information was collected for each bridge:

1) year built;
2) general condition information;
3) slab condition information;
4) slab-girder interface condition; and
5) site conditions.

The researchers surveyed six bridges in San Antonio, Texas in March 2003. The bridges were built in the 1950's or early 1960's, and some had been modified in the last 25 years. The bridges were all 4- or 9-span continuous bridges with welded girder splices, supported by pins or rollers. The spans ranged from 50 to 60 feet. They had 5 to 7 longitudinal girders in each span with a 7-ft typical transverse spacing. The girders ranged in depth from 27 to 36 in. with weights from 108 pounds per foot to 178 lb per ft. In general, the girders' condition ranged from well painted and no rust to flaking paint and flaky layers of rust. One bridge had rainwater squirting out between the slab and the girder every time a vehicle drove over the bridge. For such a case, there appears to be a good likelihood of rust on the top side of the girder flange. Given such evidence, it is assumed that a few bridges had a significant amount of rust on the top flange of the girder. This raised concerns about the effect of the rust on the coefficient of friction at the steel-concrete interface. To obtain data on this issue, the coefficient of friction was measured at the top of a steel girder taken from an older bridge during demolition. These tests are discussed later in this thesis.

The cast-in-place concrete slabs ranged in thickness from 6¾ in. to 8 in. Study advisors at TXDOT pointed out that most of the bridges built in the 1950's

and 1960's (when most of the candidate bridges were built) use a 7-in. thick concrete deck. Generally, the slabs appeared to be in good condition, with little or no signs of spalling or leaching. What spalling existed was near the outside girders where the slab was cast on the side of the top girder flange, and was most likely due to thermal expansion. Only the outer section of the girders on the outside of the span had the underside of the concrete deck below the top surface of the top flange of the girder, a byproduct of the construction technique used at the time. Thus, it would be difficult to add plates to the vertical edges of the outermost girders of these bridges.

Unfortunately, the steel-concrete interface was the least promising aspect of the existing bridges. Some of the bridges had a significant amount of rust on the top flanges of the girders, presumably from water entering at the expansion joints. This was observed on girders in which the slab was removed because the bridge was being demolished.

In general, the bridges were very accessible and relatively low to the ground, with a height of about 15 feet. Some bridges were as high as 35 to 40 feet above the ground. Traffic was generally heavy on the surveyed bridges, but most bridges had four lanes, allowing the closure of one or several lanes for retrofit construction.

In this and future chapters, a typical candidate bridge girder is referenced as given here and shown in Figure 4.3. The girder is 50 ft long and simply supported bridge. It has a 7 in. thick, 7 ft wide concrete slab composed of concrete with a specified compressive strength of 3000 psi on an A36 steel girder, 36 in. deep with flanges that are 12 in. wide and 1 in. thick, separated by a web with a thickness of ⅝ in. The girder is simply supported, as opposed to continuous, due to the findings of the research performed by Johnson and Molenstra (1991). The girder carried a uniformly distributed ultimate load of 1.9

kip/ft (dead and live). Point loads are not considered due to the research performed by Johnson and Molenstra (1991), as well. Calculations are performed considering positive bending only, neglecting the reinforcement in the slab.

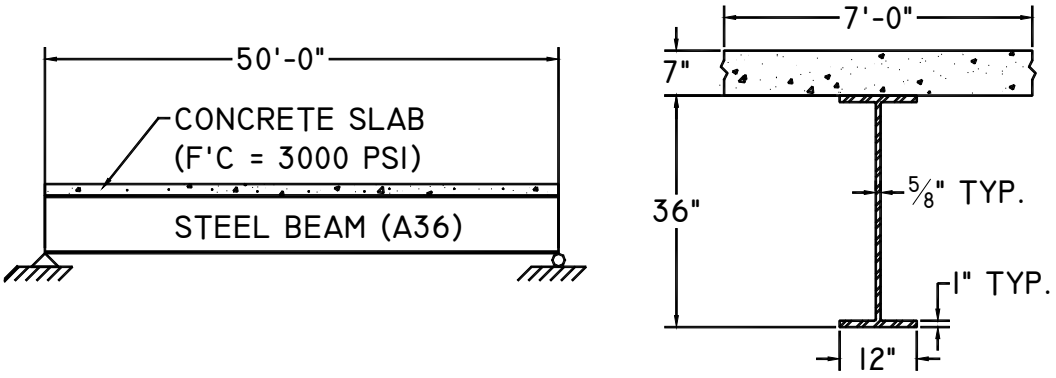

Figure 4.3: Typical candidate bridge girder

4.4.2 Test Slab and Girder Design for Single-Connector, Direct-Shear Static Load Test

The test block was designed to test one connector at a time. The concrete slab's thickness, reinforcing bar sizes and bar spacing were designed so that it represented a typical existing concrete bridge deck from a candidate bridge. The resulting block was 7 in. thick, with #4 and #5 reinforcing bars spaced (Figure 4.4). To eliminate edge effects, the concrete slab block was chosen to have a nominal length and width of 2 ft. As discussed in Chapter 5, fiberglass waffle-slab molds were used as forms for the blocks for ease of construction. The molds were slightly tapered vertically, with an inside area of 23.5 in. square on the top and 22.5 in. square on the bottom.

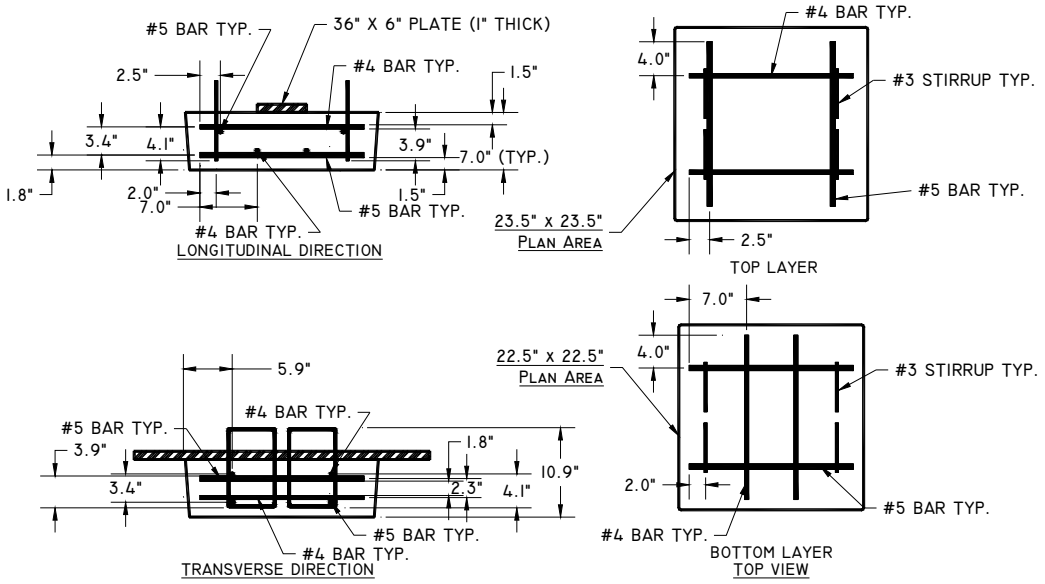

Figure 4.4: Placement of reinforcement (original design)

The component of the test specimen representing the steel girder was designed to represent one-half of the top flange of the girder, resulting in a plate 6 in. wide by 1 in. thick. This plate was intended to represent half of the top flange of a prototype girder, typical dimensions of which are given in Chapter 2. Only the top flange of the girder was represented because the objective was to investigate shear behavior of the connection between the concrete and that top flange. The plate was designed to be 3 ft long to extend beyond the concrete block and fit in the test setup, and also to prevent edge effects around the connector.

Based on the literature, an connector diameter of ¾ in. was chosen. As discussed in Chapter 2, most empirical research shows that connector strength and stiffness are not dependent on the material strength of the connector steel (Ollgaard, Slutter and Fisher 1971). To increase connector strength and stiffness, the connector diameter should be increased, rather than its tensile strength. Thus, the researchers were not as concerned about the ultimate tensile strength of the

connectors, and initially used connectors of low-carbon steel to prevent galvanic corrosion.

4.4.3 Selection of Embedment Depth for Single-Connector, Direct-Shear Static Load Test

Since AASHTO (2002) requires a 2-in. clear cover and the block has been selected as 7 in. thick, the nominal embedment depth was maximized to 5 in. for most of the connectors. The high-tension, friction-grip bolt connection method had slightly smaller nominal embedment depths because the bolt head thickness is not counted in the embedment depth. To meet the clear cover requirements, however, the top of that bolt head was located 2 in. below the top of the concrete surface. The effective embedment depth was also 5 in. for all methods except the high-tension, friction-grip bolt and the expansion anchor. The Kwik Bolt II expansion anchor is pulled significantly toward the plate when tightened, making its effective embedment depth less than 5 in. Most connectors discussed in this thesis have a minimum ratio of embedment depth to diameter (H/d) equal to 6.67 (an embedded length of 5 in., divided by a diameter of ¾ in.), 67 % greater than the minimum requirement of 4 for stud connectors, as given by AASHTO (2002). The AASHTO (2002) specification specifies the minimum height-to-diameter ratio for welded studs, for which the height equals the embedment depth. To be more general, this thesis will address the embedment depth-to-diameter ratio.

4.4.4 Selection of Materials for Single-Connector, Direct-Shear Static Load Tests

The materials used in the experimental program were chosen to represent those found in the existing candidate bridges, many of which were built in the 1950's and 1960's using A36 steel girders, and concrete with a specified 28-day compressive strength between 2500 psi and 3000 psi, and a specified 7-day tensile

strength of 750 psi. To meet the specified tensile strength requirement, the concrete often can reach a compressive strength, fc, of 4500 psi after curing 28 days. As a result, the steel plates used in these tests were ordered as A36, with a minimum specified yield strength of 36 ksi. The concrete used in the test blocks had a targeted 28-day compressive strength range of between 2500 psi and 3000 psi. Since the performance of connectors is worse in low-strength concrete, if the connector behavior is satisfactory for concrete with a compressive strength close to the specified compressive strength, it is satisfactory for concrete with a compressive strength higher than specified. A retarder, typically used in the construction of a concrete bridge deck in the summer in Texas, was added to the concrete mixture, because it would have been used in a typical candidate bridge. Connector strength varied based on commercial availability. Initially, low-carbon steel (commonly A36) was specified. To obtain more frictional resistance, higher-strength material was later used for some methods so more clamping force could be applied. The high-tension, friction-grip bolt (1¼-in. diameter) and undercut anchor used higher-strength materials. Chapter 5 outlines the materials used in the experimental testing.

4.5 DEVELOPMENT OF TEST SETUPS

In the sections below, the development of the setups for the friction test and the static load test is described.

4.5.1 Development of Setup for Friction Test

A simple, portable friction test was designed and built to obtain field experimental values for the static coefficient of friction. As shown in Figure 4.5, a concrete block of known weight is pulled with a force that is measured and recorded when the block starts to slip.

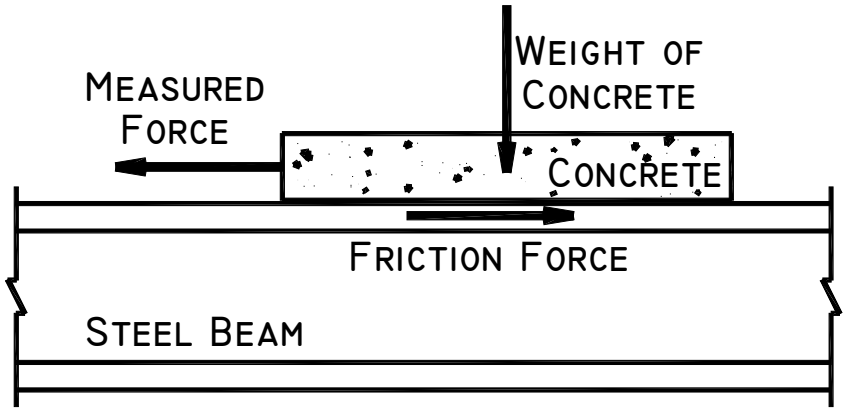

Figure 4.5: Schematic diagram of friction test

The static coefficient of friction can be calculated using Equation 4.1:

$$\mu_s = \frac{F}{W} \qquad \textbf{(4.1)}$$

Where: μ_s = static coefficient of friction;

F = measured force [parallel to interface] at first slip; and

W = known weight of concrete block.

4.5.2 Development of Setup for Single-Connector, Direct-Shear Static Load Test Setup

Development of the setup used to obtain the static shear-slip relation of the investigated connection methods, is described in detail by Hungerford (2004). The setup was designed to represent most accurately the shear-transfer model used by designers for composite action. As discussed above, the push-out test, commonly used to obtain this information has several shortcomings. Therefore, a direct-shear setup was developed to test one connector at a time (Figure 4.5). This setup was designed so that it could easily be altered to perform fatigue and a group-connector tests for future phases of this project.

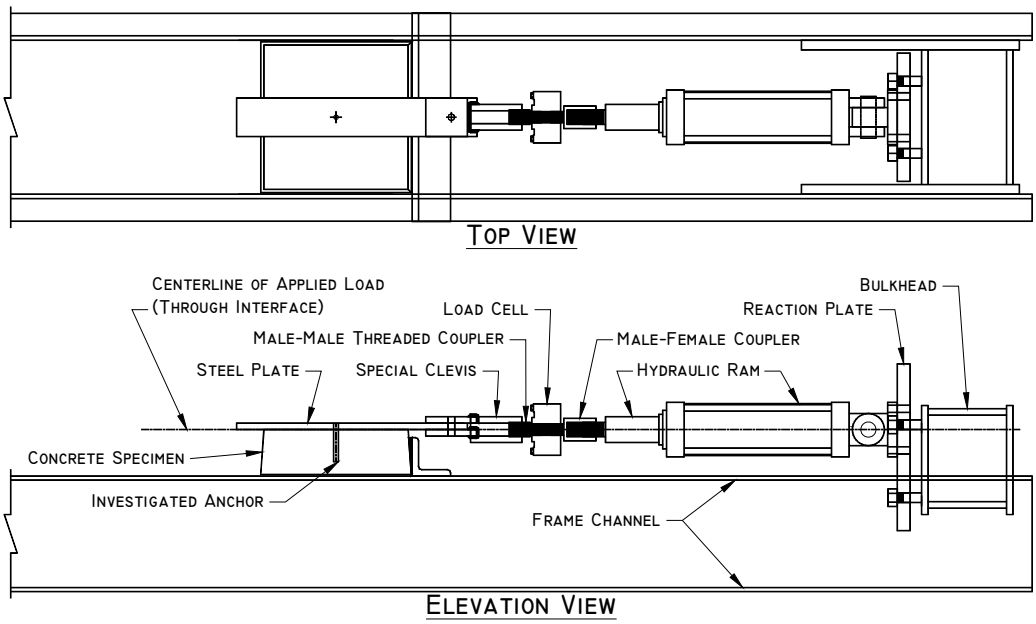

Figure 4.6: Single-connector, direct-shear static load test setup

On the left of Figure 4.6, is the concrete block, turned upside-down from its original design shown in Figure 4.4 (the vertical taper is in the opposite direction). This modification is discussed in Chapter 5. Directly above the block is the steel plate, representing half the girder flange. The concrete block and steel plate are attached by the investigated connection method, shown as a connector. The plate is attached with a large bolt to a special clevis, which is screwed to the load cell via a male-male threaded coupler. A hydraulic ram is connected to the load cell through a female-male threaded coupler, and is secured to a very stiff reaction plate with four large bolts. The bolts are welded to a bulkhead that is attached to the channels comprising the test frame.

Two main advantages of the single-connector, direct-shear test setup shown above over the push-out test are discussed in Chapter 2. First, the centerline of the applied loading passes through the concrete block-steel plate

interface, minimizing the eccentricity of the connector. Second, the setup is self-contained, and thus does not require a reaction floor or wall.

4.6 DEVELOPMENT OF EXPERIMENTAL FATIGUE TEST AND SETUP

A high-cycle fatigue test, in which the connector is subjected to millions of load cycles, is proposed to be performed in the later stages of this research project on the connection methods that exhibit adequate structural behavior in the single-connector, direct-shear static load test. This section provides some suggestions for fatigue testing of shear connectors. Although the researchers designed the setup to do high-cycle fatigue tests, it probably can be easily converted to perform low-cycle fatigue tests.

Chapter 2 provides background information concerning previous research on the behavior of connectors in fatigue. While varying opinions exist on the importance of reversing the applied load, it is believed that no reversed loading is necessary. The high-cycle fatigue tests can be performed uni-directionally, since stress range has been shown to be the critical variable, rather than minimum stress (Slutter and Fisher 1966). Since the graph of stress range versus the logarithm of the number of cycles to failure (S-log N) typically is a straight line, at least two stress ranges should be tested for each connection method.

For connection methods that show adequate high-cycle fatigue behavior, a low-cycle fatigue test is proposed to investigate inelastic behavior and incremental collapse. Low-cycle fatigue tests also investigate the effects of reversed loading on the connector. As discussed in Chapter 2, the ultimate static strength of a connector that has undergone low-cycle fatigue loading has been shown to be reduced by 10 % compared to the static capacity of the structure before it has been subjected to any cyclic loads for fully composite design (Grundy and Taplin 2003). In addition, the slip capacity of the connector has

been shown to be reduced by 30 % compared with results from prior research (Chapter 2).

The test setup used for the single-connector, direct-shear static load tests shown in Figure 4.6 was designed so that it could be adapted for fatigue loading in future stages of this project. Only a few components need to be added to the original test setup for the single-connector, direct-shear cyclic load test, since the hydraulic ram and load cell already fatigue-rated. The additional hydraulic equipment consists of a closed-loop pump, servo-controller, and servo-valve.

4.7 DEVELOPMENT OF INSTRUMENTATION FOR SINGLE-CONNECTOR, DIRECT-SHEAR STATIC LOAD TESTS

Since the primary objective of the experiments was obtaining the load-slip curve of the investigated connection methods, test instrumentation was relatively simple. It consisted of a load cell to measure the applied shear, a washer load cell to measure the tension in the connector (if applicable), and two Linear Variable Differential Transformers (LVDTs) to measure slip at the steel-concrete interface (Figure 4.7).

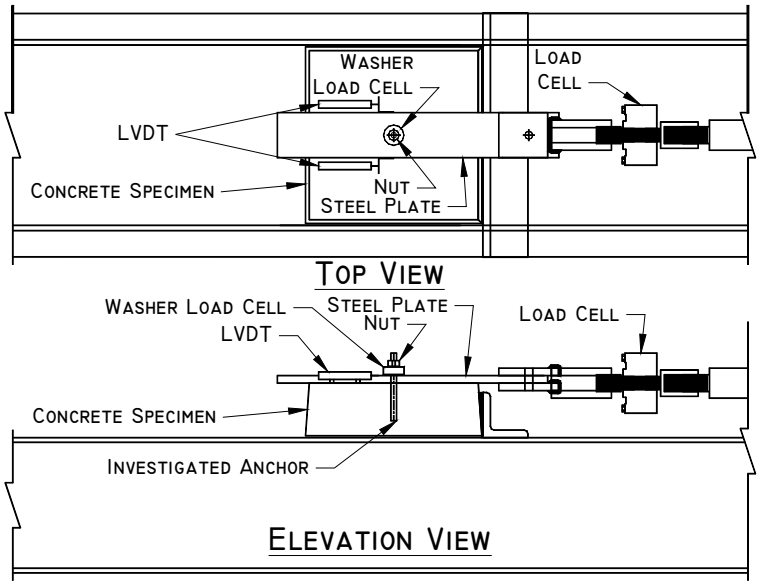

Figure 4.7: Schematic of instrumentation used in single-connector, direct-shear static load tests

The test equipment and instrumentation has the following minimum capabilities:

1) hydraulic ram;
   - 100-kip tension static capacity;
   - 40-kip ultimate fatigue capacity;
   - 15-kip range (fatigue);
   - 2-in. stroke;
2) load cell;
   - 100-kip static capacity;
   - fatigue capability;
3) washer load cell;
   - 48 k tension capacity;
4) linear variable differential transformers (LVDTs);
   - 2-in. stroke; and

- 1/10000-in. precision.

CHAPTER 5
IMPLEMENTATION OF EXPERIMENTAL PROGRAM

5.1 INTRODUCTION

In this chapter, the implementation of the experimental program described in Chapter 4 is discussed. Details of the following topics are covered:

- test matrix and test designations;
- concrete casting procedure;
- concrete, steel, connector, grout, and anchor gel materials;
- connection method installation;
- test equipment for friction and single-connector, direct-shear static load tests; and
- test procedures for friction and single-connector, direct-shear static load tests.

Field friction tests were performed on a bridge undergoing demolition in San Antonio, Texas. The single-connector, direct-shear static load tests were performed in the Ferguson Structural Engineering Laboratory at the University of Texas Pickle Research Center in Austin, Texas. Compressive-strength tests of concrete and grout were performed at the Construction Materials Research Group Building at the Pickle Research Center.

5.2 TEST MATRIX AND TEST DESIGNATIONS

Table 5.1 shows the test matrix and designations for the single-connector, direct-shear static load tests. The six basic retrofit connection methods covered in

this thesis are shown in boldface. Also listed in the table are variations of these basic connection methods. Variations are listed below the respective basic connection method, and designated in brackets. The basic connection methods are shown in the diagrams of Chapter 3. Any proprietary connector has the manufacturer's product name shown in parentheses, since often, the test designation was created using that name. Connection methods not shown in boldface are reported by Hungerford (2004).

Initially it was planned to perform three replicate tests of each basic connection method. It was subsequently realized, however, that constraining a series to three replicate tests was in some cases either excessive or unnecessary. For example, the expansion anchor, tested first, had poor structural performance for this application. Thus, it was decided that only one replicate would be performed for this connection method so that the remaining two concrete blocks could be used for other connection methods if necessary. To improve performance of the expansion anchor, the researchers developed a variant (KWIKG), in which the gap between the concrete and the connector would be with grout, as described in Chapter 3. The grout used was the same as on the post-installed welded stud tests, and contained too much aggregate to allow the connector to set into the hole properly, again resulting in poor structural performance. Thus, only one test was performed on the altered expansion anchor (KWIKG). On the other hand, 9 tests were performed on the epoxy coated to plate connection method (3MEPX) because several construction variables were investigated for their effect on the structural performance of the connection method. For reasons such as these, more or fewer than three replicates may have been performed for each particular connection method.

Table 5.1: Test matrix and designations

Connection Method (Manufacturer's Product Name)	Test Designation	No. of Tests Performed
Cast-in-Place Welded Headed Stud	CIPST	3
Post-Installed Welded Headed Stud	**POSST**	**3**
Post-Installed Welded Threaded Rod	POSTR	2
Stud Welded to Plate	**STWPL**	**3**
Double-Nut Bolt	**DBLNB**	**3**
Concrete Screw (Wedge-Bolt)	WEDGB	3
Concrete Screw [with Anchor Gel] (Wedge-Bolt)	[WEDGG]	[3]
Concrete Screw [with Steel Sheath] (Wedge-Bolt)	[WEDGS]	[1]
High-Tension, Friction-Grip Bolt	**HTFGB**	**3**
High-Tension, Friction-Grip Bolt [1¼-in. Dia.]	**[HTFAT]**	**[3]**
Expansion Anchor (Kwik Bolt II)	**KWIKB**	**1**
Expansion Anchor [with Grout] (Kwik Bolt II)	**[KWIKG]**	**[1]**
Undercut Anchor (Maxi-Bolt)	**MAXIB**	**3**
Undercut Anchor [High-Strength] (Maxi-Bolt)	**[MAXHS]**	**[1]**
Undercut Anchor [HS with Anchor Gel] (Maxi-Bolt)	**[MAXHG]**	**[1]**
Threaded Rod Adhesive Anchor (Hilti-HAS)	HASAA	3
Wedge Rod Adhesive Anchor (Hilti-HIT-TZ)	HITTZ	3
HY-150 Adhesive Coated to Plate	HY150	1
3M Epoxy Coated to Plate	3MEPX	9
Total Number of Tests		50
Total Number of Tests Discussed in This Thesis		**25**

5.3 CONCRETE CASTING

Fifty concrete blocks were cast for the single-connector, direct-shear static load tests on a day when the temperature reached 95 F. All blocks were cast from the same batch of concrete. The concrete blocks were cast in fiberglass molds intended for waffle-slab construction (Figure 5.1), since the interior of the molds

had virtually the same plan area as the original design of the concrete test blocks. The original design called for a plan area of 24 in. square to avoid edge effects, and a depth of 7 in. to represent the deck of a typical candidate bridge. The waffle-slab molds were tapered vertically with a 23.5-in. square plan area on the top and 22.5-in. square plan area 7 in. below the top. The brim, shown in Figure 5.1, denotes the top of the form.

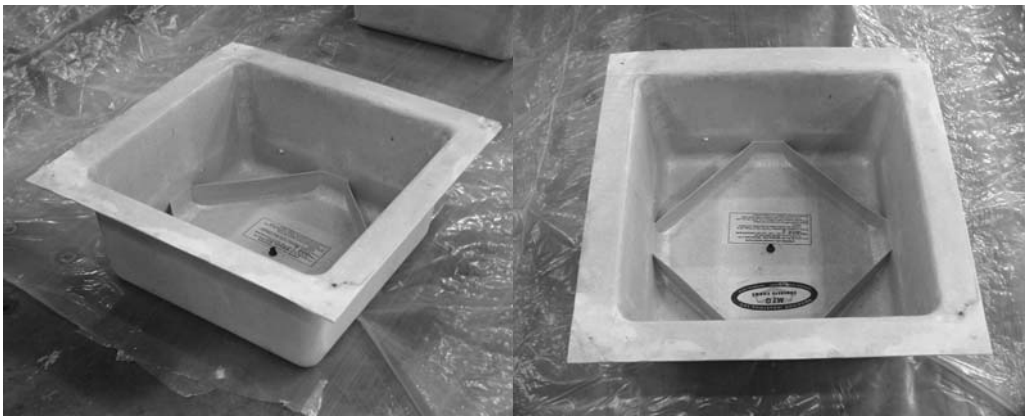

Figure 5.1: Fiberglass mold used as forms for casting concrete blocks

The waffle-slab molds were 12 in. deep, so plywood was set on reinforcing bar chairs at the bottom of the form (Figure 5.2) to reduce the depth to 7 in. A bead of sealant was placed around the edge of the board to ensure no concrete paste drained through to the bottom of the form. Next, the form was coated with oil to debond the concrete from the form; finally, the reinforcing bar cages were placed into the forms (Figure 5.3).

The reinforcing bar cages were designed to represent the standard candidate bridge slab, as shown in Figure 4.3 of Chapter 4. Stirrups (#3 size) were placed to extend above the top of the block, to enable the blocks to be lifted and maneuvered easily. Figure 5.3(a) shows a typical reinforcing bar cage sitting on four 1.5-in. reinforcing bar chairs that provided the required clear cover. Figure 5.3(b) shows all 50 forms with cages set prior to casting.

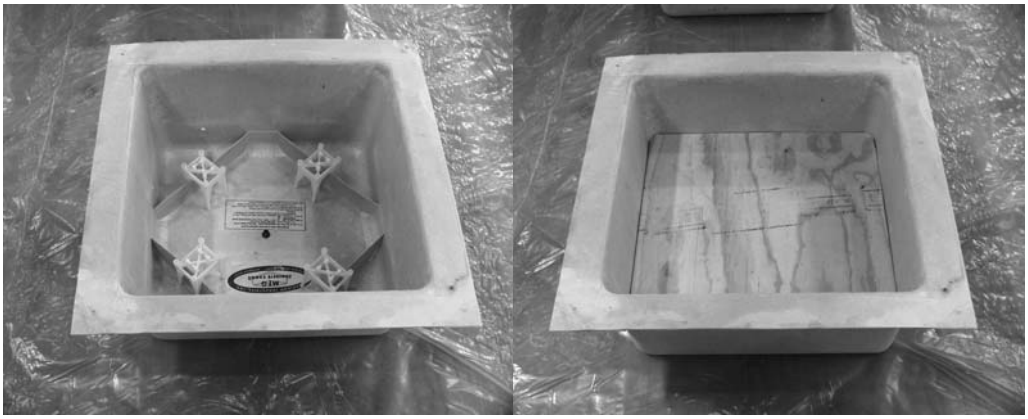

Figure 5.2: Creating 7-in. depth: (a) Reinforcing bar chairs to hold plywood; (b) Plywood

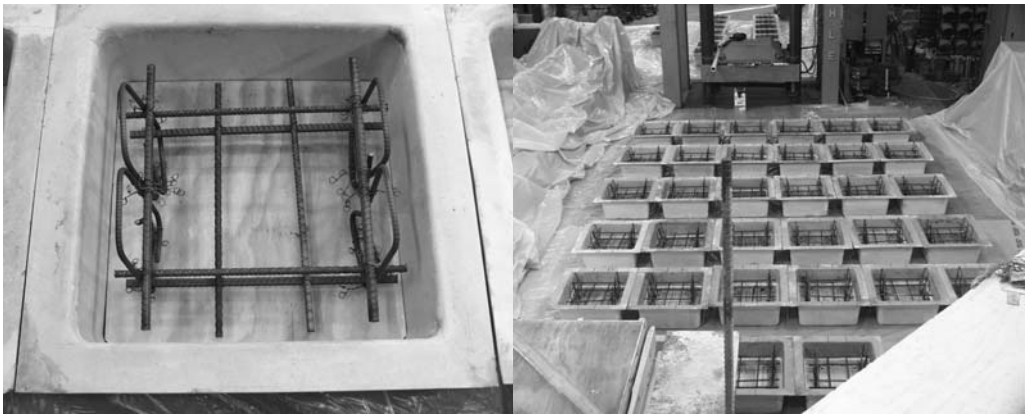

Figure 5.3: Reinforcing bar cage(s)

The concrete was ordered in one batch of five cubic yards (5 yd^3), as described in Section 5.4.1. Concrete was poured into each of the forms in one lift using a one-cubic-yard bucket. The edges of the forms were filled first so the reinforcing bar cages would not rise up when the concrete was placed. This was successful. The concrete was vibrated briefly, screeded and trowelled. At the time of casting, it was planned to use the top of the slab as the steel-concrete interface in the tests. Because the steel plates were to be placed on top of the forms, care was taken to trowel smooth only the center of the block (Figure 5.4),

leaving the edges only roughly trowelled. It was later decided to place the steel plate on the other side of the blocks, requiring the blocks to be turned over and making the uneven top surface a hindrance. This point is explained further in Section 5.7.2.

Figure 5.4: (a) Pouring and vibrating concrete; (b) Finishing concrete

The steel plates were placed on the fresh concrete about 15 minutes after trowelling, to allow the air bubbles and paste to rise to the top first. The steel plate was gently moved back and forth into position to ensure a smooth interface, as shown in Figure 5.5.

Figure 5.5: (a) Steel plate placed into position; (b) Completed pour

After casting, large plastic sheets were placed over the blocks, as shown in the upper corners of Figure 5.3(b). Twice daily for five days, the sheets were lifted and the concrete was sprayed with water. After five days, the sheets were removed and the blocks were allowed to air-cure.

5.4 MATERIALS USED IN TESTS

The properties of the concrete, steel plate, and connector materials are discussed in the following sections.

5.4.1 Properties of Concrete Used in Blocks

The concrete used in the single-connector, direct-shear static load tests was a 4-sack mixture design with ¾-in. aggregate and Pozzolith® retarder, a type of admixture often used in bridge construction during the summer in Texas. Discussions with TxDOT indicated that the original specified compressive strength of concrete used in older candidate bridges was in the range of 2500 to 3000 psi. The specified compressive strength of concrete for the test blocks was 2500 psi with a 4-in. slump. Expected entrapped air was 1 to 2 %. The water-cement ratio was 0.40 by weight. The mixture design (Capitol Aggregates Mixture Design #261) is given in Table 5.2. The percent difference between the specified quantity of a given component and the amount actually batched is given in the far-right column of the table.

Table 5.2: Mixture design, weights per cubic yard of concrete

Component	Description (Source)	Specified Quantity	$\frac{Batched - Specified}{100 \times Specified}$
Type I Cement	ASTM C150 (S.A.)	376 lb	-0.3
Fine Aggregate	ASTM C33 (Aus)	1541 lb	-0.3
¾-in.Course Aggregate	ASTM #67 (Aus)	1927 lb	-0.2
Water	TXDOT 421/ AASHTO T-26	151.2 lb	-1.8
Pozzolith® 100 XR	Master Builders Type B & D	5.6 oz	0.0
S.A.-San Antonio, TX; Aus-Austin, TX;			

Pozzolith® used has the following effects (Masterbuilders 2004):

- increased compressive and flexural strength (especially early-age);
- increased durability;
- reduced water content required for a given workability; and
- retarded setting characteristics.

As delivered, the concrete had a slump of 6 in. rather than 4, but since a low compressive strength was desired, the batch was accepted. Figure 5.6 shows the development of strength of the concrete over the first 28 days. Three cylinder tests were performed at 7 days, 14 days, and 28 days; two cylinder tests were performed at 21 days. The concrete had an average 28-day compressive strength of 2960 psi. The admixture is claimed by the manufacturer to give the concrete high early strength, and increase the workability

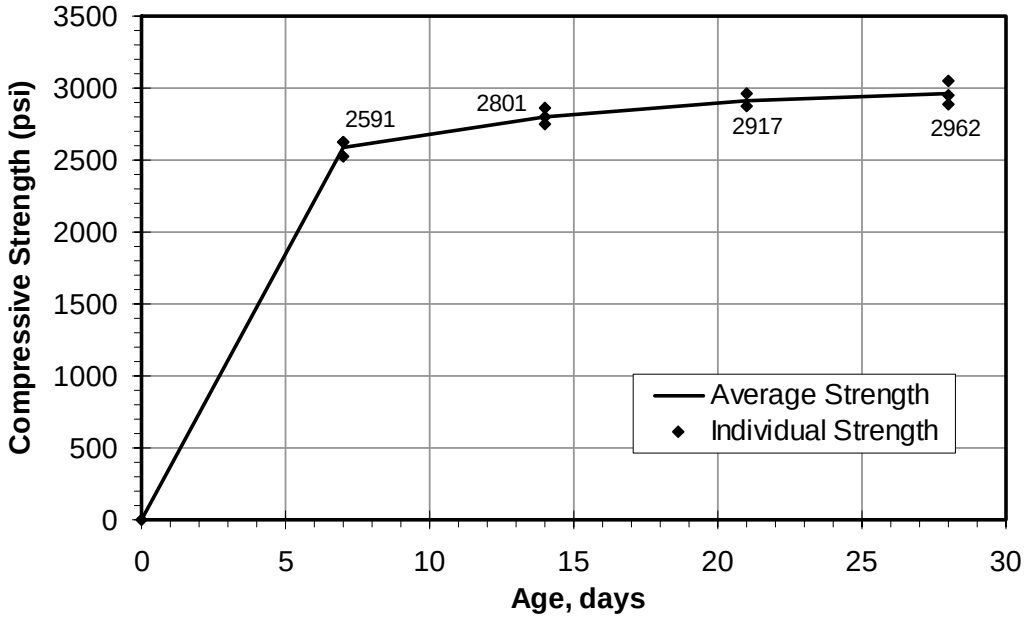

Figure 5.6: Compressive strength of concrete over first 28 days

The age of the concrete at time of testing ranged between 41 days and 202 days, and compressive strengths ranged from 3200 to 3500 psi based on three cylinders tested monthly.

Of the fifty test blocks cast, only one was reused. One block previously used for an undercut anchor test was reused (with the connector removed) for a pilot test using HY-150 epoxy coated to the steel plate to transfer the shear. When a capacity of only 6 kips was achieved, this slab and corresponding steel plate were discarded.

5.4.2 Properties of Steel Used for Plates

The steel used for the plate was specified to have a minimum yield strength of 36 ksi, approximately equivalent to the specified minimum yield strength of the girders in a typical candidate bridge, typically ASTM A36 (F_y = 36 ksi) or A7 (F_y = 33 ksi) steel.

Two displacement-controlled tension tests were performed following ASTM E8 on a 6- x 1- x ¼-in coupon of the steel plate taken perpendicular to the length of the plate (transverse to the rolling direction). The coupons were milled by the laboratory machinist to the required dimensions and tolerances of ASTM A370.

A typical stress-strain curve, for the second steel coupon (Figure 5.7), shows no drop in stress after the proportional limit. The results of the first coupon test differ from the second by less than 1 %. Three static yield points were obtained for each coupon test and are shown in the yield plateau of Figure 5.7. A static yield point is defined here as the lowest stress attained after loading has been halted for 3 minutes. The distortion in the plot at a strain of about 0.025 % is due to an increase in loading rate after strain hardening had begun.

On average, the steel had an dynamic yield strength of 43.0 ksi based on the 0.2-percent offset. The average static yield strength was 39.9 ksi based on the average of six static yield points. The average dynamic ultimate strength was 66.9 ksi. The average ratio of dynamic yield strength to ultimate strength was 0.64. The average ultimate strain was about 34 % based on a 2-in. gage length.

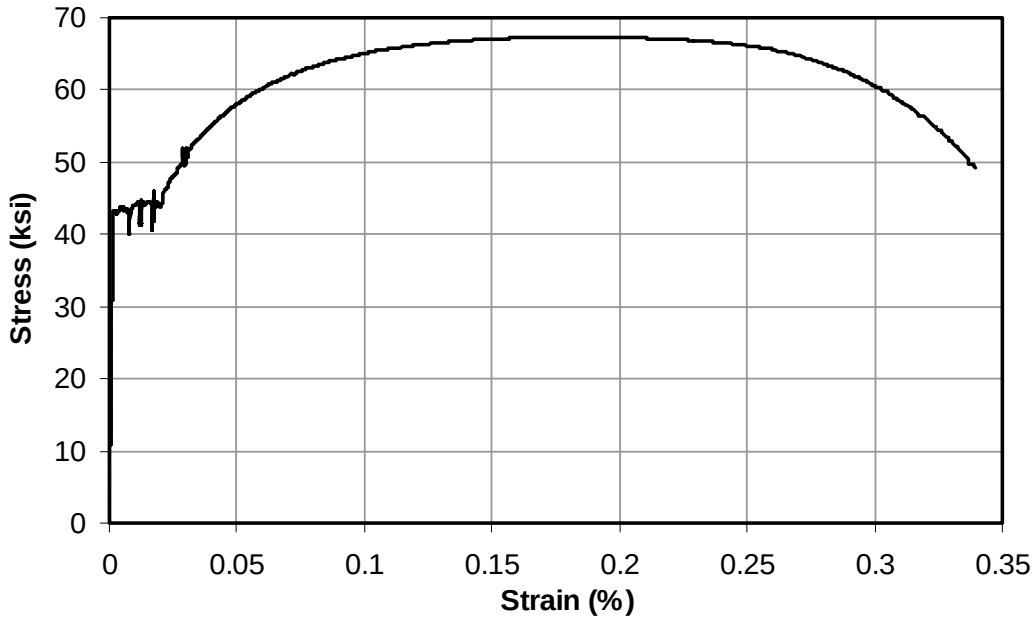

Figure 5.7: Typical stress-strain curve for steel used for plates

A hole was required in the each of the steel plates so the 1¼-in. clevis bolt could pass through. Figure 4.5 of Chapter 4 shows a schematic of the test setup. The center of the hole was placed 2.5 in. from the leading edge for each of the steel plates. All holes for the clevis bolt were drilled using a Slugger™ drill with a 1-5/16-in. diameter annular bit, with the exception of the steel plate used for the expansion anchor test (KWIKB). The center point for the connector hole was placed 20.5 in. from the leading edge of the steel plate, and the hole diameter varied depending on which connection method was being tested. All holes for the connectors were drilled using the Slugger™ drill. Figure 5.8 shows a diagram of the steel plate with the locations for the clevis bolt and connector marked.

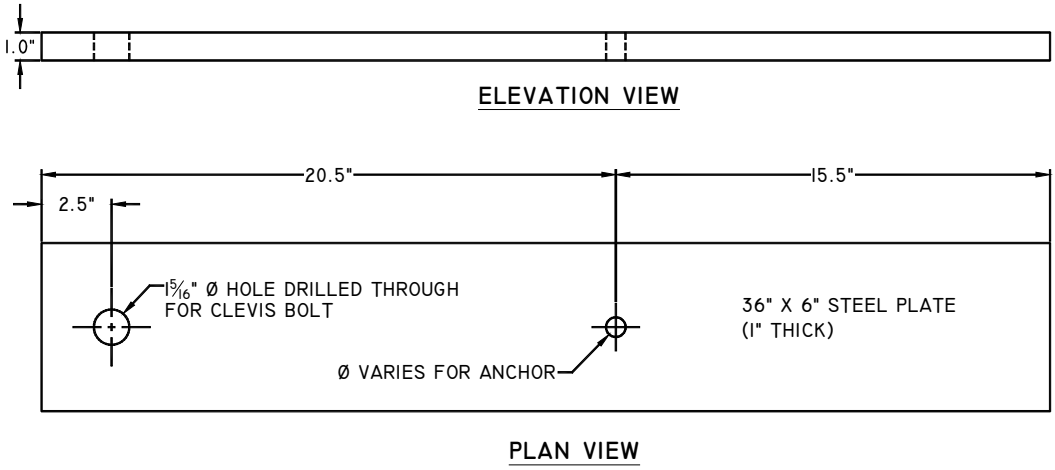

Figure 5.8: Hole locations in steel plate

Originally, an attempt was made to use a drill press located in the laboratory facility for the holes in the steel plates for the expansion anchor tests. Three replicates were originally envisioned. It was cumbersome to clamp the steel plate down for each hole, however, and it was believed that drilling multiple steel plates simultaneously presented a significant danger. In addition, oil still had to be used to cool the drill bit and was more difficult to clean up. The Slugger™ drill was self-contained and cleanup was easy because drilling was performed over a disposable plastic sheet that captured the oil and shavings. The final and perhaps most significant reason for using the Slugger™ is it would be the drill most likely used in the field for this type of retrofitting. Near the end of this phase of testing, it was realized that the oil could be easily recycled by capturing it in a shallow pan.

No steel plates were reused for any of the connector testing. A steel plate used for one of the undercut anchor tests was reused for a pilot test using adhesive

to transfer the shear as described in the section above. The test was showed poor performance, and the reused steel plate and slab were discarded.

5.4.3 Additional Information on Connectors Tested Here

As discussed in Chapter 4, all connectors had a ¾-in. nominal diameter except the HTFAT friction-grip bolts, which had a nominal diameter of 1¼ in. Originally, lower strength grades of steel (for example, A36) when available, were chosen for the connectors in an attempt to ensure ductile behavior of the connector and prevent breakout of the concrete. Thus, the original tests conducted on the expansion, undercut, adhesive, and concrete screw connectors used low-carbon steel with a specified yield strength of about 36 ksi. Although the actual yield strengths were larger than this (as observed from the pre-tension force applied), once it was shown breakout did not occur, two undercut anchors of ASTM A193-B7 steel were tested. This material is equivalent to ASTM A325 material, with a specified minimum tensile strength of 120 ksi. Since the expansion anchors showed poor structural performance (high slip and low capacity), they were and not considered further.

The welded studs used in the experiments were supplied by Alpha Stud Welding of Houston, Texas. The bolts, nuts and washers for the double-nut bolts and high-tension, friction-grip bolts were supplied by Austin Bolt Company. The nuts and washers for the expansion and undercut anchors were provided by the respective manufacturers. Only the welded studs had a certified material report providing the mechanical properties. A sample connector from each connection method was installed in a installation test block prior to testing to ensure proper installation.

5.4.3.1 Welded Connectors (Cast-in-Place Stud, Post-Installed Stud and Stud Welded to Plate)

Stud welding was performed by a technician of Alpha Stud Welding in Houston. Figure 5.9 shows a picture of a welded headed stud, used for the cast-in-place and post-installed connection methods.

Figure 5.9: Standard welded stud

Figure 5.10 shows the stud welded to plate components used for testing. The fillet weld shown in Figure 5.10(b) used E70 electrodes and was performed by a Ferguson Laboratory technician. Table 5.3 shows the properties reported by the manufacturer (Stud Welding Associates, Elyria, Ohio), for a specific heat of 5,760 studs.

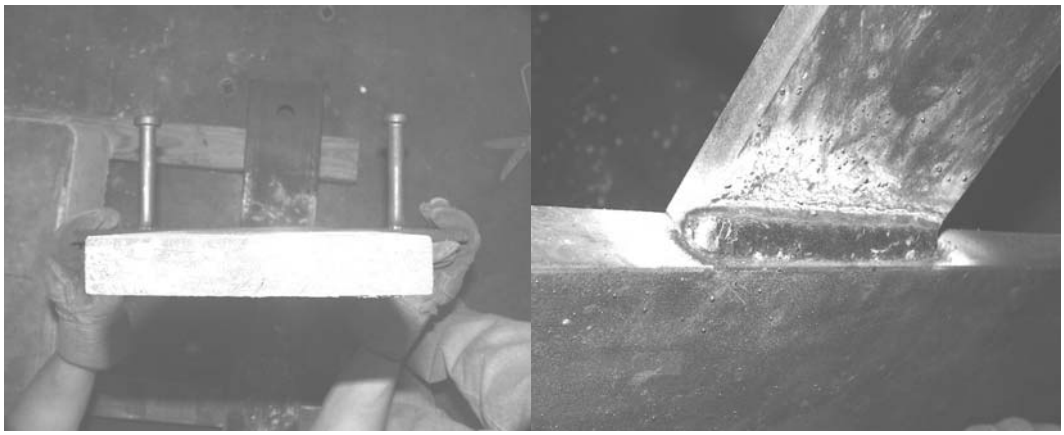

Figure 5.10: Stud welded to plate

Table 5.3: Material properties for welded studs

	AISI Grade	Minimum Yield	Minimum Tensile	Elong. (%)	Rdctn (%)
Welded Stud	C1015	53,100 psi	66,200 psi	28.8	67.8

5.4.3.2 Double-Nut Bolt

The connector used for the double-nut bolt was a Grade 8 tap bolt (entire shank threaded) as shown in Figure 5.11. Grade 8 material is comparable to ASTM A490 material, which has a specified ultimate tensile strength of 150 ksi. The bolts were 8 in. long and threaded the entire length of the shank. Three heavy hex nuts conforming to the requirements of ASTM A563 Grade DH were used. Two nuts were placed on the top (concrete side of the steel plate) to prevent twisting during tightening, and one on the bottom side for tightening. Steel washers meeting the requirements of ASTM F436 were used on both sides of steel plate. A large threaded length was required because three nuts were required in addition to the steel plate. Tap bolts were chosen because of the lower cost compared with threading a standard bolt an extra inch or two.

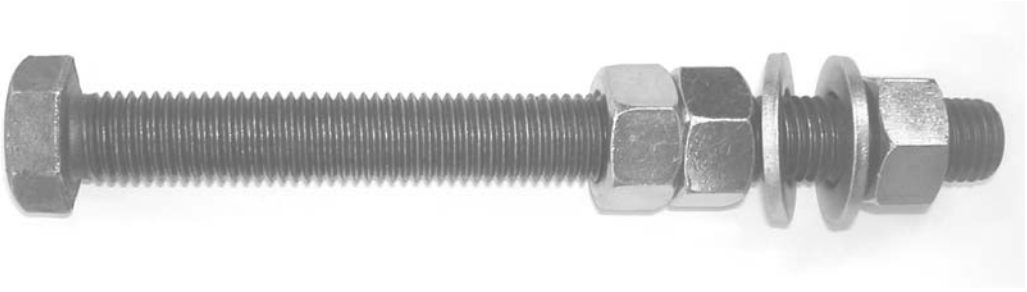

Figure 5.11: Double-Nut Bolt

5.4.3.3 High-Tension, Friction-Grip Bolt

Two diameters and strengths of standard structural bolts were used in the testing program: an A325 ¾-in. diameter and an A490 1¼-in. diameter with minimum specified ultimate tensile strengths 120 ksi and 150 ksi respectively. Each bolt was 7 in. long (Figure 5.12 and Figure 5.13). Heavy hex nuts conforming to ASTM A563 Grade DH were used with the high-tension, friction-grip bolts. Hardened steel washers meeting ASTM F436 were used on both sides of the slab. For the ¾-in. diameter bolt, a standard washer was used with an outside diameter of 1-15/32 in. Research presented at an ACI-355 meeting showed from experiments on bolts that the crushing strength of the concrete could reach $8 \times f_c'$ due to confining effects (Klingner 2003). By calculation, this was sufficient to prevent crushing under the preload given the size of the standard washers. With this in mind a standard 2½-in. O.D. washer was initially used for the 1¼-in. diameter HTFAT bolt. Cracks were observed in the installation test block, however, when it was installed. A 3-in. O.D. washer was subsequently used to lower the stress on the concrete.

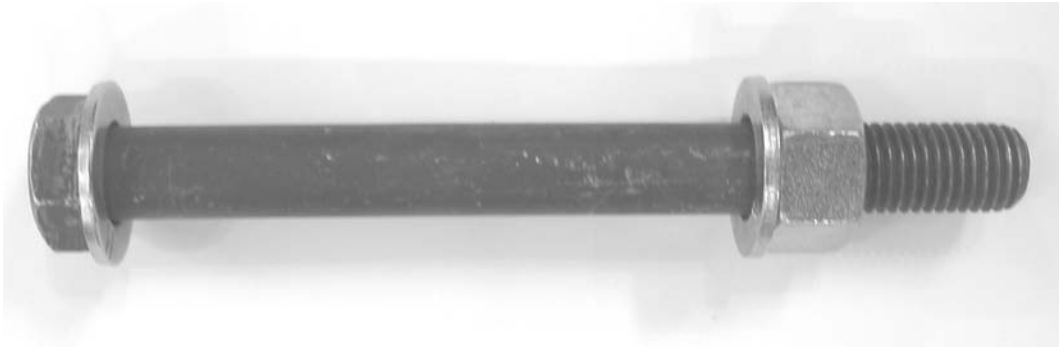

Figure 5.12: High-Tension, friction-Grip Bolt (¾-in. diameter)

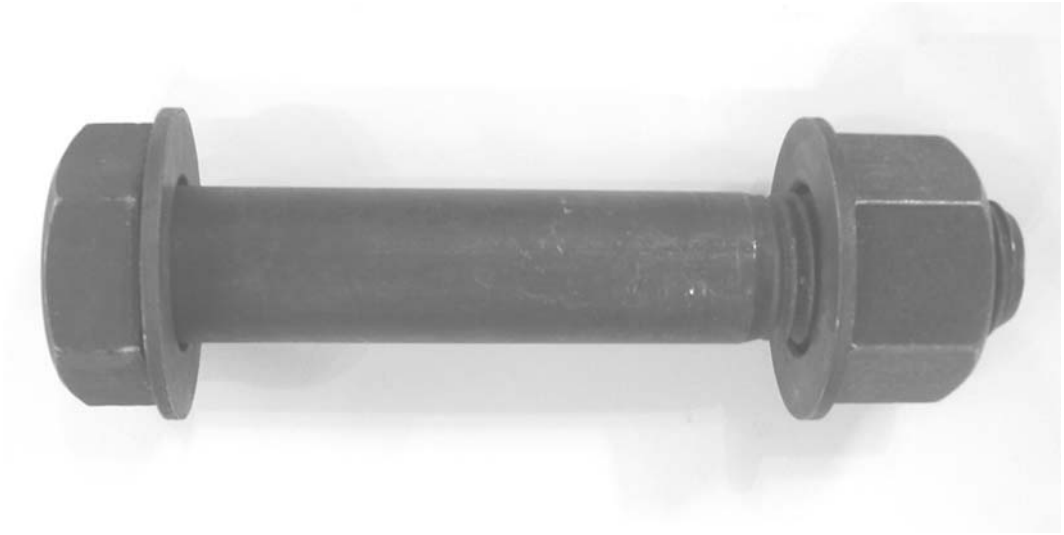

Figure 5.13: High-Tension, friction-Grip Bolt (1¼-in. diameter)

5.4.3.4 Expansion Anchor

The expansion anchors were designated by the manufacturer as Hilti Carbon Steel Kwik-Bolt II ¾-8, as shown in Figure 5.14. The following material properties are taken from the Hilti Product Technical Guide 2002 Edition (Hilti 2002). The expansion anchors were made of ASTM A510 carbon steel (F_y = 41 ksi; F_u = 75 ksi) with chemical composition of AISI 1038. The wedges are manufactured from AISI 1010 carbon steel. Nuts are carbon steel conforming to ASTM A563 Grade A, and meet dimensional requirements of AISI B18.2.2. Washers are carbon steel conforming to SAE 1005-1033, and meet dimensional requirements of ANSI 18.22.1 Type A Plain. All carbon steel parts are zinc-plated in accordance with ASTM B633, Type III Fe/Zn 5.

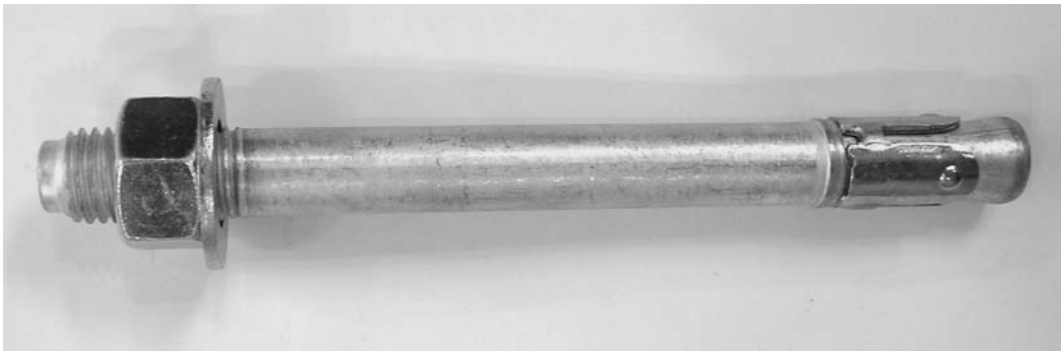

Figure 5.14: Expansion Anchor

5.4.3.5 Undercut Anchor

Two strengths of undercut anchors were tested. The standard test connection method used Drillco A36 Maxi-Bolts ¾-in. x 9-in. with a 6-in. sleeve. The bell-shaped portion of the connector, called the conical nut, is made of ASTM A193-B7 material. The expansion sleeve is ASTM A513 Type 5 material. An A325 washer is used with a heavy hex nut conforming to ASTM A194 Grade 2H standards.

To obtain higher clamping force, the higher-strength ASTM A193 Grade B7 Maxi-Bolt was also used. Only the specified material strength changed for this connector; the conical nut, expansion sleeve, washer, and nut were made of the same materials listed above.

Figure 5.15: Undercut Anchor (A36 or ASTM A193-B7)

Finally, one additional modification was made to the high-strength undercut anchor. An anchor gel was placed around the connector in the concrete and steel to fill the gap to reduce movement of the connector in the hole before bearing against the edge. Five-Star® RS Anchor Gel ("RS Anchor…" 2004) was used and is discussed in Section 5.4.5.

5.4.4 Grout

Grout was required for the following connection methods investigated here: post-installed welded stud (POSST); double-nut bolt (DBLNB); stud welded to plate (STWPL); welded-threaded rod (POSTR); and the high-tension, friction–grip bolt (HTFGB). The researchers investigated several different types, looking for the following characteristics:

1) the grout had to be at least as strong as the hardened concrete (3000 psi);
2) the grout had to reach this strength quickly, since the bridge would have to be closed for the time it took the grout to reach the specified strength;
3) the grout could not shrink significantly, which would cause it to crack and allow water around the connector, nor could it significantly expand and cause high stress to the surrounding concrete. Thus, a non-shrink grout was desired; and
4) the grout had to be effective in small spaces (for example, 2-in. diameter for the stud welded to plate connection method) and large spaces (for example, 3.5-in. diameter for the post-installed welded stud connection method).

The grout selected for this project was Five-Star® Highway Patch ("Five-Star..." 2004), which met all desired characteristics. The grout has a 2-hour

compressive strength of 2000 psi, a 1-day strength of 5100 psi, and a 7-day strength of 7000 psi based on the ASTM C109 standard ("Five-Star..." 2004). The shrinkage of ±0.05 % is effectively negligible.

This one-part blend of dry cement and fine aggregate was mixed with the appropriate amount of water (Table 5.4) using a power drill and mixing paddle (Figure 5.16).

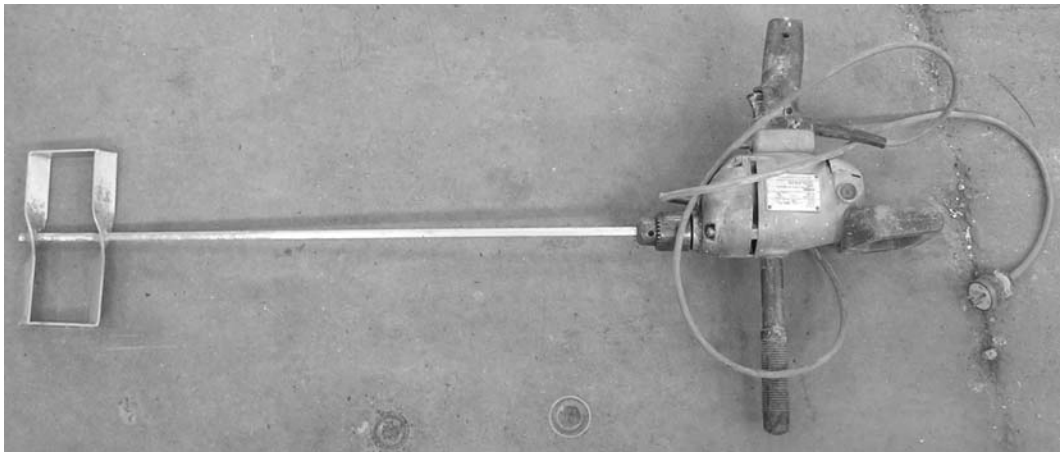

Figure 5.16: Grout mixing paddle

Table 5.4: Grout proportions per cubic ft of grout

Component	Quantity
Five-Star® Highway Patch Mix	125 lb.
Water	5925 mL. (Min.); 7110 mL. (Max.)

5.4.5 Anchor Gel

A structural epoxy was used to fill the gap between the connector and the hole for some of the connection methods, such as the undercut anchor and concrete screw. Five-Star® RS Anchor Gel, a two-part epoxy commonly used to fill cracks in concrete, was recommended by the manufacturer for this application. It is mixed in a one-to-one volume ratio using a mixing gun and nozzle. It meets

the requirements of ASTM C881 Types I and IV, Classes B and C, Grade 3. The manufacturer asserts that the gel consistency can be ideal for vertical and overhead surfaces and is used for grouting bolts, dowels, pins, and special fasteners ("RS Anchor..." 2004). Five-Star® RS Anchor Gel has a bond strength of 2900 psi at 2 days, and a compressive strength of 10,800 psi. Although the data sheet for the product does not specify the curing time required to achieve this compressive strength, a Five-Star representative stated that it could be reached in 6 to 8 hours. The epoxy has a gel time of 7 minutes at 73 F by ASTM C881. The manufacturer recommends not filling a gap larger than ¼ in. Five-Star® RS Anchor Gel was used on one high-strength undercut anchor (MAXHG); three concrete screws (WEDGG); and two welded-threaded rods (POSTR).

5.5 INSTALLATION OF CONNECTION METHODS

This section outlines the installation of the six connection methods discussed in this thesis. Chapter 3 included a schematic diagram and general installation steps for each connection method.

Although the original intent was to place the steel plate on the top, finished face of the slab, several concerns about the finished surface led to using the bottom surface instead. Despite waiting fifteen minutes after vibrating for the paste to rise to the surface, the steel plate [Figure 5.5(a)] trapped air, creating voids under the steel plate during initial curing on most of the blocks. Ridges of paste formed under the plates, and some laitance collected there as well. Because of the ridges, not all steel plates fit flush against the concrete while maintaining when the plate was oriented in the plane of the interface so that its edges were parallel to the edges of the test block. Thus, if a test was performed, there could be eccentricity in the loading. The bottom surface of the slab, in contrast, was

more representative of the interface in the candidate bridges, with no voids, ridges, or laitance.

The effect of the aggregate settling towards the bottom would not be captured if the block was used as designed. It was believed any natural settling of aggregate might lead to a lower strength and stiffness of the concrete if the top were used as the interface. For all of these reasons, it was decided to turn the blocks over for testing. Consequently, the face of the block cast against the plywood base in the form faced upwards, and the steel plate was attached to this surface.

Because the block was turned over, the reinforcement, which was asymmetric about the horizontal axis, was not as representative of a candidate bridge. It was believed, however, and other research has indicated (Tadros, Badie and Girgis 2001), that sufficient confinement is achieved by simply running the transverse reinforcing bars continuously along the girder lines. Since the slab contained both top and bottom reinforcement in both the longitudinal and transverse directions, the test results should not be significantly affected. Since the cast-in-place benchmark tests were cast when it was intended to use the finished surface as the interface, these tests were conducted with the reinforcement (and slab) in the opposite configuration to all other tests. As stated above, this is believed to have made little difference.

Each connector for the single-connector, direct-shear static load tests was installed in the center of the bottom of the slab. The center point was measured individually for each test with a carpenter's square. A 5-in. nominal embedment depth was created using a rotary hammer dill at the time of testing for most of the connectors. A pre-fabricated hole was formed in the concrete using PVC pipe for the post-installed welded studs. The carpenter's square was used to visually ensure that the drill was perpendicular to the slab. The expansion and undercut

anchors were installed into the concrete slab after the slab was placed into the test setup. The other connectors were installed prior to placing the concrete block into the test setup. Setup of static load tests is discussed further in Section 5.7.2.

5.5.1 Preparation of Welded Connectors for Installation

Before casting the concrete blocks, eight standard steel test plates (36- x 6- x 1-in.) and six smaller plates (5- x 5- x ½-in.) were taken to Houston, Texas to have one connector welded to each plate at Alpha Stud Welding Company. The certified welder performed several test runs before welding ¾- x 5-3/16-in. headed studs to the pre-marked locations on six of the standard steel plates. Three of these were used for the cast-in-place welded stud tests, and the other for the post-installed welded stud tests. The final two standard steel plates had ¾- x 6-3/16-in. rods with 10 threads per in. stud welded to the pre-marked locations. These welded threaded rod tests are discussed by Hungerford (2004). A welded headed stud was attached to each of the smaller plates. These smaller plates were used for the stud-welded-to-plate connection method.

The headed studs were 3/16 in. longer than the installed required length because this additional material was melted and used in the root of the weld. Thus, the final length of the installed studs was 5 in.

5.5.1.1 Installation of Cast-in-Place Welded Studs

Since the cast-in-place benchmark tests were cast when it was intended to use the finished surface as the interface, these tests were conducted with the reinforcement (and slab) in the opposite configuration to all other tests. As stated above, this is believed to have made little difference.

This connector was installed in three steps:

1) Before the concrete was cast, the steel plates with the pre-welded studs were marked so that they could be placed with the stud in the center of the concrete slab as in all other tests.
2) Concrete was poured into the form around the reinforcing bar cage, vibrated, and finished smooth on top.
3) The studs were gently moved back and forth into the concrete, and the concrete was vibrated lightly around the stud. Special care was taken to ensure that the vibrator did not touch the steel plate, stud, or reinforcement during the final vibrating.

Hungerford (2004) gives more detailed information on all aspects of the cast-in-place welded studs. Since these connectors were used as the benchmark against which to compare other tests, general installation procedures are repeated here.

5.5.1.2 Installation of Post-Installed Welded Studs

In the field, a coring machine would be used to make a hole large enough to fit a stud-welding gun (3.5-in. diameter). Since the coring machine requires a larger surface area to clamp it down than permitted by the 2-ft. by 2-ft. concrete slab, a hole was pre-cast in the test block. This connector was installed in eleven steps:

1) Before casting, a PVC pipe (3.5-in. O.D. by 7-in. high) was placed into the center of the form to create a void representing a cored hole that would be produced in the field.
2) A bead of sealant was placed around the bottom ring of the PVC cylinder to adhere the pipe to the plywood bottom of the form.

3) Duct tape was placed over the top of the PVC pipe so that no concrete would fall into the hole. The tape was slit down the center after the concrete had been placed, vibrated, and finished.
4) The three standard steel plates with headed studs welded to them were placed onto the wet slab [as shown in Figure 5.5(a)] with the stud placed into the PVC pipe through the slit in the tape. These last two steps were inconsequential since the bottom of the slab was used, as discussed earlier.
5) The PVC pipe was gently tapped out with a hammer, leaving a smooth void similar to that left by a coring machine.
6) The researchers wanted to prevent shrinkage cracks from forming in the grout. Because the void had a high surface area and a low volume, a large amount of water was expected to be absorbed from the grout by the hardened concrete. To prevent this, the concrete around the void was saturated by filling the void with water-soaked paper towels 24 hours before placing the grout.
7) The steel plate was placed on the laboratory floor, with the welded stud pointing upward.
8) A bead of sealant was placed around the bottom of the concrete block (the face that would make the steel-concrete interface). The sealant was used to prevent any paste from the grout from leaking through the interface.
9) The block was placed onto the steel plate so that the connector was centered in the hole.
10) Five-Star® Highway Patch grout (Section 5.4.4) was placed into the hole and puddled thoroughly to eliminate voids.
11) The top of the hole was leveled smooth with a flat piece of wood.

Using impermeable 4- x 8-in. molds, several cylinders of grout were cast for each test block so an accurate strength could be obtained, based on the average of the cylinder tests. The grout was allowed to cure for at least one day and cylinders were tested immediately before performing the static load test. Chapter 6 reports the results of the compressive strength of the grout mixes.

5.5.2 Installation of Stud Welded to Plate

The installation of this connector is similar to the installation for the post-installed welded stud, so reference is made to the installation of that connector. This connector was installed in nine steps:

1) A headed stud was welded to each of six smaller 5- x 5- x ½-in. steel plates in the shop.
2) Two of these smaller plates were fillet-welded to the steel plate representing half of the girder flange, so that the welded studs were in the same location longitudinally as the other connection methods tested.
3) The small plates were placed flush with the interface of the concrete and steel (Figure 5.9).
4) Using a rotary hammer drill, two 2-in. diameter holes were drilled through the concrete for the studs. The holes were drilled from the bottom side only, causing some breakout on the top of the concrete block, as noted in Chapter 6.
5) Steps 7 through 11 of the post-installed welded stud installation procedure. The holes were not presoaked with water prior to casting the grout.

This is the only connection method in which two connectors were tested in a group.

5.5.3 Installation of Double-Nut Bolt

The installation of this connector is similar to the installation for the post-installed welded stud, so reference is made to the installation of that connector. This connector was installed in nine steps:

1) A 13/16-in. hole was drilled into the steel using a Slugger™ drill. This diameter was chosen because it was readily available, and would likely be used in the field. It is believed that a ¾-in. diameter hole could have been used, however, since the holes in the concrete and steel are match-drilled, that is, drilling is performed from only one side of the bridge so that the hole drilled in the concrete is concentric to the hole drilled in the steel. Making the hole ¾ in. in diameter would minimize slip, but might increase difficulty of installation.
2) Two nuts were placed on the tap bolt so that when the nuts and washer sat against the steel plate, the top of the head of the bolt was 5 in. above the steel plate. A nut, standard washer, and "Squirter Direct Tension Indicator (DTI)" load-indicating washer were placed on the bottom of the steel plate. The nut was tightened to the specified minimum pre-tension of the bolt utilizing the DTI washer.
3) A 2-in. diameter hole was drilled through the concrete using a rotary hammer drill. The holes were match-drilled from both sides to prevent breakout of the concrete.
4) Steps 6 through 11 of the post-installed welded stud installation procedure.

The installation of this connection method was the only one in which a handheld cordless drill with a small propeller-like attachment was used for the grout mixing. This proved to be inadequate, resulting in a poorly mixed grout that

had lower strength than the other mixes. This is discussed further in Chapters 6 and 7.

5.5.4 Installation of High-Tension, Friction-Grip Bolt

The ¾-in. ASTM A325 high-tension, friction-grip bolt was installed in seven steps.

1) A 2-in. diameter hole was drilled 2.7 in. deep into the center of the finished side of the concrete slab using a rotary hammer drill, creating a nominal embedment depth of 4.3 in. for the bolt. The depth was chosen such that the top of the head of the bolt was 2 in. below the top surface of the concrete block to meet clear cover requirements [2 in. (Clear Cover) + 15/32 in. (Bolt head thickness) + 0.177 in. (maximum washer thickness) = 2.70 in.]. For Specimen HTFGB01, the hole was accidentally drilled one in. too deep, leaving an embedment depth of 3.3 in.
2) The bottom of the hole was made as flat as possible using a chisel.
3) The concrete block was turned over to avoid breakout. Pilot tests performed on a sample slab showed that drilling through the slab caused some breakout of the concrete. The center was marked again with appropriate adjustments made in the location of the center point if the 2-in. diameter hole was slightly off center.
4) A ¾-in. diameter hole was drilled through to the 2-in. diameter hole. Drilling the 2-in. diameter hole first prevented any breakout of the concrete for the ¾-in. hole. A standard 13/16-in. diameter hole was drilled into the steel plate for the bolt. As with the double-nut bolt connection method, a ¾-in. diameter hole could have been drilled to reduce slip when friction is overcome.

5) For the HTFGB01 and HTFGB02 tests, a bead of epoxy was placed around the 2-in. diameter hole under the washer to ensure a flat surface for bearing when tightening the bolt. The bolt and washer were placed into the hole prior to placing the epoxy. Holding the bolt and washer about 3 in. above the bottom of the hole, the epoxy was injected onto the bottom of the surface. Then the bolt and washer were pressed firmly into the epoxy and the excess epoxy was wiped away.
6) After the epoxy cured (approximately 1 hour after injection by manufacturer's specifications), the steel plate was attached onto the slab over the connector. The steel plate was oriented in the plane of the interface so that its edges were parallel to the edges of the test block. The third test did not use any epoxy.
7) For the first test, the bolt was tightened up to 28 kips, the specified minimum preload for a ¾″ A325 bolt, monitored using a washer load cell (Figure 5.16) with standard washers on each side. The bolt was pre-tensioned on the laboratory floor so the bolt head could be held to prevent the bolt from twisting. For the final two tests, a "Squirter DTI" load-indicating washer was used in conjunction with a standard washer to measure the preload.

The slab with the steel plate attached was lifted and placed into the setup for testing.

Figure 5.17: Washer Load Cell

5.5.4.1 Installation of High-Tension, Friction-Grip Bolt (1¼-in. Diameter)

The 1¼-in. diameter ASTM A490 high-tension, friction-grip bolt was installed using the same steps as above, with two exceptions:

1) First, a hole with an effective diameter of 3.5 in. was drilled 3 in. deep using a 2-in. diameter cruciform rotary hammer drill bit in four adjacent locations [2 in. (Clear Cover) + 25/32 in. (Bolt head thickness) + 0.177 in. (maximum washer thickness) = 2.96 in.], as illustrated in Figure 5.17. The nominal embedment depth was 4 in. for this connection method. The drilling proved difficult for the adjacent holes because the drill kept slipping into a hole already drilled, although it was manageable for drilling only a few inches into the concrete. This drilling technique is not recommended, however, for a hole that needs to be drilled all the way through the concrete slab. A coring machine would probably be preferable for such a situation.
2) Because a DTI washer was not readily available for this size bolt, the applied tension was estimated as a function of torque, using a Skidmore bolt tension calibrator. Once the desired tension was

obtained in the Skidmore, the applied torque was measured using a torque wrench, and the same torque was used to install the connector. The 1¼-in. diameter bolt was installed into the installation test block first, using a standard 2.5-in. O.D. washer. Upon tightening the connector, the block cracked. Thus, a 3-in. O.D. washer was used for this connection method. For the first test specimen, a bolt pre-tension of 75 kips was selected. The block slightly cracked under the final tightening, so slightly less torque was applied to the remaining bolts, resulting in a pre-tension of approximately 71 kips.

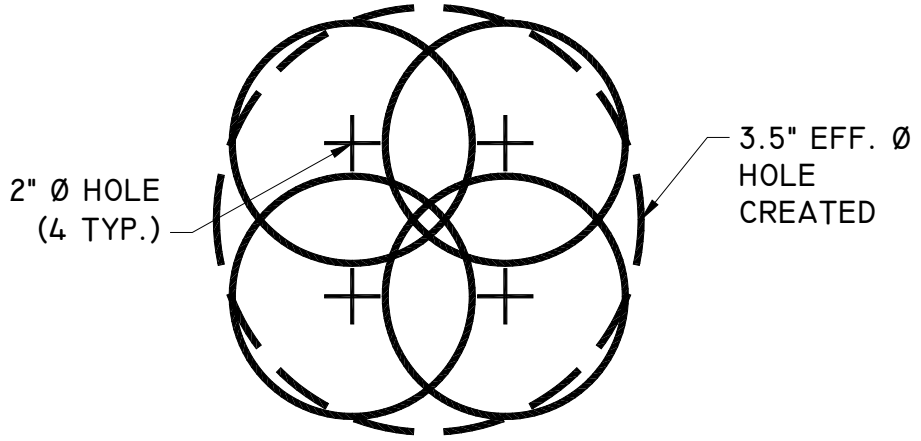

Figure 5.18: Method for drilling 3.5-in. hole with 2-in. rotary hammer drill bit for HTFAT connector

5.5.5 Installation of Mechanical Anchors

The mechanical anchors (expansion and undercut) were installed according to their respective manufacturer's instructions. Trial installations were performed on a installation test block for each connection method to ensure that the installation would be as specified. Mechanical anchors were installed after the

slab had been placed into the test setup because the bottom of the block does not need to be accessed. The connectors are held from twisting by their self-contained mechanisms, as opposed to a bolt, which requires the head to be held while the nut is turned. The expansion anchor uses dimples on the wedges to keep the bolt from twisting when the nut is tightened. The undercut anchor uses the friction of the conical undercut sleeve against the concrete to prevent twisting.

5.5.5.1 Installation of Expansion Anchor

The expansion anchor was installed in five steps:

1) A ¾-in. diameter hole was drilled 5.5 in. into the concrete using a rotary hammer drill, as shown in Figure 5.18. This is the standard hole depth to produce the specified effective embedment of 4-¾ in. The controlling minimum base material thickness of $1.3 \times h_{ef}$ (=6.175 in.) is met with the 7-in. concrete slab.
2) The hole was cleaned out using compressed air through a chuck.
3) The connector was tapped into the hole using a 2-lb. hammer. Hammering was necessary to place the connector since the wedge of the connector is larger than the connector's nominal diameter and the hole was drilled to that nominal diameter.
4) A steel plate was placed over the connector. The washer load cell (Figure 5.16) was placed onto the connector with hardened steel washers on both sides. The nut was tightened, using a torque wrench, to the manufacturer's recommended torque of 180 ft-lb (interpolated from tables, Hilti 2002).

For Specimen KWIKB01, the first test performed, the tension was taken off after 10 minutes, and reapplied to half of its original value. Then the connector was unloaded completely, the plate was realigned, and the

manufacturer's recommended torque was applied. This was done to account for any relaxation that might occur due to the increased concentrated load caused by the connector. Over the nearly six-month testing period, however, it was learned that in a real field application, the preload could be maintained using one of the methods outlined in Section 3.2.5.1 of Chapter 3. Therefore, the full preload was applied to the rest of the connectors, except MAXIB01, to realize the full benefit of pre-tension.

After tightening, the tension as measured by the washer load cell was read from the data acquisition system and noted to predict the shear at first slip. As discussed in Chapter 6, the applied tension corresponding to Hilti's recommended torque was relatively low. The Kwik-Bolt II is classified as a "medium duty" connector by the manufacturer. Its low cost and relative ease of installation made it a candidate for testing. As described in Chapter 6, however, its poor structural performance eliminated it from further consideration for this application.

An attempt was made to fill the gap between the connector and the concrete with Five-Star® Highway Patch grout in an additional test (KWIKG). Because the aggregate in the grout was too large and the connector could not be set properly, this test yielded exceptionally poor results.

Figure 5.19: Drilling into concrete with rotary hammer drill (Hole predrilled in plate)

5.5.5.2 Installation of Undercut Anchor

The Maxi-Bolt undercut anchor requires two more installation steps than the expansion anchor, and each step involves more detail than the expansion anchor:

1) First, a hole was drilled 6 in. into the center of the bottom of the slab using a 1.172-in. diameter carbide-tipped drill bit supplied by Drillco with a rotary hammer drill. This satisfied the minimum hole depth for this connector, which was 4½ in. according to the manufacturer.

2) The hole was undercut using the diamond insert blades of an undercutting tool (Figure 5.20) on a special undercutting drill (Figure 5.19) provided by the manufacturer. The drill used with the undercutting tool was a handheld, high-speed core drill rotating faster than 1000 RPM. The undercutting tool is about 4 ft long and approximately 1 in. in diameter, with undercutting blades inside its shaft. The drill has a spring-loaded mechanism that expands the diamond undercutting blades outward when the drill is pushed down against the concrete. The diamond blades cut away the concrete to form the undercut in only about 30 seconds when functioning properly. Water was poured into the hole prior to using the undercutting tool to keep the diamond blades cool.
3) The hole was cleaned out using compressed air through a chuck.
4) The anchor-setting tool (Figure 5.22) was screwed onto the threads of the Maxi-Bolt, and the arrangement was set on the shim plates. Steel plates with 1¼-in. holes were placed over the concrete to shim a special tool used to set the connector so that the sleeve would expand into the undercut hole. Similar adjustments had to be made when using the undercutting tool because the stop was set for a different embedment depth and could not be changed. The connector was placed into the hole with the sleeve in its original unexpanded position. By rotating the nut on top of the setting tool, the connector and conical nut were drawn upward, causing the sleeve to expand into the undercut hole. The setting tool has an automatic stop, ensuring that the sleeve is expanded the correct amount. At this point, the connector was loose in the hole and could be pushed to the bottom of the hole.

5) The steel loading plate was placed over the Maxi-Bolt. The washer load cell was placed and the connector pre-tensioned to the manufacturer's recommended load (11 kips) using the data acquisition system.

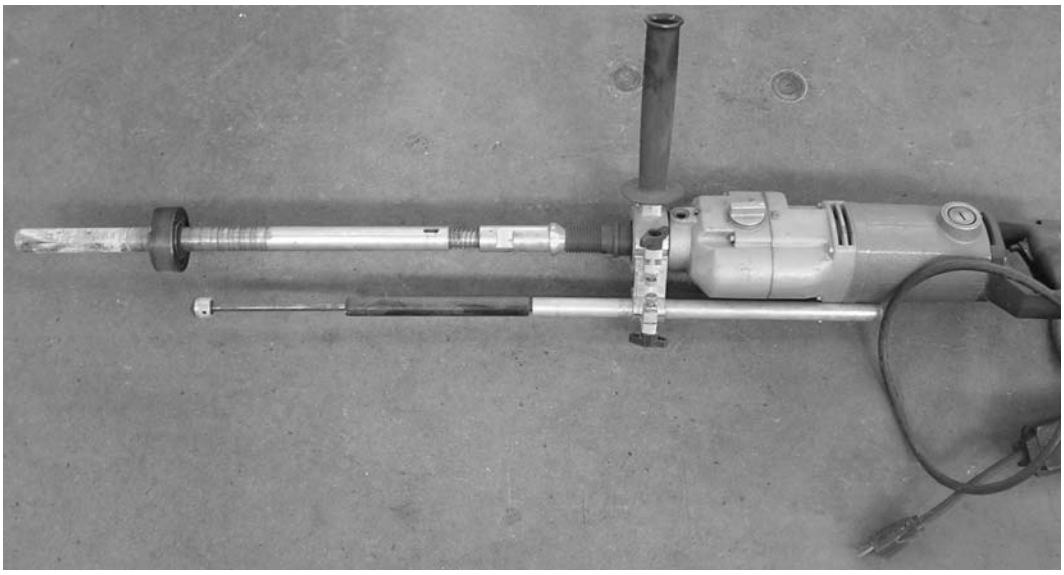

Figure 5.20: Undercutting Drill

Figure 5.21: Diamond insert blades on undercutting tool

Figure 5.22: Setting tool for undercut anchor

Several aspects of this installation procedure can cause difficulties. First, the depth of the undercut is somewhat difficult to judge. Next, the diamond

undercutting blades are very delicate and require water to keep them cool and sharp. If the diamond blades are only slightly chipped, the undercutting operation is not possible. Thus, the blades must be maintained in excellent condition. More discussion on the relatively difficult installation issues of the undercut anchor is given in Chapter 7.

A final point on the installation of the undercut anchors needs to be made. The expansion sleeve used on the standard undercut anchor is 5-in. long, which makes the top of the sleeve flush with the steel-concrete interface when installed into the hole. For most situations, a standard 1-in. sleeve is placed on top of the 5-in. expansion sleeve to fill the annular gap in the steel plate. For this application, however, where the purpose is to find a shear connection method with minimum slip, leaving the interface of the two sheaths at the steel-concrete interface may lead to poor structural performance. In place of the 1-in. second sheath, a 2-in. long sheath is available.

Therefore, three different installation techniques were investigated. For the first test for the undercut anchor connection method, no second sheath was used. For the second test, the standard 1-in. sheath was used so that the two sheaths met at the interface of the concrete block and steel plate. Finally, for the third test, the 5-in. sheath was cut 1 in. shorter, and the 2-in. second sheath was used so the sheaths did not meet at the steel-concrete interface. The results of the tests were significantly different, as discussed in Chapters 6 and 7. The final installation technique is recommended. The pre-tension for Specimen MAXIB03 was applied for ten minutes, and then reduced 40 % to account for relaxation.

5.5.5.2.1 Undercut Anchor (with Anchor Gel)

The Five-Star® RS Anchor Gel was used with one high-strength undercut anchor, using a dual-cartridge system for mixing and placing the epoxy. The

mixing gun was not supplied by the manufacturer in a timely fashion, so a technician from one of Five-Star's distributors recommended a standard pumping gun purchased at a local hardware store. Two sealant guns were used side-by-side, since they fit the two dispenser bottles. Each gun was pumped simultaneously to ensure a one-to-one mixing ratio by volume. The mixture was pumped through the nozzle and discarded until a uniform gray color was discharged. The nozzle provided by the distributor fit but did not attach securely to the Five-Star® RS Anchor Gel cartridge system. The nozzle was pushed off the cartridge by the gel, not allowing the epoxy to mix. Therefore, the two-part gel was dispensed onto a sheet of cardboard and mixed by hand until it became a uniform gray color. It is understood that the mixing proportions and procedures significantly affect the strength of the grout, but the mixing nozzle supplied by the manufacturer was able to be secured to the cartridge dispenser. Therefore, when the two components of the anchor gel were dispensed, the nozzle fell off the cartridge dispenser. Thus, the mixing procedure described above was performed.

The connector was installed using the same procedure as the undercut anchor, with one additional step:

1) The hole for the connector was filled about one-quarter full with anchor gel. Then, the undercut anchor was twisted into the hole. It was quickly realized that the gel did not completely cover the connector, so the connector was removed and coated with gel. Once again, the connector was twisted into the hole. Since no gel squeezed out of the top, it is unlikely that the gel completely surrounded the connector. Given the fast curing time of the anchor gel and the fact that six connectors were being installed simultaneously, only two attempts were made at coating the connector. The annular gap was

less than ¼-in. and the temperature was about 70 F when the epoxy was placed.

5.6 TEST EQUIPMENT

The test equipment used for the field friction and single-connector, direct-shear static load tests are given in the following sections.

5.6.1 Test Equipment for Field Friction Test

Figure 5.22 shows the testing assembly used to measure the static coefficient of friction in the field. The figure shows the top half of a steel girder from a bridge undergoing demolition in San Antonio, Texas. On top of the flange on the left side is a pulling mechanism, which was used to apply a load in the horizontal direction. It is simply a machinist's table capable of sliding in a horizontal plane. Oil was used to ensure a smooth and virtually frictionless motion when the crank on the left was rotated. A threaded rod attached to a steel bar bolted to the pulling mechanism serves as a boom to which a spring scale is attached. Finally, a concrete block weighing 22.0 lb is attached to the scale on the right side of the figure. The scale reads the applied load in kg or lb when the concrete block slips. In an effort to represent the slab-girder interface as accurately as possible, the concrete block was cast against a steel plate. Twenty-four tests were performed on four girders from a recently demolished bridge in San Antonio, Texas. The results are summarized in Chapter 6.

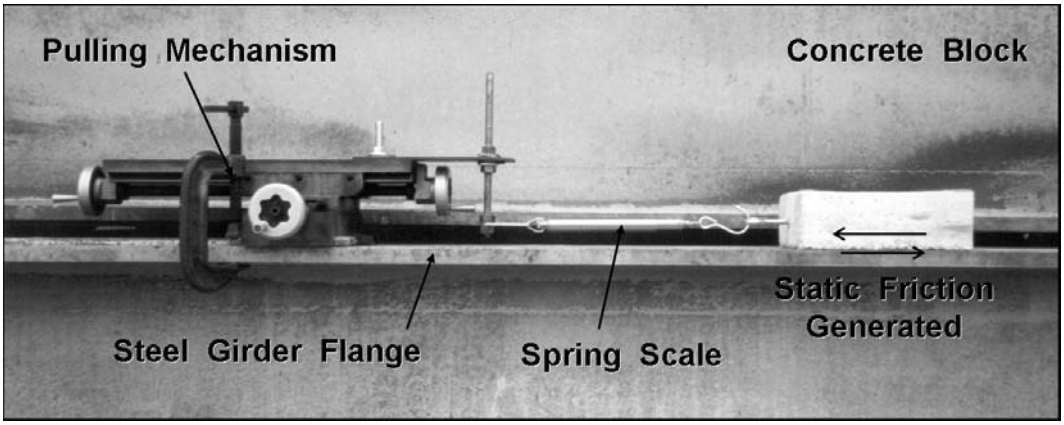

Figure 5.23: Field friction test setup

5.6.2 Test Equipment for Single-Connector, Direct-Shear Static Load Test

The single-connector, direct-shear static load test setup is shown in Figure 5.23. The frame was previously used by researchers at the University of Texas, so only minor modifications were required for the single-connector, direct-shear setup. The frame is designed to be self-contained, so it does not need a reaction wall or floor. Two 23-ft long, MC 18x58 channels run parallel, 2 ft apart [Figure 5.24(a)]. A series of plates welded together form a "bulkhead" and is bolted between the channels, shown in Figure 5.24(b). The bulkhead acts as a reaction for the hydraulic loading system. Four 1½-in. diameter bolts are attached to the front face of the bulkhead, and were used to attach the reaction plate. A hydraulic ram (Figure 5.25) with a tension capacity of over 100 kips was bolted to the reaction plate. The ram rests on a small section of a wide-flange girder so the weight of the loading apparatus is not applied to the test specimen.

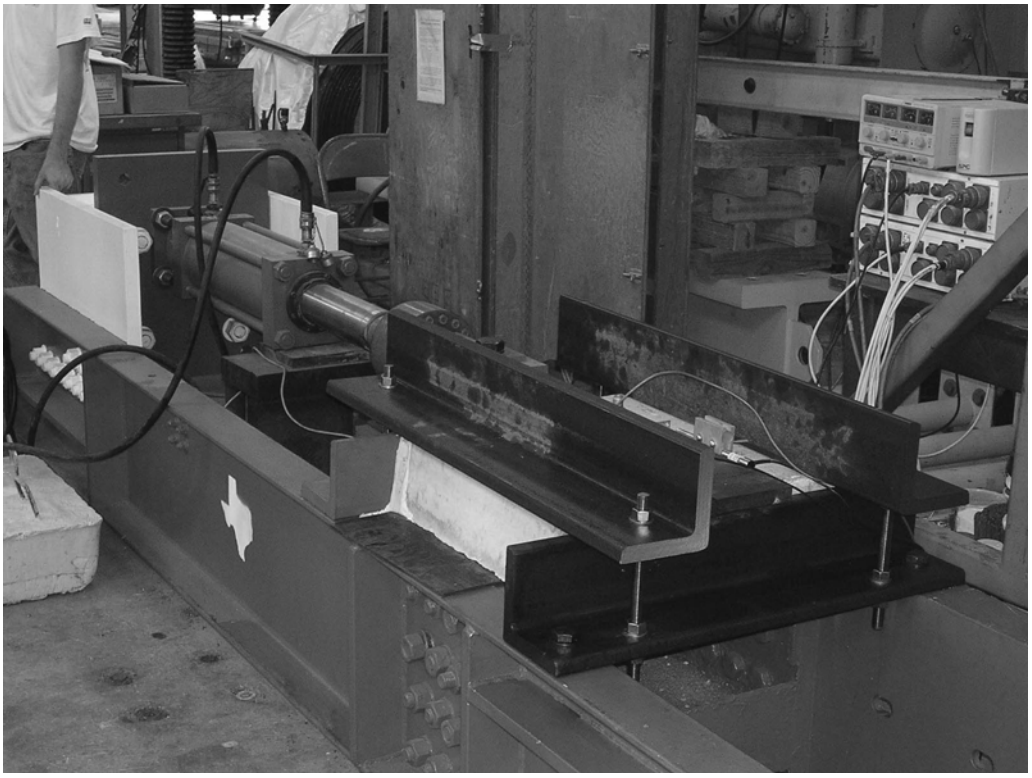

Figure 5.24: Single-connector, direct-shear static load (SCSL) test setup

Figure 5.25: (a) Self-contained test frame; (b) Bulkhead used as reaction wall

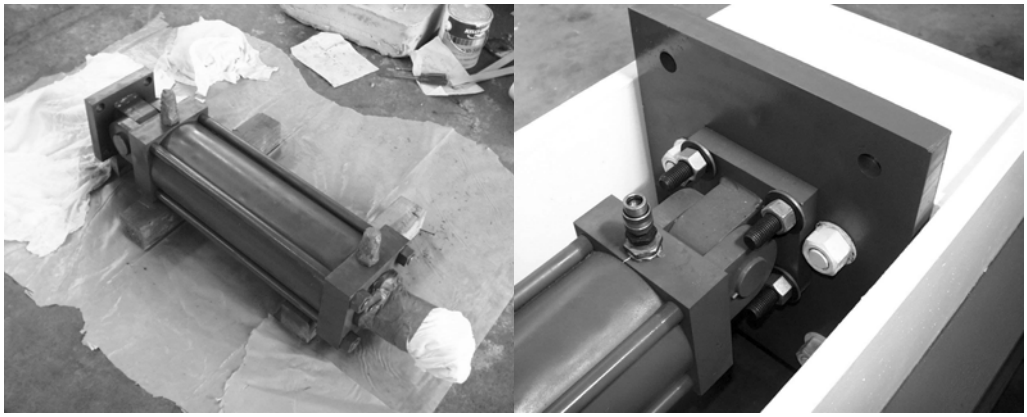

Figure 5.26: (a) Hydraulic ram (over 100-kip capacity); (b) Reaction plate

The capacity of the load cell was chosen so that the test setup could be slightly altered for group tests of two or four connectors in later stages of this research project (21-kip capacity per welded stud, with 4 studs, equals 84 kips). A 2-in. diameter threaded rod and reducing coupler was screwed onto the ram piston to connect to the load cell, as shown in Figure 5.26. Next, a special clevis was attached to the load cell with a 2-in. diameter threaded rod. The clevis was designed to connect to the steel plate used in the tested connection so that the centerline of the hydraulic ram would pass through the steel-concrete interface. A schematic diagram showing the line of action is given in Figure 4.5 of Chapter 4.

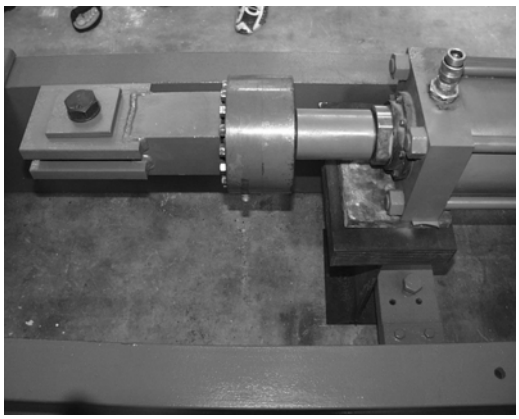

Figure 5.27: From left to right: clevis, load cell, coupler, and hydraulic ram

The concrete block was positioned onto a supporting plate (Figure 5.27) in the test frame and reacted against a welded-in-place angle. Three additional angles (Figure 5.23) were placed around the block to secure it into the frame. The steel plate representing half the girder flange in the candidate bridge was placed on top of the block with the investigated connection method. The special clevis was attached to the steel plate with a 1¼-in. bolt. The LVDTs (and washer load cell, if applicable) were attached to the specimen. Finally, a 680-lb group of steel blocks welded together (Figure 5.28) was placed on top of the steel plate to represent the tributary dead load of a typical candidate bridge (4 ft x 2 ft x 7 in.).

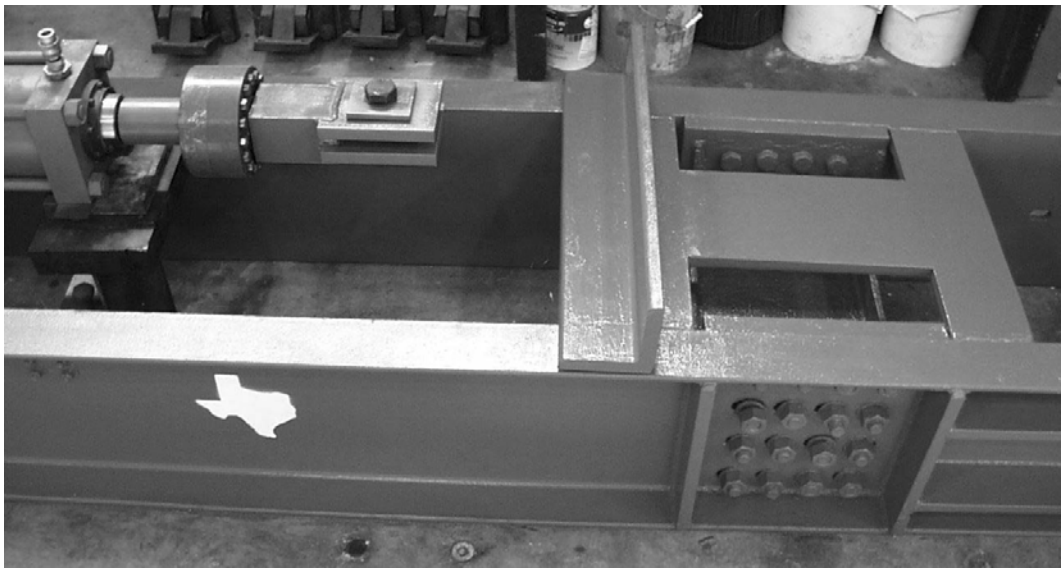

Figure 5.28: Welded-in-place angle and plate for supporting specimen

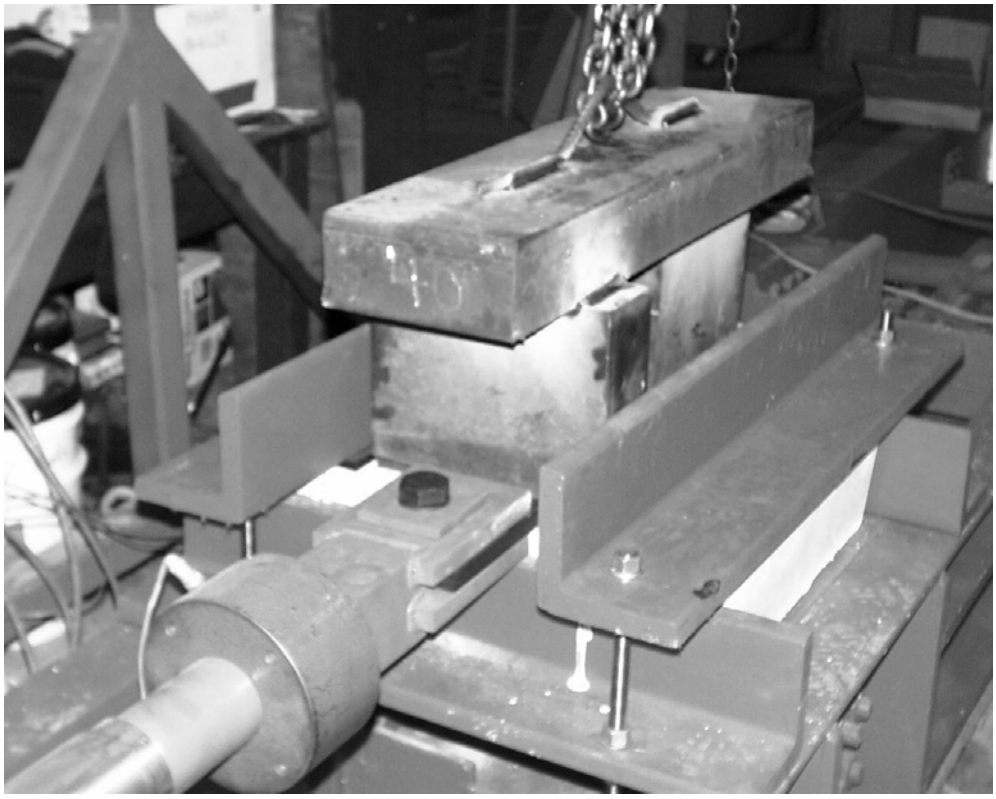

Figure 5.29: Complete test setup with top angles and dead weight

Hungerford (2004) covers the design of the static load test setup in detail, but a brief description is given here for completeness. The setup was designed so that it could also be easily altered for fatigue testing on a single connector or group of connectors by simply adding a servo-valve and servo-controller, as discussed in Chapter 4.

5.6.3 Instrumentation Used in Single-Connector, Direct-Shear Static Load Tests

The applied shear was measured with a 100-kip load cell shown in Figure 5.26. It had a rated accuracy of about 0.5 % of full scale. Tension in the connectors was measured using a HSI-Houston Scientific International Load Cell

Model 2054-001, referred to in this thesis as a "washer load cell." It had a maximum error of about 20 %, as determined by calibration on a Skidmore machine. The relative slip of the connector was measured with two Sensotech Model JEC Linear Variable Differential Transformers (LVDTs) (Figure 5.29). The two LVDTs had a 2-in. stroke and a linearity of 0.15 and 0.21 %. The two load cells used an excitation voltage of 10 V; the two LVDTs used an excitation voltage of 30 V. Thus, 6 channels had to be read.

Figure 5.30: LVDTs on left and right side of steel plate with load cell in center

5.6.4 Data Acquisition and Reduction

The loads and displacements were measured using a National Instruments Data Acquisition System (DAQ). The raw voltage data were read and converted to engineering units using LabView software. Data for the static load tests were

obtained every 0.5 seconds. A graph of the load vs. slip was presented in real time on the computer monitor for test control.

5.7 TEST PROCEDURES

5.7.1 Procedures for Friction Tests

The static coefficient of friction was obtained in two ways—from the field tests and from the single-connector, direct-shear tests.

5.7.1.1 Procedures for Field Tests

Field friction tests were conducted on the flanges of steel girders of an older bridge undergoing demolition in San Antonio, Texas. The test procedure used in the field was relatively simple. First, the pulling mechanism was clamped to the flange of the girder using a C-clamp. Next, the spring scale was attached to the boom arm described in Section 5.6.1. Then, the concrete block was placed onto the girder with the side cast against the steel facing down. The scale was adjusted vertically so it was parallel to the girder using the two nuts on the threaded rod. Finally, the crank on the pulling mechanism was rotated slowly, pulling the spring scale. Another researcher watched the scale, reading the values aloud so the loading rate was maintained slow and constant. When the concrete block slipped, the last load read aloud was recorded. Finally, since the girders were on a sloping surface, the angle of the flange relative to horizontal was measured and recorded.

5.7.1.2 Establishment of Coefficient of Friction from Single-Connector, Direct-Shear Tests

Several connection methods used friction to transfer shear at the steel-concrete interface. Since the applied tension and the shear at which slip started

were recorded, the coefficient of friction can be calculated for the connection methods using Equation 4.1.

5.7.2 Procedure for Single-Connector, Direct-Shear Static Load Tests

The procedures for setting up and running the direct-shear test are outlined in this section. Hungerford (2004) describes these procedures in more detail, but they are summarized here for completeness.

First, the concrete block was positioned onto the I-shaped plate shown in Figure 5.27 with the lifting stirrups facing downward. For the connection methods in which the connector was installed in the test frame, the steel plate representing half the girder flange was positioned on top of the concrete block. By this point, the holes for the clevis and connector had been drilled. The hole for the connector was positioned near the center of the concrete block, so that the steel plate was in line with the clevis and hydraulic ram. The position of the connector was marked through the hole in the steel plate. The steel plate was removed and the hole was drilled into the concrete. Finally, the steel plate was positioned over the hole and the connector was installed.

For the connection methods in which the connector was installed prior to placing the block into the test frame, the block was positioned into the frame so that the steel plate aligned with the clevis.

With the steel plate attached and aligned with the clevis, the rear angle (Figure 5.23) was positioned and bolted to the test frame. Hydrostone, a high-strength gypsum compound, was used to fill the gap between the front (welded) angle and the concrete block. Because the waffle-slab mold used as a form for the concrete blocks was slightly tapered, the boundary between the angle and the block was not flush. The Hydrostone was poured into plastic bags to prevent spilling and facilitate cleanup.

Before the Hydrostone set, the two top angles shown in Figure 5.23 were placed on top of neoprene pads on the corners of the concrete block. The 5- x 3- x ½-in. pads were placed onto the corners to prevent any confining effects around the connector region.

The LVDTs were attached to the concrete block using a two-part epoxy. Spacers were used to ensure that the LVDTs were parallel to the steel plate. A bracket was attached to the each side of the steel plate to measure the relative displacement between the steel plate and the concrete block (Figure 5.29). If applicable, the washer load cell was placed. Instrumentation was zeroed on the data acquisition system, and the connector was pre-tensioned as recommended.

The last step for setting up the test was to add the dead weight to the top of the steel plate. The weight was attached loosely to chains, so that in the event of a sudden failure of the connector, the weight would not topple and damage any of the testing apparatus. After ensuring that everything was set and secured, the test was performed. The connector was loaded at an average rate ranging between 0.1 and 0.3 kips/second. Each test was displacement-controlled and lasted about 15 minutes. The resulting load-slip curves for the connection methods discussed in this thesis are given in Chapter 6.

CHAPTER 6
EXPERIMENTAL RESULTS

6.1 INTRODUCTION

In this chapter, are presented the results of the tests discussed in the previous chapter. First, results of the friction tests are given, followed by results of the single-connector static load tests for the connection methods discussed in this thesis. Results for the other connection methods investigated in this project and not discussed further here are reported in Hungerford (2004). Finally, an analysis is presented of the probable cost of materials to retrofit a typical candidate bridge using each connection method tested in this project. Test results are discussed in Chapter 7.

6.2 RESULTS OF FRICTION TESTS

The static coefficient of friction between steel and concrete was obtained in two separate ways—from the field tests and from the single-connector static load tests.

6.2.1 Results of Field Tests

Friction tests were conducted on steel girders from a bridge built in 1961 and reconstructed in 1976 undergoing demolition in San Antonio, Texas (I-410 over Honeysuckle Lane). The results of the field tests performed at various locations along four girders are given in

Table 6.1. Three tests were performed at each location on a girder. The table reports the values of the horizontal load applied at first slip, F_i, where "i" is the girder number. As mentioned in Chapter 5, a 22.0-lb block cast against a steel

plate was used to apply the known normal force to the steel girder. Since the girders tested were in the field on a sloped surface, the angle of the girder relative to horizontal, θ, was recorded in degrees. The static coefficient of friction was calculated using Equation 6.1. The geometry used to derive the equation is shown in Figure 6.1. The block was always pulled upward, against gravity, leading to the negative sign in the numerator.

$$\mu = \frac{F - W \times \sin(\theta)}{W \times \cos(\theta)} \qquad \textbf{(6.1)}$$

Where: μ = static coefficient of friction;

F = measured force [parallel to interface] at first slip;

W = known weight of concrete block; and

θ = angle from horizontal.

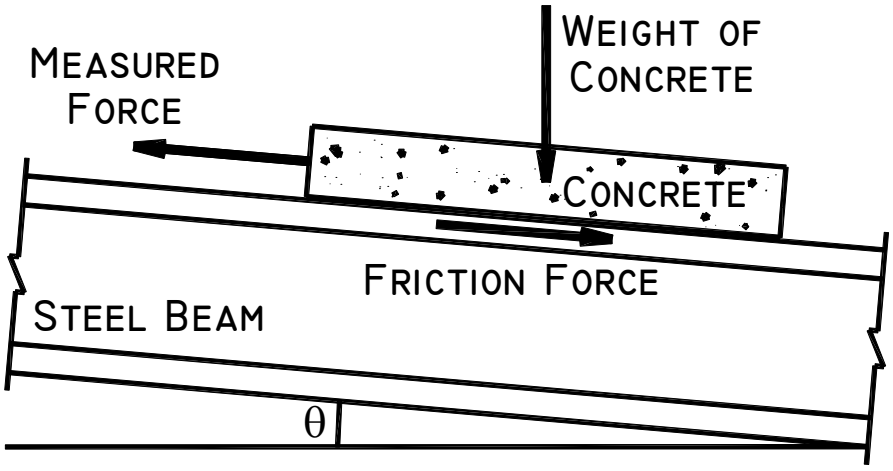

Figure 6.1: Geometry of field friction test

For all field tests, the mean static coefficient of friction was 0.63, with a minimum value of 0.50, and a maximum value of 0.77, a standard deviation of 0.061, and a median of 0.64. As stated in Chapter 4, previous research based on tests performed by seven researchers, showed average values for the dynamic

coefficient of friction ranging from 0.3 to 0.65 (Cook 1989). Further analysis of the test results is given in Chapter 7.

Table 6.1: Field friction test results for each of four girders

	Left End			Middle			Right End		
F_1 (lb)	16.0	14.3	14.9	14.9	13.8	16.2	16.3	16.1	15.4
μ_1*	0.67	0.60	0.62	0.62	0.57	0.68	0.69	0.68	0.65
F_2 (lb)	14.9	18.2	15.4	16.0	15.4	15.4	-	-	-
μ_2*	0.62	0.77	0.65	0.67	0.65	0.65	-	-	-
F_3 (lb)	16.0	12.7	13.8	12.5	14.9	15.4	-	-	-
μ_3*	0.66	0.51	0.56	0.50	0.61	0.63	-	-	-
F_4 (lb)	13.2	15.4	13.8	-	-	-	-	-	-
μ_4*	0.57	0.67	0.59	-	-	-	-	-	-

*θ = 3° for Girder 1, 3° for Girder 2, 4° for Girder 3, and 2° for Girder 2

6.2.2 Results of Single-Connector Static Load Tests

Several investigated connection methods used friction from a pre-tensioned, post-installed connector as the primary shear-transfer mechanism. Since the applied tension and shear were recorded throughout the test, the coefficient of friction was calculated by dividing the shear at first slip by the corresponding tension.

The initial portion of a typical shear-slip plot for one connection method is shown in Figure 6.2. The load at first slip was consistently and reasonably (if somewhat arbitrarily) taken as the intersection of the load-slip curve with a line parallel to the initial tangent to that curve, at an offset of 0.002 in.

Table 6.2 shows the results from the applicable tests, given in alphabetical order of the test designation.

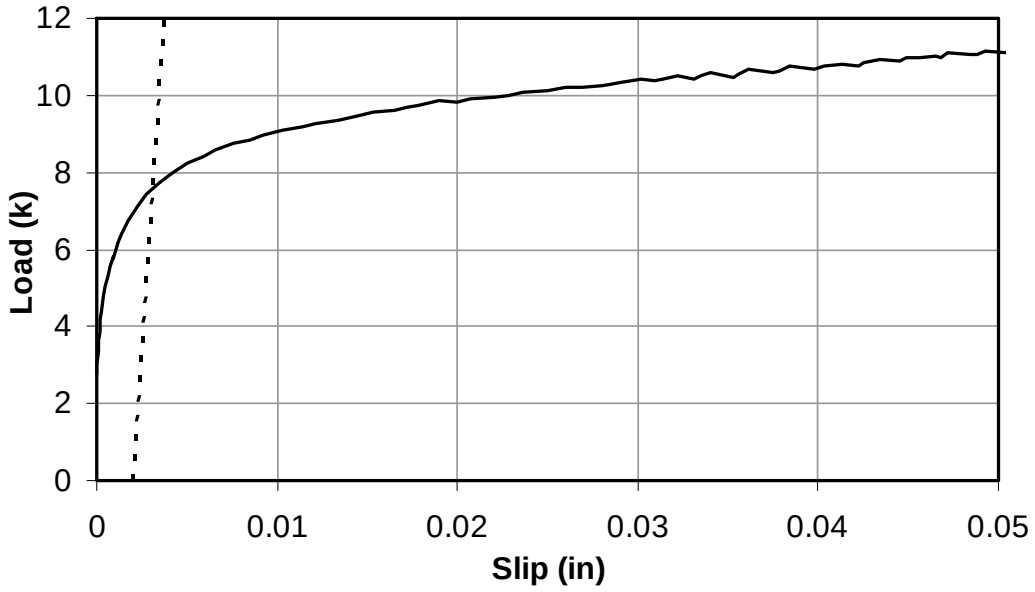

Figure 6.2: Offset rule used to obtain shear at slip

The average static coefficient of friction was 0.40 with a standard deviation of 0.22. Further analysis of the results is given in Chapter 7. Not all of the tests performed using friction as the primary force transfer mechanism are reported in the table. Specimens HASAA03 and HITTZ02 had HY-150 epoxy between the concrete block and steel plate, giving artificially high friction results. More discussion of these two connection methods is given in Hungerford (2004). The tension was not measured for Specimens MAXHS01 and MAXHG01. For Specimens HTFGB02 and HTFGB03, the tension was measured using the "Squirter DTI" load-indicating washers described in Chapters 4 and 5.

Table 6.2: Coefficient of friction results from single-connector tests

Test Designation	Shear (k)	Tension (k)	Static Coefficient of Friction
HASAA01	12.0	14.0	0.86
HASAA02	11.1	16.1	0.69
HITTZ01	6.1	9.0	0.68
HITTZ03	7.2	17.6	0.41
HTFAT01	12.0	75.0	0.16
HTFAT02	18.7	71.4	0.26
HTFAT03	15.8	71.4	0.22
HTFGB01	8.0	25.7	0.31
HTFGB02	12.4	28.0*	0.44
HTFGB03	10.0	28.0*	0.36
KWIKB01	3.0	7.8	0.39
MAXIB01	8.5	18.0	0.47
MAXIB02	3.3	15.8	0.21
MAXIB03	1.8	16.0	0.11

*Tension estimated using DTI washer

6.3 RESULTS OF SINGLE-CONNECTOR STATIC LOAD TESTS

Results of tests on the six connection methods discussed in this thesis are summarized in Table 6.3. The results from the benchmark cast-in-place welded headed stud tests are listed first, followed by results for retrofit methods, arranged in descending order of the average load at the key slip of 0.2 in. Ultimate slip is taken as that corresponding to 90 % of the ultimate load on the descending branch. In some tests, the LVDTs were removed prior to failure of the connection so that they would not be damaged. Other tests were stopped after the ultimate load was reached, but before connection failure, because one side of the clevis was being subjected to moment for which it had not been designed. Tests stopped

for either of these reasons have a greater ultimate slip than recorded, and are denoted by an asterisk in Table 6.3. General observations about each connector method are given below.

Figures 6.37 through 6.47 at the end of this chapter show the load-slip curves for each connection method, along with the method's average load-slip curve. The applied shear is displayed on the vertical axis, while the average slip measured by the two LVDTs is shown on the horizontal axis. The average load-slip curve was determined by averaging the load values at any given value of slip. In addition to the data for each investigated connection method, each plot shows the average results for the cast-in-place welded headed studs (CIPST) as a benchmark. The CIPST Average is shown as a lighter solid line and should not be confused with data for the investigated connection method.

Anomalies that occurred before and during the tests are also described in each appropriate section below. Although a significant number of anomalies appear, they are difficult to avoid in real construction. When they were detected during construction or before a test, the test was conducted in any event, to assess the effect of such construction anomalies on load-slip performance, and to identify shear-transfer methods that would be relatively insensitive to such anomalies. Test results were generally unaffected by these anomalies. This point is discussed in more detail in Chapter 7.

Table 6.3: Results of single-connector static load tests

Test ID	Load at 0.2-in. Slip (kips)	Ultimate Load (kips)	Slip at Ultimate Load (in.)	Ultimate Slip (in.)
CIPST01	17.7	24.3	0.764	0.806
CIPST02	19.9	21.7	0.325	0.477
CIPST03	14.7	17.8	0.506	0.574
HTFAT01	30.7	37.6	0.387	0.416*
HTFAT02	39.3	39.7	0.266	0.364*
HTFAT03	37.2	45.0	0.317	0.487
HTFGB01	23.5	30.7	0.474	0.637*
HTFGB02	27.8	34.3	0.521	0.525*
HTFGB03	26.2	33.5	0.588	0.785
DBLNB01	25.4	31.1	0.627	0.672*
DBLNB02	22.6	30.6	0.564	0.613*
DBLNB03	24.7	28.4	0.430	0.443*
POSST01	22.0	22.8	0.426	0.492
POSST02	22.2	22.4	0.243	0.374
POSST03	22.5	23.3	0.301	0.359
STWPL01	21.2	21.3	0.221	0.290*
STWPL02	17.6	18.4	0.447	0.505*
STWPL03	19.5	21.6	0.418	0.464
KWIKB01	14.6	23.7	1.06	1.06
MAXHS01	7.10	24.1	0.510	0.703*
MAXIB03	2.89	33.7	1.27	1.29

*Indicates that LVDTs were removed prior to failure of connection.

For some tests, the steel plate representing half the girder flange lifted significantly (that is, ¼ in. to ½ in.) off end of the concrete block opposite to the ram. When the representative concrete slab was being designed, the dead weight of only the tributary area was taken into account. The stiffness of the surrounding

slab was not accounted for, allowing the plate to lift in some cases. In Chapters 7 and 8, a solution to this problem is proposed for the next phase of testing.

For the most part, the plate did not lift significantly before the ultimate load at the connection was reached. In some cases, the plate lifted and the connector experienced significant tension. An example of this is shown in the Specimen CIPST01 (Figure 6.37), in which no dead load was applied to the steel plate.

As a frame of reference, most of the figures in this chapter showing photos of the SCSL tests are oriented so that the loading system is to the left of the picture. In other words, the steel plate is pulled to the left. The figures for the expansion anchor are oriented so that the loading system is to the right or above the picture.

6.3.1 Results for Cast-in-Place Welded Stud

Hungerford (2004) discusses the results of the cast-in-place welded stud tests in detail. Since this connection method is the benchmark to which the structural behavior of all other connection methods is compared, several key results are also given in this thesis.

The average ultimate static load of the three tests is 21.3 kips. The AASHTO (2002) design code gives a predicted ultimate strength of 21.0 kips for 3000-psi concrete. This was achieved in spite of some evident anomalies in orientation. Also, the third test in the series had a weld that was possibly defective. In addition, a small void (1/16-in.) was observed around the connector. This was the only test in which the connector failed at the root of the weld. An incomplete weld penetration was apparent all around the stud. This lowered the average ultimate strength of the connection method. The standard push-out test

on which the code design values are based inherently averages the results for single anchors because tests are typically performed on eight connectors at a time.

Finally, the ultimate strength of the average of the results is only about 19.5 kips. This is not a major concern because the ultimate strengths of the individual tests occur at different slip values, causing the maximum of the average curves to be lower than the average of the maximum of each curve. Detailed discussion of the cast-in-place welded stud connection method is given in Hungerford (2004).

6.3.2 Results for Post-Installed Welded Stud

The grout used for POSST01 and POSST02 was the first large batch mixed in this project. A small batch had been made previously to fill the gap for one expansion anchor (KWIKG01). In the KWIKG batch, a rod had been used for mixing and found to be inadequate (the 1-day compressive strength was only 3420 psi). Thus, a mixing paddle attached to a power drill were used to mix grout for the POSST tests.

Two Five-Star® Highway Patch grout mixtures were made for the set of three POSST tests. Chapter 5 outlines the specified mixture design proportions of the grout. The volume of the first batch fell well short of what was expected, however, leaving only two test cylinders to be cast. The volume of grout was increased for the POSST03 test, but was still insufficient, and only three cylinders were cast. This is discussed further in Chapter 7. As discussed in Chapter 5, the compressive strength of the grout was tested using 4- x 8-in. cylinders cast in plastic cylinder molds. Test POSST01 was performed 24 hours after casting the grout, and Tests POSST02 and POSST03, 48 hours after.

The first grout mixture did not reach the manufacturer's specified 1-day strength of 5100 psi, and it is unlikely the second mixture would have either,

although a 1-day test was not performed due to a shortage of cylinders. Nevertheless, the static load tests on POSST02 and POSST03 were performed when the cylinder strength of the grout was above 5100 psi. Table 6.4 shows the results of the cylinder tests for each batch and connector tests. The number of cylinders tested to obtain the strength at each age is shown in parenthesis in the first column. The specimen is shown in brackets next to the strength of the grout at the time of performing the static load test.

Table 6.4: Grout compressive strength for POSST tests

Mixture # (# of cylinders tested at each time period)	24-hour strength (psi) (Specified = 5100 psi)	48-hour strength (psi)
I (1)	4500 [POSST01]	5250 [POSST02]
II (3)	N/A	5370 [POSST03]

As listed in Table 6.3, for the POSST tests all loads corresponding to a slip of 0.2 in. are very close to each other. In Specimen POSST02, the hole for the headed stud was filled with grout when the concrete block was inadvertently suspended above the steel plate about 1/8 in. The block was accidentally knocked by a forklift while the grout was a few hours old, resulting in a small gap between the steel plate and the concrete block. In addition, the specimen was probably incorrectly aligned, because it appears to have undergone some twisting in the plane of the interface during testing. Due to the separation of the steel and concrete, the LVDT on one side of the steel plate was close to the bottom edge of the bracket that was bonded onto the plate as shown in Figure 6.3. Readings from the LVDTs show scatter from the very beginning of testing, reaching a maximum difference of about 0.06 in. at an average slip of about 0.06 in. In other words, the steel plate apparently rotated in the plane of the interface until was applied concentrically. The difference of 0.06 in. in recorded slip values was consistent

throughout the remainder of the test. It is unlikely that the slip values were affected by the placement of the LVDT on the bottom edge of the bracket.

The stud in Specimen POSST02 sheared above the weld (on the side of the weld away from the plate), while the studs in Specimens POSST01 and POSST03 sheared at the weld. POSST02 likely sheared above the weld because the steel plate lifted slightly away from the concrete slab. In each POSST test, the welded studs failed near the steel-concrete interface. Plate lifting did not appear to cause connector tension in any of these tests.

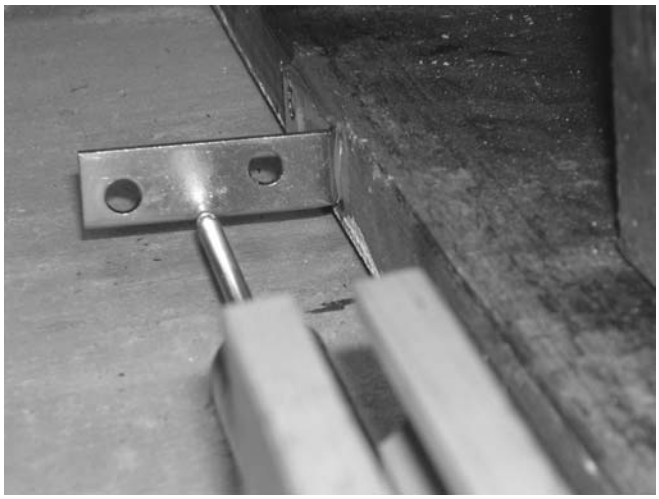

Figure 6.3: LVDT close to bottom of bracket (POSST02)

Crushing of the slab ahead of the connector was mostly confined to the grout, as shown in Figure 6.4. The white ring shown in the figure is sealant used to contain the water in the grout during casting. The inner circumference of the ring marks the interface of the grout and concrete.

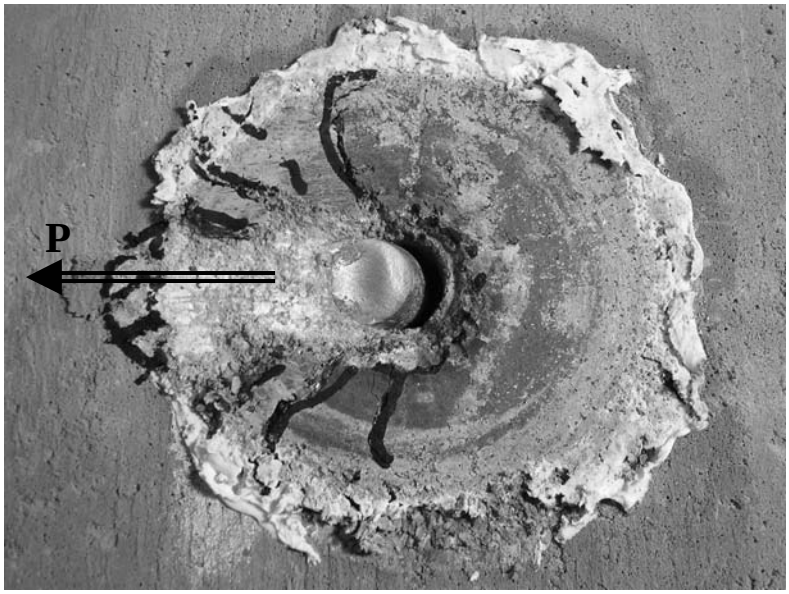

Figure 6.4: Crushing of POSST slabs mostly confined to grouted region.

6.3.3 Results for Stud Welded to Plate

As discussed in previous chapters in this thesis, the term "small plate" refers to the 5- x 5- x ½-in. plate to which a stud was pre-welded, while the term "steel plate" refers to the 36- x 6- x 1-in. standard plate representing half the girder flange used in all tests. Since this method involved two welded studs rather than the single connectors of other methods tested here, the load results reported in Table 6.3 have been divided by 2 for consistency. Testing only one small plate would have induced an eccentricity in the plane of the interface that would not be present in the field.

Two batches of Five-Star® Highway Patch grout were mixed for the three STWPL tests. The grout was placed in two lifts. Two batches were made sequentially because more grout was required than could be batched in a single bucket. All three tests were performed two days after casting. Only one cylinder was cast for this connection method because of a shortage of grout due to poor

mixing. The bags of grout used for these two mixtures had been exposed to the atmosphere for several weeks, resulting in the dry mixture becoming saturated. Therefore, large clumps of dry mixture could not be properly blended with the water during mixing. Additional water was added above the maximum recommended by the manufacturer to aid in mixing the dry clusters. About 200 mL of extra water (11 % of the maximum recommended) was added to the first batch; and about 600 mL (34 % of the maximum recommended) of extra water was added to the second batch.

Table 6.5 shows the results of the cylinder tests for each batch and connector test. Both mixtures are shown together since each represented one of the two lifts in the casting. The number of cylinders tested to obtain the strength at each age is shown in parenthesis in the first column. The specimen is shown in brackets next to the strength of the grout at the time of performing the static load test.

Table 6.5: Grout compressive strength for STWPL tests

Batch number (number of cylinders tested at each time period)	24-hour strength (psi) (Specified = 5100 psi)	48-hour strength (psi)
I and II (1)	N/A	3580 [STWPL01, 02, 03]

Specimen STWPL01 was loaded until the load started to decrease and it was obvious that the maximum load had been obtained. The clevis and the LVDTs were thought to be in danger because the plate was lifting significantly (about ½ in.), so loading was stopped at a slip of about 0.28 in. Previous research on welded studs had shown a slip at ultimate load ranging from 0.23 to 0.42 in. (Ollgaard, Slutter and Fisher 1971). Therefore, it was believed the test could be stopped without much loss in valuable data. In addition, edge effects were

believed to be causing the concrete slab to split, as shown in the top and bottom of Figure 6.5. The front part of the block (left side in that figure) was simply being pulled from the back part (right side). The lines marked on the figure show the transverse crack oriented perpendicular to the direction of loading. The marked lines parallel to the steel plate were used to mark the holes for drilling through the concrete.

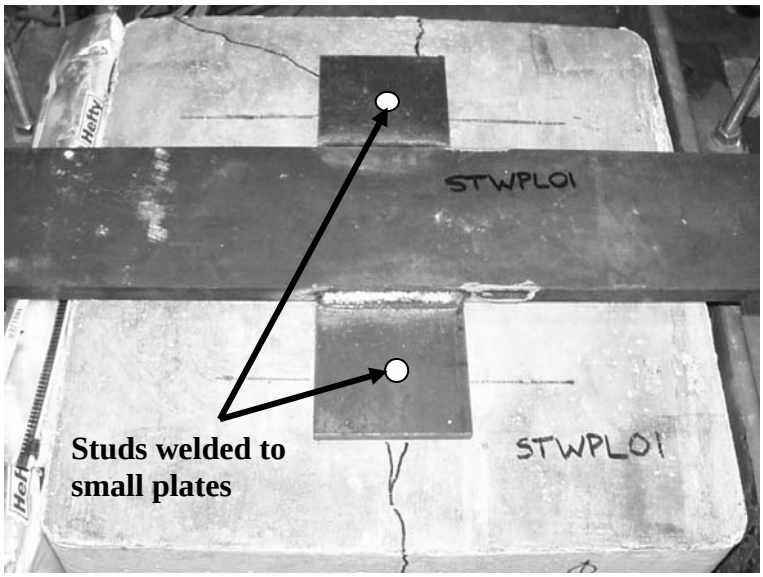

Figure 6.5: STWPL01 at failure (slab separating)

Specimen STWPL02 was loaded until its maximum load was reached. Again, it was believed that no more useful information was being obtained due to the edge effects, and the test was halted. The plate had lifted about ¼ in. at the final loading.

Specimen STWPL03 was the only test in which the connection was loaded to failure, although only one of the two studs sheared. The plateau at a load of about 14 kips in each of the three tests is due to the block cracking. The block actually had 28 kips on it at this point, but the load was divided by 2 because two

connectors were used in each test. Edge effects may have been significant for this connection method.

As discussed in Chapter 5, the 2-in. diameter holes were drilled completely through the concrete slabs from one side, causing some breakout on the top surface of the slab. This phenomenon was expected and believed to be insignificant, since the top surface of the block serves no structural purpose. Figure 6.6 shows the grout used to fill one of the holes in Specimen STWPL02. Some shrinkage cracks can be seen on the surface of the grout. Most likely, these occurred because the hole was not saturated with water the night before as discussed in Chapter 5. The cracks likely outline the 2-in. diameter hole. Concerns over the sensitivity of grout quality to variations in mixture proportions and mixing procedures are discussed in Chapter 7.

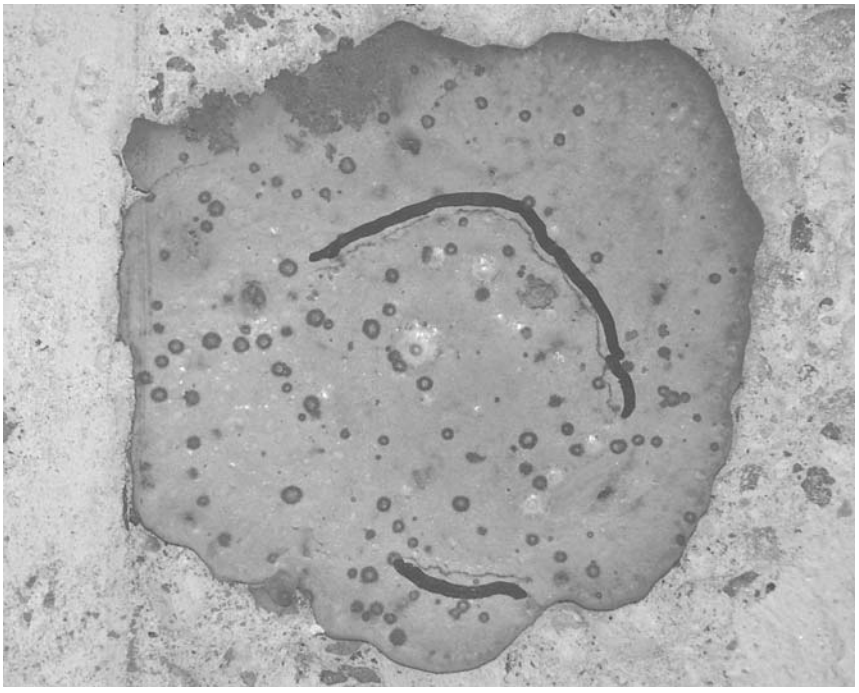

Figure 6.6: Grout on top surface of STWPL02 test with shrinkage cracks.

Specimen STWPL02 had one of the small plates welded slightly above the top of the steel plate so it was not in contact with the concrete slab, as shown in Figure 6.7. A washer for a ¾-in. diameter bolt was placed in the gap to show how far the small plate was above the concrete slab.

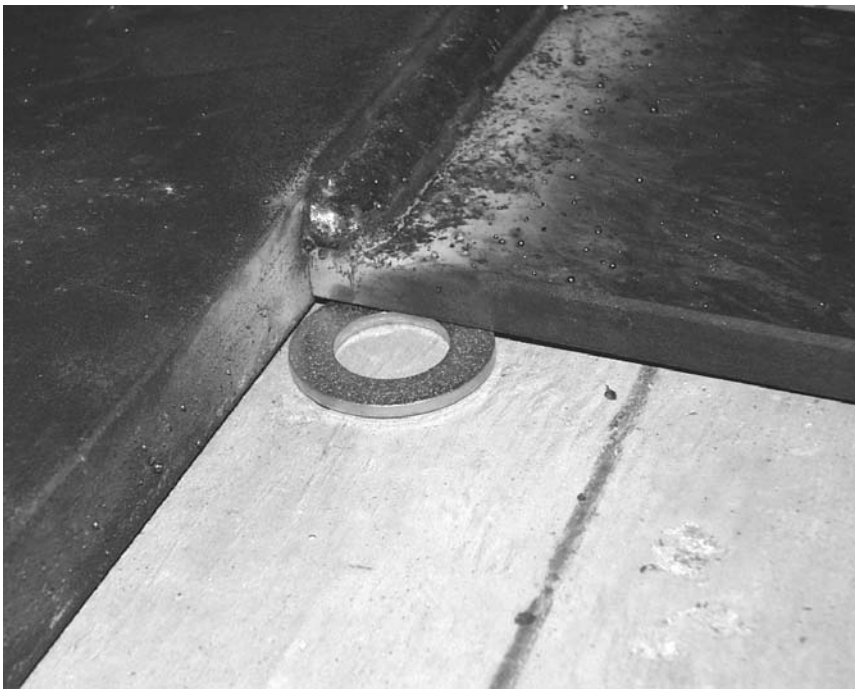

Figure 6.7: Gap between small plate and concrete slab

For the STWPL connection method, the LVDTs were placed on the steel plate directly behind the fillet weld attaching the small plates, as shown in Figure 6.8. The LVDTs were placed at the location of the connector in all of the other connector tests to reduce the influence of flexibility in the concrete block and steel plate, on the recorded slip values. The LVDTs for Specimen STWPL03 were placed on the same side of the steel plate measuring the slip in front of and behind the small plate to prevent excessive flexibility in the fillet weld that would lead to inaccurate results by measuring the displacement away from the

connectors. Measurements revealed only a 1-percent difference in the displacements.

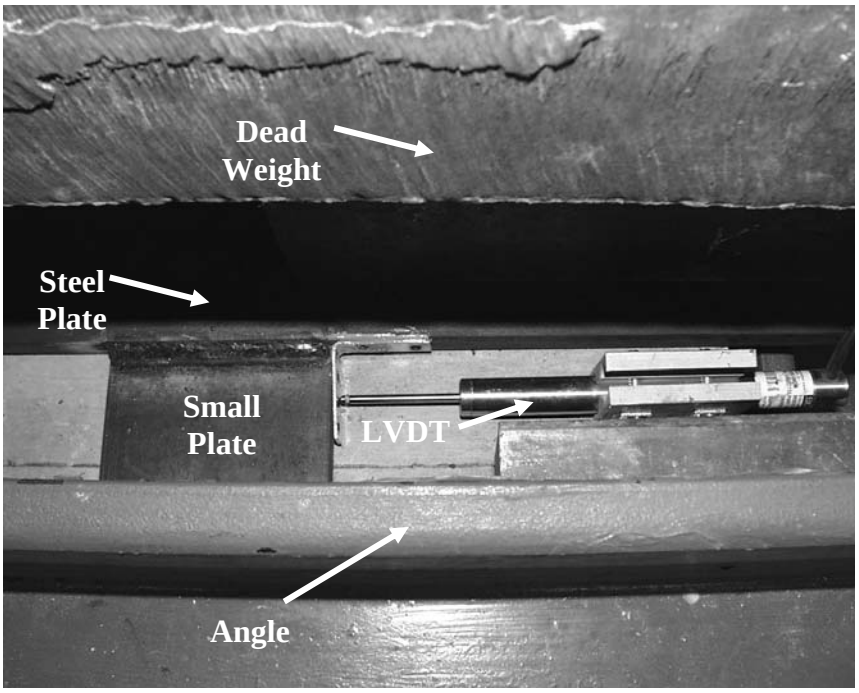

Figure 6.8: Placement of LVDTs for STWPL tests.

6.3.4 Results for Double-Nut Bolt

One Five-Star® Highway Patch grout mixture was made for the set of three DBLNB tests. Test DBLNB01 was performed 24 hours after casting the grout, and Tests DBLNB02 and DBLNB03, 48 hours after.

Neither grout batch reached the manufacturer's specified 1-day compressive strength of 5100 psi. As discussed in Chapter 5, mixing was performed with a less powerful hand drill and smaller mixing device, leading to a less-complete mixing. Table 6.6 shows grout compressive strengths for the DBLNB specimens. The number of cylinders tested to obtain the strength at each

age is shown in parenthesis in the first column. The specimen is shown in brackets next to the strength of the grout at the time of the static test.

Table 6.6: Grout compressive strength for DBLNB tests

Mixture # (# of cylinders tested at each time period)	24-hour strength (psi) (Specified = 5100 psi)	48-hour strength (psi)
I (2)	3170 [DBLNB01]	3180 [DBLNB02, 03]

The LVDTs were removed prior to failure on each specimen for this connection method. The specimens in fact were never completely failed. Testing was stopped at final loads of about 29, 28, and 26 kips respectively because it was believed that the ultimate load had been reached and that subsequently acquired data would indicate only the separation of the concrete slab. The connectors in these tests were high-strength and did not fail. Rather, incipient breakout failure was observed. For Specimen DBLNB01, no cracks were observed and the plate was not lifting at a load of 25 kips and a slip of 0.2 in. Specimen DBLNB02 had no cracks at 28 kips of applied load. No cracking or lifting was observed for Specimen DBLNB03 at a load of 26 kips. Because the researchers did not continuously observe the specimens during testing, the exact loads at which each crack formed are unknown. Nevertheless, given that all loads were above 25 kips without observed cracking, it is believed the test data were not significantly influenced by the plate lifting or the cracking of the concrete slab from breakout. Figure 6.9 shows the deformed connector with the washer still in place. It shows that as with the POSST connection method, cracks propagated beyond the grout. This is reasonable, because the hole for the DBLNB specimens was 1 in. smaller in diameter than for the POSST specimens. Figure 6.10 shows the connector with the washer removed so the gap behind the connector can be clearly seen. The shank deformed severely in shear over the length of the two nuts. Figure 3.11

shows the configuration of the nuts and washers used for the double-nut bolt connector.

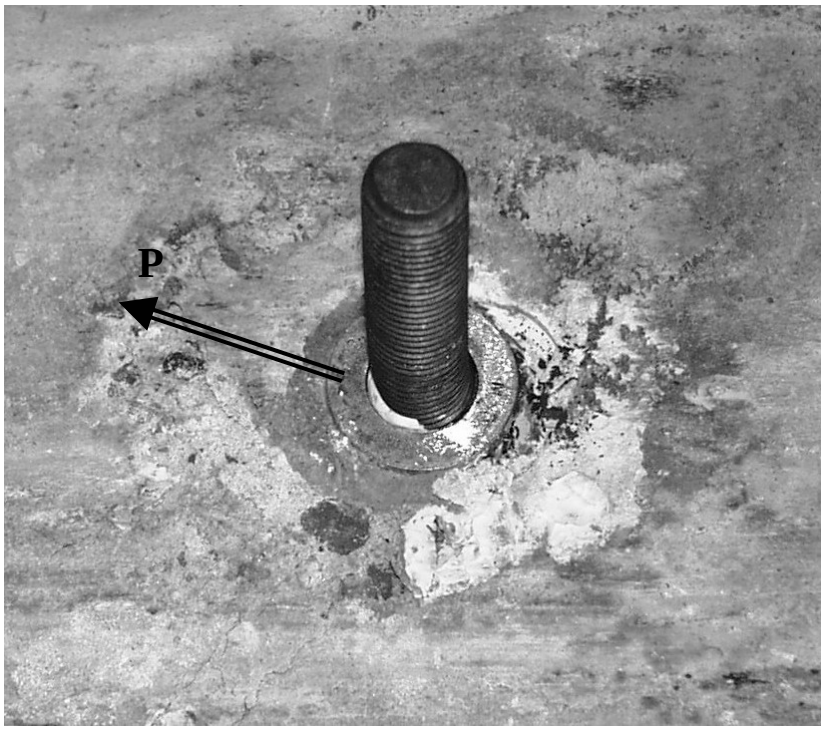

Figure 6.9: Typical DBLNB failure with washer still in place

Specimen DBLNB03 was probably aligned incorrectly because it appears to have twisted in the lane of the interface. Readings from the LVDTs differ between each other and grow further apart as the test progresses, reaching a maximum difference of about 0.03 in. around an average slip of 0.2 in. The readings then start to converge, and are nearly identical at an average slip of 0.36 in. At that point one of the two LVDTs shows a sharp increase in reading, leading to a difference of nearly 0.1 in. at an average slip of about 0.45 in. It is believed the slip data for this specimen are unreliable above an average slip of 0.35 in.

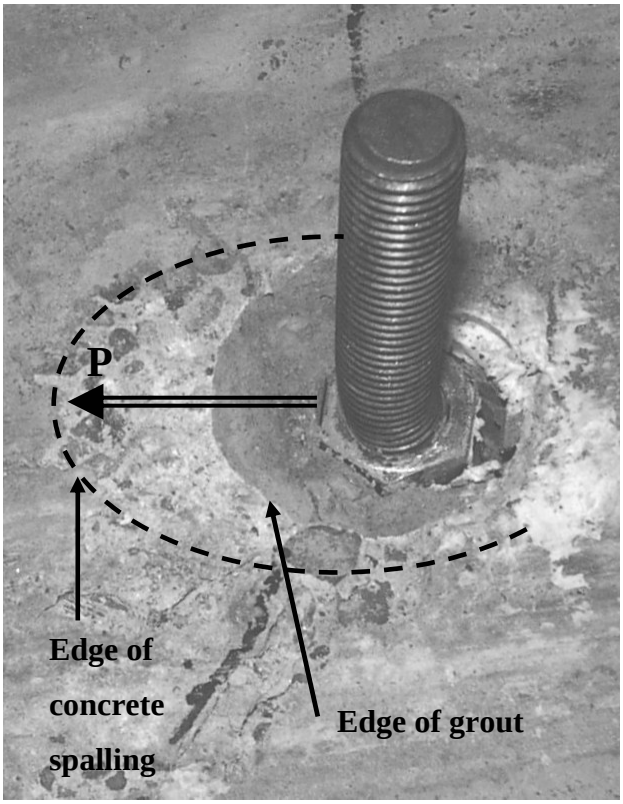

Figure 6.10: DBLNB01 with washer removed and cracks marked

6.3.5 Results for High-Tension, Friction-Grip Bolt

As mentioned in Chapter 5, Specimen HTFGB01 had a nominal embedment depth of only 3.3 in., 1 in. less than the other replicates. HTFGB02 and HTFGB03 had 4.3-in. embedment depths. In addition, to ensure a flush contact surface, epoxy was placed below the head of the connector (and washer) for Specimens HTFGB01 and HTFGB02. To assess the effects of the epoxy, none was used for HTFGB03. As mentioned in Chapter 5, a standard 1-15/32-in. washer was used on the concrete side and the steel side of the connector. No grout was used for this connection method because it does not depend on the grout for structural performance. This is discussed further in Chapter 7.

For this connection method, the LVDTs were removed on the first two specimens prior to failure. These specimens in fact were never completely failed. Testing was halted at final loads of about 18 and 33 kips respectively, because it was believed that the ultimate load had been reached and subsequently acquired data would simply reflect the separation of the concrete slab. The connectors used in these tests were high-strength and consequently had a high resistance to fracture. Because of the high strength of the connectors, a breakout failure in the concrete was starting to be observed, as shown in Figure 6.11. At a load of 29 kips, a crack was observed in the perpendicular to the direction of load (vertically in the figure), completely across the block. Figure 6.12 shows the deformation of the connector of Specimen HTFGB01 after testing.

The connector in Specimen HTFGB03 failed in shear as shown in Figure 6.13 and Figure 6.14. At a slip of 0.5 in., the plate had not lifted. Only transverse cracking, was observed, and the plate lifted only slightly at failure.

Given the discussion above, the epoxy placed at the head of the connector seemed to have made a difference in performance. This issue is discussed further in Chapter 7. In addition, although Figure 6.41 apparently shows that the connectors in each of the tests experienced significant tension, the plate for HTFGB03 did not lift. Thus, the tension created in the connector was likely due to the connector rotating in the concrete (as shown in Figure 6.14). This is the opposite of what happened in the STWPL tests, in which the steel plate lifted a significant amount causing tension in the connector. Since the data for Specimen HTFGB03 fall between those of the other two tests for this connection method, it is believed that all data are valid.

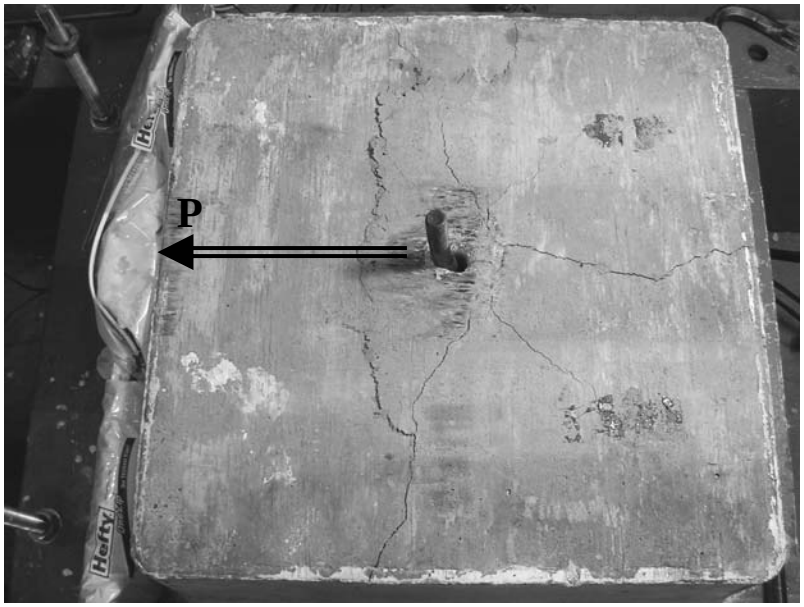

Figure 6.11: Breakout failure of Specimen HTFGB01

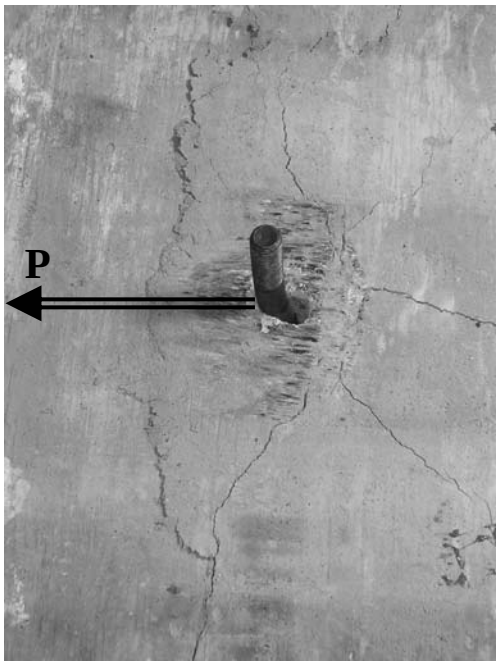

Figure 6.12: Deformation of connector in Specimen HTFGB01

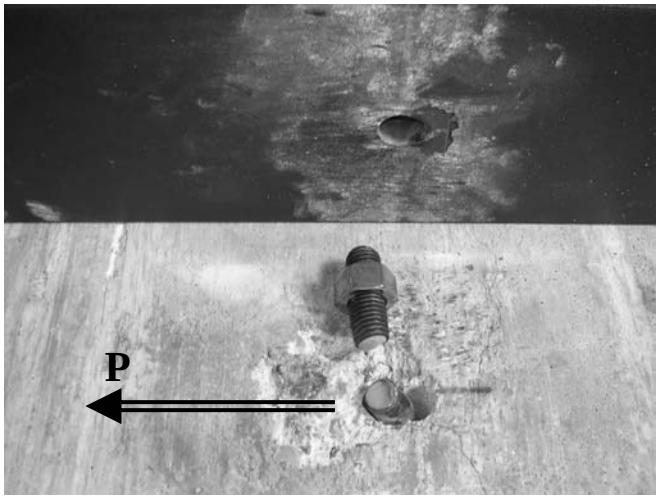

Figure 6.13: Shear failure of Specimen HTFGB03

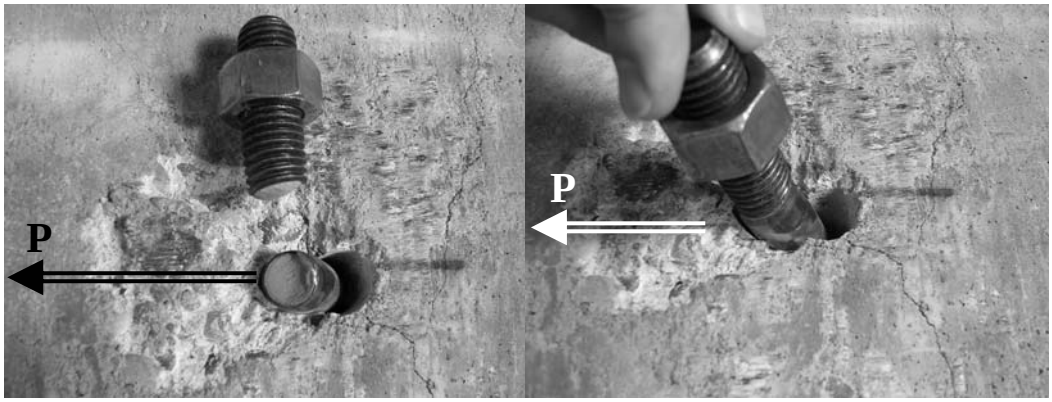

Figure 6.14: Close-up of Specimen HTFGB03 after failure

6.3.5.1 Results for High-Tension, Friction-Grip Bolt (1¼-in. Diameter)

As discussed in Chapter 5, epoxy was used on the first two of the specimens for this connection method to ensure a flat surface for the washer, as shown in Figure 6.15. Epoxy was not used for the third test (Figure 6.16). In all three tests, the bottom of the hole was "flattened" as well as possible using a hammer and chisel. A 3-in. O.D washer was used for each of the three tests. As mentioned in Chapter 5, a hole with an effective diameter of about 3.5 in. was

drilled using a 2-in. diameter bit in four adjacent locations. Figure 5.16 in Chapter 5 illustrates the intended drilling pattern, while its implementation is shown in Figure 6.15(b). This drilling technique was investigated as an alternative to a coring machine. As with the ¾-in. high-tension, friction-grip bolts, no grout was used in these tests.

Specimen HTFAT01 was not tested to failure because it was believed that the clevis was in danger of being overstressed. Judging from the other tests, it is unlikely that the specimen had much more slip capacity. The peak load had been reached. Although the LVDTs were removed prior to failure on Specimens HTFAT01 and HTFAT02, Specimen HTFAT02 failed soon after this . The ultimate slip capacity was close to 0.4 in. for each specimen, as shown in Figure 6.42. HTFAT03 failed before the LVDTs were removed. Transverse cracks were observed at the plateau in the load around 23 kips for each test. The concrete block may not have been large enough for this size of connector.

Figure 6.15: Specimens HTFAT01 and HTFAT02 with epoxy

Figure 6.16: Specimen HTFAT03 with no epoxy

As shown in Figure 6.17, the HTFAT connectors show little deformation in the concrete. Unlike most of the other connector tests, the steel plate underwent significant bearing deformation(Figure 6.18).

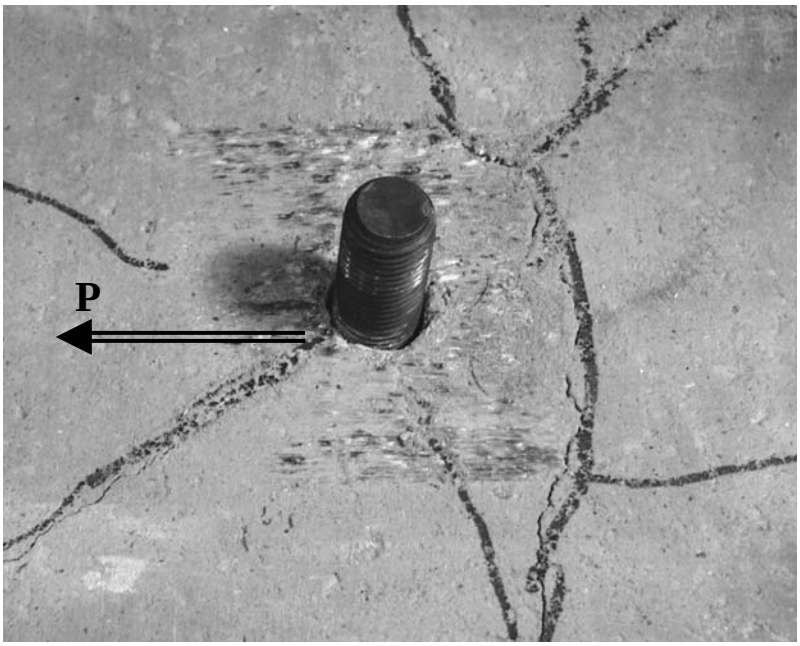

Figure 6.17: Small deformation in slab (SpecimenHTFAT01)

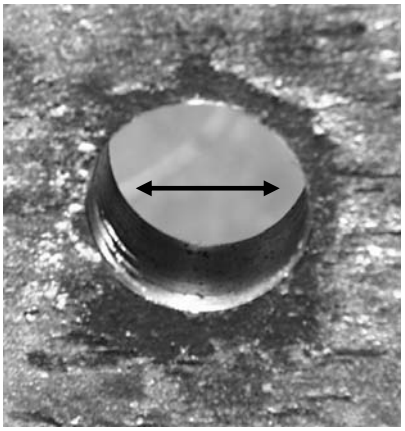

Figure 6.18: Significant bearing deformation in steel plate (Specimen HTFAT01)

Both large-diameter, high-tension, friction-grip bolts caused significant crushing of the entire concrete slab (Figure 6.19), which was the cause of failure.

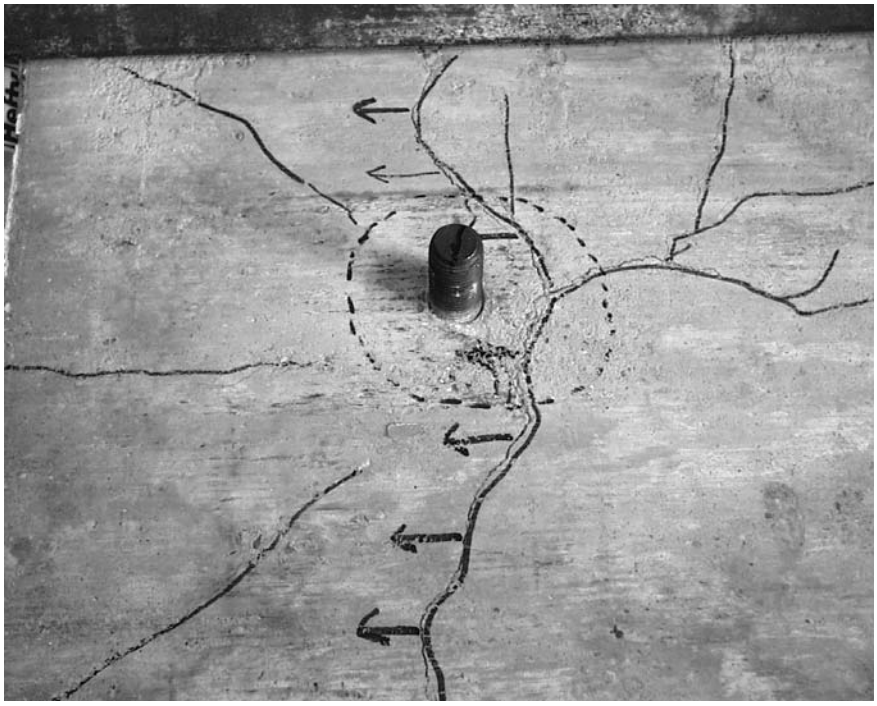

Figure 6.19: Significant cracking of concrete slab for Specimen HTFAT02

6.3.6 Results for Expansion Anchor

The expansion anchor (KWIGB) was the first connection method installed and tested. Given its poor structural performance relative to the cast-in-place welded headed stud, as shown in Figure 6.43, this anchor was eliminated from this investigation. Only one anchor was tested for this connection method, and it is shown at failure in Figure 6.20. It displayed high deformation capacity, (Figure 6.21), probably due to the steel plate lifting and the anchor experiencing significant tension. Figure 6.21(b) shows the anchor kinking at the interface between the concrete block and the steel plate. As shown in Figure 6.22, the plate had significant deformation on the side adjacent to the interface,.

To obtain its hysteretic behavior, the specimen was unloaded after a brief initial loading. Figure 6.43(b) shows that the anchor underwent some inelastic deformation during this load cycle, because the loading branches do not match.

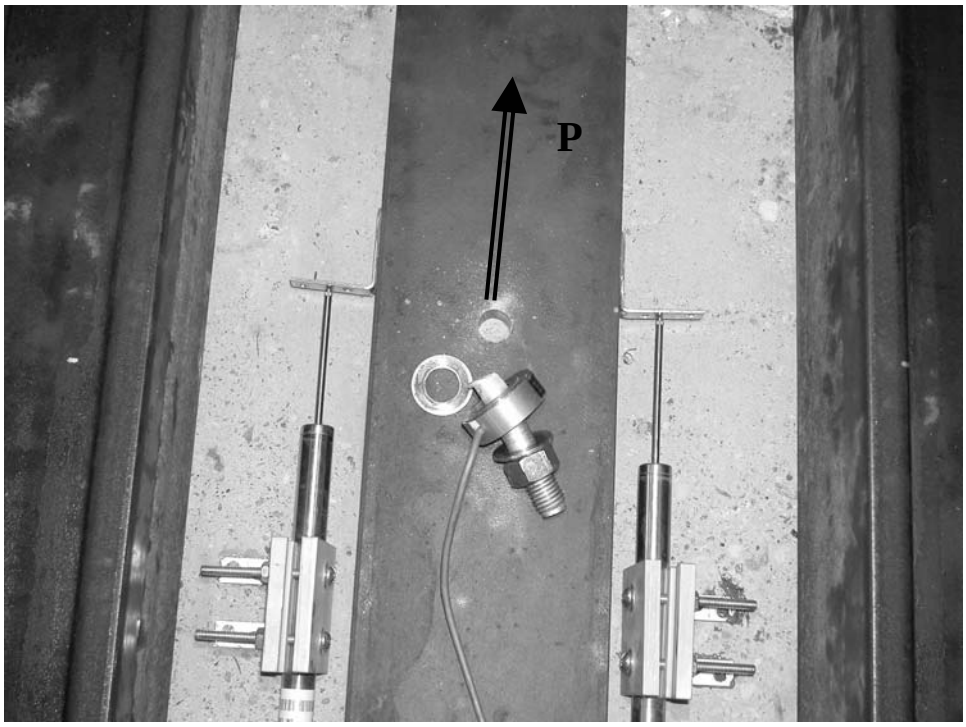

Figure 6.20: Failure of Specimen KWIKB01

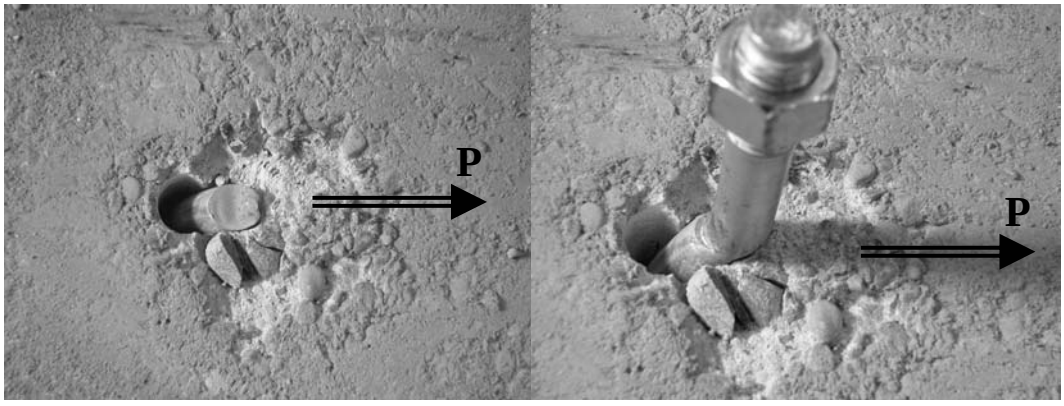

Figure 6.21: Concrete deformation for Specimen KWIKB01

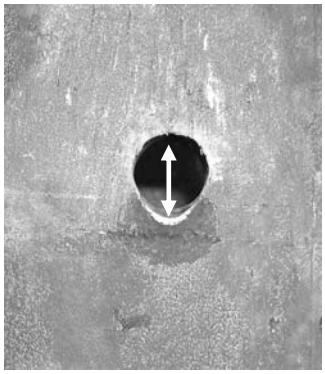

Figure 6.22: Deformation in plate on concrete side for Specimen KWIKB01

6.3.7 Results for Undercut Anchor

Specimen MAXIB03 is the only undercut anchor reported in Table 6.2 because the other two specimens were installed differently and it is believed that the third specimen most accurately represents probable field installation. MAXIB01 was installed without an upper sheath (shown just left of the middle of Figure 5.14 in Chapter 5) covering the threads in the hole. MAXIB02 was installed with the bottom of the upper sheath in the shear plane at the interface of the concrete and steel. MAXIB03 was installed with the bottom of the upper sheath below the shear plane in the concrete. No average is plotted for these three tests because they are viewed as three different conditions.

In each undercut anchor test, the applied tension exceeded the manufacturer's recommended pre-tension of 11.0 kips. Due to a subsequently discovered error in the calibration of the washer load cell led, the researchers actually applied more pre-tension than intended.

The pre-tension applied to the three specimens varied based on the various sheath configurations. Since no upper sheath was used in MAXIB01, the anchor could be tightened well above the manufacturer's recommended pre-tension. The highest possible pre-tension was desired so friction could act as the primary force

transfer mechanism under working loads. The upper sheath in MAXIB02 was brought into contact with the steel plate upon tensioning, effectively limiting the tension that could be applied to the anchor. As observed in Table 6.2, the applied tension forcing the concrete and steel together was lower than in MAXIB01. For Specimen MAXIB03, the lower expansion sheath was cut so that the interface of the sheaths was 1 in. below the concrete-steel interface. The 2-in. upper sheath was used, but was cut shorter to account for the lifting that occurred under tensioning. Unfortunately, as shown in Table 6.2, this measure was not effective. To develop of the highest clamping force with the Maxi-Bolt apparently requires removal of the upper sheath.

The LVDTs were not removed for any of the three MAXIB tests. MAXIB01 failed in pryout (Chapter 2), as shown in Figure 6.23 through Figure 6.29.

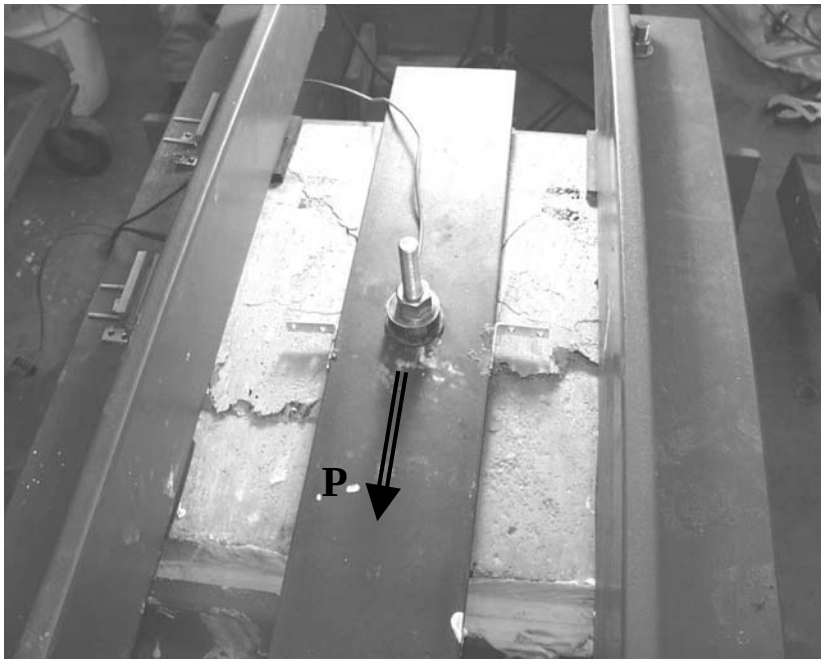

Figure 6.23: Pryout of Specimen MAXIB01

As Figure 6.24 shows, the plate lifted significantly during Test MAXIB01. Figure 6.25 shows a crack along the side of the concrete specimen characteristic of a pryout failure; Figure 6.26 shows the extent of the damage to the concrete block; and Figure 6.27 shows the large deformation in the concrete around the anchor. In contrast, only slight deformation was observed in the steel plate, as shown in Figure 6.28. Figure 6.29 shows how much the anchor bent during the test.

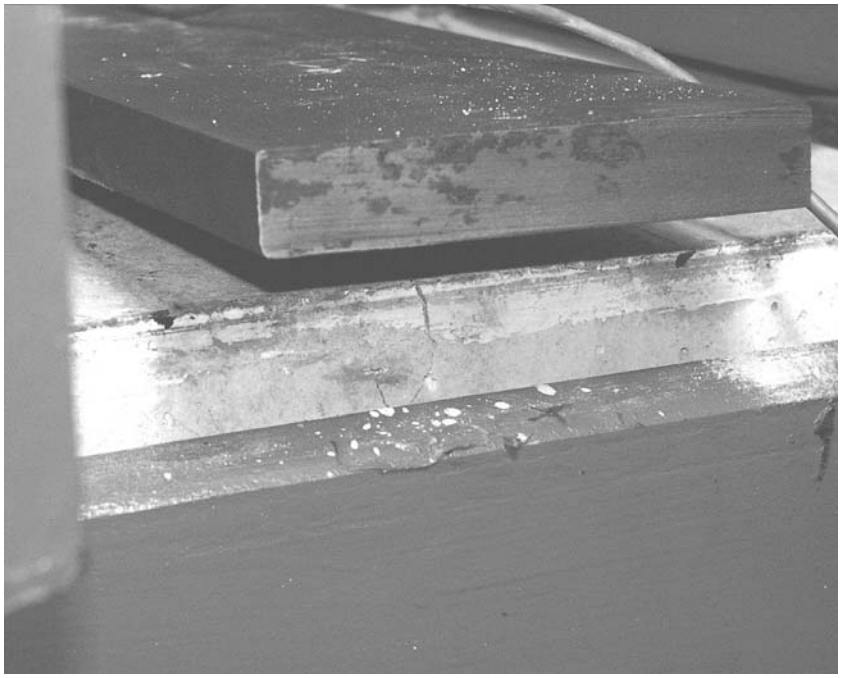

Figure 6.24: Steel plate lifted from pryout, Test MAXIB01

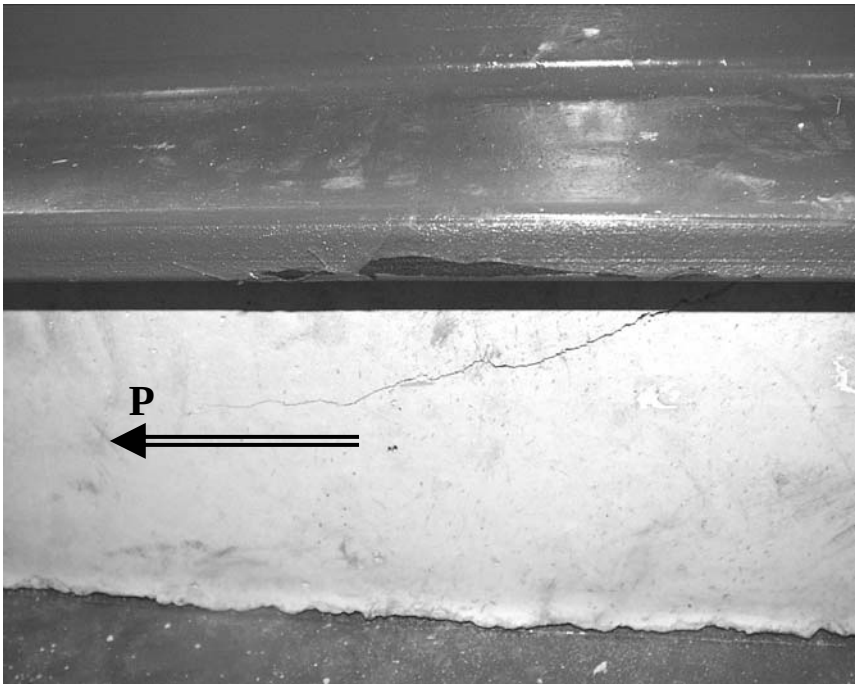

Figure 6.25: Pryout crack in side of slab for MAXIB01

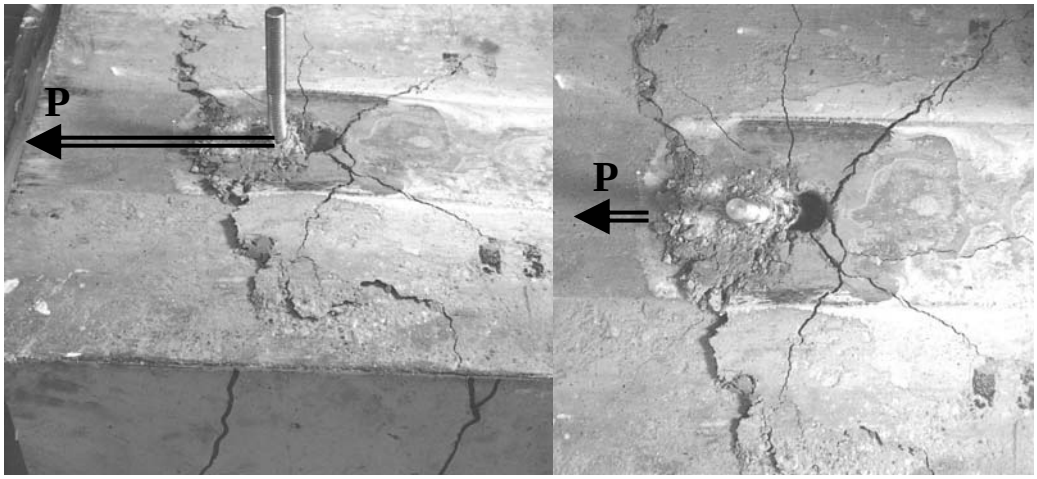

Figure 6.26: MAXIB01 with steel plate removed

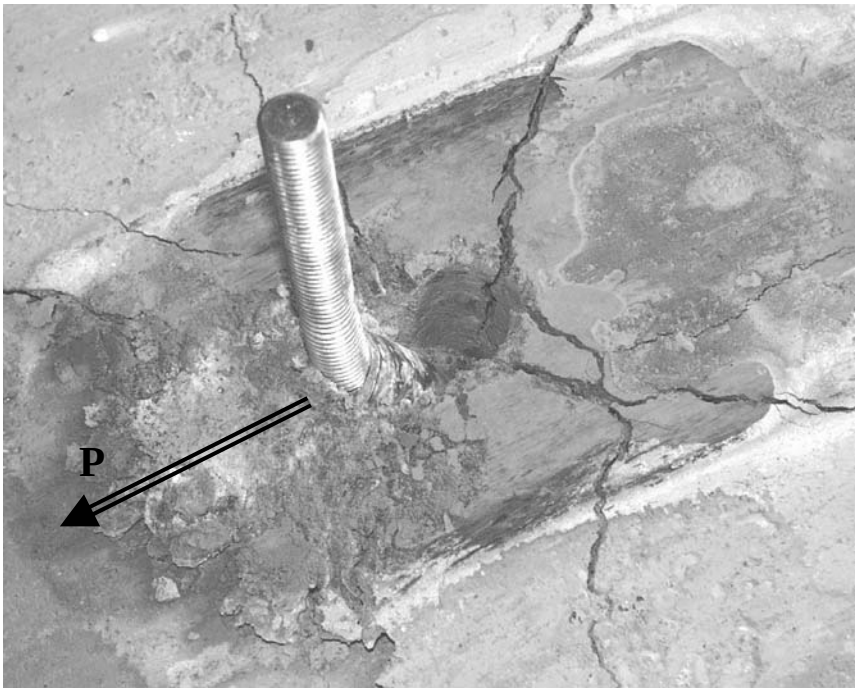

Figure 6.27: Concrete deformation of Specimen MAXIB01

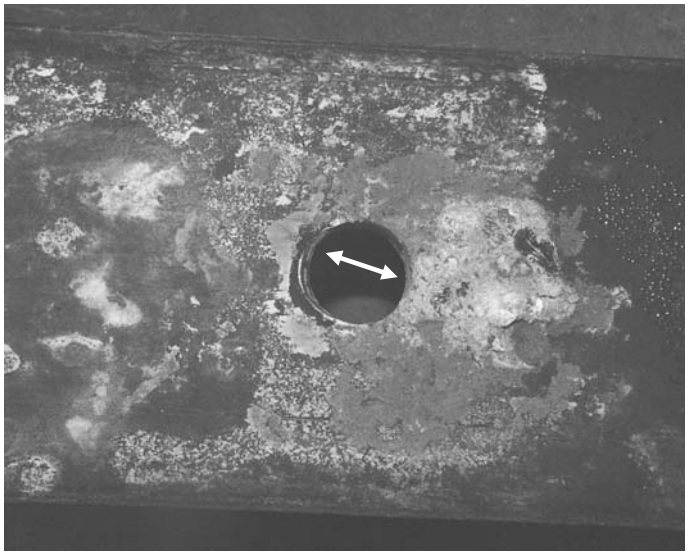

Figure 6.28: Slight steel plate deformation of MAXIB01

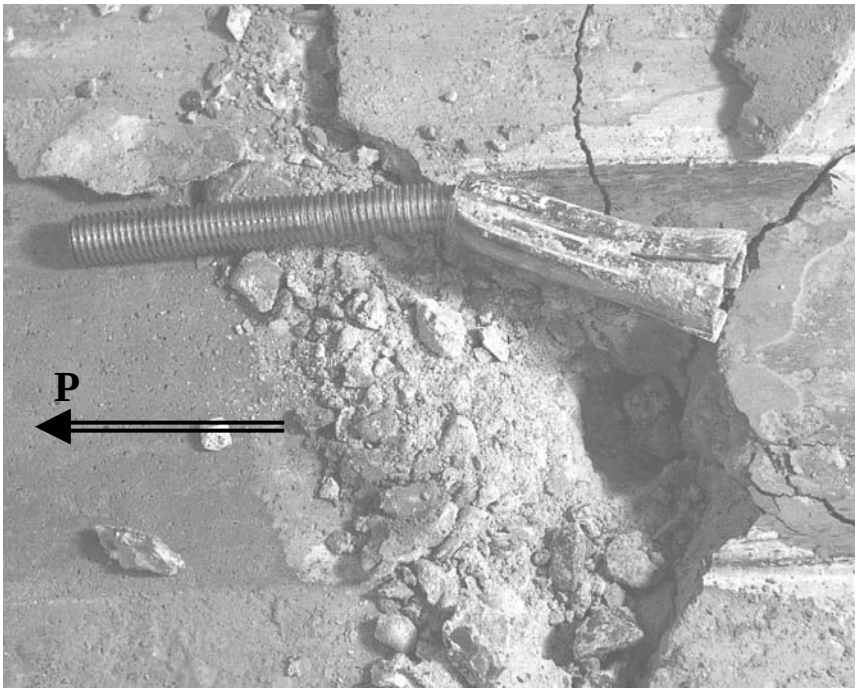

Figure 6.29: MAXIB01 anchor after removal from slab

MAXIB02 had the interface of the two sheaths at the shear plane, which would be the typical installation configuration using the standard 1-in. long upper sleeve. No pryout was observed for this specimen (Figure 6.30 and Figure 6.31). The anchor sheared at the interface of the two sheaths (which corresponded to the shear plane between the concrete slab and steel plate). This is one of the reasons that Specimen MAXIB02 had the lowest capacity of the connection method—the steel plate did not have to shear through the sheath, but just through the anchor. Yet, it also could not bend and transfer the load through flexure, as MAXIB01 did. Significant steel plate deformation occurred due to the large sheath (Figure 6.32).

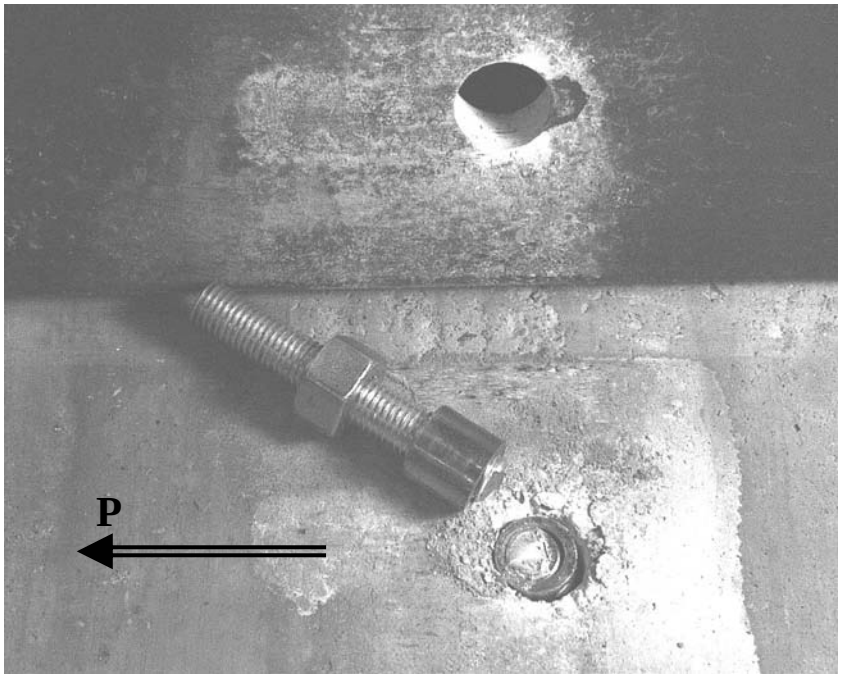

Figure 6.30: Sheath at shear plane and no pryout failure for MAXIB02

Figure 6.31: No cracks in side of slab for MAXIB02

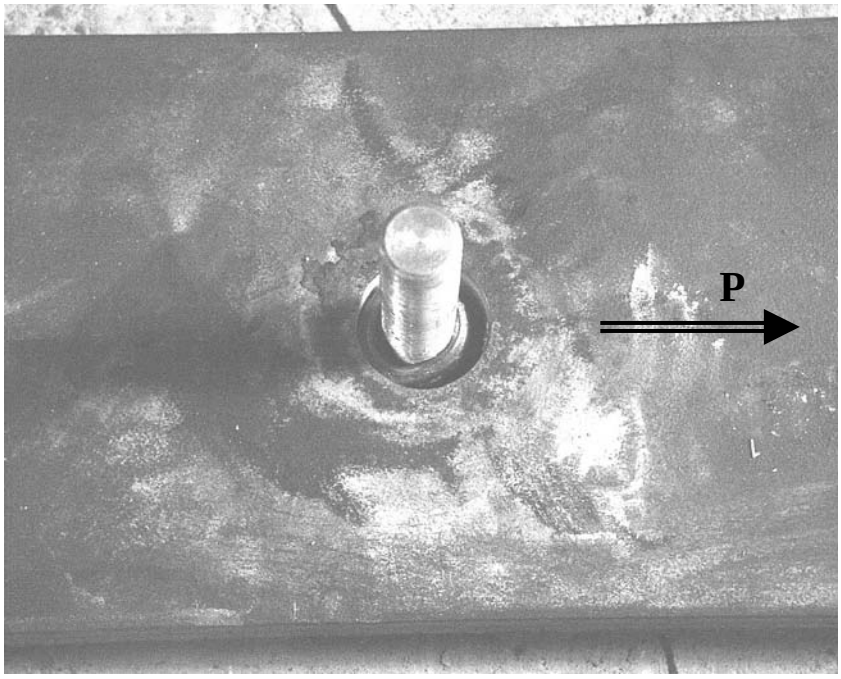

Figure 6.32: Gap between steel plate and anchor sleeve after testing MAXIB02

The interface of the two sheaths in Specimen MAXIB03 was located in the concrete about 1 in. below the steel-concrete interface. The anchor in Specimen MAXIB03 sheared off below the shear plane (at the interface of the two sheaths) after some pryout, as shown in Figure 6.33. The anchor apparently experienced significant tension (Figure 6.44).

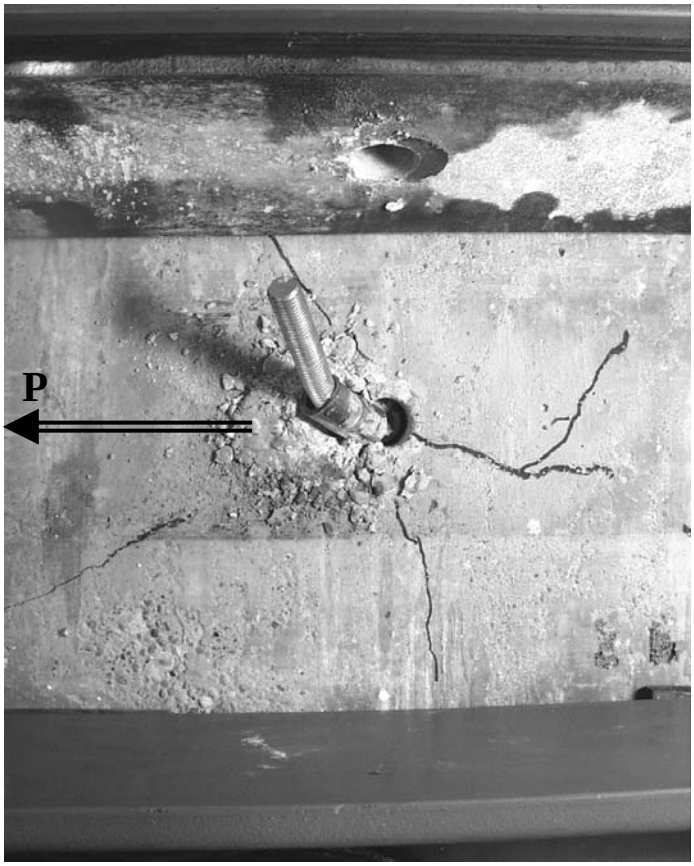

Figure 6.33: MAXIB03 failure at interface between sleeves

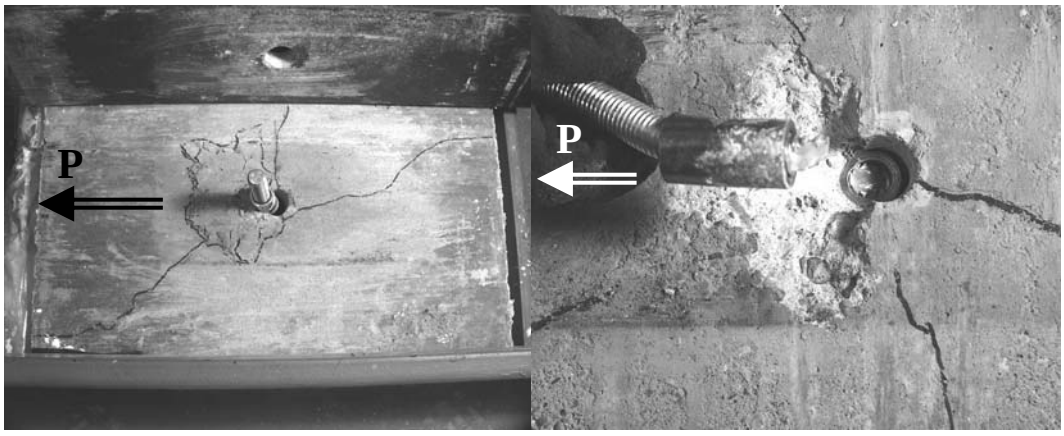

Figure 6.34: Close-up of MAXIB03 after failure

6.3.7.1 Results for Undercut Anchor (High-Strength)

The high-strength undercut anchor used in Specimen MAXHS01 (A193-B7 steel) was installed with the interface of the two sheaths about 1 in. into the concrete. The anchor did not fracture in the test. Pryout had begun, but the anchor appeared to be close to shearing through the shank (Figure 6.35). Figure 6.36 shows significant deformation in the steel plate, due to the sheath. The LVDTs were removed prior to the end of testing because the displacements were becoming so large it was believed the devices were in danger of being damaged.

Both high-strength undercut anchor tests had a slight sudden increase in slip without an increase in load at about 13 kips, due to the formation of a transverse crack in the concrete block. Several possible explanations are given below for cracking at this relatively low load. First, the anchor rotated significantly in the hole in the concrete after slip occurred, causing only the top and bottom of the anchor to bear against the concrete. This may have caused the block to split at the top due to the concentrated bearing force. Although no direct evidence of this was observed, it is also possible that the blocks in these tests had a local imperfection due to incomplete consolidation of concrete.

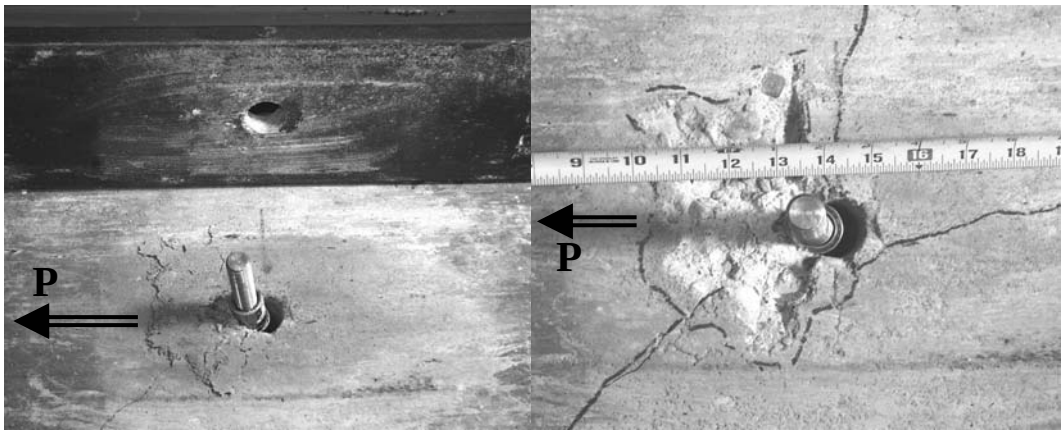

Figure 6.35: Crushing deformation of MAXHS01

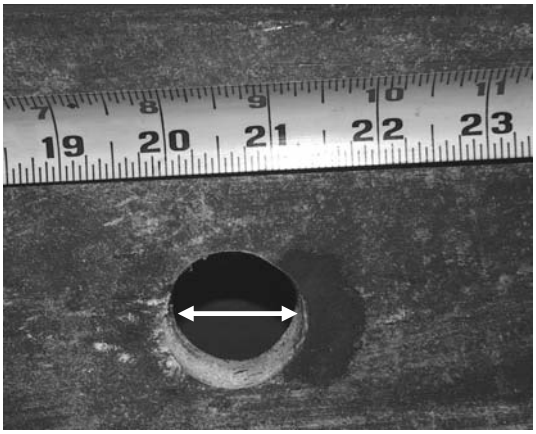

Figure 6.36: Steel plate deformation of MAXHS01

6.3.7.2 Results for Undercut Anchor (High-Strength with Anchor Gel

As discussed in Chapter 5, the anchor for Specimen MAXHG01 was coated with Five-Star® RS Anchor Gel in an attempt to reduce the anchor's slip into bearing. Because of the various problems discussed in Section 5.5.5.2.1, little epoxy was placed around the anchor. As shown in Figure 6.46, Specimen MAXHG01 performed slightly better than the other undercut anchors, for which no "slip into bearing" was observed. This improvement is likely due in part to the anchor gel, and also to the back of the hole in the steel plate being closer (by chance) to the anchor

The drop in the load at about 13 kips is due to a transverse crack in the block. Possible explanations for this are discussed in the section above. The steel plate was barely lifting at a slip of 0.4 in.

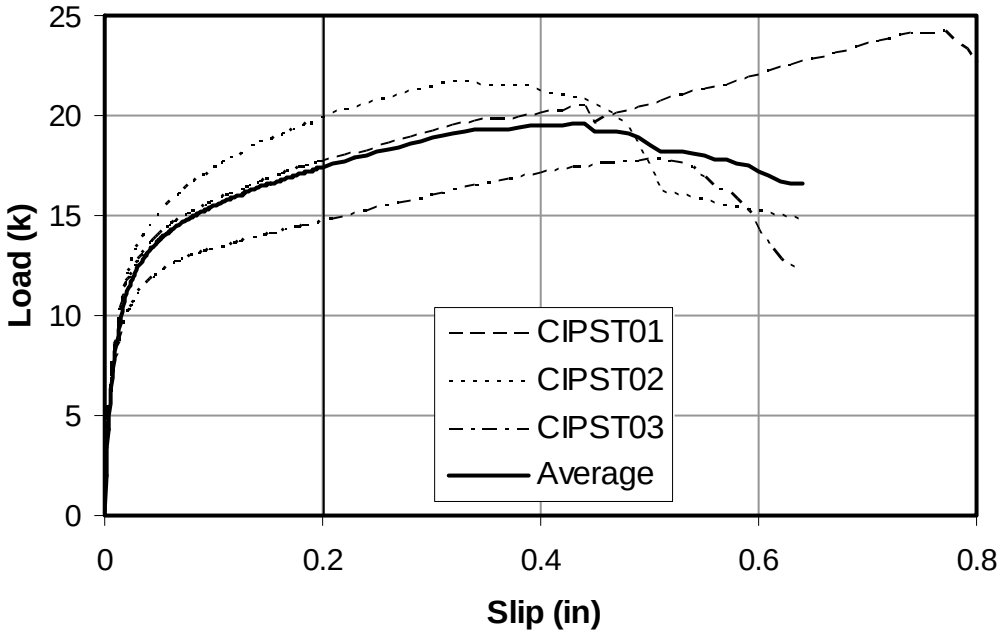

(a) Complete data set

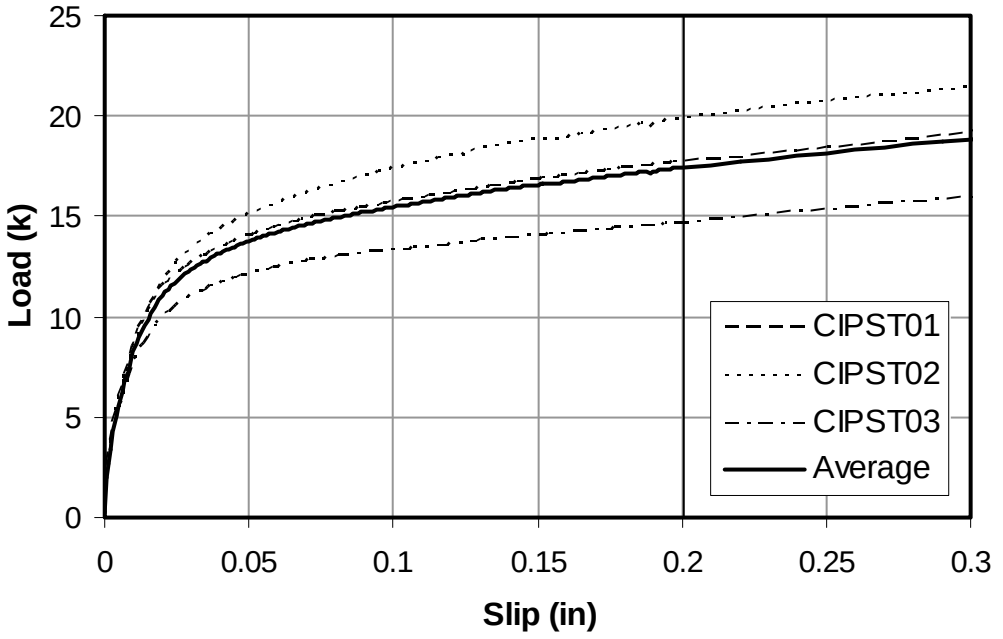

(b) Slip ranging from 0 to 0.3 inches

Figure 6.37: Load-slip curves for CIPST tests

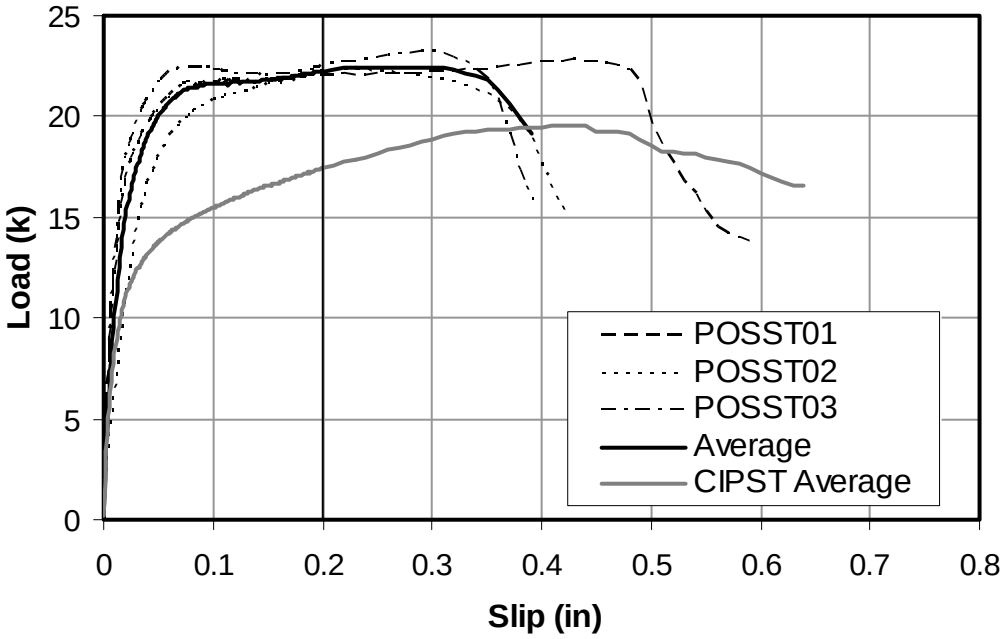

(a) Complete data set

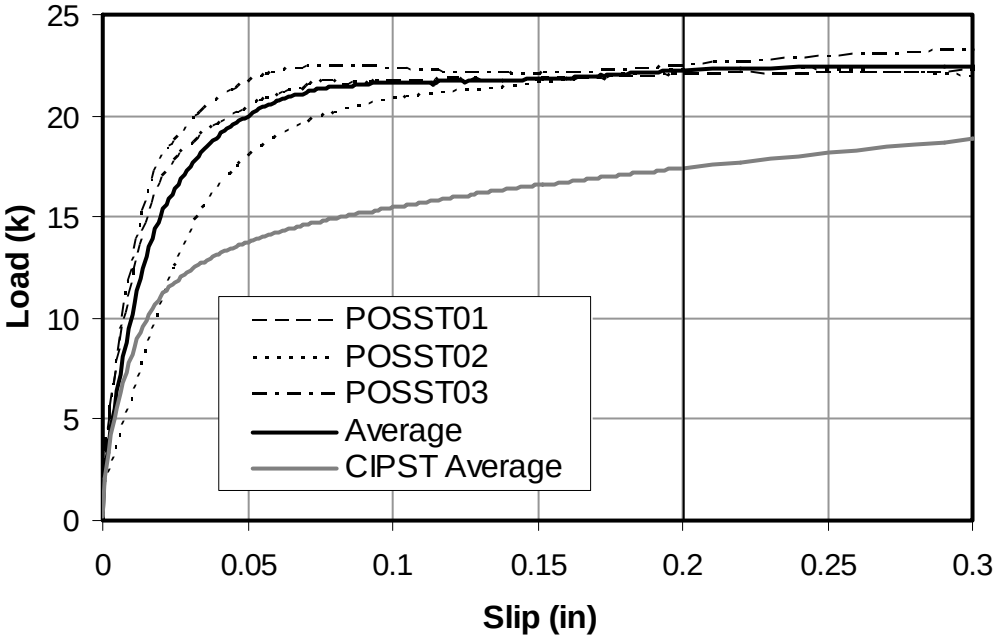

(a) Complete data set

Figure 6.38: Load-slip curves for POSST tests

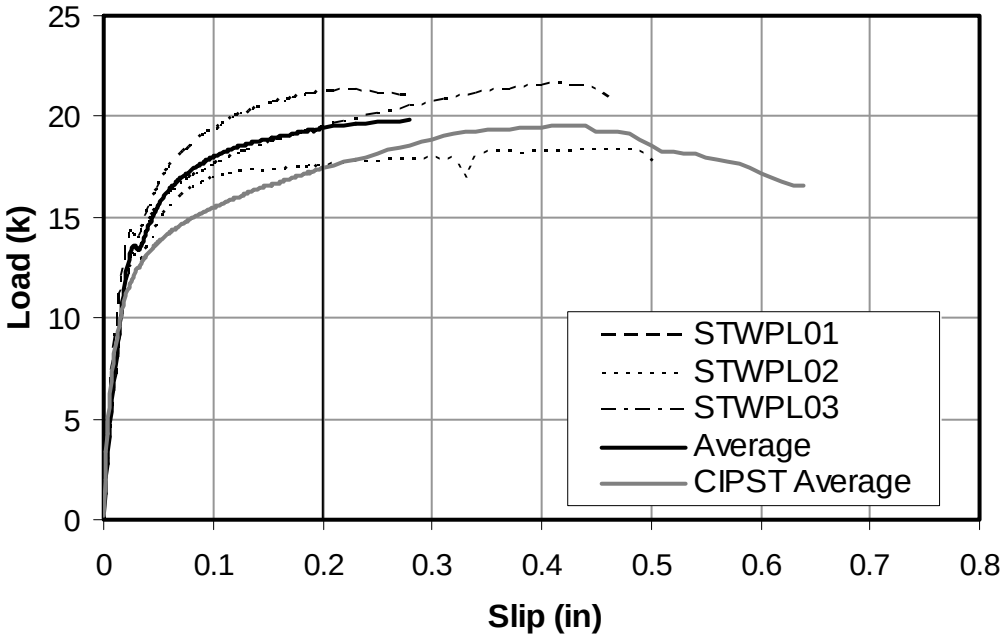

(a) Complete data set

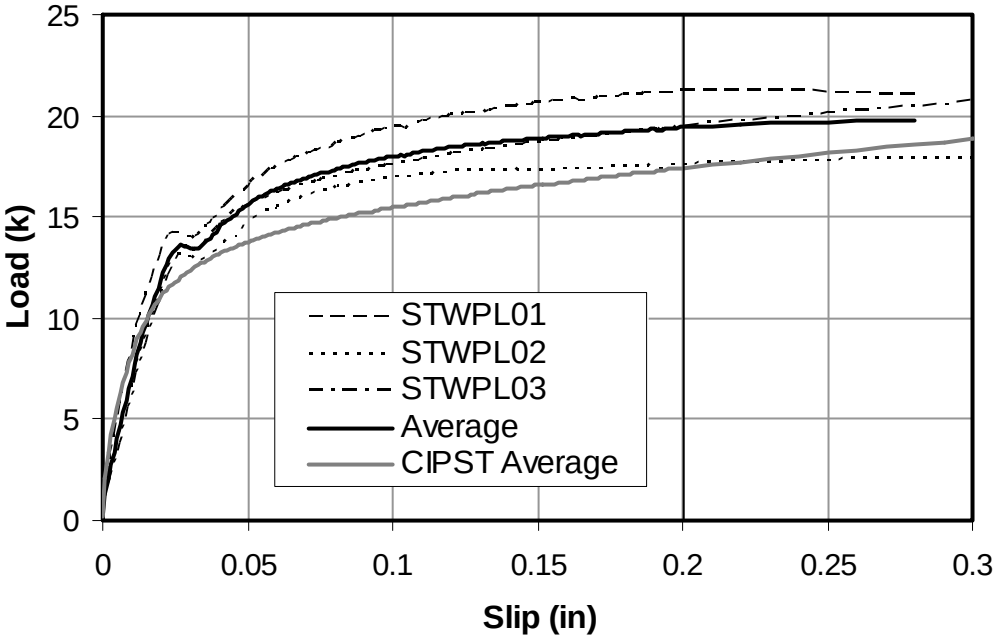

(b) Slip ranging from 0 to 0.3 inches

Figure 6.39: Load-slip curves for STWPL tests

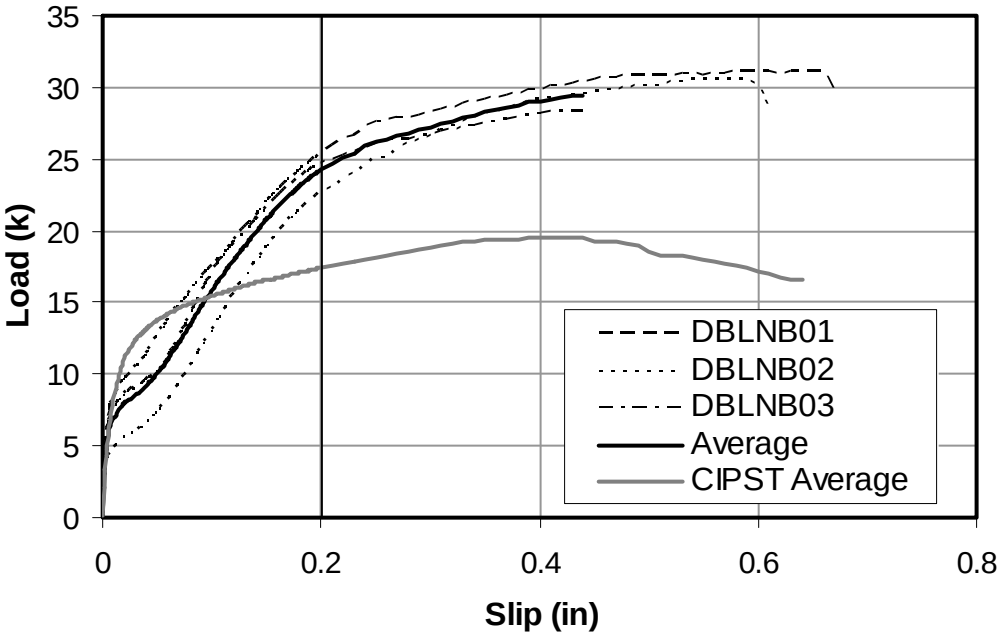

(a) Complete data set

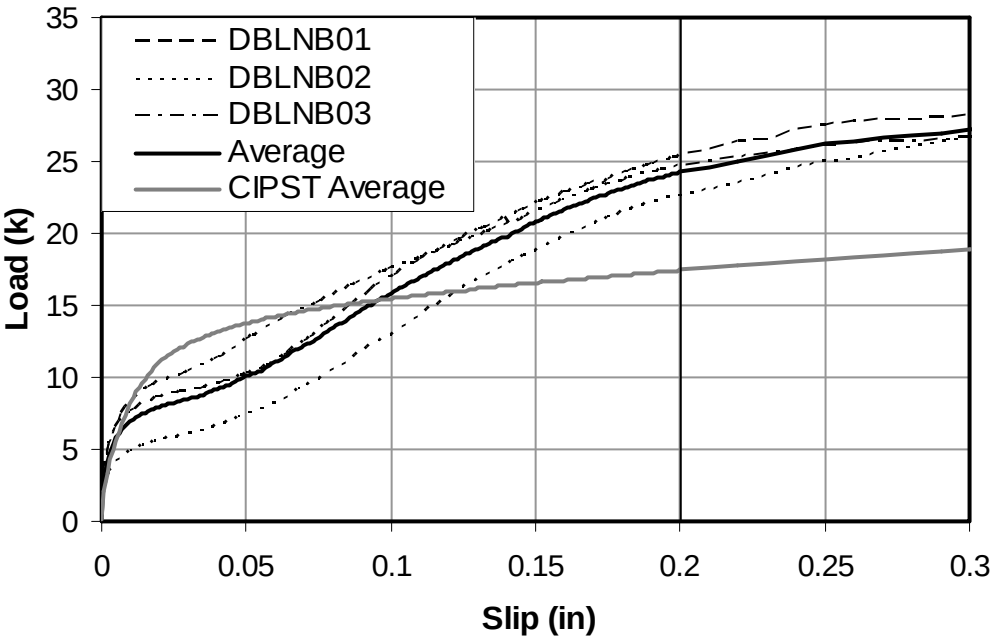

(b) Slip ranging from 0 to 0.3 inches

Figure 6.40: Load-slip curves for DBLNB tests

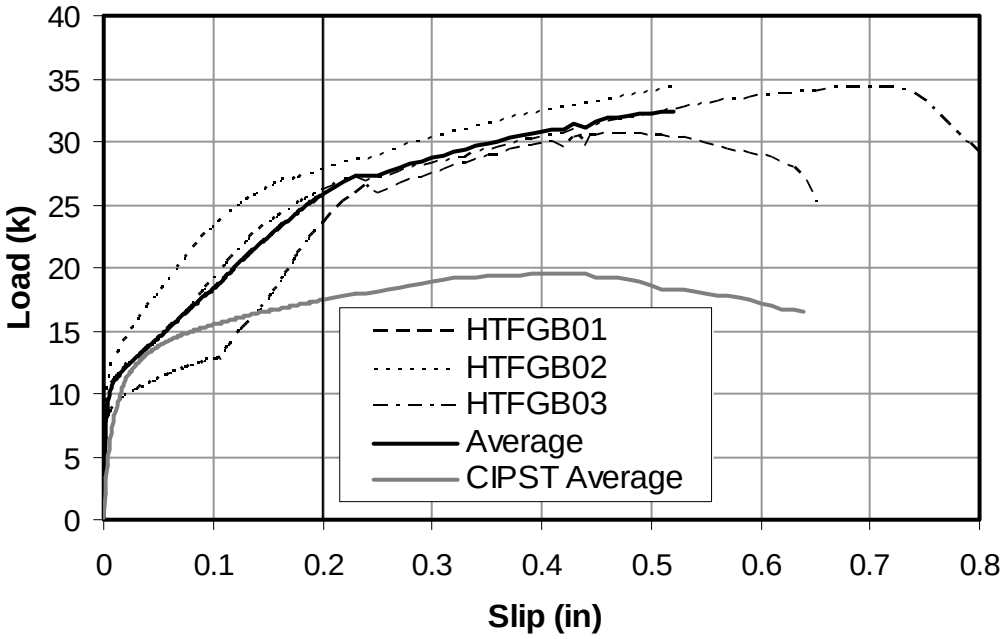

(a) Complete data set

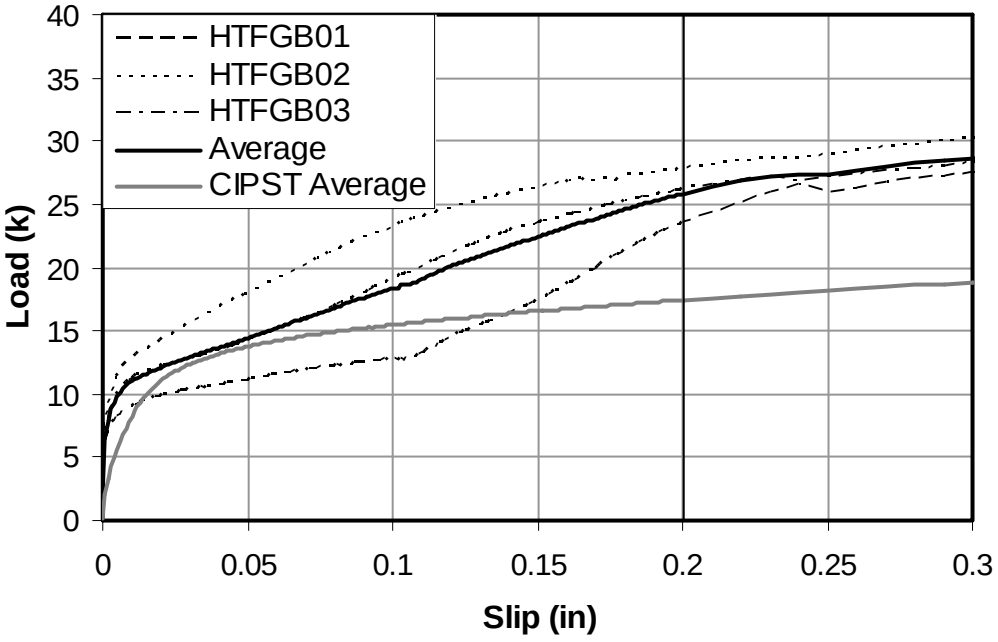

(b) Slip ranging from 0 to 0.3 inches

Figure 6.41: Load-slip curves for HTFGB tests

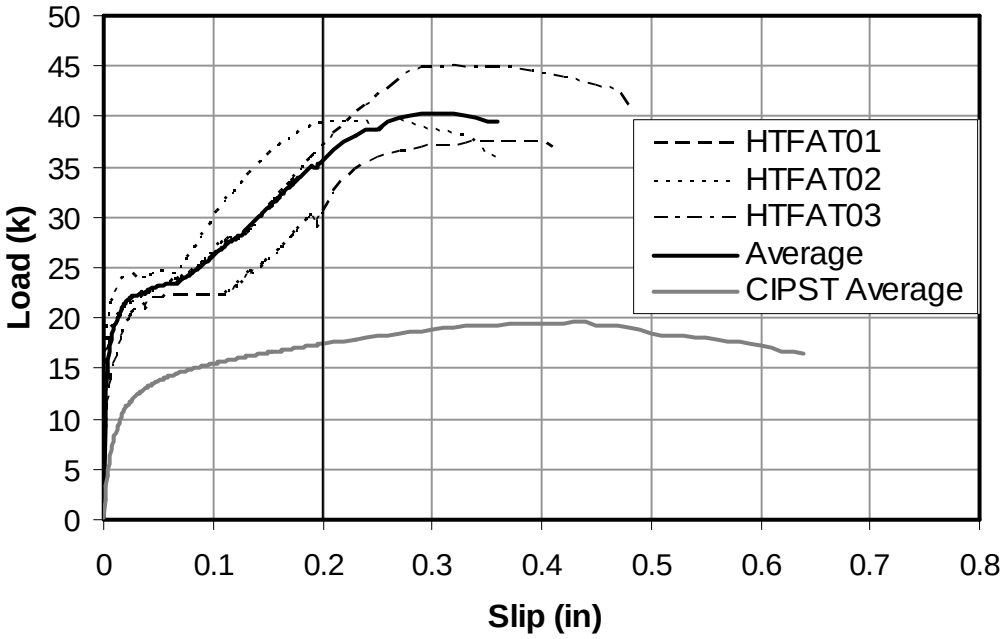

(a) Complete data set

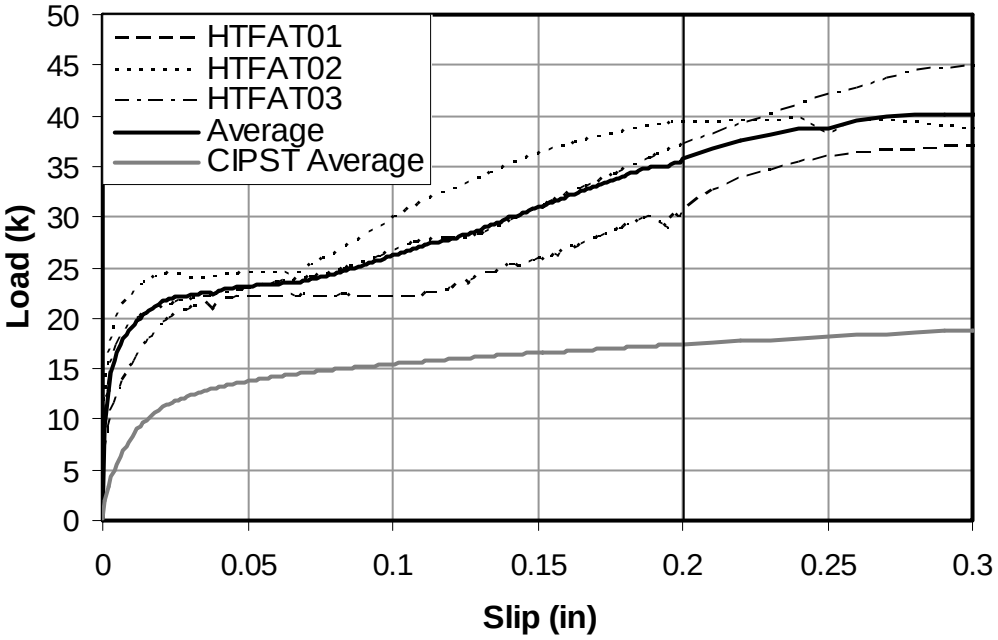

(b) Slip ranging from 0 to 0.3 inches

Figure 6.42: Load-slip curves for HTFAT tests

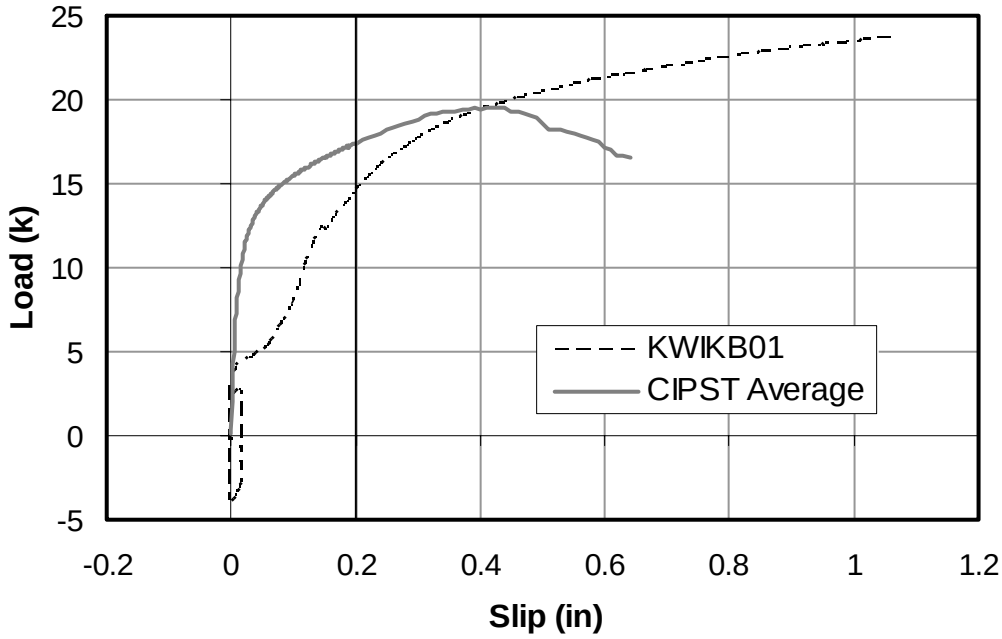

(a) Complete data set

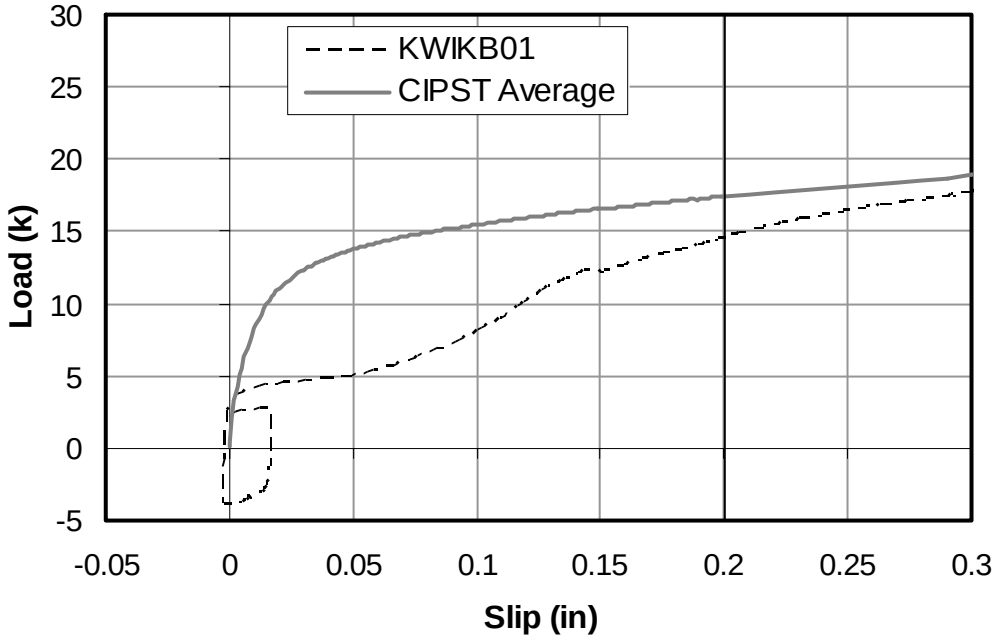

(b) Slip ranging from 0 to 0.3 inches

Figure 6.43: Load-slip curves for KWIKB test

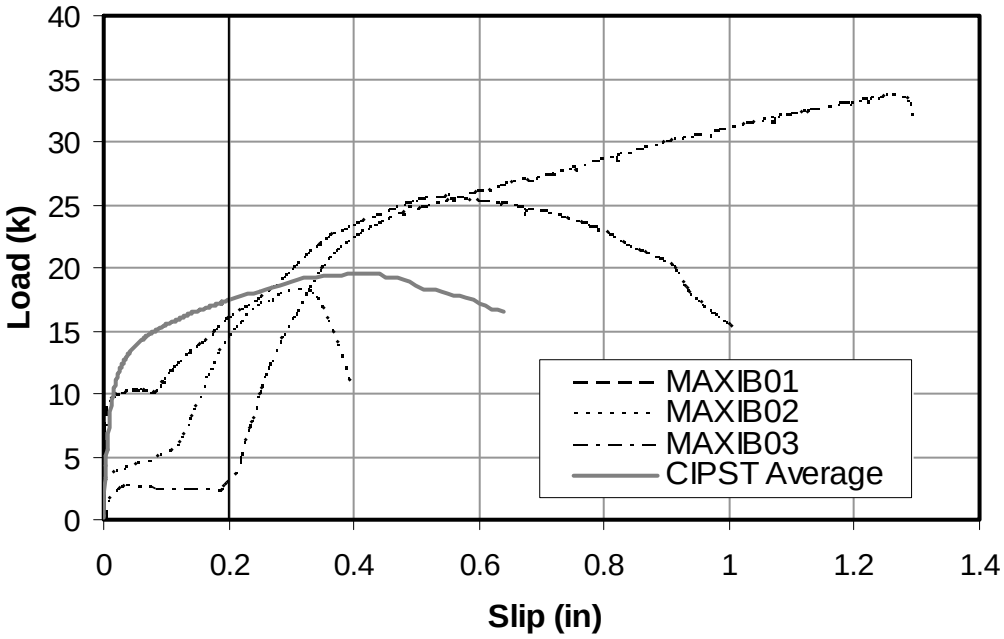

(a) Complete data set

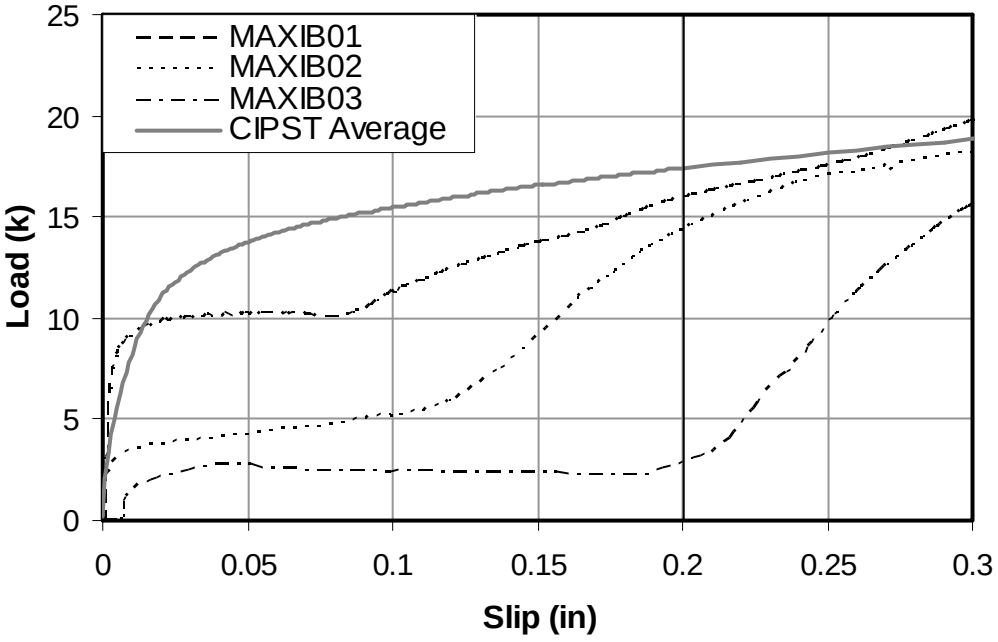

(b) Slip ranging from 0 to 0.3 inches

Figure 6.44: Load-slip curves for MAXIB tests

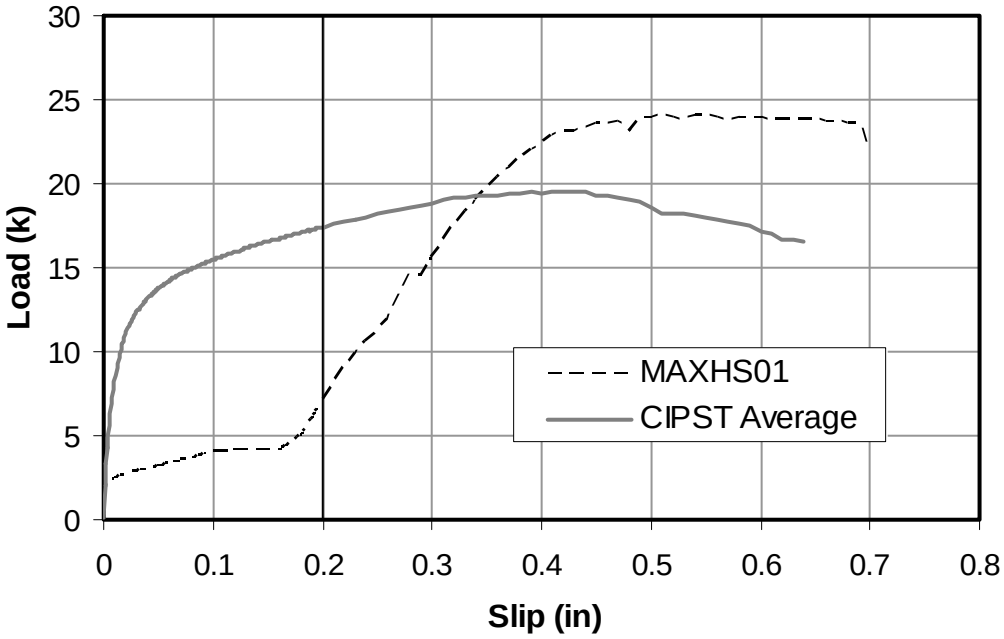

(a) Complete data set

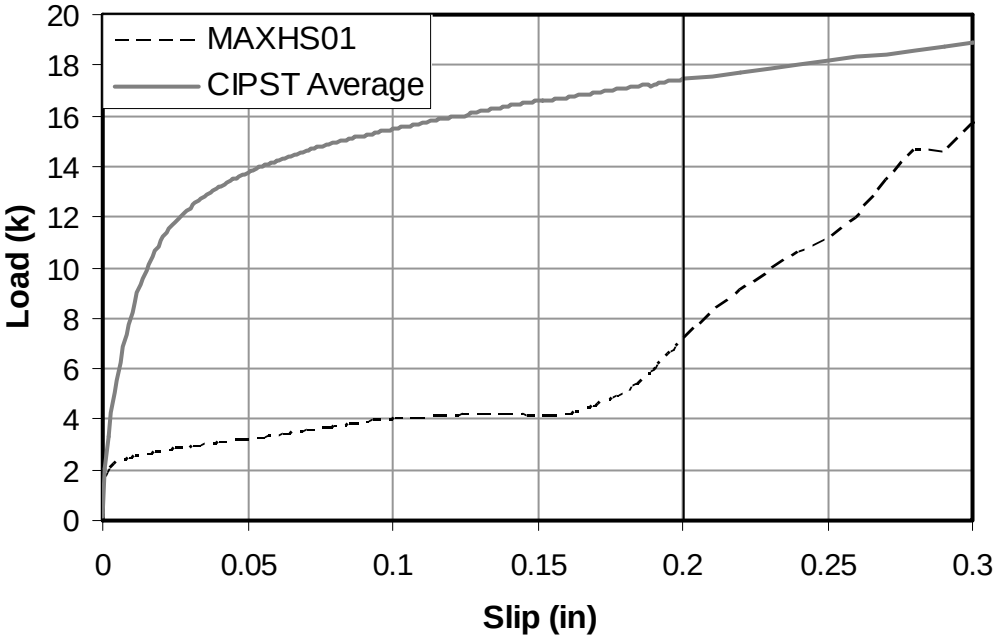

(b) Slip ranging from 0 to 0.3 inches

Figure 6.45: Load-slip curves for MAXHS test

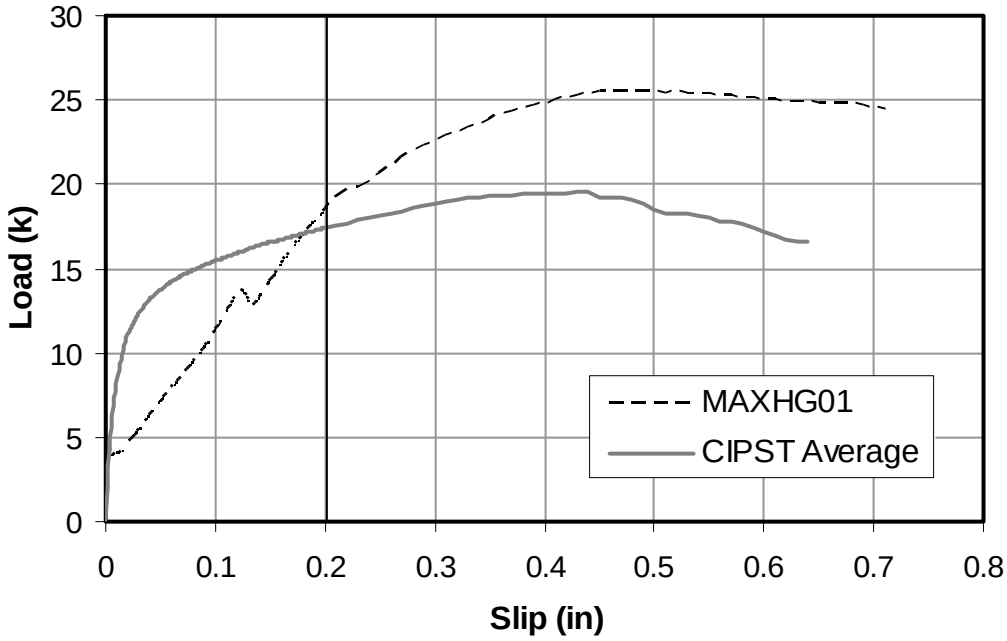

(a) Complete data set

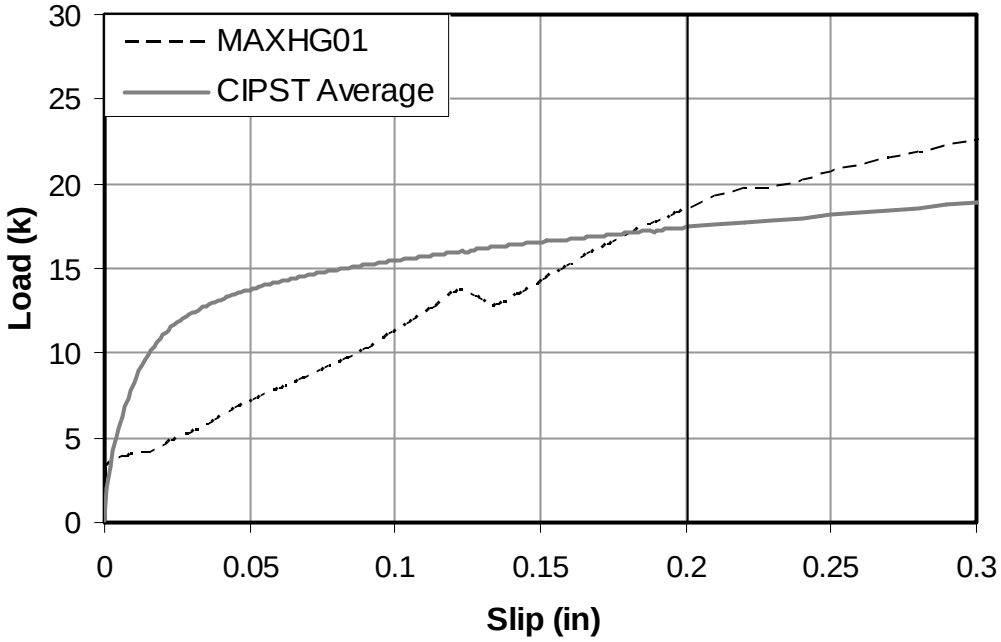

(b) Slip ranging from 0 to 0.3 inches

Figure 6.46: Load-slip curves for MAXHG test

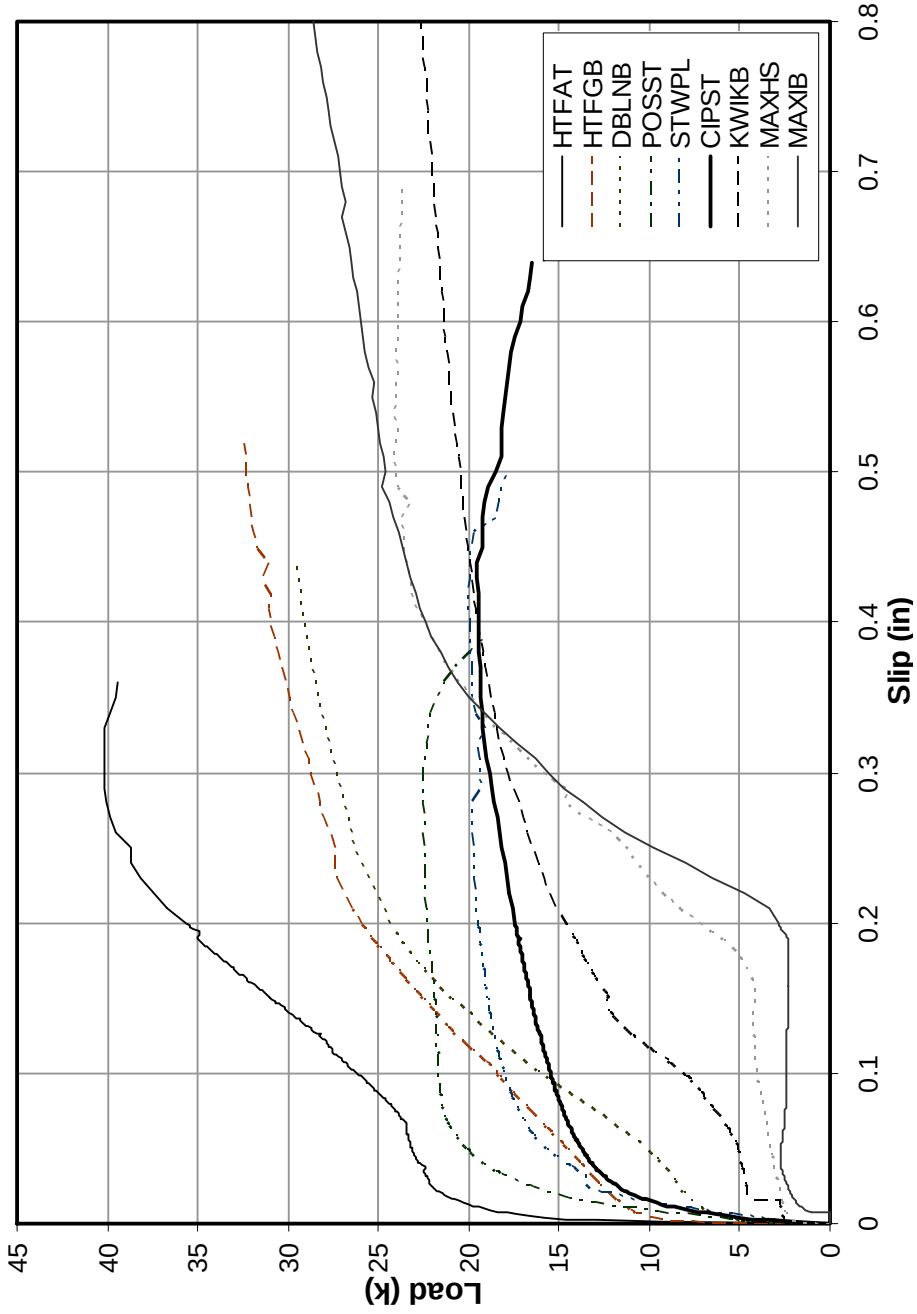

Figure 6.47: Compilation of average results for connection methods

CHAPTER 7
FURTHER EVALUATION AND DISCUSSION OF EXPERIMENTAL RESULTS

7.1 INTRODUCTION

In this chapter, the results reported in Chapter 6 are evaluated and discussed. Additional results of tests for coefficient of friction are covered first, followed by additional results for the single-connector, direct-shear static load tests. Chapter 8 summarizes the conclusions drawn from this chapter as well as previous chapters.

7.2 COEFFICIENT OF FRICTION

Previous research by Cook led to the recommendation of a design value for the dynamic coefficient of friction, μ, of 0.40 with a Φ-factor of 0.65 (Cook 1989). Since the design value for coefficient of friction is critical to some of the connection methods investigated in this project, and since little research had been performed on existing, weathered steel girders, the static coefficient of friction was measured in this project both in field tests and in the single-connector, direct-shear static load tests. These data are discussed below.

7.2.1 Discussion of Field Results

Twenty-four tests were conducted on four girders of a demolished bridge in San Antonio, Texas. Results are listed in Table 6.1. For the field tests, the average static coefficient of friction was 0.63, with a minimum value of 0.50, and a maximum value of 0.77. The standard deviation was 0.061, with a median of 0.64. Using a lower 5 % fractile gives a recommended design value of 0.60.

These tests were performed using a concrete block weighing 22.0-lb, three orders of magnitude below the pre-tension force applied by some of the connectors investigated in this phase of the project.

7.2.2 Discussion of Test Results for Static Coefficient of Friction

The coefficient of friction was calculated for 14 of the single-connector, direct-shear static load tests by dividing the applied shear by the applied tension at first slip. As described in Chapter 6, the shear at first slip was estimated using an offset method. Results are given in Table 6.2. The mean static coefficient of friction was 0.40, with a minimum value of 0.11, and a maximum value of 0.86. The standard deviation was 0.22, with a median of 0.37. Using a lower 5 % fractile gives a recommended design value of 0.28, less than half of the design value from the field tests. Several possible reasons for the discrepancy between the field and the laboratory tests are discussed below.

Two connection methods showed exceptionally low values for the coefficient of friction: the 1¼-in. diameter high-tension, friction-grip bolt (HTFAT) and the undercut anchor (MAXIB). Several possible explanations for these lower results are given. The HTFAT tests were the only ones in which the applied tension was not directly measured with a washer load cell or load-indicating washer; the torque method was used to estimate the pre-tension. Therefore, the tension may not have been as high as estimated, giving erroneously low results for μ. The mean coefficient of friction for this connection method was 0.21. Although not directly known, the applied pre-tension was relatively high (over 2.5 times that of the other connectors), possibly crushing the concrete locally at the steel-concrete interface, and thereby affecting the coefficient of friction. Even though the computed coefficient of friction for the high-tension,

friction-grip bolts was quite low, the actual slip loads were the highest among all connection methods, due to the very high tension force in the connectors.

The MAXIB undercut anchors slipped at a much lower shear than anticipated for the two tests in which the second sheath was used. For Specimen MAXIB01, in which a second sheath was not used, the calculated coefficient of friction was 0.47. Specimens MAXIB02 and MAXIB03, with second sheaths, gave values of 0.26 and 0.22 respectively. It is probably that the second (upper) sheath in Specimen MAXIB02 or MAXIB03 went into bearing against the steel plate, limiting and reducing the pre-tension as more torque was applied to the nut. For those tests, the tension was clamping the sheath to the steel plate, not the concrete block to the steel plate. In these two tests, the applied tension suddenly dropped significantly (20 %) after reaching about 20 kips of pre-tension during the time the anchor was being tensioned. This was probably when the sheath encountered the steel plate. The first test showed no drop in tension at a higher pre-tension of 30 kips, implying that the other two anchors did not yield when they reached 20 kips of pre-tension. The pre-tension was later relaxed 40 % for Specimen MAXIB01 to account for relaxation, leading to the value of tension reported in Table 6.2.

Excluding the data for the HTFAT and MAXIB connection methods, the mean static coefficient of friction was 0.52, with a minimum value of 0.31, and a maximum value of 0.86. The standard deviation was 0.20, with a median of 0.43. Using a lower 5 % fractile gives a recommended design value of 0.40, as Cook suggested in his research to find the dynamic coefficient of friction. Thus, a design value of 0.40 is proposed for the coefficient of friction. A Φ-factor of 0.65 appears reasonable, considering the rather large variation in the measured coefficients of friction.

7.3 DISCUSSION OF RESULTS FOR SINGLE-CONNECTOR, DIRECT-SHEAR STATIC TESTS

Section 7.3.1 compares the test results of the connection methods discussed in this thesis, while Section 7.3.2 provides further analysis of each connection method.

7.3.1 Comparison of Test Results

Figure 7.1 shows a load-slip graph for the average of each of the six standard connection methods, as well as for a three of the four variations discussed in this thesis. The grouted expansion anchor is not shown because its capacity was so low (about 6 kips). The cast-in-place welded stud is also shown as a reference. The connection methods are listed in the key of the figure in order of highest shear at a slip of 0.2 in. Only MAXIB03 is shown for the MAXIB connection method since it incorporates the sheath configuration that would most probably be used in the field for this application: a second sheath, with the interface between the two sheaths below the steel-concrete interface. Connection methods MAXHG and MAXHS involve only one replicate each.

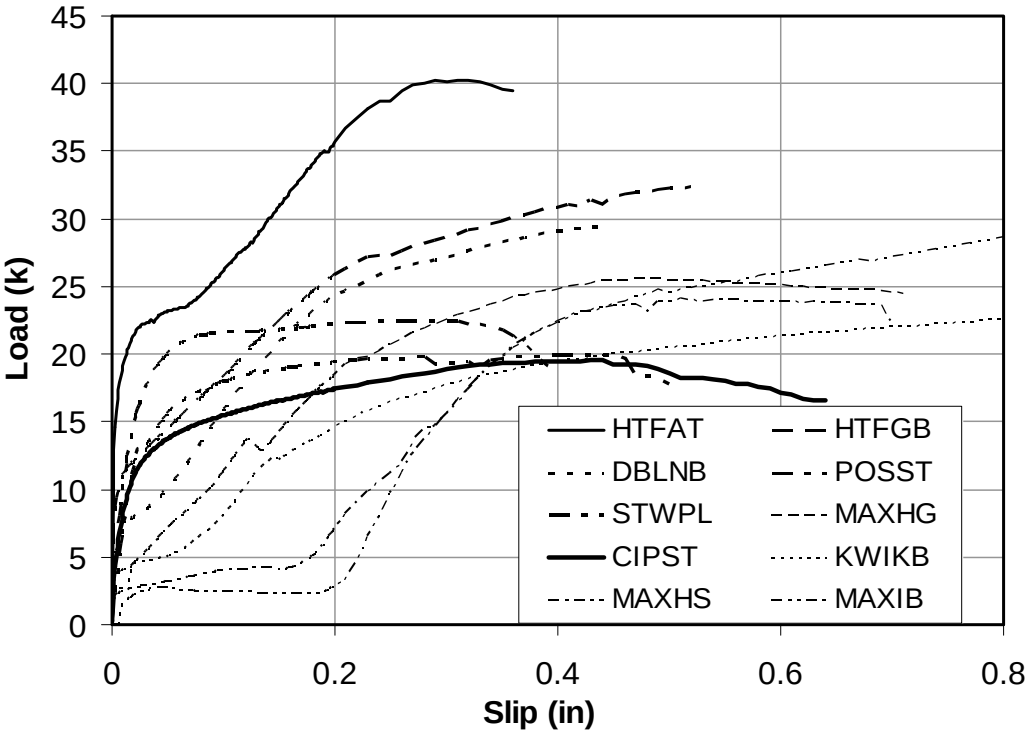

Figure 7.1: Load vs. slip for connection methods

As shown in Figure 7.1, the connection methods are shown to have mean ultimate shear capacities ranging from about 19.5 kips to 40 kips. These numbers must be interpreted carefully because each connector in a connection method reaches its ultimate capacity at a different slip value, causing the ultimate of the average capacity to be lower than the average of the ultimate values for each connection method. The plots end at the lowest final slip recorded for the tests for a connection method, making it appear that the maximum capacity was not reached for some connection methods (for example, HTFGB). Since the ultimate capacity was reached for each test, the average of the numerical ultimate capacities for a connection method is presented in Table 7.1. These values are based on the results given in Table 6.2, and are given in the order used in previous chapters.

Figure 7.1 shows that all connection methods discussed in this thesis have a higher average ultimate capacity than the benchmark cast-in-place welded stud. Table 7.1 shows that the stud welded to plate connection method is the only one with a lower individual average ultimate capacity than the cast-in-place welded stud. Section 7.3.2.3 discusses this further.

Table 7.1: Average of individual ultimate capacities of connection methods

Connection Method Description	Test Designation	Average Ultimate Capacity (kips)
Cast-in-Place Welded Headed Stud	**CIPST**	**21.3**
Post-Installed Welded Headed Stud	POSST	22.8
Stud Welded to Plate	STWPL	20.4
Double-Nut Bolt	DBLNB	30.0
High-Tension, Friction-Grip Bolt	HTFGB	32.8
High-Tension, Friction-Grip Bolt [1¼-in. Dia.]	HTFAT	40.8
Expansion Anchor	KWIKB	23.7
Undercut Anchor (MAXIB03)	MAXIB	33.7
Undercut Anchor [High-Strength]	MAXHS	24.1
Undercut Anchor [HS with Anchor Gel]	MASHG	25.5

Figure 7.2 shows averages of the initial portion of each methods' average load-slip curves, to observe more clearly the relative initial stiffness of each connection method. The connection methods are listed in the same order as Figure 7.1. The HTFAT, HTFGB, POSST, and STWPL connection methods have an initial stiffness greater than that of the benchmark CIPST connection method. The DBLNB connection method achieves a capacity greater than the CIPST connection method achieves by a slip of 0.1 in., but slightly dips below the load-slip curve of the CIPST connection method, initially. The standard undercut and expansion anchors, however, have significant slips at ultimate capacities. The

initial load-slip curve is important when evaluating the effectiveness of the investigated connection methods.

Previous research has shown that the ultimate slip a bridge connector experiences is about 0.2 in. (Chapter 2). Thus, it appears that the shear resistance developed by a connector at low levels of slip is the most meaningful measure of the structural effectiveness of the corresponding connection method. The shear resistance developed by a connector at large slip may be of little practical value, since the corresponding displacements of the bridge girder may be unacceptably large. In this thesis, a value for the critical design slip of 0.2 in. is chosen based on the studies noted above. That is, the shear resistance at a slip of 0.2 in. is taken as the primary indicator of useful shear capacity.

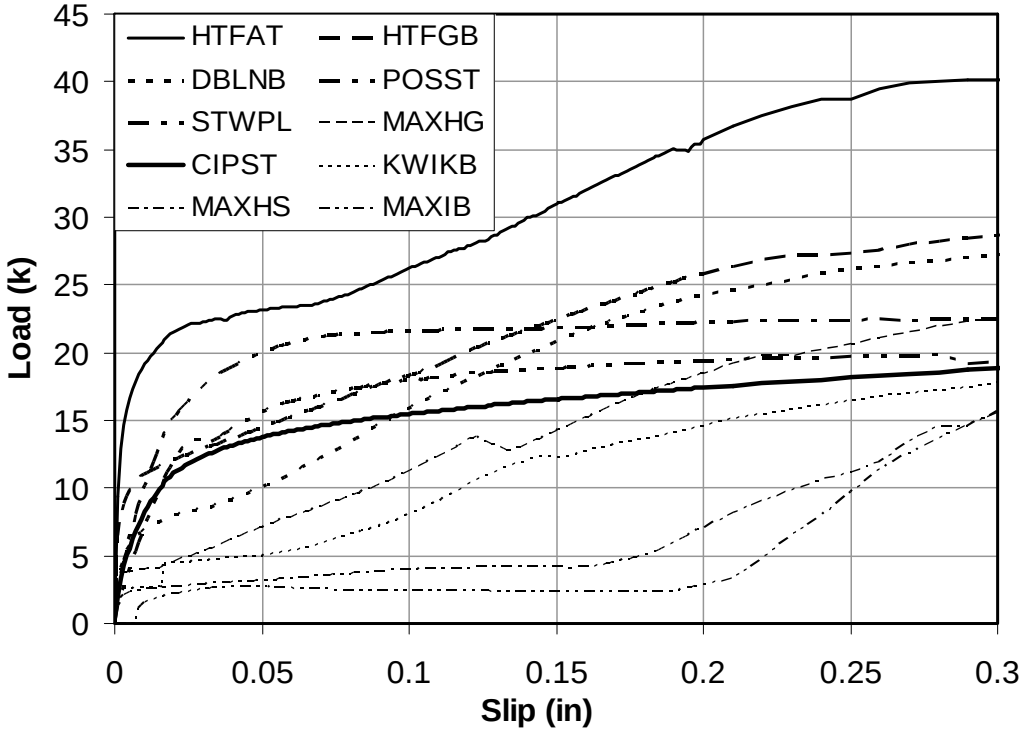

Figure 7.2: Load vs. slip for connection methods for slip ranging from 0 to 0.3 in.

7.3.2 Evaluation of Behavior of Connection Methods

Although it is of interest to compare the average load-slip relationships of the connection methods, a major objective of the experimental program in this phase of the project was to better understand the behavior of the individual connectors. To that end, the following sections discuss the behavior of the each connection method.

Several design equations have been proposed in the literature to calculate the ultimate capacity of a connector in concrete. As discussed in Chapter 2, the AASHTO (2002) code equations are based on the work performed by Ollgaard, Slutter and Fisher (1971). They are given in Equation 7.1:

$$Q_u = 0.4 * d^2 * \sqrt{f'_c * E_c} \leq 60{,}000 * A_s \qquad \textbf{(7.1)}$$

Where: Q_u = specified ultimate strength of connector;
d = diameter of connector;
f_c' = specified compressive strength of concrete;
E_c = modulus of elasticity of concrete; and
A_s = cross-sectional area of connector.

The units of the variables are required in lb and in. Equation 7.1 depends only on the strength of the concrete and the size of the connector. The strength of the connector is not explicitly taken into account, although the 60,000 constant coefficient in the limit of Equation 7.1 is based on the ultimate tensile strength of a headed stud.

Oehlers and Johnson (1987) proposed the following equation for predicting the ultimate capacity of a cast-in-place welded headed stud. The equation is dependent on the strength of the concrete, the size of the connector, and the strength and stiffness of the connector material:

$$Q_u = 5.0 * A_s * f_u * \left(\frac{E_c}{E_s}\right)^{0.4} * \left(\frac{f'_{cu}}{f_u}\right)^{0.35} \qquad \textbf{(7.2)}$$

Where: F_u = specified ultimate tensile strength of connector;

E_s = modulus of elasticity of connector material; and

f_{cu}' = specified compressive strength of concrete of cube.

The compressive strength of the concrete in Equation 7.2 uses the 50-mm cube, rather than a cylinder, as used in Equation 7.1. The cube strength of concrete is typically about 20 % higher than the cylinder strength, although no adjustment was made in Table 7.2. Cylinders were used for concrete and grout specimens in this phase of the project.

Table 7.2 compares the observed results of each test to the predicted values given by Equation 7.1 and Equation 7.2. It lists the measured compressive strength of the concrete, f_c, and grout, f_g, if applicable, as well as a weighted average, f_{avg}, based on the annular comparative areas of the grout and concrete surrounding the connector, assuming a 4-in. crushing zone. For example, the POSST connection method had a 3.5-in. diameter cylinder of grout surrounding the connector, leaving a 0.5-in. annular region of concrete for the 4-in. crushing zone observed. This led to a weighted-average compressive strength using 76.6 % of the grout strength and 23.4 % of the concrete strength. The STWPL and DBLNB connection methods had 2-in. diameter cylinders of grout. The stiffness of the concrete was calculated as using $57 \times \sqrt{fc'}$. The HTFAT connection method used a 1¼-in. diameter connector; all of the other connectors were ¾ in. in diameter. The stiffness of the steel was taken as 29,000 ksi. The ratio of measured-to-calculated strength is given.

For Equation 7.1, the difference in the strength of the grout for a connection method did not affect the calculated ultimate capacity in even the third

significant figure in any of the three specimens in the connection method, so each connection method displays the same result. The varying strength of the grout affected the solution in each specimen of a connection method using Equation 7.2, as displayed in the table. Equation 7.1 is less sensitive to the grout strength than Equation 7.2.

Table 7.2: Material properties and test results compared to Eqs. 7.1 and 7.2

Designation	f_c (psi)	f_g (psi)	f_{avg} (psi)	E_c (ksi)	F_u (ksi)	Result (k)	E 7.1 (k)	O/P Ratio	E 7.2 (k)	O/P Ratio
CIPST01	3200		3200	3220	66.2	24.3	22.9	0.94	21.0	0.87
CIPST02	3200		3200	3220	66.2	21.7		1.05	21.0	0.97
CIPST03	3200		3200	3220	66.2	17.8		1.28	21.0	1.18
POSST01	3200	4500	4200	3690	66.2	22.8	26.5	1.16	24.4	1.07
POSST02	3200	5250	4770	3940	66.2	22.4		1.18	26.2	1.17
POSST03	3250	5370	4870	3980	66.2	23.3		1.14	26.5	1.14
STWPL01	3440	3580	3480	3360	66.2	21.3	24.3	1.14	22.0	1.03
STWPL02	3440	3580	3480	3360	66.2	18.4		1.32	22.0	1.20
STWPL03	3440	3580	3480	3360	66.2	21.6		1.13	22.0	1.02
DBLNB01	3440	3170	3370	3310	150	31.1	23.8	0.76	36.9	1.18
DBLNB02	3440	3180	3380	3310	150	30.6		0.78	36.9	1.20
DBLNB03	3440	3180	3380	3310	150	28.4		0.84	36.9	1.30
HTFGB01	3320		3320	3280	120	30.7	23.5	0.77	31.6	1.03
HTFGB02	3320		3320	3280	120	34.3		0.84	31.6	0.92
HTFGB03	3320		3320	3280	120	33.5		0.77	31.6	0.94
HTFAT01	3320		3320	3280	150	37.6	65.3	1.74	101.5	2.70
HTFAT02	3320		3320	3280	150	39.7		1.64	101.5	2.56
HTFAT03	3320		3320	3280	150	45.0		1.45	101.5	2.25
KWIKB01	3200		3200	3220	75	23.7	22.9	0.96	22.8	0.96
MAXIB01	3200		3200	3220	58	25.7	22.9	0.89	19.3	0.75
MAXIB02	3200		3200	3220	58	18.3		1.25	19.3	1.05
MAXIB03	3200		3200	3220	58	33.7		0.68	19.3	0.57
MAXHS01	3250		3250	3250	120	24.1	23.1	0.96	31.2	1.30
MAXHG01	3500		3500	3370	120	25.5	24.4	0.96	32.5	1.28

The table clearly shows that the calculations are not always conservative compared with the results of the experimental program. Both of the equations

overestimated the strength of each of the specimens for the POSST, STWPL, and HTFAT connection methods. The average of the CIPST results met the predicted calculation of Equation 7.2 and fell 7.0 % short of the calculation of Equation 7.1. It is also obvious that the design equations, based on push-out tests on welded headed studs, do not accurately predict the ultimate strength of many of the retrofit connection methods. Specific reasons for this are proposed later in this chapter. Despite the inability to predict accurately the ultimate strength of the connection methods using Equation 7.1 and Equation 7.2, the results of the experimental program give an accurate comparison between the investigated connection methods and the benchmark cast-in-place welded headed stud. Discussion of the results is given below under each connection method's heading.

7.3.2.1 Cast-in-Place Welded Stud

Hungerford (2004) provides the background research, results, and conclusions of the cast-in-place welded headed stud. Summary information repeated for completeness.

Table 7.2 shows that two of the three cast-in-place welded studs developed capacities less than predicted by Equation 7.1. This equation is based on many tests with considerable scatter. Figure 7.3 shows the load-slip relation for welded studs from the standard push-out test obtained from the literature. Equation 7.3 gives a commonly used relation between slip and ultimate load proposed by Ollgaard, Slutter and Fisher (1971). The data were normalized using the more precise version of Equation 7.1 (Ollgaard, Slutter and Fisher 1971) for the ultimate connector strength, Q_u, and a concrete strength of 3000 psi. Data by An and Cederwall (1996) are normalized by Equation 7.2 since this equation is referenced in their work.

$$Q = Q_u * \left(1 - e^{-18*\Delta}\right)^{0.4} \qquad \textbf{(7.3)}$$

Where: Q = shear applied to connector;

Q_u = ultimate strength of connector; and

Δ = slip of connector.

The data are quite scattered. Most of the data used to obtain Equation 7.1 and Equation 7.3 are from tests performed with concrete having a compressive strength of around 5000 psi. Data from tests in which the concrete strength was around 3000 psi fall closer to the data from the experimental results of this phase of the project. The results reported by Klaiber *et al*. (1983) were for two connectors, and thus the reported load was divided in two for comparison here.

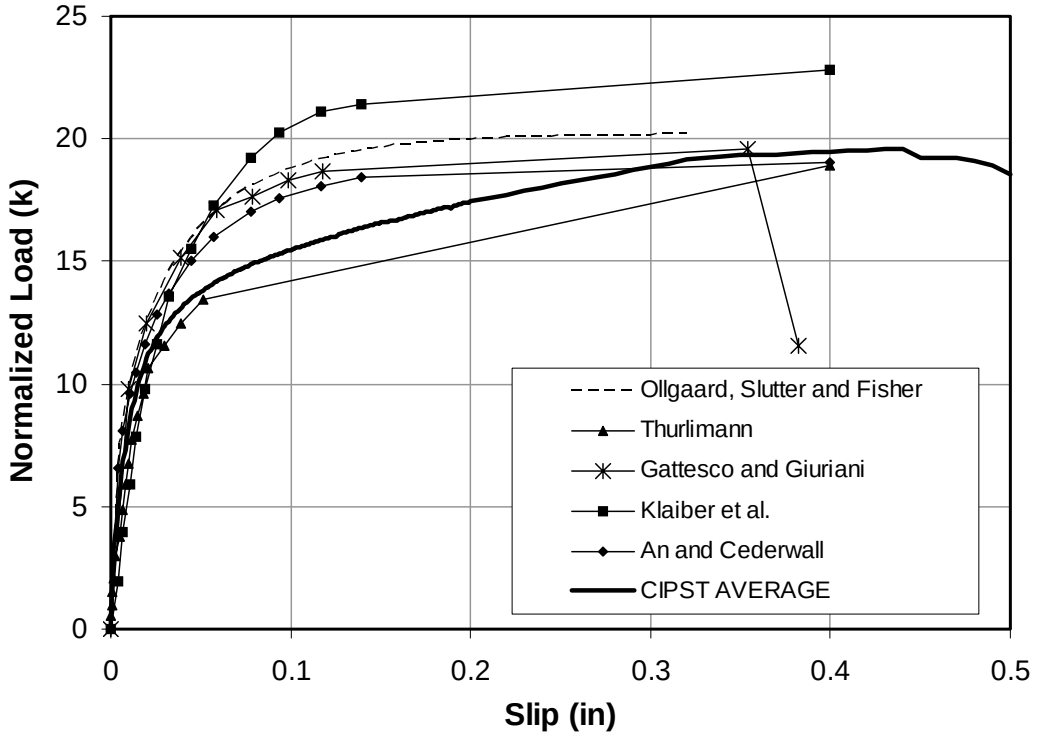

Figure 7.3: Load-slip relationship for cast-in-place welded studs

The average data for the CIPST tests fall above only the data from Thurlimann. Initial stiffness and ultimate strength are similar, however, for all of the results. Thurlimann (1959) reports that the slip of an individual connector in a

standard push-out test may vary as much as 100 %; the data for the three CIPST tests certainly corroborate this.

7.3.2.2 Post-Installed Welded Stud

Both Equation 7.1 and Equation 7.2 overestimated the ultimate strength of the POSST connection method. Based on the average ultimate strength for the connection method reported in Table 7.1, the results fall 14 % and 11 % below the results given by Equation 7.1 and Equation 7.2 respectively. This may be due to several reasons. The crushing region around the connector was not confined to the grout (Figure 6.3). Therefore, it is difficult to estimate what value of f_c' should be used in Equation 7.1 and Equation 7.2. A weighted average based on the comparative areas of the grout cylinder (3.5-in. diameter) and the concrete crushed zone (4-in. diameter) was used. To obtain design values for the post-installed welded stud, more static tests (possibly on a group of connectors, as discussed in Chapter 8), would be desirable.

As mentioned in Chapter 6, Specimen POSST02 had a gap between the concrete block and the steel plate due to inadvertently moving the concrete block during the initial hours of grout curing. The results show only a 2.8-percent decrease in ultimate capacity compared to the average of the other two tests for that connection method. A 2.2-percent difference exists between the other two tests. The strength of the grout of Specimen POSST02 was similar to Specimen POSST03, with a 3.9-percent difference in ultimate capacities. Thus, the gap did not significantly affect the connector behavior. A gap would be virtually impossible to create in the field, since the headed stud is welded directly to the girder flange and the hole is filled with grout from the top of the bridge.

7.3.2.3 Stud Welded to Plate

Neither Equation 7.1 nor Equation 7.2 accurately estimated the ultimate strength of the STWPL connection method. Based on the average ultimate strength of the connection method reported in Table 7.1, the results fall 16 % and 7.2 % below the results given by Equation 7.1 and 7.2 respectively. This may be due to reasons similar to those given in the POSST section. The value of the compressive strength of the surrounding material is difficult to characterize, leading to considerable uncertainty in the results given by the equations.

As mentioned in Chapter 6, Specimen STWPL02 had a gap of about ⅛ in. between the concrete block and one of the small plates with a welded stud. This specimen had a 14-percent lower ultimate capacity than the average of the other two tests, possibly because of the gap (combined with the eccentricity). The other two tests differed by 1.4 %. The strength of the grout was the same for all of the tests. This type of gap obtained in Specimen STWPL02 could potentially occur in the field, as opposed to the gap in the POSST02 test, because the small plate may not be welded to the girder flange with the top flush with the concrete.

Although no push-out tests were performed by the researcher who first used this connection method (Leite 2001), it was implemented on a bridge in Brazil. The connectors were 1- x 1- x 10-in. square steel bars spaced longitudinally at 23.5 in. This approaches the maximum spacing of 24 in., required by AASHTO (2002). Longitudinal strains measured in the girders of the retrofitted bridge were lower than calculated using finite-element analysis (Leite 2001). This implies a higher degree of composite action than anticipated, and probably implies satisfactory performance of the retrofit connector method.

7.3.2.4 Double-Nut Bolt

A large difference between the calculated values of Equation 7.1 and Equation 7.2 was obtained for the double-nut bolt connection method because of the connector's high ultimate tensile strength. The resulting average capacity of the connection method met the code-based equation (Equation 7.1) by a margin of 26 %, but fell short of the result predicted by Oehlers and Johnson (1987) (Equation 7.2) by nearly 19 %. A difference of 13 kips was obtained between the capacities predicted by the two equations.

The equation given by Oehlers and Johnson (1987) takes into account the strength of the connector, which for the Grade 8 tap bolt is 2.5 times the strength of a typical headed stud (on which the equation is based). By limiting the ultimate tensile strength of the connector to 60 ksi, Equation 7.2 overestimates the capacity by about 48 %. Limiting the strength of the connector eliminates a considerable benefit of Equation 7.2. As discussed in the next section, the strength of the HTFGB connection method, which used A325 bolts (F_u = 120 ksi) was accurately predicted by Equation 7.2, leading one to believe that an appropriate cap may be 120 ksi for the equation. Using this cap, the results are 5.8 % below the predicted value given by the equation, a significant improvement from the 19-percent underestimation without a cap on connector tensile strength.

As mentioned in Chapter 6, based on the slip data, Specimen DBLNB03 appeared to have been misaligned. This specimen's capacity was 7.9 % lower than the average of the other two tests, which differed by 1.6 %. The strength of the grout was virtually the same for all three tests.

7.3.2.5 High-Tension, Friction-Grip Bolt

The results of the three tests on this connection method met or exceeded, in five of the six replicates, the load-slip behavior predicted by Equation 7.1 and

Equation 7.2. Equation 7.2 accurately predicts the strength of the connection method within 3.9 % of the average of the connection method. Only Specimen HTFGB01 is underestimated (by 2.8 %), probably because its embedment depth was 1 in. less than in the other two tests, with an H/d ratio of 4.4. Equation 7.1 underestimates the strength of the average of the HTFGB connection method by 40 %, probably because the higher strength of the connector material is not taken into account.

Specimen HTFGB03 was the only replicate in which epoxy was not used below the connector head to provide a flat bearing surface. It was also the only replicate that failed in shear, without pryout. Since pryout is an undesirable failure mode, and HTFGB03 had virtually the same capacity as the other two tests, it appears that using epoxy under the connector head is not a good idea. It is believed that in Specimens HRFGB01 and HTFGB02, the epoxy may have prevented local crushing of the concrete under the edge of the connector head, and naturally contributed to an undesirable pryout failure. In any case, the bottom of the hole must still be flattened, however, to provide a good bearing surface.

Based on the results of Table 6.2, the coefficient of friction can be readily taken as 0.4, using a Φ-factor of 0.65. This results in a low shear capacity, however, given the maximum pre-tension of only 28 kips. Thus, practically speaking, it is probably that the ¾-in. diameter high-tension, friction-grip bolt is useful for using friction as the primary shear transfer mechanism under working loads. Given that it takes more steps to install than some of the other structurally effective methods, it has somewhat of a disadvantage. Unfortunately, as discussed below, increasing the diameter of the connector to obtain more clamping force appears to be ineffective.

7.3.2.5.1 High-Tension, Friction-Grip Bolt (1¼-in. diameter)

This connection method did not meet the predicted strength of 60.3 kips given by the AASHTO (2002) design equation. The average ultimate strength obtained in the tests was only 40.8 kips, falling 32 % below Equation 7.1.. Although the tests were halted before failure of the connector, the load was decreasing when the test was stopped. Since the design equations tested ¾-in. diameter and 7/8-in. diameter connectors in concrete that was typically stronger than that used in this experimental program, the code equations do not appear appropriate for this connector. Equation 7.2 overestimates the average strength for the HTFAT connection method by a factor of 1.49. This connector is much stronger than the connectors used in the tests to generate the equation. Using the cap of 120 ksi recommended here for F_u in Equation 7.2, the predicted capacity still overestimates the results by a factor of 1.15.

Based on the results of Table 6.2, the average coefficient of friction for this connection method was only 0.21, almost half of the design value recommended in Section 7.2. Although the allowable pre-tension is 2.8 times that of a ¾-in. diameter connector, only a small increase in the shear capacity is obtained using friction.

7.3.2.6 Expansion Anchor

The expansion anchor develops very large slip at low levels of applied shear. As indicated in Figure 7.2, the shear resistance of the expansion anchor at 0.2 in. slip is very low. Consequently, the expansion anchor is not considered suitable as a retrofit shear connector for strengthening bridges.

7.3.2.7 Undercut Anchor

Using ¾ in. for the diameter in Equation 7.1 produced accurate estimates of the strength of this connection method for all five undercut anchors tested. It would be incorrect to include the sheath in that diameter.

As mentioned in Chapter 6, the three anchors for the MAXIB connection method were installed in different ways. Equation 7.1 gives the closest estimates of capacity for undercut anchors without a second sheath. Equation 7.2 underestimates the capacity for the MAXIB connector method, and overestimates the capacity of the higher strength MAXHS and MAXHG connector methods. MAXIB02, installed like MAXHS01 and MAXHG01, had a lower ultimate capacity, probably because of the lower strength of the connector.

Given the connector's inability to transfer shear through friction and the oversized hole in the concrete required for installation resulting in high slip values, as well as the high relative cost of the connector, the undercut anchor is not recommended for this application.

7.4 MATERIAL COSTS AND EASE OF INSTALLATION OF CONNECTORS USED IN CONNECTION METHODS IN PROJECT

Comparative connector costs and relative ease of installation are given in Chapter 3 for the connection methods discussed in this thesis. The same information is given in Table 7.3 for all connection methods of this study. Costs include materials (connectors, grout and adhesive as applicable), but do not include labor costs, because these could be highly contractor-dependent. The comparative cost analysis was performed assuming 300 connectors (the number required for a 50-ft long span with six girders, with rows of two connectors, spaced longitudinally at 2 ft.). Costs are normalized to the cost of the cast-in-place, welded headed studs. Costs for the epoxy-coated-to-plate method were

estimated assuming that the adhered area was approximately equal to that of two cast-in-place welded studs spaced at 2 ft, with an additional safety factor of about 1.5 due to the brittle failure of the connection. No other connection methods were so adjusted for relative strength or failure mode.

In Table 7.3, sets of connection methods with significantly different material costs are separated by double lines. Four basic ranges of material costs are evident, with one set of methods being roughly comparable with the benchmark.

Table 7.3: Normalized material costs of connection methods in project

Connection Method Designation	Relative Ease of Installation	Normalized Material Cost
CIPST	Easy	1.0
POSST	Easy	3.1
WEDGB	Easy	3.3
HTFGB	Hard	3.9
POSTR	Medium	4.2
STWPL	Medium	5.6
KWIKB	Easy	8.7
HASAA	Medium	10.5
HITTZ	Medium	10.7
DBLNB	Medium	11.9
HTFAT	Hard	12.1
MAXIB	Easy	24.8
3MEPX	Medium	45.2

CHAPTER 8
SUMMARY, CONCLUSIONS, AND RECOMMENDATIONS FOR FURTHER RESEARCH

8.1 SUMMARY

This thesis covers one part of a larger project to investigate methods to develop composite action in non-composite floor systems in existing bridges using retrofit shear-connection methods. In this thesis, the term "connection method" refers to any way of connecting the concrete slab and steel girder to transfer shear. This includes mechanical fasteners, and adhesives applied at the steel-concrete interface. The term "connector" refers to any type of metal fastener, and excludes adhesive-only connections. The term "basic connection method" refers to the connection method installed in its simplest form, as shown in the schematic diagrams of Chapter 3. Fifteen basic connection methods were investigated, of which twelve were subjected to single-connector, direct-shear static load tests. An additional seven variations of some of the basic connection methods were tested (for example, adding anchor gel to fill the gap for the undercut anchor). Tests were performed on single connectors to better evaluate structural behavior. Since the most cost-effective implementation of this project would be realized by taking advantage of partially composite design, in which the strength of the bridge is governed by the strength of the connectors, it is important to understand the behavior of the individual connector. A direct-shear test was therefore performed at this stage of the project, as compared to the more conventional push-out test.

Six retrofit shear-connection methods are discussed in this thesis, with the remainder covered by Hungerford (2004). Of the fifteen connection methods studied here, seven are recommended for further testing in later stages of this overall investigation.

Since some connection methods use friction as the primary shear-transfer mechanism, the static coefficient of friction, μ, between concrete and steel, was measured in the field on four steel girders of a recently demolished bridge in San Antonio, Texas. In addition, the coefficient of friction was deduced from some single-connector, direct-shear static load tests, using the measured shear and tension forces. The results show large scatter for the latter tests, but are reasonably consistent with previous research.

Detailed conclusions for each of the objectives are given in the sections below. Recommendations for further testing are given in Section 8.9.

8.2 CONCLUSIONS, OBSERVATIONS, AND RECOMMENDATIONS

8.2.1 Conclusions Regarding Coefficient of Friction

Friction is perhaps the simplest way of transferring shear between the concrete slab and steel girder to create composite action. Even without shear connectors, some friction can be developed. Past studies indicate, however, that a reliable and predictable degree of composite action cannot be developed in this manner, particularly at higher load levels (Cook 1977, Bowen and Engelhardt 2003). For this project, the ability to transfer shear through friction, by the installation and tensioning of various connectors, was investigated. To determine the shear that can be transferred by friction requires data on the coefficient of friction between steel and concrete.

Two types of tests were conducted to obtain data on the coefficient of friction. In addition, previous research was investigated to determine an

appropriate design value (Cook 1989). Based on an evaluation of previous research, the results of the field friction tests, and the results of the static load tests, a design value for μ of 0.40 is proposed. The Φ-factor of 0.65 proposed by Cook (1989) appears reasonable, considering the large scatter in data.

8.2.2 Conclusions Regarding Results from Single-Connector, Direct-Shear Static Tests

Static shear tests were conducted on twelve basic connection methods as well as on an additional seven variations of the basic connection methods. Of the nineteen connection methods tested (basic connection methods plus variations), seven connection methods are recommended for further testing (Table 8.1). Twelve connection methods exhibited poor structural performance for application as retrofit shear connection methods, and are not recommended for further consideration (Table 8.1). In Table 8.1, variations to the basic connection method are shown in brackets.

Table 8.1: Recommendations regarding retrofit connection methods

Connection Methods Recommended for Further Testing	Connection methods Not Recommended for Further Testing
High-Tension, Friction-Grip Bolt	Expansion Anchor
Double-Nut Bolt	Expansion Anchor [with Grout]
Post-Installed Welded Headed Stud	Undercut Anchor
Epoxy Coated to Plate	Undercut Anchor [High-Strength]
Threaded Rod Adhesive Anchor	Undercut Anchor [HS with Anchor Gel]
Concrete Screw [with Steel Sheath]	High-Tension, Friction-Grip Bolt [1¼″-Dia.]
Stud Welded to Plate	Post-Installed Welded Threaded Rod
	Wedge Rod Adhesive Anchor
	HY-150 Adhesive Coated to Plate
	Concrete Screw
	Concrete Screw [with Anchor Gel]

In the sections below, more conclusions are presented on the connection methods discussed in this thesis. First, however, observations are made regarding the installation equipment, grout, and anchor gel.

8.2.3 Observations and Recommendations on Installation Equipment

The tools used for installation of the connection methods are discussed in Chapters 3, 5, 6, and 7. Based on experience with this equipment in this test program, as discussed in Chapters 6 and 7, the following observations and recommendations are made regarding the installation equipment.

8.2.3.1 Observations and Recommendations Regarding Coring Machine versus Rotary Hammer Drill

A coring machine is required for drilling holes larger than 2 in. in diameter if the hole is to be drilled completely through the concrete slab. A rotary hammer drill should be used for drilling holes 2 in. or less in diameter, or holes larger than

2 in. in diameter that are only a few inches deep. The latter can be achieved by drilling a series of adjacent holes using a 2-in. diameter bit, creating a larger "effective" diameter, as shown in Chapter 5.

Chapter 3 lists the disadvantages of using a coring machine in the field. Those include the requirement to clamp the machine down while drilling, and the need for a constant water supply. In addition, the larger-diameter bit used has a higher chance of hitting reinforcing bars. The rotary hammer drill, on the other hand, is handheld and requires only a bucket of water for cooling. Whenever possible, a rotary hammer drill should be used instead of a coring machine.

For the seven connection methods recommended in Section 8.2.2 for further testing in the later phases of this project, a coring machine is required for only one method—the post-installed welded stud. The other five connection methods that require drilling can be installed using a rotary hammer drill. The final recommended method (Epoxy Coated to Plate) does not require drilling.

8.2.3.2 Observations and Recommendations Regarding Slugger™ Drill

A special-purpose, hollow-bit drill, referred to here as a "Slugger™," is a portable tool used for coring through steel. This type of drill can be used easily in the field to drill holes into the top girder flange, from below or above the bridge deck. Klaiber *et al*. (1983) found drilling through the steel to be difficult for the high-tension, friction-grip bolt due to buildup of the steel shavings in the concrete hole. The only other concern with using the drill would be the environmental impact of using machine oil to cool the bit. A portable container could be fabricated to capture the oil during drilling to avoid damage to the environment.

8.2.4 Observations and Recommendations on Grout and Anchor Gel

The two sections below present observations and recommendations on the grout and anchor gel used in this test program.

8.2.4.1 Observations and Recommendations Regarding Grout

Of the seven connection methods recommended for further testing, four require grout. Five-Star® Highway Patch grout was used for those connection methods. The manufacturer's recommendations for batching and mixing (Chapter 5) should be followed.

Since Ollgaard, Slutter and Fisher (1971) and others (An and Cederwall 1996) show that the stiffness and ultimate strength of a connector is directly dependent on the material surrounding it (Chapter 2), it is important for the grout to have a high, predictable strength. The Five-Star® Highway Patch grout has a specified 1-day compressive strength of 5100 psi, about 70 % higher than the 28-day strength of the concrete used in this testing program. It also has a 7-day strength of 7000 psi, but since it was anticipated that the candidate bridge would need to be opened as soon as possible after retrofitting, the 1-day strength was chosen and targeted. Significant time is saved by using the 1-day strength, without much loss in performance. It was found that the strength of the grout was very sensitive to mixing procedures and component proportions, as discussed below.

The mixture must be thoroughly mixed using a power drill and large mixing paddle (POSST). A mortar mixer is also acceptable. Mixing using a cordless drill with a smaller propeller-like mixing apparatus (DBLNB) was not successful, nor was hand mixing with a smooth rod (KWIKG). Both resulted in low grout strengths.

The maximum amount of water recommended by the manufacturer cannot be exceeded (STWPL). This amount of water is quite small and should be mixed sparingly with the dry grout constituents.

The hole in which the grout is being placed must be saturated with water 24 hours prior to casting to prevent absorption of water by the surrounding

concrete, and consequent shrinkage cracks in the grout. There should not be any standing water in the hole, however, at the time of casting. Any shrinkage cracks could allow water to penetrate to the connector. To further prevent shrinkage cracks, the grout should be moist- cured for three days or sealed.

The hole should be properly cleaned and roughened to ensure a good bond, as recommended by the manufacturer and other researchers (Klaiber *et al*. 1983). The manufacturer recommends mixing the grout at temperatures between 35 F and 90 F, and also recommends not mixing more grout than can be placed in ten minutes.

The mixture proportions yielded a smaller volume than calculated even accounting for a 15 % waste, probably due to a large amount of grout adhering to the side of the bucket after mixing. To account for this as well, it is wise to prepare about 25 % more grout than is theoretically needed.

Cylinders were used to test the grout because the molds were readily available, easier to cast, and easier to test than the 50-mm cubes. The cylinder strength results are expected to be about 20 % less than the cube strength that the ASTM C109 standard used by the manufacturer reports. Even allowing for this, however, the 1-day compressive strengths fell short of meeting the 5100 psi recorded value for the cases where proper mixing or proportions were not used.

8.2.4.2 Observations and Recommendations Regarding Anchor Gel

The Five-Star® RS Anchor Gel, a two-part epoxy commonly used to fill cracks, was recommended by the manufacturer for filling the gap between the connector and the steel (and possibly concrete) for some connection methods. It proved to be inadequate for the connection methods for which it was used, however. Hungerford (2004) discusses this in more detail.

8.3 OBSERVATIONS AND RECOMMENDATIONS REGARDING POST-INSTALLED WELDED STUD (POSST)

The post-installed welded stud demonstrated excellent structural performance because of the large annular ring of high-strength grout surrounding it. The design strength (taken as the strength at 0.2 in. of slip) and initial stiffness of the POSST connection method were substantially larger than those of the cast-in-place welded stud, considered as the benchmark. In addition, the POSST connection method had a large slip capacity. For these reasons, this connection method is recommended for further testing. Two disadvantages of this connection method are that it requires a coring machine and welding to the top of the steel flange with a stud-welding gun.

8.4 OBSERVATIONS AND RECOMMENDATIONS REGARDING STUD WELDED TO PLATE (STWPL)

The stud welded to plate connection method exhibited good structural performance, with a design strength and initial stiffness above the benchmark, and about the same slip capacity as the benchmark. Although it is very similar to the POSST connection method, it requires only a rotary hammer drill and uses a more reliable welding technique because the welding is done on the vertical edge of the girder flange, which can be easily cleaned and checked for soundness. For these reasons, this connection method is recommended for further testing.

8.5 OBSERVATIONS AND RECOMMENDATIONS REGARDING DOUBLE-NUT BOLT (DBLNB)

The double-nut bolt displayed good structural performance with a design strength greater than the benchmark. The initial stiffness was slightly lower than that of the benchmark because of the plate (girder flange) had to slip into bearing after the initial frictional resistance between the top and bottom nuts was

overcome. At a slip of about 0.1 in., the connection method has a higher strength than the benchmark; It also had a larger slip capacity than the benchmark. The advantage of this connection method over those listed above is that is does not require any welding in the field. For of these reasons, This connection method is recommended for further testing.

8.6 OBSERVATIONS AND RECOMMENDATIONS REGARDING HIGH-TENSION, FRICTION-GRIP BOLT (HTFGB)

The high-tension, friction-grip bolt exhibited very good structural performance, with a design strength, initial stiffness, and slip capacity, much greater than those of the benchmark. For of these reasons, This connection method is recommended for further testing. This connection method also has the potential to perform well under fatigue loading, although the coefficient of friction, μ, used for design is quite low, requiring a significant number of connectors to eliminate slip.

8.7 OBSERVATIONS AND RECOMMENDATIONS REGARDING EXPANSION ANCHOR (KWIKB)

The expansion anchor exhibited poor structural performance, with a design strength and initial stiffness well below the benchmark. Although this connection method is extremely easy to install, the large "slip into bearing" required to achieve substantial strength makes it inadequate for this application. Using grout to reduce the "slip into bearing" proved ineffective. For these reasons, this connection method is not recommended for further testing.

8.8 OBSERVATIONS AND RECOMMENDATIONS REGARDING UNDERCUT ANCHOR (MAXIB)

The undercut anchor demonstrated poor structural performance, with a design strength and initial stiffness well below the benchmark. Although this connection method is relatively easy to install, the large "slip into bearing" required to achieve substantial strength is inadequate for this type of application. Using anchor gel to reduce the "slip into bearing" proved ineffective. For these reasons, this connection method is not recommended for further testing.

8.9 RECOMMENDATIONS FOR FURTHER TESTING

This thesis covers the initial phases of a broader investigation of methods to develop composite action in non-composite floor systems. This section provides recommendations for further testing for subsequent phases of the investigation, and also a method of assessing the effectiveness of the connectors installed in a bridge.

Since the first phase of testing studied the behavior of connection methods under static loading, the next phase should evaluate the behavior of the recommended methods under fatigue loading. Tests should be performed on single connectors to isolate individual connector behavior. Since each investigated connection method may undergo several million cycles, it is important to model the test accurately, as any small flaws in each cycle can produce large inaccuracies in the overall behavior (Gattesco and Giuriani 1996). In general, the same test setup can be used to perform the cyclic tests as was used in the static tests described here, with only a few additional components required. An additional modification to the test setup may be beneficial and reduce any unintentional tension force applied to the connector. This issue, along with a recommended modification, is discussed in detail by Hungerford (2004).

High-cycle fatigue testing should be performed first using several stress ranges to obtain the appropriate S-N curve. The high-cycle fatigue tests can be performed uni-directionally since stress range has been shown to be the critical variable, and minimum stress does not control (Slutter and Fisher 1966). Chapter 2 provides background information concerning previous research on the behavior of connectors in fatigue.

For connection methods that show adequate high-cycle fatigue behavior, a low-cycle fatigue test is recommended to evaluate behavior beyond the elastic range. This test, which subjects the connectors to only thousands of cycles under quasi-static loading, can be used to investigate incremental collapse, and also evaluate the effects of reversed cyclic loading (Gattesco and Giuriani 1996).

Low-cycle fatigue tests are important for connectors in regions of high shear, especially for partial composite design, where the connectors often yield and govern the strength of the bridge. As discussed in Chapter 2, the ultimate static strength of a connector that has undergone low-cycle fatigue loading, in a bridge designed for full-composite action, has been shown to be reduced by 10 % compared to the static capacity of an otherwise identical structure tested monotonically to failure (Grundy and Taplin 2003). In addition, the slip capacity of a connector has been shown to be reduced by 30 % compared with the database of results obtained by other researchers from monotonic testing (Chapter 2). Again, this is critical if the strength of the bridge depends on the connectors.

In addition to tests on single-connector specimens, a limited number of tests on specimens with multiple connectors may be beneficial. For this purpose, the conventional push-out test may be appropriate. Specimens for push-out test typically include four to eight connectors per specimen. This type of test can provide data on the ability of connectors to redistribute and share load. Push-out

tests can also provide data that are directly comparable to the large existing database from push-out tests.

8.9.1 Bridge Monitoring

Once the findings of this project are finalized, it is recommended that a existing bridge be retrofitted and monitored to assess the performance of the retrofit. A useful explanation of how to monitor a bridge economically and easily using strain gages is given by Leite (2001). As described in Chapter 2, properly placed strain gages on the top flange of the steel beam below the location of a shear connector can also be used to qualitatively assess the effectiveness of the connector (Toprac 1965).

REFERENCES

AASHO Standard Specifications for Highway Bridges, 1957. 7th ed. Washington, D.C.: American Association of State Highway Officials, 1957.

AASHO Standard Specifications for Highway Bridges, 1961. 8th ed. Washington, D.C.: American Association of State Highway Officials, 1961.

AASHTO LRFD Bridge Design Specifications, 1998. Customary U.S. Units. 2nd ed. Washington, D.C.: American Association of State Highway and Transportation Officials, 1998.

AASHTO Standard Bridge Design Specifications, 1977. 11th ed. Washington, D.C.: American Association of State Highway and Transportation Officials, 1977.

AASHTO Standard Bridge Design Specifications, 2002. 17th ed. Washington, D.C.: American Association of State Highway and Transportation Officials, 2002.

AISC Specification for the Design, Fabrication, and Erection of Structural Steel for Buildings. New York: American Institute of Steel Construction, 1961.

An, Li, and Cederwall, Krister. "Push-out Tests on Studs in High Strength and Normal Strength Concrete." Journal of Construction Steel Research 36.1 (1996): 15-29.

Bode, Helmut, Leffer, Andreas, and Martin Mensinger. "The Influence of the Stress Range History on the Fatigue Behaviour of Headed Studs." Composite Construction IV, May 28-June 2. Banff, Alberta, Canada: Engineering Foundation Conferences, 2000.

Bowen, C.M. and Engelhardt, M.D. "Analysis, Testing, and Load Rating of Historic Steel Truss Bridge Decks." Research Report No. 1741-2. University of Texas at Austin: Center for Transportation Research, 2003.

BS 5950. Code of Practice for Design of Composite Beams. London: British Standards Institution, 1990.

Cook, John P. Composite Construction Methods. New York: John Wiley & Sons, 1977.

Cook, Ronald A. Behavior and Design of Ductile Multiple-Anchor Steel-to-Concrete Connections. Diss. University of Texas at Austin, 1989. Austin: Ferguson Laboratory, 1989.

DD ENV 1994-1-1 Eurocode 4: Design of Composite Steel and Concrete Structures, Part 1.1: General Rules and Rules for Buildings. London: British Standards Institution, 1994.

Engelhardt and Klingner. **Summary of project 0-4124 presented by Dr. Engelhardt and Dr. Klingner.** 14 pages

Engelhardt, Michael D. Class Notes. "Composite Beams." Aug. 2003.

ENV 1994-1-1:1992 Eurocode 4, Design of Composite Steel and Concrete Structures, Part 1-1: General Rules and Rules for Buildings. Draft. Brussels, Belgium, Oct. 1992.

"Epoxy Bonds Composite Beams." Engineering News-Record. 10 Oct. 1963: 103.

Eurocode 3: Design of Steel Structures: Part 1.1: General Rules and Rules for Buildings. Brussels, Belgium: European Committee for Standardization (CEN), 1993.

Faella, Ciro, Martinelli, Enzo, and Emidio Nigro. "Shear Connection Nonlinearity and Deflections of Steel-Concrete Composite Beams: A Simplified Method." Journal of Structural Engineering. 129.1 (2003): 12-20.

"Five-Star Highway Patch Data Sheet." Online. Internet. 18 Feb. 2004. Available www.fivestarproducts.com/html/f1b7e.html.

Gattesco, N., and E. Giuriani. "Experimental Study on Stud Shear Connectors Subjected to Cyclic Loading." J. Construct. Steel Res. 38.1 (1996): 1-21.

Gattesco, N., Giuriani, E., and A. Gubana. "Low-Cycle Fatigue Test on Stud Shear Connectors." Journal of Structural Engineering 123.2 (1997): 145-150. 12416.

Gilbert, R. Ian, and Mark Andrew Bradford. "Time-Dependent Behavior of Continuous Composite Beams at Service Loads." Journal of Structural Engineering 121.2 (1995): 319-327. 5053.

Grigorian, Carl E., Yang, Tzong-Shuoh, and Egor P. Popov. "Slotted Bolted Connection Energy Dissipaters." Steel Tips. Report No. UCB/EERC-92/10. University of California at Berkeley: Structural Steel Educational Council, 1992.

Grundy, Paul, and Geoff Taplin. "Low Incremental Collapse Capacity of Composite Beams." Proc. of IABSE Symposium for Structures for High-Speed Railway Transportation. Antwerp, Belgium: 27-29 Aug. 2003.

Haensel, J. "Composite Bridge Design: The Reanimation of Steel Bridge Construction." J. Construc. Steel Res. 46.1-3 (1998): 54-55. 44.

Hegger, Josef, et al. "Studies on the Ductility of Shear Connectors when Using High-Strength Steel and High-Strength Concrete." International Symposium on Connections between Steel and Concrete. Ed. Eligehausen, R. Stuttgart, Germany: 10-12 Sept. 2001.

Hicks, S. J., and R. E. McConnel. "The Shear Resistance of Headed Studs Used with Profiled Steel Sheeting." Composite Construction III, June 9-14. Irsee, Germany: Engineering Foundation Conferences, 1996. 97-109.

Hilti North America. Product Technical Guide. 2002. www.hilti.com

Johnson, R.P., and Molenstra, Ir N. "Partial Shear Connection in Composite Beams for Buildings." Proc. Instn Civ. Engrs, Part 2 91 (1991): 679-704. 9744.

Klaiber, F. W., et al. "Strengthening of Existing Single Span Steel Beam and Concrete Deck Bridges." Final Report, Part I, Engineering Research Institute, Iowa State University, 1983.

Klingner, Richard E. Class Notes. "Behavior and Design of Fastening to Concrete." Oct. 2002.

Klingner, Richard E. Personal Interview. Nov. 2003.

LRFD Manual of Steel Construction. 3rd ed. U.S.A: American Institute of Steel Construction, 2001.

Masterbuilders website. www.masterbuilders.com. Got information about pozzolith 100 XR product on 2/9/2004.

Matus, Roberto Arroyo, and Jean Francois Jullien. "A New Shear Stud Connector Proposal." Composite Construction III, 9-14 June. Irsee, Germany: Engineering Foundation Conferences, 1996. 70-96.

Nakajima, A., et al. "Cyclic Shear Force—Slip Behavior of Studs under Alternating and Pulsating Load Condition." Engineering Structures (2003): 537-545.

Oehlers, D.J., and R.P. Johnson. "The Strength of Stud Shear Connections in Composite Beams." Structural Engineering 65B.2 (1987): 44-48.

Oehlers, Deric J., Seracino, Rudolf, and Michael F. Yeo. "Effect of Friction on Shear Connection in Composite Bridge Beams" Journal of Bridge Engineering 5.2 (2000): 91-98. 16405.

Oehlers, Deric John, and George Sved. "Composite Beams with Limited-Slip-Capacity Shear Connectors." Journal of Structural Engineering (1995): 932-938.

Ollgaard, Jorgen G., Slutter, Roger G., and John W. Fisher. "Shear Strength of Stud Connectors in Lightweight and Normal-Weight Concrete." AISC Engineering Journal 8.2 (1971): 55-64.

Roberts, T. M., and O. Dogan. "Fatigue of Welded Stud Shear Connectors in Steel-Concrete-Steel Sandwich Beams." J. Constuct. Steel Res. 45.3 (1998): 301-320.

"RS Anchor Gel Data Sheet." Online. Internet. 18 Feb. 2004. Available www.fivestarproducts.com/html/f1b8d.html.

Slutter, Roger G., and John W. Fisher. "Fatigue Strength of Shear Connectors." Highway Research Record 147 (1966): 65-88.

Tadros, Maher K., Badie, Sameh S., and Amgad M. Girgis. "Innovative Interface Systems for Steel-Girders/Concrete-Deck Connection." International Symposium on Connections between Steel and Concrete. Ed. Eligehausen, R. Stuttgart, Germany: 10-12 Sept. 2001.

Thurlimann, B. “Fatigue and Static Strength of Stud Connectors.” Journal of the American Concrete Institute 30 (1959)

Topkaya, Cem. Behavior of Curved Steel Trapezoidal Box Girders During Construction. Diss. University of Texas at Austin, 2002. Austin: Ferguson Laboratory, 2002.

Toprac, A. A. “Fatigue Strength of ¾-Inch Stud Shear Connectors.” Highway Research Record. 103 (1965): 53-77.

United States. Dept. of Transportation. Texas National Bridge Inventory: 2002. Federal Highway Administration. Online. Internet. 6 June 2003.

Viest, I. M., Fountain, R. S., and C.P. Siess. “Development of the New AASHO Specification for Composite Steel and Concrete Bridges.” HRB Bull. 174. (1958): 1-17.

Viest, Ivan M., et. al. Composite Construction: Design for Buildings. New York: Mcgraw-Hill, 1997.

Yamamoto, Yasutoshi, et al. “Shallow Shear Anchor Bolts for Structural Seismic Strengthening of Columns with Wing Wall.” International Symposium on Connections between Steel and Concrete. Ed. Eligehausen, R. Stuttgart, Germany: 10-12 Sept. 2001.

Zhang, Yong-gang, Klingner, Richard E., and Herman L. Graves, III. “Seismic Response of Multiple-Anchor Connections to Concrete.” International Symposium on Connections between Steel and Concrete. Ed. Eligehausen, R. Stuttgart, Germany: 10-12 Sept. 2001.

VITA

Brad Anthony Schaap was born in Omaha, Nebraska on August 30, 1979, the son of Ronald James Schaap and Darlene Kay Schaap. After graduating from Omaha North High, he attended Washington University in Saint Louis, receiving his Bachelor of Science in Civil Engineering in May of 2002. In August of 2002, he began his study in the Graduate School at the University of Texas at Austin, working as a research assistant at the Phil M. Ferguson Structural Engineering Laboratory.

This document was typed by the author.